# Laboratory Medicine 2014

Guest Editors: Mina Hur, Patrizia Cardelli, and Giulio Mengozzi

Laboratory Medicine 2014

Laboratory Medicine 2014

Guest Editors: Mina Hur, Patrizia Cardelli, and Giulio Mengozzi

Contents

Editorial

Laboratory Medicine 2014

Mina Hur,[1] Patrizia Cardelli,[2] and Giulio Mengozzi[3]

[1] *Department of Laboratory Medicine, School of Medicine, Konkuk University, 120-1 Neungdong-ro, Hwayang-dong, Gwangjin-gu, Seoul 143-729, Republic of Korea*

[2] *Department of Clinical and Molecular Medicine, Sant'Andrea Hospital, School of Medicine and Psychology, Sapienza University, Via di Grottarossa 1035/1039, 00189 Rome, Italy*

[3] *Department of Laboratory Medicine, Clinical Biochemistry Laboratory, "City of Health and Science" University Hospital, Corso Bramante 88, 10126 Turin, Italy*

Correspondence should be addressed to Mina Hur; dearmina@hanmail.net

Clinical laboratory tests are the scientific basis for the diagnosis and management of diseases. In addition to the traditional areas of laboratory testing, including clinical chemistry, hematology, microbiology, immunology, and transfusion medicine, genetic testing is also broadening its role in the clinical laboratory field. While many new research procedures and analytical methods are becoming available, they all should be strictly validated before being adopted in the clinical practice as routine assays. Clinical laboratories have an important role to play in this translational process from bench to bedside.

Based on the success of the inaugural issue in 2013, Biomed Research International annualized the special issue on laboratory medicine, and this special issue is the second one succeeding the first success. This issue includes a wide variety of laboratory-related topics as illustrated by four review articles and 15 research papers. A review article by J.-L. Choi et al. provides a comprehensive review on progresses in clinical application of platelet function tests. I. Mozos describes laboratory markers of ventricular arrhythmia risk in renal failure. Another review by T.-K. Er et al. deals with current approaches for predicting a lack of response to anti-EGFR therapy in *K-ras* wild-type patients. Y. Liu and G. Shi review the recent advances regarding the role of chemotactic G protein-coupled receptors in control of migration of subsets of dendritic cells.

Two interesting papers cover the basic field of laboratory medicine. The paper by H. Jin et al. was the first to compare the characteristics of erythrocytes derived from cord blood and granulocyte colony-stimulating factor-mobilized adult peripheral blood. H.-Y. Kim et al. showed that increased mitochondrial DNA copy number might be a useful biomarker associated with polycyclic aromatic hydrocarbons toxicity and hematotoxicity.

Seven papers deal with the growing area of molecular diagnostic applications. The paper by S. H. Kim et al. identifies *Candida guilliermondii* and *Candida famata* correctly by using matrix-assisted laser desorption/ionization-time of flight mass spectrometry and gene sequencing. Y. J. Hong et al. evaluated a multiplex real-time PCR and melting curve analysis for the detection of herpes simplex and varicella-zoster virus in clinical specimens. Y. Kim et al. evaluated three automated nucleic acid extraction systems for identification of respiratory viruses in clinical specimens by multiplex real-time PCR. An interesting paper by S. Kim et al. showed differences in disease risk estimations among three commercial genetic-testing services, implying that the genetic services need further evaluation and standardization. Another paper by S. Kim et al. analyzed *in vivo* expressions of the pharmacodynamic marker inosine monophosphate dehydrogenase (IMPDH) mRNA to investigate its usefulness in assessing effects of mycophenolic acid. Y. J. Hong et al. reported the significance of Lewis phenotyping in various tissues and concluded that the gastric Lewis phenotype must be used for the study on the association between the Lewis phenotype and *Helicobacter pylori*. C.-W. Park et

al. proposed that the degree of hepatitis C virus (HCV) quasispecies measured by ultradeep pyrosequencing might be useful to predict progression of hepatocellular carcinoma in the patients with chronic HCV.

Six papers come from the conventional areas of hematology and chemistry. L. A. S. Nunes et al. established reference intervals for the hemogram and iron status biomarkers in a physically active male population. T.-D. Jeong et al. investigated the association between the reduction in the estimated glomerular filtration rate and the prevalence of monoclonal gammopathy of undetermined significance in healthy Korean males. Another paper by T.-D. Jeong et al. indicated that total cholesterol concentration is correlated with the levels of bone turnover markers, suggesting that it might predict osteoporosis in premenopausal women. T. Ruskovska et al. emphasized that the variability of results of total (anti)oxidants which are obtained using different assays should be taken into account when interpreting data from clinical studies of oxidative stress, especially in complex pathologies such as chronic hemodialysis. E. Gruszewska et al. concluded that the changes in concentrations of total sialic acid and free sialic acid during the same liver diseases indicate significant disturbances in sialylation of serum glycoproteins. Lastly, B. De Berardinis et al., on behalf of GREAT international, reported the usefulness of combining Galectin-3 and bioimpedance vector analysis in predicting short and long term events in patients admitted for acute heart failure.

Given that laboratory medicine plays a vital role in translating research findings into clinical practice, we hope that this special issue would broaden the readership of Biomed Research International and contribute to the scientific development in this field.

Mina Hur
Patrizia Cardelli
Giulio Mengozzi

Research Article

Profiling of Biomarkers for the Exposure of Polycyclic Aromatic Hydrocarbons: Lamin-A/C Isoform 3, Poly[ADP-ribose] Polymerase 1, and Mitochondria Copy Number Are Identified as Universal Biomarkers

Hwan-Young Kim,[1,2] Hye-Ran Kim,[2,3] Min-Gu Kang,[1] Nguyen Thi Dai Trang,[2] Hee-Jo Baek,[4] Jae-Dong Moon,[4] Jong-Hee Shin,[1] Soon-Pal Suh,[1] Dong-Wook Ryang,[1] Hoon Kook,[4] and Myung-Geun Shin[1,2,4]

[1] *Department of Laboratory Medicine, Chonnam National University Medical School and Chonnam National University Hwasun Hospital, 160 Ilsimri, Hwasun-eup, Hwasun-gun, Jeollanam-do 519-809, Republic of Korea*
[2] *Brain Korea 21 Plus Project, Chonnam National University Medical School, Gwangju, Republic of Korea*
[3] *Laboratory of Metabolism, National Cancer Institute, National Institutes of Health, Bethesda, MD, USA*
[4] *Environment Health Center for Childhood Leukemia and Cancer, Chonnam National University Hwasun Hospital, Hwasun, Republic of Korea*

Correspondence should be addressed to Myung-Geun Shin; mgshin@chonnam.ac.kr

This study investigated the profiling of polycyclic aromatic hydrocarbon- (PAH-) induced genotoxicity in cell lines and zebrafish. Each type of cells displayed different proportionality of apoptosis. Mitochondrial DNA (mtDNA) copy number was dramatically elevated after 5-day treatment of fluoranthene and pyrene. The notable deregulated proteins for PAHs exposure were displayed as follows: lamin-A/C isoform 3 and annexin A1 for benzopyrene; lamin-A/C isoform 3 and DNA topoisomerase 2-alpha for pentacene; poly[ADP-ribose] polymerase 1 (PARP-1) for fluoranthene; and talin-1 and DNA topoisomerase 2-alpha for pyrene. Among them, lamin-A/C isoform 3 and PARP-1 were further confirmed using mRNA and protein expression study. Obvious morphological abnormalities including curved backbone and cardiomegaly in zebrafish were observed in the 54 hpf with more than 400 nM of benzopyrene. In conclusion, the change of mitochondrial genome (increased mtDNA copy number) was closely associated with PAH exposure in cell lines and mesenchymal stem cells. Lamin-A/C isoform 3, talin-1, and annexin A1 were identified as universal biomarkers for PAHs exposure. Zebrafish, specifically at embryo stage, showed suitable *in vivo* model for monitoring PAHs exposure to hematopoietic tissue and other organs.

1. Introduction

Polycyclic aromatic hydrocarbons (PAHs) are ubiquitous environmental toxicants found in air, water, plants, and soils which are present as volatile, semivolatile, and particulate pollutants [1]. PAHs have been of increasing concern in the human health field due to their wide-spread dispersion in the environment and the adverse health effects associated with PAHs exposure such as carcinogenesis and endocrine disruption. Although the adverse effects of individual PAHs are not exactly alike, the United States Environmental Protection Agency (EPA) has designated 32 PAHs compounds as priority pollutants (http://www.epa.gov/). The toxicity of PAHs is structure dependent. Benzopyrene (BaP) among 32 PAH compounds is notable for being the first chemical carcinogen to be discovered [2, 3].

The most commonly used biomarkers of PAHs exposure are metabolites of PAHs, particularly 1-hydroxypyrene (1-OHP), and PAH-DNA or protein adducts [3]. 1-OHP is the principal product of pyrene metabolism, representing 90% of its metabolites [4]. Following inhalation, the half-life of 1-OHP is on average about 18–20 hours [5–7]. Pyrene is the only known precursor of 1-OHP [8]; it forms a consistent proportion of higher molecular weight PAHs in the environment [9]. Main analytical methods employed to measure 1-OHP are high performance liquid chromatography (LC) combined with fluorescence detection and gas chromatography with mass spectrometry [10, 11].

Biomarkers to assess exposure to PAHs at high levels are well studied, but more work is needed to validate these biomarkers when exposure occurs at low, environmental levels. Most reported biomarkers for PAHs exposure were mainly targeted against nuclear genome and proteome as well as metabolites in either serum or urine. Moreover, biomarkers as mentioned in several studies [3] did not reflect PAHs exposure sensitively in genomic and proteomic level.

Enormous strides have recently been made in our understanding of the biology and pathobiology of mitochondria. Many diseases have been identified as caused by mitochondrial dysfunction, and many pharmaceuticals have been identified as previously unrecognized mitochondrial toxicants. A much smaller but growing reports indicate that mitochondria are also targeted by environmental pollutants [12]. Past evidence had indicated that the mtDNA repair capacity is limited and that the proximity of mtDNA to sites of reactive oxygen species generation suggested that mtDNA may be more susceptible to mutation than nuclear DNA. Our laboratory has recently reported that hnRNP protein and the change of mitochondrial genome are recognized as novel and useful markers for benzene exposure [13]. Moreover, there is currently a paucity of data on the direct effects of PAHs in primary hematopoietic cells and various cell lines.

In zebrafish, hundreds of genes involved in the formation of virtually every organ system have been identified by large-scale mutagenesis screening [14]. Consequently, the phenotypes resulting from loss of gene function through mutation can be compared to malformations resulting from embryonic exposure to contaminants. This "chemical genetic" approach has been used recently to identify specific mechanisms of developmental toxicity [15, 16].

Therefore, this study investigated to identify new biomarkers and pathobiological role for PAHs exposure, especially BaP using targeted mitochondrial genomic and proteomic approach in cell line, peripheral blood/mesenchymal stem cell, and *in vivo* zebrafish model.

2. Materials and Methods

2.1. Reagents and Cell Lines. Cell lines (K562, THP-1, MOLT-4, and HL-60 cells) were obtained from the American Type Culture Collection, which were cultured in RPMI 1640 medium (Gibco Laboratories, Grand Island, NY, USA) supplemented with 10% fetal bovine serum (Gibco) (see Supplementary Table 1 in Supplementary Material available online at http://dx.doi.org/ 10.1155/2014/605135).

Previous published protocol was used for the isolation and characterization of bone marrow-derived mesenchymal stem cells (h-TERT) [17]. For *in vitro* cell line study, cells were cultured and maintained in RPMI media containing 10% fetal bovine serum and four types of PAHs such as BaP, pentacene, fluoranthene, and pyrene were added in the cell culture media with 100 μM concentration.

2.2. Chemicals. BaP (purity > 99%), fluoranthene (99%), pentacene (>99%), and pyrene (>99%) were purchased from Sigma (Sigma-Aldrich, St. Louis, MO, USA). Stock PAHs solutions were made in dimethyl sulfoxide (DMSO) (Sigma-Aldrich) at concentration of 100 μM.

2.3. Cytotoxicity Assay. Cytotoxicity assays were carried out using the Enhanced Cell Viability Assay Kit (EZ-CyTox, Daeil Lab Service Co., Seoul, Korea) protocol. The absorbance (A450) of each well was measured using a VERSA Max microplate reader (Molecular Devices, Sunnyvale, CA, USA).

2.4. Determination of mtDNA Copy Number. mtDNA copy number was determined according to our published protocol [13]. For *in vitro* model study, the purified PCR product of *cytochrome b (Cytb)* gene was inserted into pGEM-T easy vector and E. coli JM 109 cells (Promega, Madison, WI, USA) were transformed in order to obtain recombinant plasmids. The mtDNA copy number was calculated using the following formula: $[X \, \mu g/\mu L \text{ plasmid DNA}/4419 \text{ (plasmid length)} \times 660] \times 6.022 \times 10^{23} = Y$ molecules/μL, where X represents the concentration of plasmid DNA and Y represents copy number. For *in vivo* model study, a mixture of 25 μL containing 12.5 μL 2x QuantiTect SYBR green PCR master mix (Qiagen, Valencia, CA, USA), 400 μM *Cytb* primers forward (5$'$-TTCTGAGGGGCCACAGTAAT-3$'$) and reverse (5$'$-GGGGTTATTTGATCCGGTTT-3$'$), and 50 ng of total DNA were used for the PCR with the CFX96 real-time system (Bio-Rad, Hercules, CA, USA). For PCR, 95°C for 15 minutes was followed by 35 cycles of 20 seconds at 94°C, 30 seconds at 52°C, 30 seconds at 72°C, and a melting reaction with a decrease of 1°C per cycle between 72°C and 92°C.

2.5. Direct Sequencing of mtDNA Control Region. This study used a published protocol to amplify and sequence the mtDNA *control region* gene and minisatellites (303 poly C, 16189 poly C and 514 (CA) repeat) [13]. The mtDNA sequences obtained were analyzed using the Revised Cambridge Reference Sequence (http://www.mitomap.org/), Blast2 program (http://www.ncbi.nlm.nih.gov/blast/bl2seq/wblast2.cgi), and the MitoAnalyzer (http://www.cstl.nist.gov/biotech/strbase/mitoanalyzer.html) to identify mtDNA aberrations.

2.6. Proteomic Assay of Mitochondria-Rich Cellular Fraction

2.6.1. One-Dimensional SDS-Polyacrylamide Gel Electrophoresis. Briefly, an equal amount of proteins (30 μg) was then separated on NuPAGE 4–12% Bis-Tris Gel (Invitrogen; Carlsbad CA, USA). After separation, the gel was stained with GelCode Blue Stain Reagent (Thermo scientific) and the blue-stained

gel lanes were removed by manual cutting. Each blue-stained gel lane was separately cut into 5 slices. Each of these gel slices was then further cut into sizes of ~1 mm^3 and transferred to a clean 1.5 mL tube.

2.6.2. Enzymatic In-Gel Digestion. The separated proteins were excised from the gel and the gel pieces containing protein were destained with 50% acetonitrile (ACN) containing 50 mM NH$_4$HCO$_3$ and the gel pieces were vortexed until Coomassie Brilliant Blue was completely removed. These gel pieces were then dehydrated in 100% ACN and vacuum-dried for 20 min with SpeedVac. For the digestion, gel pieces were reduced using 10 mM dithiothreitol in 50 mM NH$_4$HCO$_3$ for 45 min at 56°C, followed by alkylation of cysteines with 55 mM iodoacetamide in 50 mM NH$_4$HCO$_3$ for 30 min in the dark. Finally, each of gel pieces was treated with 12.5 ng/μL sequencing grade modified trypsin (Promega) in 50 mM NH$_4$HCO$_3$ buffer (pH 7.8) at 37°C overnight. Following digestion, tryptic peptides were extracted with 5% formic acid in 50% ACN solution at room temperature for 20 min. The supernatants were collected and dried with SpeedVac. Resuspended samples in 0.1% formic acid were purified and concentrated using C18 ZipTips (Millipore, Billerica, MA, USA) before mass spectrometry (MS) analysis.

2.6.3. Nano-LC-Electrospray Ionization-MS/MS Analysis. The tryptic peptides were loaded onto a fused silica microcapillary column (12 cm × 75 μm) packed with C18 reversed phase resin (5 μm, 200 Å). LC separation was conducted under a linear gradient as follows: a 3–40% solvent B (ACN containing 0.1% formic acid) gradient (solvent A; DW containing 0.1% formic acid), with a flow rate of 250 nL/min, for 60 minutes. The column was directly connected to linear trap quadropole linear ion-trap mass spectrometer (Finnigan, San Jose, CA, USA) equipped with a nanoelectrospray ion source. The electrospray voltage was set at 1.95 kV, and the threshold for switching from MS to MS/MS was 500. The normalized collision energy for MS/MS was 35% of main radio frequency amplitude and the duration of activation was 30 ms. All spectra were acquired in data-dependent scan mode. Each full MS scan was followed by five MS/MS scans corresponding to the range from the most intense to the fifth intense peaks of full MS scan. Repeat count of peak for dynamic exclusion was 1, and its repeat duration was 30 seconds. The dynamic exclusion duration was set for 180 seconds and the width of exclusion mass was ±1.5 Da.

2.6.4. Database Searching and Validation. The acquired LC-electrospray ionization-MS/MS fragment spectra were searched in the BioWorksBrowser (version Rev. 3.3.1 SP1, Thermo Fisher Scientific Inc.) with the SEQUEST search engines against National Center for Biotechnology Information (http://www.ncbi.nlm.nih.gov/) nonredundant human database.

2.7. Quantitative mRNA Expression Study. Total RNA was extracted using the QIAamp RNA Blood Mini kit (Qiagen). Reverse transcription produced cDNAs using Superscript III

(Applied Biosystems). The expression of poly[ADP-ribose] polymerase 1 (PARP-1) and lamin A/C (LMNA) mRNA was quantified using QuantiTect SYBR green PCR master mix (Qiagen), PARP-1 forward: 5′-GAGGAAGTAAAGGAA-GCCAA-3′, PARP-1 reverse: 5′-CACAACTTCAACAGG-CTCT-3′, LMNA forward: 5′-AAGCTTCGAGACCTG-GAG-3′, LMNA reverse: 5′-TCCAAGAGCTTGCGGTA-3′, and β-actin mRNA as a normalization control. The ΔΔCt method was used to calculate relative changes in gene expression determined by real-time quantitative PCR using CFX96 (Bio-Rad). Normalization was achieved using Ct values of PARP-1 and LMNA mRNA from PAHs-treated cells and β-actin mRNA. The ΔCt$_{\text{calibrator}}$ value (mean PARP-1 and LMNA—mean β actin) was obtained from the mean Ct value of PARP-1 and LMNA mRNA and β-actin mRNA from the control cells ($n = 10$). The ΔΔCt value was calculated as ΔCt minus ΔCt$_{\text{calibrator}}$. The final relative quantification of PARP-1 and LMNA mRNA was expressed as ΔΔCt.

2.8. Western Blot. Extracted protein samples (20 μg per well) were separated on a 12% SDS-Bis-Tris polyacrylamide gel. After transfer, the nitrocellulose membrane was incubated over night with 10 mL of primary antibodies against PARP-1, LMNA (Santa Cruz Biotechnology, Delaware Avenue, CA, USA), and β-actin (Santa Cruz Biotechnology) at 4°C. The membrane was then incubated with the appropriate goat anti-mouse IgG antibody (1 : 1000) (Jackson ImmunoResearch Laboratories, West Grove, PA, USA) to detect biotinylated protein markers in 10 mL of blocking buffer with gentle agitation for 1 hour at room temperature. The proteins were visualized using a chemiluminescence detection system (Amersham ECL system, London, UK).

2.9. In Vivo Study. For *in vivo* model study, zebrafish embryos 30 h after fertilization (hpf) were exposed to BaP at concentrations of 200, 400, 600, 800, and 1000 nM. Seventy embryos were cultured in 40 mL of BaP solution in each petri dish, and there were three replicates for each of the five treatments. Embryos were collected at 54 hpf, 78 hpf, and 102 hpf. Embryos were maintained under the same temperature and pH conditions for the duration of experiments.

3. Results

3.1. The Change of Cell Morphology. PAH-untreated h-TERT cells showed compact cellularity with spindle shape. Cells were tightly attached to each other and to the substrate. Generally, direct exposure of PAHs such as BaP, pentacene, fluoranthene, and pyrene depressed the proliferative capacity of h-TERT cells and the cell morphology was altered in each PAH-exposure group. Cells became detached from the subsurface, and cell-to-cell attachments were lost (Figure 1).

3.2. The Change of Total Cell Counts. Depending on the type of PAHs, each cell count showed different aspects. The total number of cells in the THP-1 and Molt-4 cell lines decreased 11 days after PAHs exposure. The change in the total number of cells in the THP-1 and Molt-4 cell lines decreased in
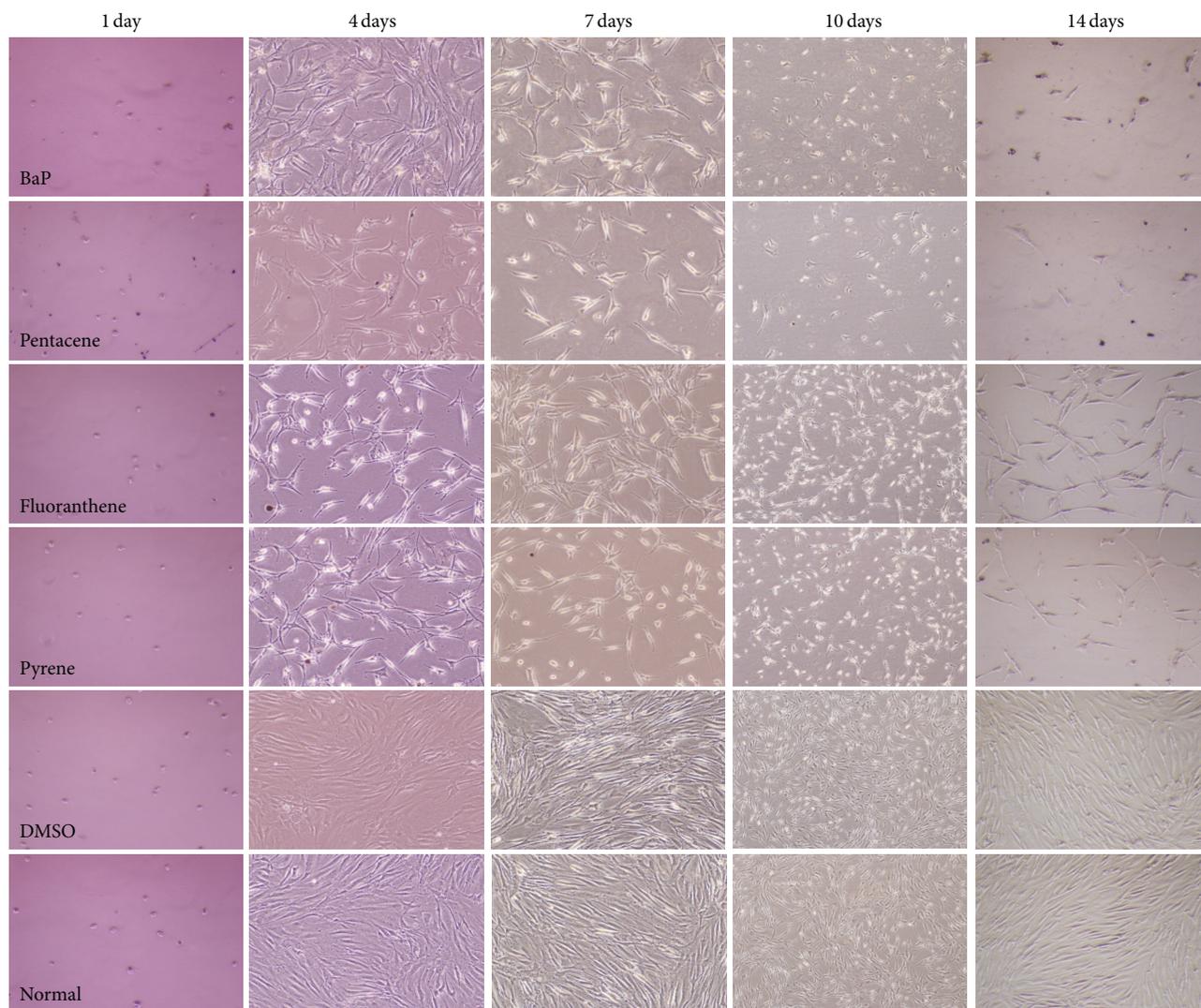
FIGURE 1: Morphological change of human mesenchymal stem (h-TERT) cells after PAHs exposure. PAH-untreated cells (DMSO and normal) showed compact cellularity with spindle shape. h-TERT cells were tightly attached to each other and to the substrate. Generally, direct exposure of PAHs depressed the proliferative capacity of h-TERT cells with a thread-like or round shape and loose cell-to-cell attachment. Each PAHs compound showed different cytotoxic effect. DMSO and normal indicated only DMSO-treatment and culture solution itself (no treatment of PAHs and DMSO), respectively.

a time-dependent manner. In comparison to control group, fluoranthene displayed profound significant reduction in cell count (Figures 2(a) and 2(b)). The change in the total cell count for the THP-1 and Molt-4 cell lines had a similar pattern after PAHs exposure. Cytotoxicity study carried out the experiment with $100 \, \mu$M of PAHs after selecting the minimum concentration that is poisonous to cells.

3.3. *Viability and Apoptosis.* Viability significantly decreased after two days of exposure to fluoranthene. On the third day of PAHs exposure, viability reduced remarkably in all the cells (Figures 2(c) and 2(d)). Each type of cell lines displayed different proportionality of apoptosis. Several hundreds of PAHs exposure biomarkers were identified in comparison to control group (Supplemental Figure 1).

3.4. *Increased mtDNA Copy Number.* Mitochondrial contents were increased with different pattern: mtDNA copy number was dramatically elevated after 5-day treatment of fluoranthene and pyrene in both cell line and *in vivo* zebrafish model. mtDNA copy numbers were generally increased after PAHs exposure in a dose and time-dependent manner in the cell lines. These findings suggested that loss of compensatory ability in response to high levels of oxidative stress was induced by high concentrations of PAHs (Figure 3).

3.5. *Sequence Alteration of mtDNA Control Region.* Changes of the mtDNA sequence were comprehensively studied by direct sequencing of the mtDNA control region and gene scanning for the determination of mtDNA length and
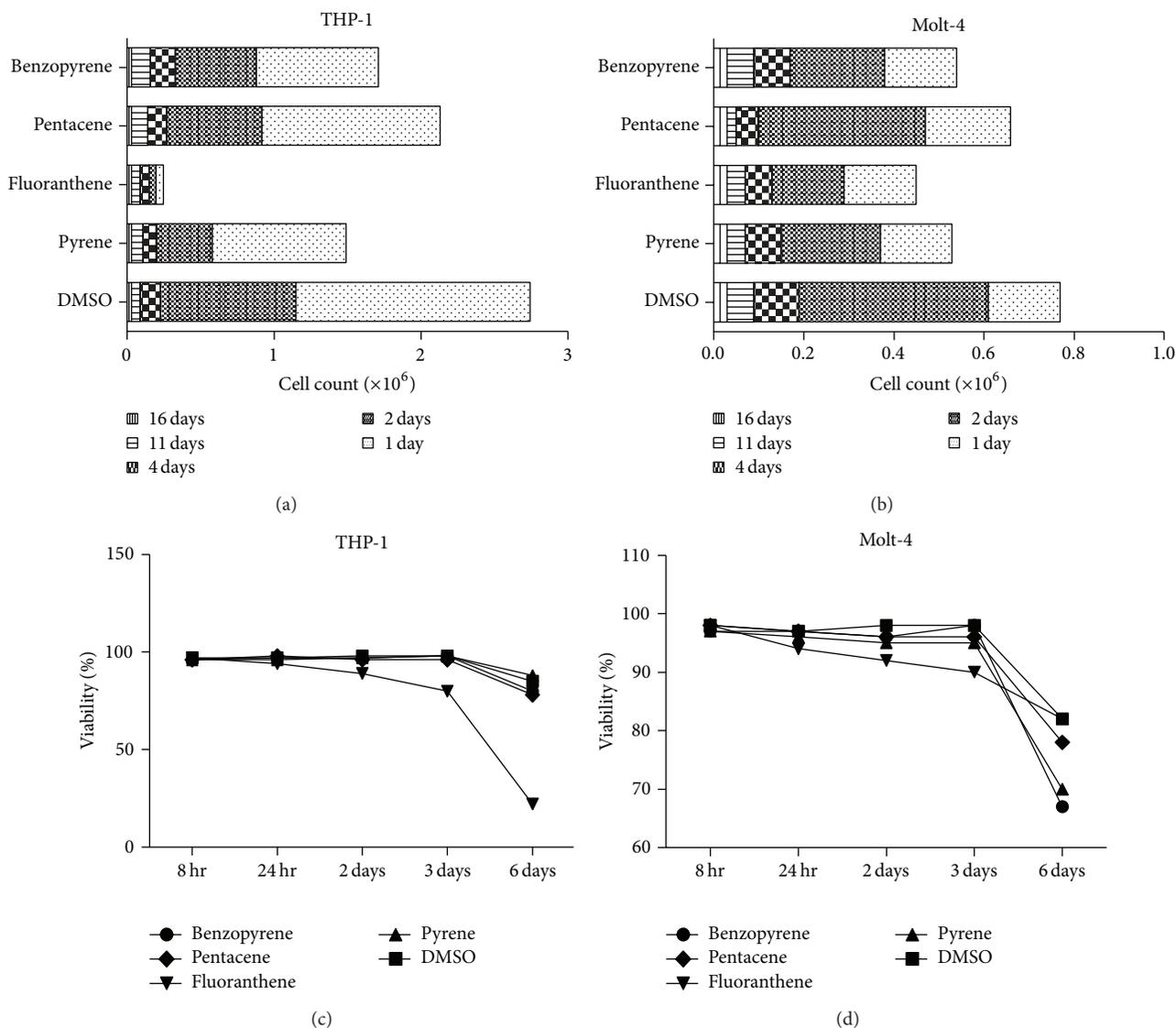
Figure 2: The change of cell count and viability after PAHs exposure in THP-1 and Molt-4 cell line. Depending on the type of PAHs, each cell count showed different aspects. In comparison to DMSO treated (0.1%) group, fluoranthene displayed profound significant reduction in cell count, especially in THP-1 and Molt-4 cell line ((a) and (b)). Viability was significantly decreased after fluoranthene exposure for two days. On the third day of PAHs exposure, viability was reduced remarkably in both cell lines ((c) and (d)).

heteroplasmic mutations. No alteration of mtDNA sequences was observed after direct exposure of PAHs during 7 days (Supplemental Figure 2). No alteration of mtDNA minisatellites such as 1618 poly C, 303 poly C and 514 (CA) repeat was found after PAHs exposure.

3.6. Mitochondrial Protein Markers. Several hundreds of cellular proteins in mitochondrial-rich cytoplasmic fraction were profoundly deregulated in comparison to control group (Figure 4). The notable deregulated proteins for PAHs exposure were displayed as follows: LMNA and annexin A1 for BaP; LMNA and DNA topoisomerase 2-alpha for pentacene; PARP-1 for fluoranthene; and talin-1 and DNA topoisomerase 2-alpha for pyrene (Tables 1 and 2).

3.7. Confirmation of Mitochondrial Protein Markers

3.7.1. Increased mRNA Expression of PARP-1 and LMNA Gene. mRNA expression of PARP-1 and LMNA gene was generally increased in THP-1 and h-TERT cell lines after exposure of PAHs with different pattern. This finding was confirmed using embryogenesis in zebrafish model (Figure 5).

3.7.2. Increased Protein Expression of PARP-1 and LMNA Gene. The expression of PARP-1 protein was increased after exposure of BaP, pentacene, and fluoranthene. The LMNA proteins were increased after exposure of BaP (Figure 6).

3.8. Morphological Abnormalities of Zebrafish. At 54 hpf, embryos treated with 400 nM BaP exhibited mild pericardial
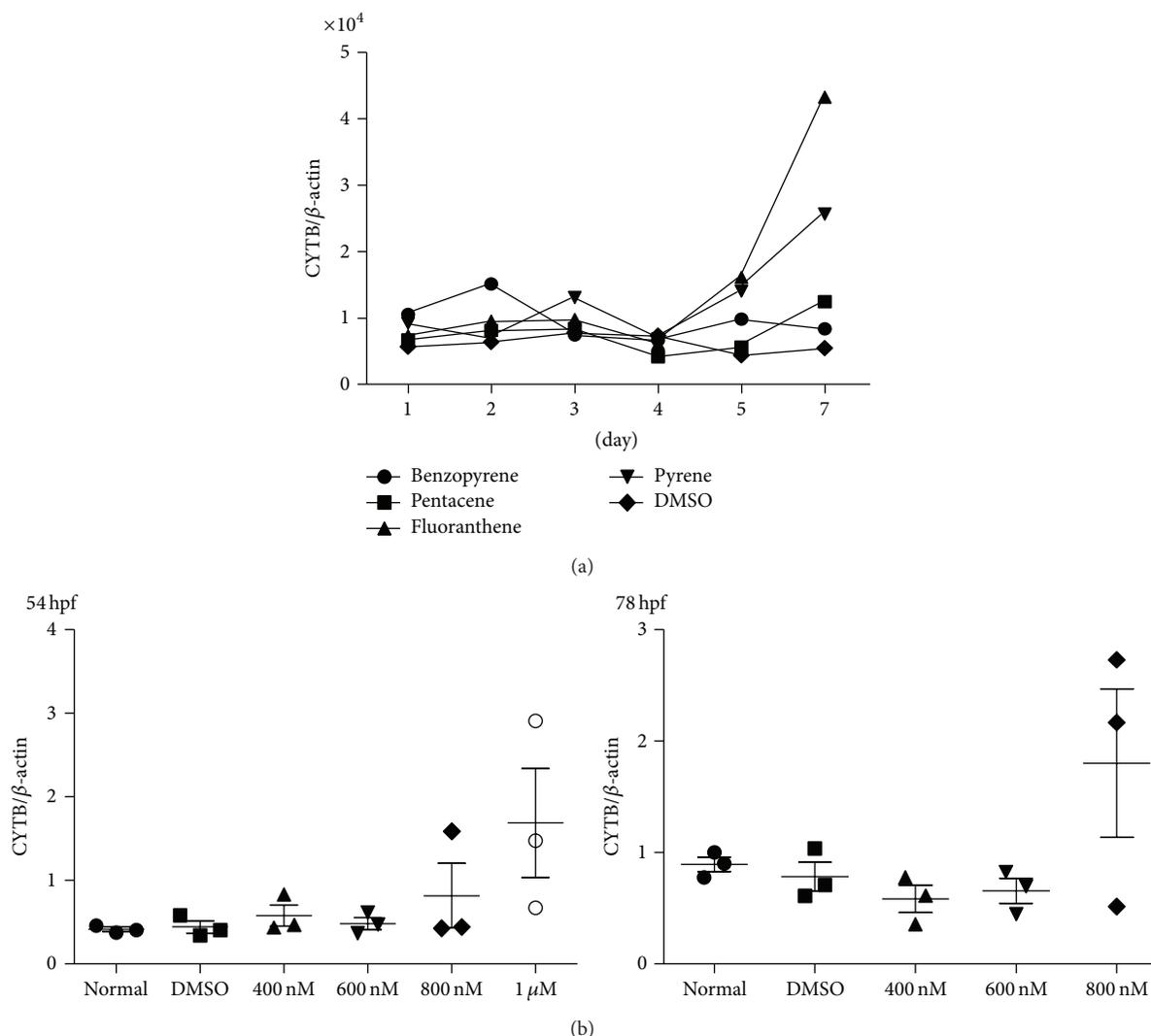
FIGURE 3: The change of mtDNA copy number after PAHs exposure. mtDNA copy number was increased after exposure of PAHs with different pattern in THP-1 cell line (a) and *in vivo* zebrafish model (b). mtDNA copy number was dramatically elevated after 5-day treatment of fluoranthene and pyrene in both THP-1 cell line and *in vivo* zebrafish model. hpf, hours per fertilization in zebrafish; normal, no treatment group; and DMSO, only DMSO (0.1%) treated group.

edema and showed dorsal curvature of the body axis (Figure 7). Dorsal curvature was more severe by higher concentration of BaP as edema accumulated. Notably, eye and jaw growths were similarly reduced by BaP treatment.

4. Discussion

PAHs are known genotoxic agents and induce DNA damaging effects, such as DNA adducts, DNA strand breaks, chromosomal aberrations, sister chromatid exchanges, and micronucleus formation [18]. The main sources of human exposure to PAHs are occupation, passive and active smoking, and food, water, and air pollution [19]. The total intake of carcinogenic PAHs in the general population has been estimated to be $3 \mu g/day$ [20]. Levels of occupational exposure of BaP, which is one of the main PAHs compounds, vary

widely in different industrial activities and job titles, ranging from 0.1 to $48\,000 \, ng/m^3$ [21–23]. In smokers, BaP levels range from 0.5 to 7.8 $\mu g/100$ cigarettes when exposure is from mainstream smoke and from 2.5 to 19.9 $\mu g/100$ cigarettes when it comes from side-stream smoke. Levels from passive smoking are lower, ranging from 0.0028 to 0.76 $\mu g/m^3$ of BaP [24]. Besides occupational exposure, dietary intake seems to be the most important source of PAHs in nonsmokers [24, 25]. There is a high variation in atmospheric PAHs levels across geographical areas with BaP concentrations ranging from 0.01 to $100 \, ng/m^3$ BaP [26]. Airborne PAHs are usually analyzed by gas chromatography/mass spectrometry [27, 28] or high performance LC [29–31], mostly from particles collected in a filter after extraction with organic solvents.

In order to exert its deleterious effects, BaP must be bioactivated. The formation of BaP *o*-quinones has been

(a)

(b)
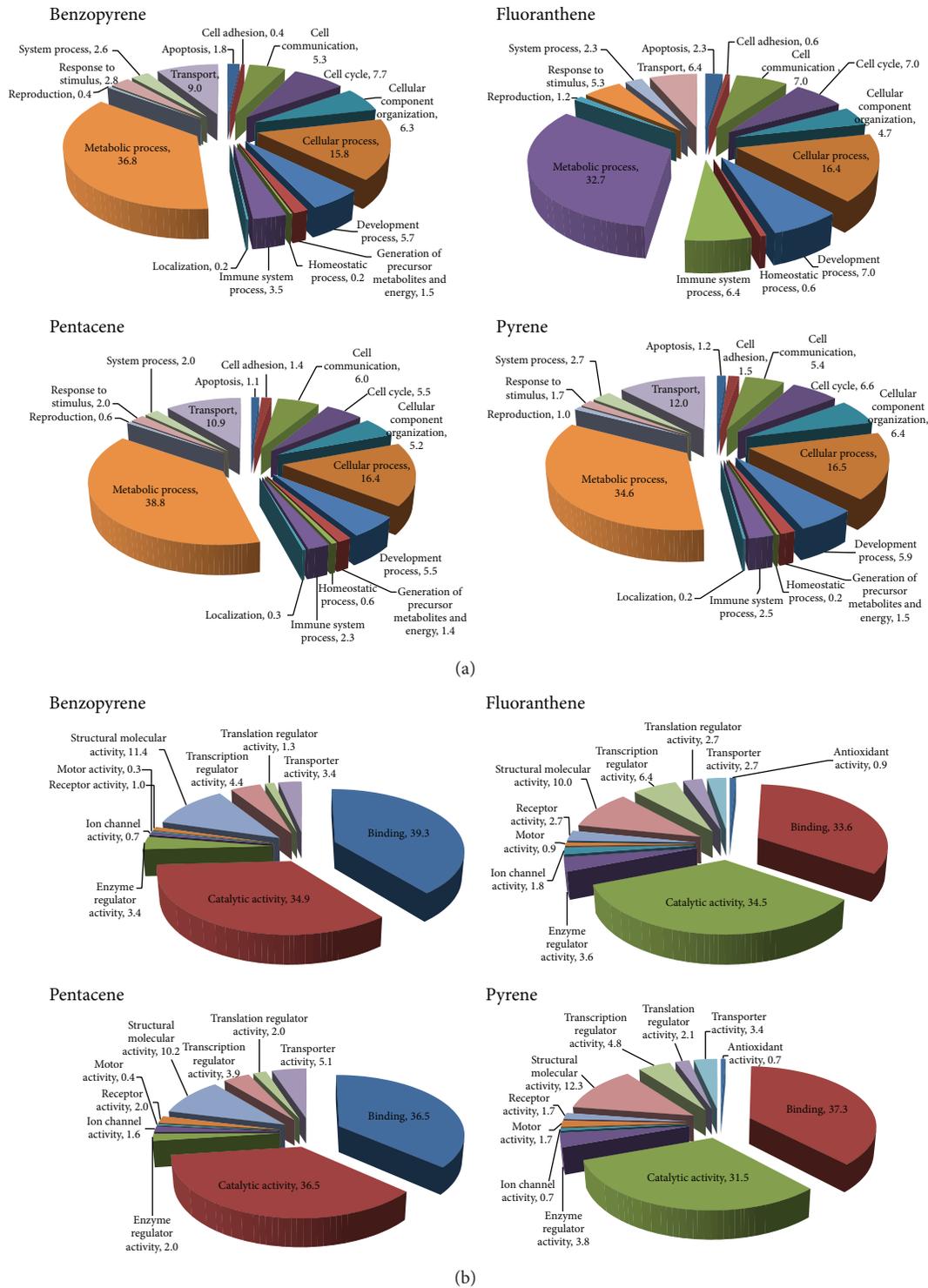
Figure 4: Functional grouping of potential candidate biomarkers for PAHs exposure. Identified potential biomarkers were categorized as their biological process (a) and molecular functions (b). These candidate biomarkers for PAHs exposure were isolated using proteomic analysis of mitochondria-rich cellular fraction in THP-1 cell line.

described as one of the BaP activation pathways. Cytochrome P4501A (CYP1A) is able to produce BaP-7, 8 diol that is further oxidized to BaP-7, 8-dione by AKR1A1 [32]. BaP binds to and activates the aryl hydrocarbon receptor (AhR), being

metabolized by the cytochrome P4501A, the microsomal epoxide hydrolase, and the glutathione-S-transferase α [33]. AhR is a ligand-activated transcription factor involved in the regulation of biological responses to planar aromatic

TABLE 1: Summary list of identified potential biomarkers for PAHs exposure.

PAHs	Protein	Fold change
Benzopyrene	Vimentin	19.39
	Annexin A1	13.38
	Lamin-A/C	10.04
	NADPH: adrenodoxin oxidoreductase, mitochondrial isoform 2 precursor	5.3
	Squalene synthase	5.3
	Heterogeneous nuclear ribonucleoproteins A2/B1 isoform B1	4.82
	T-complex protein 1 subunit theta	4.35
	Talin-1	4.35
Pentacene	Lamin-A/C	6.9
	DNA topoisomerase 2-alpha	6.38
	Annexin A1	6.38
	Poly[ADP-ribose] polymerase 1	5.85
	Squalene synthase	5.33
	Talin-1	5.33
	PREDICTED: u5 small nuclear ribonucleoprotein 200 kDa helicase-like, partial	4.81
Fluoranthene	Poly[ADP-ribose] polymerase 1	6.21
	Elongation factor 1-gamma	5.21
	Heat shock 70 kDa protein 1A/1B	5.21
	Heterogeneous nuclear ribonucleoproteins A2/B1 isoform B1	5.21
	Probable ATP-dependent RNA helicase DDX5	5.21
	T-complex protein 1 subunit theta	5.21
Pyrene	Talin-1	16.82
	DNA topoisomerase 2-alpha	8.17
	Filamin-C isoform b	7.16
	E3 SUMO-protein ligase RanBP2	5.65
	CAD protein	5.14
	Poly[ADP-ribose] polymerase 1	5.14

TABLE 2: Results of PARP-1 and LMNA protein by repeat proteomic analysis.

Protein	Fold change	
	First result	Second result
PARP-1 (accession no: 156523968)		
DMSO versus BaP	3.41	3.58
DMSO versus pentacene	5.85	4.31
DMSO versus fluoranthene	6.21	5.34
DMSO versus pyrene	5.14	3.41
LMNA (accession no: 27436948)		
DMSO versus BaP	10.04	4.16
DMSO versus pentacene	No change	0.97
DMSO versus fluoranthene	4.50	3.00
DMSO versus pyrene	4.14	1.80

DMSO, only DMSO-treatment as control; PARP-1, poly[ADP-ribose] polymerase 1; LMNA, lamin A/C; BaP, benzopyrene.

hydrocarbons. AhR ligands have been generally classified into two categories, synthetic or naturally occurring. The first ligands to be discovered were synthetic and members of halogenated aromatic hydrocarbons. Naturally occurring compounds that have been identified as ligands of AhR include derivatives of tryptophan [34, 35]. The major contributors to air PAHs in the urban and suburban atmosphere are mobile sources from diesel and gasoline engines. Emissions from these sources contain mainly benzo(g,h,i)perylene, pyrene, fluoranthene, and phenanthrene [36], so that measuring only BaP as an index substance may result in exposure underestimation [3].

In this study, a broad molecular investigation of the mitochondrial genome and proteome after PAHs exposure showed an increased mtDNA copy number, PARP-1, and LMNA protein, which could be used as biomarkers for exposure of PAHs in cell lines. PAHs directly might cause an increase in the generation of intracellular ROS, subsequently resulting in a change of the mtDNA content, and proteome. The oxidative stress induced by PAHs can lead to an increase
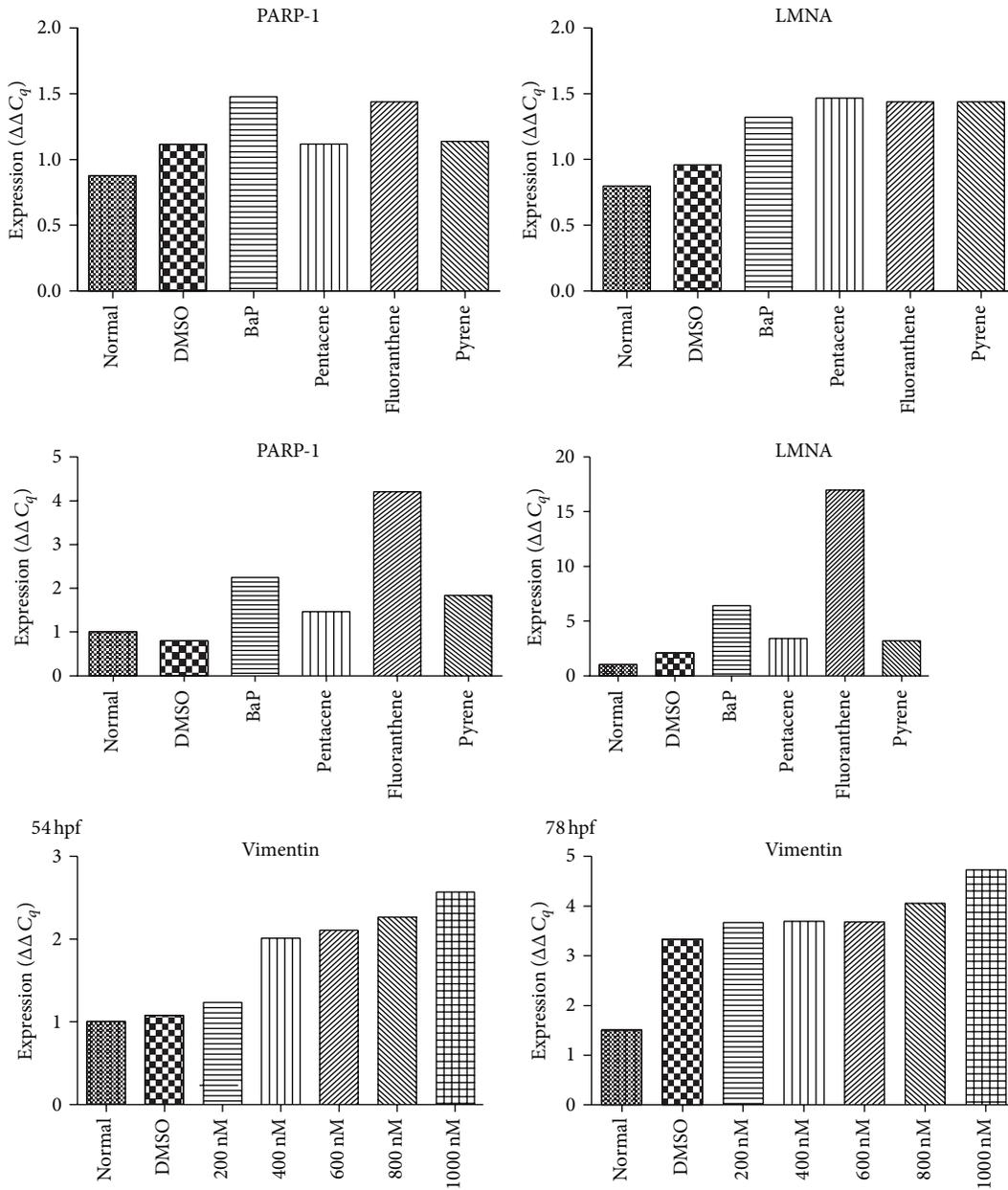
FIGURE 5: mRNA expression study of candidate biomarker genes. mRNA expression of PARP-1 and LMNA gene was generally increased in THP-1 and h-TERT cell lines after exposure of PAHs with different pattern. Normal, no treatment group; DMSO, only DMSO (0.1%) treated group.

in mitochondrial mass and mitochondrial membrane potential. The mitochondrial genome is highly susceptible to DNA damage caused by ROS and mutagens and has higher rates of mutation than does the nuclear genome. In addition, DNA damage persists longer in the mitochondrial genome. The absence of histones that provide packaging and protection of nuclear DNA and the error-prone replication and repair of mitochondrial genes all contribute to the vulnerable nature of mitochondrial DNA [37]. Therefore, the present study targeted the mitochondrial genome and proteome to identify biomarkers associated with PAH exposure. The results of the present study showed that, after PAHs exposure, mtDNA

copy number was increased. The increase of mtDNA copy number was thought to compensate for declining respiratory function during the oxidative stress after PAH exposure.

Mitochondria-rich cellular proteome was then studied to determine whether biomarkers associated with exposure of PAHs could be identified. The result showed that PARP-1 and LMNA protein might be a novel universal biomarker associated with exposure of PAHs. PARP is a monomeric protease widely present in the nuclei of most eukaryotic cells that is associated with the occurrence and development of a variety of diseases. PARP-1, the best characterized member of the PARP family, which currently comprises 18 members, is
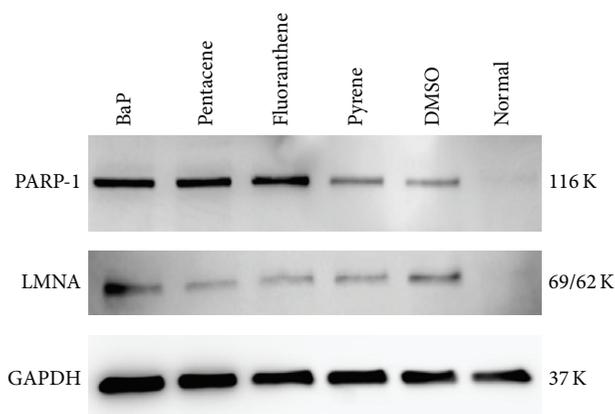
FIGURE 6: Confirmation of PARP-1 and LMNA biomarkers using Western blot. The expression of PARP-1 was remarkably increased after exposure of BaP, pentacene, and fluoranthene (100 μM concentration). LMNA protein was highly expressed after BaP exposure. Normal, no treatment group; DMSO, only DMSO (0.1%) treated group; K, kilodalton.
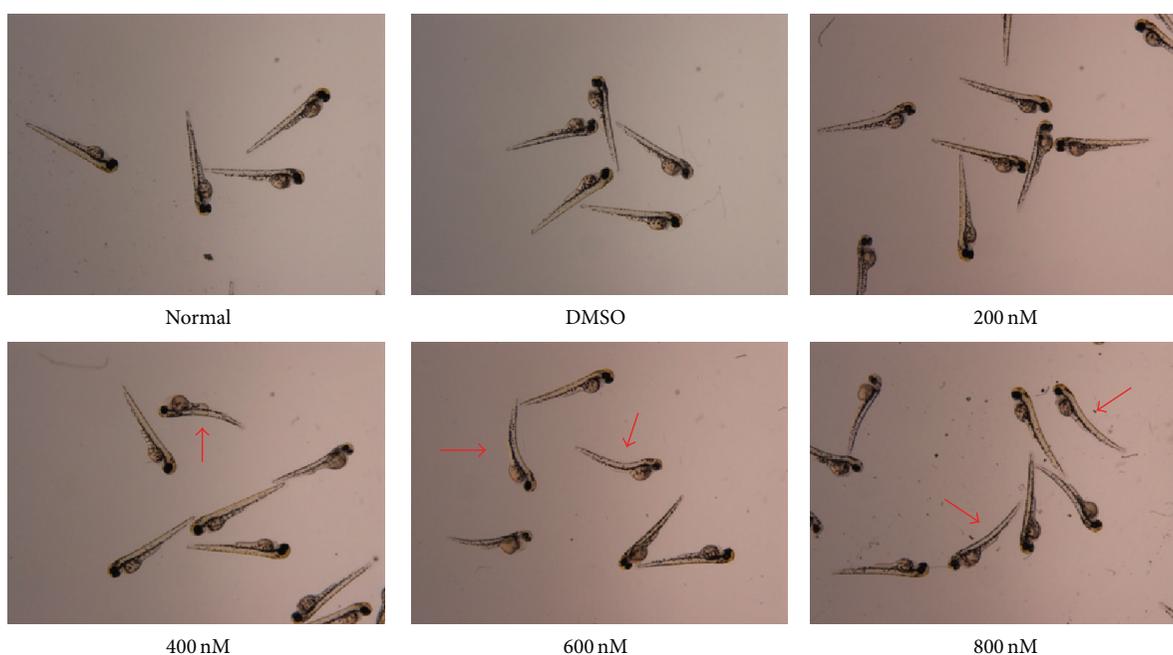
FIGURE 7: Morphological abnormalities in the general shape of zebrafish after BaP exposure. Obvious morphological abnormalities including curved backbone (arrow) were developed after exposure of more than 400 nM concentration of BaP during the embryogenesis (54 hours per fertilization).

an abundant nuclear enzyme implicated in cellular responses to DNA injury provoked by genotoxic stress. PARP is involved in DNA repair and transcriptional regulation and is now recognized as a key regulator of cell survival and cell death as well as a master component of a number of transcription factors involved in tumor development and inflammation. PARP becomes activated in response to oxidative DNA damage and depletes cellular energy pools, thus leading to cellular dysfunction in various tissues. The activation of PARP may also induce various cell death processes and promotes an inflammatory response associated with multiple organ failure [38]. It is known to activate nuclear factor-κB (NF-κB) through a variety of pathways,

which can lead to increased expression of NF-κB-dependent genes such as oncogenes, cell adhesion molecules, matrix metalloproteinases, and growth factors [39]. Inhibition of PARP activity is protective in a wide range of inflammatory and ischemia-reperfusion-associated diseases, including cardiovascular diseases, diabetes, rheumatoid arthritis, endotoxic shock, and stroke [38]. LMNA, nuclear intermediate filament proteins, is a basic component of the nuclear lamina. Mutations in LMNA are associated with a broad range of laminopathies, congenital diseases affecting tissue regeneration, and homeostasis. This study showed global profiling of toxic changes of PAHs in cell lines, h-TERT, and zebrafish model. The change of mitochondrial genome (increased

mtDNA copy number and mass) was closely associated with PAHs exposure in hematopoietic and mesenchymal stem cells. Among cellular proteins, LMNA, talin-1, and annexin A1 were remarkably elevated after exposure of PAHs; these may play a role as biomarkers for PAHs exposure. In zebrafish embryos, we observed pericardial edema and dorsal curvature of the body axis associated with BaP. Zebrafish, specifically embryo stage, showed suitable *in vivo* model for monitoring BaP exposure to hematopoietic tissue and other organs.

5. Conclusions

Direct exposure to PAHs induced alteration of the mitochondrial genome including increased mtDNA copy number. The proteomic analysis of the mitochondria-rich cellular fraction showed that PARP-1 and LMNA were a novel universal biomarker associated with exposure of PAHs. Thus mtDNA copy number, PARP-1, and LMNA protein might be useful biomarkers associated with PAHs toxicity and hematotoxicity.

Conflict of Interests

The authors declare that there is no conflict of interests regarding the publication of this paper.

Acknowledgments

References

[1] S. S. Raychoudhury and D. Kubinski, "Polycyclic aromatic hydrocarbon-induced cytotoxicity in cultured rat Sertoli cells involves differential apoptotic response," *Environmental Health Perspectives*, vol. 111, no. 1, pp. 33–38, 2003.

[2] D. H. Phillips, "Fifty years of benzo(a)pyrene," *Nature*, vol. 303, no. 5917, pp. 468–472, 1983.

[3] G. Castaño-Vinyals, A. D'Errico, N. Malats, and M. Kogevinas, "Biomarkers of exposure to polycyclic aromatic hydrocarbons from environmental air pollution," *Occupational and Environmental Medicine*, vol. 61, no. 4, article e12, 2004.

[4] S. Brzeźnicki, M. Jakubowski, and B. Czerski, "Elimination of 1-hydroxypyrene after human volunteer exposure to polycyclic aromatic hydrocarbons," *International Archives of Occupational and Environmental Health*, vol. 70, no. 4, pp. 257–260, 1997.

[5] F. J. Jongeneelen and R. P. Bos, "Excretion of pyrene and hydroxypyrene in urine," *Cancer Letters*, vol. 51, no. 2, pp. 175–177, 1990.

[6] T. J. Buckley and P. J. Lioy, "An examination of the time course from human dietary exposure to polycyclic aromatic hydrocarbons to urinary elimination of 1-hydroxypyrene," *British Journal of Industrial Medicine*, vol. 49, no. 2, pp. 113–124, 1992.

[7] F. J. van Schooten, F. J. Jongeneelen, M. J. Hillebrand et al., "Polycyclic aromatic hydrocarbon-DNA adducts in white blood cell DNA and 1-hydroxypyrene in the urine from aluminum workers: relation with job category and synergistic effect of smoking," *Cancer Epidemiology Biomarkers & Prevention*, vol. 4, no. 1, pp. 69–77, 1995.

[8] J. Jacob, G. Grimmer, G. Raab, and A. Schmoldt, "The metabolism of pyrene by rat liver microsomes and the influence of various mono-oxygenase inducers," *Xenobiotica*, vol. 12, no. 1, pp. 45–53, 1982.

[9] J. D. Butler and P. Crossley, "An appraisal of relative airborne sub-urban concentrations of polycyclic aromatic hydrocarbons monitored indoors and outdoors," *Science of the Total Environment*, vol. 11, no. 1, pp. 53–58, 1979.

[10] F. J. Jongeneelen, R. B. M. Anzion, and P. T. Henderson, "Determination of hydroxylated metabolites of polycyclic aromatic hydrocarbons in urine," *Journal of Chromatography B: Biomedical Sciences and Applications*, vol. 413, no. C, pp. 227–232, 1987.

[11] M. Bouchard, L. Pinsonneault, C. Tremblay, and J. Weber, "Biological monitoring of environmental exposure to polycyclic aromatic hydrocarbons in subjects living in the vicinity of a creosote impregnation plant," *International Archives of Occupational and Environmental Health*, vol. 74, no. 7, pp. 505–513, 2001.

[12] J. N. Meyer, M. C. K. Leung, J. P. Rooney et al., "Mitochondria as a target of environmental toxicants," *Toxicological Sciences*, vol. 134, no. 1, pp. 1–17, 2013.

[13] H. Eom, H. Kim, D. Han et al., "Mitochondrial DNA copy number and hnRNP A2/B1 protein: biomarkers for direct exposure of benzene," *Environmental Toxicology and Chemistry*, vol. 30, no. 12, pp. 2762–2770, 2011.

[14] P. Haffter, M. Granato, M. Brand et al., "The identification of genes with unique and essential functions in the development of the zebrafish, Danio rerio," *Development*, vol. 123, pp. 1–36, 1996.

[15] R. T. Peterson, B. A. Link, J. E. Dowling, and S. L. Schreiber, "Small molecule developmental screens reveal the logic and timing of vertebrate development," *Proceedings of the National Academy of Sciences of the United States of America*, vol. 97, no. 24, pp. 12965–12969, 2000.

[16] R. T. Peterson, J. D. Mably, J. N. Chen, and M. C. Fishman, "Convergence of distinct pathways to heart patterning revealed by the small molecule concentramide and the mutation heart-and-soul," *Current Biology*, vol. 11, no. 19, pp. 1481–1491, 2001.

[17] M. Gnecchi and L. G. Melo, "Bone marrow-derived mesenchymal stem cells: isolation, expansion, characterization, viral transduction, and production of conditioned medium," *Methods in Molecular Biology*, vol. 482, pp. 281–294, 2009.

[18] S. S. Franco, A. C. Nardocci, and W. M. R. Günther, "PAH biomarkers for human health risk assessment: a review of the state-of-the-art," *Cadernos de Saude Publica*, vol. 24, no. 4, pp. S569–S580, 2008.

[19] F. J. Jongeneelen, "Methods for routine biological monitoring of carcinogenic PAH-mixtures," *Science of the Total Environment*, vol. 199, no. 1-2, pp. 141–149, 1997.

[20] M. M. Mumtaz, J. D. George, K. W. Gold, W. Cibulas, and C. T. Derosa, "ATSDR evaluation of health effects of chemicals.

IV. Polycyclic aromatic hydrocarbons (PAHs): understanding a complex problem," *Toxicology and Industrial Health*, vol. 12, no. 6, pp. 742–995, 1996.

[21] J. Angerer, C. Mannschreck, and J. Gündel, "Biological monitoring and biochemical effect monitoring of exposure to polycyclic aromatic hydrocarbons," *International Archives of Occupational and Environmental Health*, vol. 70, no. 6, pp. 365–377, 1997.

[22] S. Ovrebo, P. E. Fjeldstad, E. Grzybowska, E. H. Kura, M. Chorazy, and A. Haugen, "Biological monitoring of polycyclic aromatic hydrocarbon exposure in a highly polluted area of Poland," *Environmental Health Perspectives*, vol. 103, no. 9, pp. 838–843, 1995.

[23] Z. H. Zhao, W. Y. Quan, and D. H. Tian, "Urinary 1-hydroxypyrene as an indicator of human exposure to ambient polycyclic aromatic hydrocarbons in a coal-burning environment," *Science of the Total Environment*, vol. 92, pp. 145–154, 1990.

[24] "Polynuclear aromatic compounds—part 1: chemical, environmental and experimental data," *IARC Monographs on the Evaluation of Carcinogenic Risks to Humans*, vol. 32, pp. 1–453, 1983.

[25] G. Scherer, S. Frank, K. Riedel, I. Meger-Kossien, and T. Renner, "Biomonitoring of exposure to polycyclic aromatic hydrocarbons of nonoccupationally exposed persons," *Cancer Epidemiology Biomarkers and Prevention*, vol. 9, no. 4, pp. 373–380, 2000.

[26] A. Vyskocil, Z. Fiala, D. Fialova, V. Krajak, and C. Viau, "Environmental exposure to polycyclic aromatic hydrocarbons in Czech Republic," *Human and Experimental Toxicology*, vol. 16, no. 10, pp. 589–595, 1997.

[27] J. L. Mumford, X. Lee, J. Lewtas, T. L. Young, and R. M. Santella, "DNA adducts as biomarkers for assessing exposure to polycyclic aromatic hydrocarbons in tissues from Xuan Wei women with high exposure to coal combustion emissions and high lung cancer mortality," *Environmental Health Perspectives*, vol. 99, pp. 83–87, 1993.

[28] M. C. Poirier, A. Weston, B. Schoket et al., "Biomonitoring of United States Army soldiers serving in Kuwait in 1991," *Cancer Epidemiology Biomarkers and Prevention*, vol. 7, no. 6, pp. 545–551, 1998.

[29] D. H. Kang, N. Rothman, M. C. Poirier et al., "Interindividual differences in the concentration of 1-hydroxypyrene-glucuronide in urine and polycyclic aromatic hydrocarbon-DNA adducts in peripheral white blood cells after charbroiled beef consumption," *Carcinogenesis*, vol. 16, no. 5, pp. 1079–1085, 1995.

[30] J. Lewtas, D. Walsh, R. Williams, and L. Dobiáš, "Air pollution exposure-DNA adduct dosimetry in humans and rodents: Evidence for non-linearity at high doses," *Mutation Research*, vol. 378, no. 1-2, pp. 51–63, 1997.

[31] M. Peluso, F. Merlo, A. Munnia et al., "32P-postlabeling detection of aromatic adducts in the white blood cell DNA of nonsmoking police officers," *Cancer Epidemiology Biomarkers and Prevention*, vol. 7, no. 1, pp. 3–11, 1998.

[32] N. T. Palackal, M. E. Burczynski, R. G. Harvey, and T. M. Penning, "The ubiquitous aldehyde reductase (AKR1A1) oxidizes proximate carcinogen trans-dihydrodiols to o-quinones: potential role in polycyclic aromatic hydrocarbon activation," *Biochemistry*, vol. 40, no. 36, pp. 10901–10910, 2001.

[33] S. M. Heidel, P. S. MacWilliams, W. M. Baird et al., "Cytochrome P4501B1 mediates induction of bone marrow cytotoxicity and preleukemia cells in mice treated with 7,12-dimethylbenz[a]anthracene," *Cancer Research*, vol. 60, no. 13, pp. 3454–3460, 2000.

[34] M. S. Denison and S. R. Nagy, "Activation of the aryl hydrocarbon receptor by structurally diverse exogenous and endogenous chemicals," *Annual Review of Pharmacology and Toxicology*, vol. 43, pp. 309–334, 2003.

[35] P. E. Douben, *PAHs: An Ecotoxicological Perspective*, Wiley & Sons, 2003.

[36] J. Santodonato, P. Howard, and D. Basu, "Health and ecological assessment of polynuclear aromatic hydrocarbons," *Journal of Environmental Pathology and Toxicology*, vol. 5, no. 1, pp. 1–364, 1981.

[37] B. G. Masayesva, E. Mambo, R. J. Taylor et al., "Mitochondrial DNA content increase in response to cigarette smoking," *Cancer Epidemiology Biomarkers and Prevention*, vol. 15, no. 1, pp. 19–24, 2006.

[38] A. Peralta-Leal, J. M. Rodríguez-Vargas, R. Aguilar-Quesada et al., "PARP inhibitors: new partners in the therapy of cancer and inflammatory diseases," *Free Radical Biology and Medicine*, vol. 47, no. 1, pp. 13–26, 2009.

[39] P. O. Hassa, C. Buerki, C. Lombardi, R. Imhof, and M. O. Hottiger, "Transcriptional coactivation of nuclear Factor-κB-dependent gene expression by p300 is regulated by poly(ADP)-ribose polymerase-1," *Journal of Biological Chemistry*, vol. 278, no. 46, pp. 45145–45153, 2003.

Clinical Study

Expression of *IMPDH* mRNA after Mycophenolate Administration in Male Volunteers

Sollip Kim,[1] Woochang Lee,[2] Sail Chun,[2] Tae Hyun Um,[1] and Won-Ki Min[2]

[1] *Department of Laboratory Medicine, Ilsan Paik Hospital, Inje University College of Medicine, Goyang 411-706, Republic of Korea*
[2] *Department of Laboratory Medicine, University of Ulsan College of Medicine and Asan Medical Center, 88 Olympic-ro, 43-gil, Songpa-gu, Seoul 138-736, Republic of Korea*

Correspondence should be addressed to Sail Chun; sailchun@amc.seoul.kr

Background. Mycophenolic acid (MPA) is the first-line antimetabolic immunosuppressants used in solid organ transplantation. Here, *in vivo* expressions of the pharmacodynamic marker *IMPDH* mRNA were analyzed to investigate its usefulness in assessing drug effects. *Materials and Methods*. Six healthy male volunteers who had the same genotype for genes known to be associated with drug metabolism and effects were selected to remove the confounding effect of these genotypes. Mycophenolate mofetil (MMF, 1 g) was administered once to each subject, and blood samples were collected with certain interval before and after MMF administration to measure lymphocyte expression levels of *IMPDH1* and *IMPDH2* mRNA. One week later, the experiment was repeated. *Results*. Whereas *IMPDH1* mRNA expression was stable, *IMPDH2* mRNA expression showed 2 peaks in the first week. Both *IMPDH1* and *IMPDH2* mRNA expression in the second week remarkably decreased from the first week. *Conclusion*. The temporary increase in *IMPDH2* mRNA expression in the first week might be due to a reactive reaction against the plasma MPA concentration. In the second week, the intracellular guanosine monophosphate might be depleted, rendering *IMPDH2* mRNA synthesis inactive. When MPA is regularly administered to reach a steady state, the *IMPDH2* mRNA expression may be kept low and may effectively reflect biological responses regardless of drug intake.

1. Introduction

Mycophenolate mofetil (MMF) is the first-line antimetabolic immunosuppressive agent [1] used in human solid organ transplantation. It is usually administered with calcineurin inhibitors (CNI) such as tacrolimus and cyclosporine [2]. After administration, MMF is quickly hydrolyzed to mycophenolic acid (MPA), which is its active metabolite. When MPA is combined with inositol monophosphate dehydrogenase (IMPDH) in a cell, the catalytic action of IMPDH is inhibited and inosine monophosphate (IMP) cannot be converted to xanthosine monophosphate (XMP). Therefore, intracellular guanosine monophosphate (GMP) becomes depleted over time. Consequently, DNA synthesis, which requires guanosine triphosphate (GTP), does not occur and cell proliferation is inhibited [3]. In cells, GTP is synthesized not only through the de novo pathway by IMPDH but also through an alternative pathway. However, since T- and B-lymphocytes can use only the de novo pathway, MPA selectively inhibits lymphocyte proliferation [3, 4].

Since MPA has a narrow therapeutic range and many side effects, therapeutic drug monitoring is useful for several conditions such as dual immunosuppressive therapy, reduced-dosage CNI therapy, CNI switch or withdrawal, recipients with high immunologic risk, delayed graft function, and altered gastrointestinal/hepatic/renal function [5]. However, the trough level does not reflect its pharmacodynamic effects, so the practical dosing guidelines based on drug concentration remain to be established [1, 5]. The target area under the curve (AUC) of the MPA blood concentration between 30 and 60 mg h/L remains acceptable therapeutic window [5–7]. However, this method requires repeated blood collection, so its clinical application is limited [5]. Although the limited sampling strategy showed good association to full AUC, it also requires at least 3 h stay for 3-time sampling and preexisting population pharmacokinetic model [5].

Therefore, a pharmacodynamic marker that can accurately reflect the biological effects of drugs on target cells must be developed. The activity of IMPDH, which is the intracellular target of MPA, showed limited association with clinical outcomes [5, 8–13]. High-performance liquid chromatography is the most widely used method of measuring IMPDH activity, but it is complicated and requires much time and effort. Moreover, its results vary so much that its clinical application is not widely accepted. Generally, the real-time reverse transcription- (RT-) PCR method is sensitive and can be used in clinical laboratories quickly and conveniently. So, we applied the real-time RT PCR method for *IMPDH1* and *IMPDH2* mRNA expression measurement.

The association of *IMPDH* mRNA expression with the clinical outcomes of MMF-treated kidney transplant patients has been reported [14], but no study has reported the *in vivo IMPDH* mRNA expression immediately after MMF administration to volunteers with same condition. We selected healthy volunteers who have same genotypes, gender, and race to reduce the effect of between-subject variability. Reasons for between-subject variability include differences in albumin, bilirubin and hemoglobin concentrations, renal and hepatic function, coadministration of cyclosporine, comorbidities, body weight, concomitant medication, time after transplantation, gender, race, and genetic polymorphisms in drug-metabolizing enzymes [5]. In this study, the *in vivo IMPDH1* and *IMPDH2* mRNA expressions were measured over 10 h after MMF administration to healthy people with same genotype using the real-time RT-PCR method to investigate the potential use of these two genes as pharmacodynamic markers.

2. Materials and Methods

2.1. Study Design and Healthy Volunteers.
This study was approved by the local Institutional ethics committee. All subjects provided written informed consent. The study design is shown in Supplementary Figure 1 (see Supplementary Material available online at http://dx.doi.org/10.1155/2014/870209).

A total of 75 healthy male volunteers were selected for this study. The selection criteria were as follows: (1) 18- to 50-year-old healthy Korean male volunteers with (2) a body mass index of 18.5–29.9 kg/m^2 and (3) past histories and physical examination and laboratory test results that revealed no abnormal findings. Candidates were excluded from this study when they were (1) hypersensitive to MMF or related drugs, (2) female, (3) administered with other medications up to 14 days before the study or during the study, (4) under the influence of alcohol since 2 days before the study or during the study, (5) suffering from any disease, including mental illness, (6) infected with AIDS or syphilis, positive for anti-HCV, or hepatitis B carriers, and (7) on an unusual diet (such as a low-sodium diet) for whatever reason. For the laboratory tests, the subjects' complete blood counts (hemoglobin, hematocrit, and red blood cell (RBC), white blood cell (WBC), differential, and platelet counts) and general blood chemistry (glucose, total protein, albumin,

creatinine, AST, ALT, ALP, total cholesterol, total bilirubin, and direct bilirubin) were obtained.

The single nucleotide polymorphisms (SNPs) [15–25] of the genes (*UGT1A8*, *UGT1A9*, *UGT2B7*, *IMPDH1*, and *IMPDH2*) known to affect MPA metabolism and functions were investigated in the subjects. The volunteers who showed the same genotype were selected for removing the confounding effect by genotype. Six subjects were finally selected for the *IMPDH* mRNA expression study. The subjects swallowed (not chewed) 1 g of MMF tablet with water after fasting for 8 h, after which they resumed their regular diet. From 3 days before the study, the subjects' alcohol intake, smoking, and intake of other medications, greasy foods, and excessive water were restricted. Blood samples were collected at regular intervals over 10 h before and after the MMF administration (at the baseline and after 1, 2, 3, 4, 6, 8, and 10 h). The plasma total MPA concentrations and the *IMPDH1* and *IMPDH2* mRNA expression levels in the lymphocytes were measured. One week later, when the administered drug was supposed to have been removed from the blood, the whole study protocol including MMF administration and blood sampling was repeated (Supplementary Figure 1). The time interval between week 1 and week 2 for all six volunteers was the same.

2.2. Genotyping for SNPs Associated with MPA Pharmacodynamics and Pharmacokinetics.
Based on a literature review on genotyping for SNPs associated with the pharmacodynamics and pharmacokinetics of MPA, 10 SNPs of the genes known to affect MPA metabolism and effects were selected [15–25]. The primers and probes that were used for the genotyping were designed in house using Primer3Plus, a web-based software (http://www.bioinformatics.nl/cgi-bin/primer3plus/primer3plus.cgi/). Using the gene-specific primer and the allele-specific TaqMan probe, real-time PCR was conducted. In each well of the 96-well microplates, 0.5 μL of 2X TaqMan Universal PCR Master Mix (10 μL), 40X SNP genotyping assay, and 2 μL of template DNA were added and mixed after making the total volume up to 20 μL with distilled H$_2$O. The primers, probes, and master mix were purchased from Applied Biosystems (Poster, CA). The microplate was installed on a LightCycler 480 real-time PCR system (Roche Diagnostics, Indianapolis, IN) and allowed to react for 1 min at 95°C before 40 cycles of amplification were performed. Each cycle was comprised of 15 s denaturation at 95°C and 1 min extension at 50°C. The outcomes were read using the end-point genotyping method. Information on the primers and probes is shown in Supplementary Table 1. The dye for Reporter 1 was VIC, and the quencher was NFQ; for Reporter 2, the dye was FAM, and the quencher was NFQ.

2.3. Total MPA Blood Concentrations.
Using ethylenediaminetetraacetic acid (EDTA) anticoagulated plasma, the EMIT 2000 Mycophenolic Acid Assay reagent, and the VIVA-E Drug Testing System (Siemens Healthcare, Deerfield, IL), the total and free MPA blood concentrations were measured according to the manufacturer's instruction. The analytical measurement range was 0.1–15 μg/mL. The repeatabilities at the low, intermediate, and high concentrations were 3.4%,

3.6%, and 4.9%, respectively, and the total precisions were 6.1%, 4.5%, and 6.5%, respectively.

2.4. IMPDH1 and IMPDH2 mRNA Expression Study

(1) Lymphocytes Separation. After the blood samples were collected, the monocytes were separated from the EDTA anticoagulated whole blood within 2 h. After 3 mL of Ficoll-Paque PLUS (Amersham Biosciences, Piscataway, NJ) was applied to the centrifuge tube, 6 mL of a solution that was a 1 : 1 mixture of phosphate buffer and whole blood was gently added to it to form a layer. Centrifugation was conducted at room temperature (18–20°C) at 400 g for 40 min. The upper layer was removed using a clean Pasteur pipette and the lymphocyte layer was carefully collected. To prevent contamination of the granulocytes and platelets, the sample was washed with 6 mL of phosphate buffer before it was centrifuged at room temperature at 100 g for 10 min. After the pellet was cleaned twice, it was put in a 1.5 mL guanidinium thiocyanate solution (RNA/DNA Stabilization Reagent for Blood/Bone Marrow; Roche Diagnostics, Mannheim, Germany) to be vortexed for 5 min, and then the test tube was slowly stirred for over 4 h.

(2) RNA Extraction and cDNA Translation. RNA was manually extracted from the lymphocyte suspension. The High Pure RNA Extraction Kit (Roche Diagnostics) was used according to the manufacturer's instructions. The concentration and purity of the extracted RNA were measured using a Nanodrop 2000 (Thermo Scientific, Wilmington, DE).

Within 1 h of the extraction, the RNA was translated into cDNA using AccuPower CycleScript RT PreMix dN6 (Bioneer, Daejeon, Republic of Korea) according to the manufacturer's instructions. Amplification was then done using a PTC-200 thermal cycler (MJ Research, Waltham, MA).

(3) Development and Validation of Real-Time PCR for the IMPDH1 and IMPDH2 mRNA Expressions. As an internal positive control, the *ACTB* gene that encodes β-actin was selected. Five primer sets of *IMPDH1, IMPDH2*, and *ACTB* were designed based on NM_000883.3, NM_000884.2, and NM_001101.3, respectively, using Primer3Plus. To prevent contamination by genomic DNA, at least one of the forward and reverse primers was placed at the exon-exon junction. For efficient real-time PCR, the size of the final product was limited to 150 nucleotides or less. Using the prepared primer, real-time PCR was conducted to select the primer set that had the least cycle threshold (Ct) and which showed a single peak in the melting curve analysis. Information on the selected primer is shown in Supplementary Table 2. With the selected primer, real-time PCR was conducted using the AccuPower Greenstar qPCR PreMix & Exicycler 96 Real-Time Quantitative Thermal Block (Bioneer) device. After 10 min cultivation at 95°C, a denaturation cycle at 94°C for 20 s with an extension at 54°C for 30 s was repeated 45 times. The standard DNAs of the three genes were synthesized at the concentrations of 2×10^0, 2×10^1, 2×10^2, 2×10^3, 2×10^4, 2×10^5, 2×10^6, and 1×10^8 to evaluate the linearity of

the test. The precision was calculated through four repeated measurements.

(4) IMPDH1 and IMPDH2 mRNA Expression Levels in the Volunteers. Using the extracted RNA from the lymphocytes of the six subjects, the mRNA expression levels of the *IMPDH1, IMPDH2,* and *ACTB* genes were measured. Each batch included the standard DNA, and the samples were quadruplicated. The expression level was calculated using the standard curve method for relative quantification. It was described as arbitrary unit, showing the ratio of *IMPDH* mRNA expression to *ACTB* (internal control gene) mRNA expression. For the calculations and statistical analysis, Microsoft Office Excel 2010 (Microsoft, Redmond, WA) and MedCalc statistical software version 9.2.0.2 (MedCalc Software bvba, Ostend, Belgium) were used.

3. Results

3.1. Genotyping for SNPs Associated with MPA Pharmacodynamics and Pharmacokinetics. Nine (12%) of 75 volunteers had the same genotypes. Because three subjects refused to continue to participate in this study, 6 volunteers joined the *IMPDH* mRNA expression study. The genotypes of 6 volunteers were *UGT1A8* rs1042597 CG, *UGT1A9* rs17868320 CC, rs6714486 TT, rs72551330 TT, *UGT2B7* rs7439366 CC, *IMPDH1* rs2278293 AG, rs2278294 AG, *IMPDH2* rs121434586 CT, rs72639214 CC, and rs11706052 TT.

3.2. Total MPA Blood Concentrations. The plasma total MPA level peaked 1 h after MMF intake and abruptly decreased 2 h later. The plasma concentrations of MPA of some subjects showed a second peak at 3–10 h after MMF intake, which was attributed to the enterohepatic circulation. The same pattern was seen when the experiments were repeated one week later (Figures 1(a) and 1(b)).

3.3. Validation of Real-Time PCR for the IMPDH1 and IMPDH2 mRNA Expressions. Linearity evaluation confirmed the linearity in all concentration ranges (2×10^0–1×10^8). All R^2 values of the regression lines were 0.99 or higher, showing excellent linearity. From the precision measurement, the mean Ct standard deviations of *ACTB, IMPDH1*, and *IMPDH2* were determined to be 0.44 (range, 0.01–5.59), 0.35 (0.01–1.59), and 0.11 (0.01–0.99), respectively.

3.4. IMPDH1 and IMPDH2 mRNA Expressions in the Volunteers. In the first week, the *IMPDH1* mRNA expression level did not change significantly according to the time interval, whereas the *IMPDH2* mRNA expression level peaked 1–3 h after drug intake. The level increased again 3–10 h after intake to show a double peak (Figures 1(c) and 1(e)). Expression levels of *IMPDH1* and *IMPDH2* mRNA in the second week were remarkably lower than in the first week (Figures 1(d) and 1(f)).
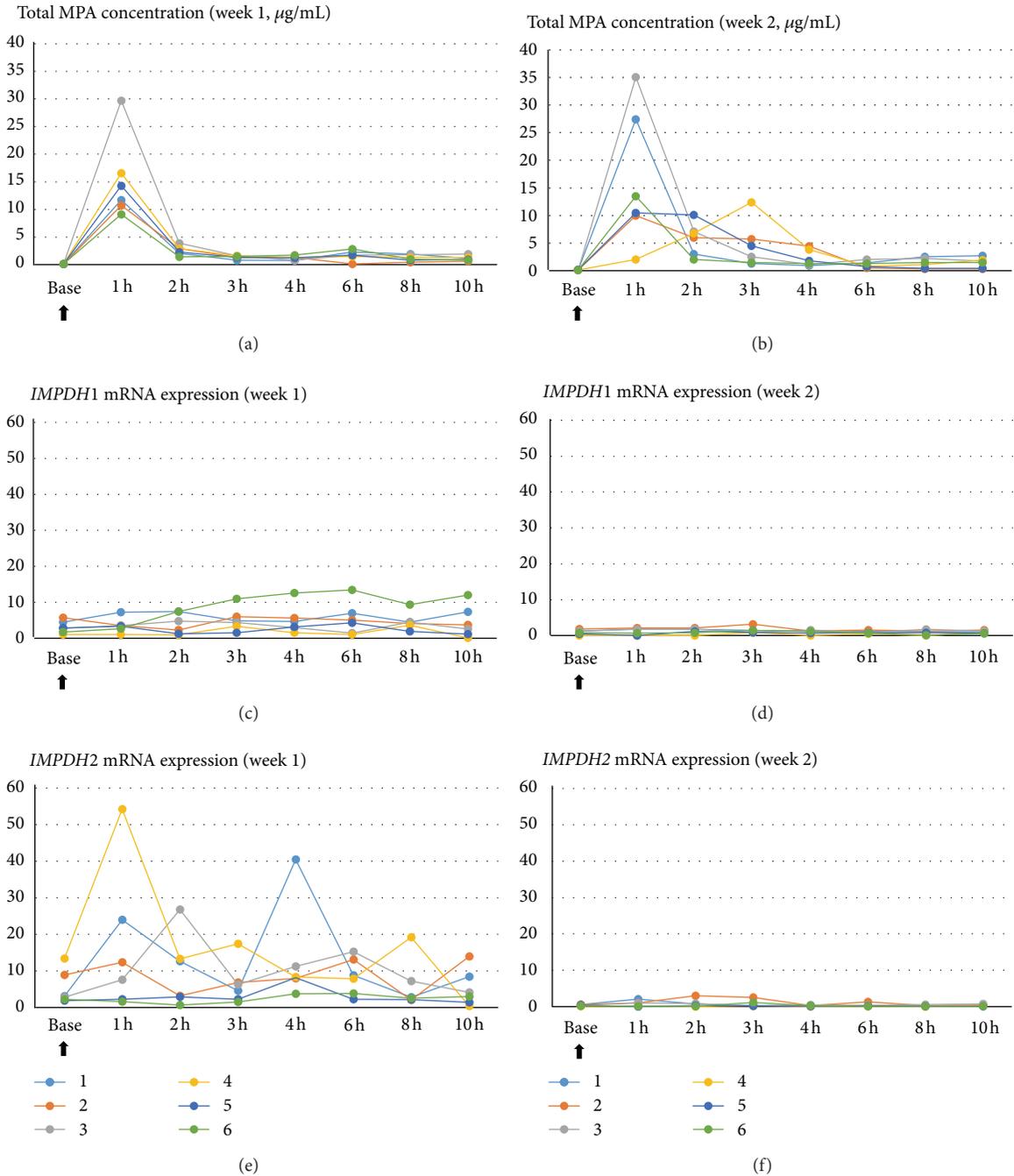
Figure 1: Plasma total MPA concentrations ((a) and (b)), *IMPDH1* mRNA expressions ((c) and (d)), and *IMPDH2* mRNA expressions ((e) and (f)) in the first week and the second week, respectively, over 10 h after the administration of MMF to the six volunteers. Black arrow means the administration of MMF. The Y-axis in mRNA expression graph is arbitrary unit, showing the ratio of *IMPDH* mRNA expression to *ACTB* (reference gene) mRNA expression.

4. Discussion

In the present study, 1 g (the typical unit dosage) of MMF was administered to volunteers to observe *IMPDH1* and *IMPDH2* mRNA expression pattern and blood MPA concentrations. The observations were done at predefined intervals over 10 h

before and after drug intake. The experiment including drug administration and samplings was repeated a week later to evaluate how fast mRNA expression decreases upon MMF intake. To exclude the influence of other factors on the mRNA expression, the study was limited to 18- to 50-year-old Korean healthy male volunteers. Ten genotypes that are known to

affect the metabolism and biological effects of MMF were tested, and the subjects who had the same genotypes were selected for inclusion in the *in vivo* study. An association of *IMPDH* mRNA expression with clinical outcomes of MMF-treated kidney transplant patients has been reported [3, 14, 26, 27], but no study has been reported on the behavior of the *in vivo IMPDH* mRNA expression immediately after drug administration with the same condition.

The *IMPDH1* mRNA expression levels in the first week were stable, while the *IMPDH2* mRNA expression levels showed two peaks, at 1–3 h and 3–10 h after intake. The first *IMPDH2* mRNA expression peak is thought to be a temporary reactive reaction to the plasma MPA concentrations, and the second peak is thought to have been a response to the increase in blood MPA concentration caused by the enterohepatic circulation. In contrast, in the second week, the *IMPDH1* and *IMPDH2* mRNA expression levels quite decreased compared with those of the first week (Figures 1(c)–1(f)). The possible reason is that *IMPDH1* and *IMPDH2* mRNA synthesis was deemed to be inactive due to the depleted intracellular GMP. Given that intracellular MPA firmly combines with IMPDH enzyme and XMP through a hydrogen bond and the van der Waals force [28], MPA is thought to consistently inhibit GMP proliferation, thereby depleting GMP. In an *in vitro* experiment, when MPA was added after culturing of mixed lymphocytes, lymphocyte proliferation was inhibited for at least 72 h [3, 26, 27]. These outcomes showed that the inhibitive effect of MPA may be maintained for a considerable length of time, as long as guanosine is not provided from outside sources. Based on this, when MPA is taken on a regular basis to reach a steady state, intracellular GMP might become depleted, and consequently, the *IMPDH2* mRNA expression level may remain low. Therefore, one-point sampling test results may effectively reflect the biological responses regardless of the time of the drug intake, enabling its use as a marker. In contrast, the drug was removed from the blood within 8 h after intake in the first- and second-week experiments. Even though a steady state was attained after drug intake that lasted for longer than a month, the blood concentration level showed a pattern of an increase followed by a decrease with the passing of time. Accordingly, the AUC must be calculated for use as a surrogate marker. Some of the 6 volunteers showed the low first peak and second peak in week 1. Unfortunately, we do not know the exact reason of this result. However, if we have more sensitive technique, maybe we could see the peak in week 1.

In this study, the *IMPDH1* and *IMPDH2* mRNA expression levels were measured via the real-time PCR method and SYBR Green. SYBR Green is an asymmetric cyanine dye that combines with double-stranded DNA, as well as with single-stranded DNA and RNA, though to a lesser extent. Even though SYBR Green has a lower specificity than the TaqMan probe, which combines only with a single helix that has a relevant base sequence, it has a high sensitivity level that allows it to be widely used to measure expression levels. Here, a combination that showed single peak was selected through fusion curve analysis that was repeated in each test to confirm the single peak and, accordingly, to secure the specificity of the test. As the standard DNA was synthesized for application, the linearity was confirmed at 8 log and the precision was excellent, with the standard deviations of the *IMPDH1, IMPDH2,* and *ACTB* gene Ct values at 0.5 or lower. Because real-time PCR is a convenient and straightforward method that can provide results within 2 h after DNA extraction, it can also be widely used in clinical laboratories.

Because RBCs comprise a large portion of the whole blood cells and express IMPDH, the IMPDH expression of RBCs is most probably obtained when the test is conducted with whole blood. In this study, the lymphocytes were separated manually using the Ficoll-Hypaque technique. However, in clinical application, a commercial RNA stabilizing lymphocyte isolation blood tube may be used to achieve more stable outcomes.

One limitation of the current study is that MMF was administered to healthy volunteers only once a week, and then the pattern of the *IMPDH* mRNA expression was observed. Because MMF is an immunosuppressive agent that can have severe side effects, it could not be administered multiple times in a row to healthy volunteers. Further studies on the expression pattern of *IMPDH* mRNA, examining patients after repeated administrations, may be needed in the future.

In conclusion, the *in vivo IMPDH1* and *IMPDH2* mRNA expression levels in healthy volunteers after MPA intake were observed weekly in this study to confirm the possible use of the *IMPDH2* mRNA expression test as an effective pharmacodynamic marker of biological responses. Moreover, the real-time RT-PCR method that was developed and verified in this study showed a wide linearity range with excellent precision. The *IMPDH1* and *IMPDH2* mRNA expression tests can also be conveniently conducted in clinical laboratories.

Abbreviations

AUC: Area under the curve
GMP: Guanosine monophosphate
GTP: Guanosine triphosphate
IMP: Inosine monophosphate
IMPDH: Inosine monophosphate dehydrogenase
MMF: Mycophenolate mofetil
MPA: Mycophenolic acid
RBC: Red blood cell
SNP: Single nucleotide polymorphism
WBC: White blood cell
XMP: Xanthosine monophosphate.

Conflict of Interests

The authors have no conflict of interests to declare.

References

[1] B. L. Kasiske, M. G. Zeier, J. R. Chapman et al., "KDIGO clinical practice guideline for the care of kidney transplant recipients: a summary," *Kidney International*, vol. 77, no. 4, pp. 299–311, 2010.

[2] KDIGO Transplant Work Group, "KDIGO clinical practice guideline for the care of kidney transplant recipients," *The*

American Journal of Transplantation, vol. 9, supplement 3, pp. S1–S155, 2009.

[3] A. C. Allison, W. J. Kowalski, C. D. Muller, and E. M. Eugui, "Mechanisms of action of mycophenolic acid," *Annals of the New York Academy of Sciences*, vol. 696, pp. 63–87, 1993.

[4] A. C. Allison and E. M. Eugui, "Mycophenolate mofetil and its mechanisms of action," *Immunopharmacology*, vol. 47, no. 2-3, pp. 85–118, 2000.

[5] D. R. Kuypers, Y. Le Meur, M. Cantarovich et al., "Consensus report on therapeutic drug monitoring of mycophenolic acid in solid organ transplantation," *Clinical Journal of the American Society of Nephrology*, vol. 5, no. 2, pp. 341–358, 2010.

[6] M. D. Hale, A. J. Nicholls, R. E. S. Bullingham et al., "The pharmacokinetic-pharmacodynamic relationship for mycophenolate mofetil in renal transplantation," *Clinical Pharmacology & Therapeutics*, vol. 64, no. 6, pp. 672–683, 1998.

[7] T. van Gelder, L. B. Hilbrands, Y. Vanrenterghem et al., "A randomized double-blind, multicenter plasma concentration controlled study of the safety and efficacy of oral mycophenolate mofetil for the prevention of acute rejection after kidney transplantation," *Transplantation*, vol. 68, no. 2, pp. 261–266, 1999.

[8] H. D. Jonge, M. Naesens, and D. R. J. Kuypers, "New insights into the pharmacokinetics and pharmacodynamics of the calcineurin inhibitors and mycophenolic acid: possible consequences for therapeutic drug monitoring in solid organ transplantation," *Therapeutic Drug Monitoring*, vol. 31, no. 4, pp. 416–435, 2009.

[9] O. Millán, N. Urtasun, and M. Brunet, "Biomarkers of the immunomodulatory effect of immunosuppressive drugs in transplant recipients," *Transplantation Reviews*, vol. 23, no. 2, pp. 120–128, 2009.

[10] L. J. Langman, H. Nakakura, J. A. Thliveris, D. F. LeGatt, and R. W. Yatscoff, "Pharmacodynamic monitoring of mycophenolic acid in rabbit heterotopic heart transplant model," *Therapeutic Drug Monitoring*, vol. 19, no. 2, pp. 146–152, 1997.

[11] M. C. Raggi, S. B. Siebert, W. Steimer, T. Schuster, M. J. Stangl, and D. K. Abendroth, "Customized mycophenolate dosing based on measuring inosine-monophosphate dehydrogenase activity significantly improves patients outcomes after renal transplantation," *Transplantation*, vol. 90, no. 12, pp. 1536–1541, 2010.

[12] P. Glander, P. Hambach, K. Braun et al., "Pre-transplant inosine monophosphate dehydrogenase activity is associated with clinical outcome after renal transplantation," *American Journal of Transplantation*, vol. 4, no. 12, pp. 2045–2051, 2004.

[13] L. R. Chiarelli, M. Molinaro, C. Libetta et al., "Inosine monophosphate dehydrogenase variability in renal transplant patients on long-term mycophenolate mofetil therapy," *British Journal of Clinical Pharmacology*, vol. 69, no. 1, pp. 38–50, 2010.

[14] F. Sombogaard, A. M. A. Peeters, C. C. Baan et al., "Inosine monophosphate dehydrogenase messenger RNA expression is correlated to clinical outcomes in mycophenolate mofetil-treated kidney transplant patients, whereas inosine monophosphate dehydrogenase activity is not," *Therapeutic Drug Monitoring*, vol. 31, no. 5, pp. 549–556, 2009.

[15] H. de Jonge and D. R. J. Kuypers, "Pharmacogenetics in solid organ transplantation: current status and future directions," *Transplantation Reviews*, vol. 22, no. 1, pp. 6–20, 2008.

[16] S. S. Thomas, S. S. Li, J. W. Lampe, J. D. Potter, and J. Bigler, "Genetic variability, haplotypes, and htSNPs for exons 1 at the human UGT1A locus," *Human Mutation*, vol. 27, no. 7, article 717, 2006.

[17] J. Wang, J. W. Yang, A. Zeevi et al., "IMPDH1 gene polymorphisms and association with acute rejection in renal transplant patients," *Clinical Pharmacology & Therapeutics*, vol. 83, no. 5, pp. 711–717, 2008.

[18] L. A. Johnson, W. S. Oetting, S. Basu, S. Prausa, A. Matas, and P. A. Jacobson, "Pharmacogenetic effect of the UGT polymorphisms on mycophenolate is modified by calcineurin inhibitors," *European Journal of Clinical Pharmacology*, vol. 64, no. 11, pp. 1047–1056, 2008.

[19] M. Miura, H. Kagaya, S. Satoh et al., "Influence of drug transporters and UGT polymorphisms on pharmacokinetics of phenolic glucuronide metabolite of mycophenolic acid in Japanese renal transplant recipients," *Therapeutic Drug Monitoring*, vol. 30, no. 5, pp. 559–564, 2008.

[20] J. Grinyó, Y. Vanrenterghem, B. Nashan et al., "Association of four DNA polymorphisms with acute rejection after kidney transplantation," *Transplant International*, vol. 21, no. 9, pp. 879–891, 2008.

[21] F. Sombogaard, R. H. van Schaik, R. A. Mathot et al., "Interpatient variability in IMPDH activity in MMF-treated renal transplant patients is correlated with IMPDH type II 3757T > C polymorphism," *Pharmacogenetics and Genomics*, vol. 19, no. 8, pp. 626–634, 2009.

[22] H. Kagaya, M. Miura, M. Saito, T. Habuchi, and S. Satoh, "Correlation of IMPDH1 gene polymorphisms with subclinical acute rejection and mycophenolic acid exposure parameters on day 28 after renal transplantation," *Basic and Clinical Pharmacology and Toxicology*, vol. 107, no. 2, pp. 631–636, 2010.

[23] A. Garat, C. L. L. Cardenas, A. Lionet et al., "Inter-ethnic variability of three functional polymorphisms affecting the *IMPDH2* gene," *Molecular Biology Reports*, vol. 38, no. 8, pp. 5185–5188, 2011.

[24] O. Gensburger, R. H. N. van Schaik, N. Picard et al., "Polymorphisms in type I and II inosine monophosphate dehydrogenase genes and association with clinical outcome in patients on mycophenolate mofetil," *Pharmacogenetics and Genomics*, vol. 20, no. 9, pp. 537–543, 2010.

[25] S. E. Tett, F. Saint-Marcoux, C. E. Staatz et al., "Mycophenolate, clinical pharmacokinetics, formulations, and methods for assessing drug exposure," *Transplantation Reviews*, vol. 25, no. 2, pp. 47–57, 2011.

[26] M. Huang, Y. Ji, K. Itahana, Y. Zhang, and B. Mitchell, "Guanine nucleotide depletion inhibits pre-ribosomal RNA synthesis and causes nucleolar disruption," *Leukemia Research*, vol. 32, no. 1, pp. 131–141, 2008.

[27] H. Daxecker, M. Raab, M. Cichna, P. Markl, and M. M. Müller, "Determination of the effects of mycophenolic acid on the nucleotide pool of human peripheral blood mononuclear cells in vitro by high-performance liquid chromatography," *Clinica Chimica Acta*, vol. 310, no. 1, pp. 81–87, 2001.

[28] M. D. Sintchak and E. Nimmesgern, "The structure of inosine $5'$-monophosphate dehydrogenase and the design of novel inhibitors," *Immunopharmacology*, vol. 47, no. 2-3, pp. 163–184, 2000.

Research Article

Usefulness of Combining Galectin-3 and BIVA Assessments in Predicting Short- and Long-Term Events in Patients Admitted for Acute Heart Failure

**Benedetta De Berardinis,[1] Laura Magrini,[1] Giorgio Zampini,[1]
Benedetta Zancla,[1] Gerardo Salerno,[2] Patrizia Cardelli,[2] Enrico Di Stasio,[3]
Hanna K. Gaggin,[4] Arianna Belcher,[4] Blair A. Parry,[5] John T. Nagurney,[5]
James L. Januzzi Jr.,[4] and Salvatore Di Somma[1]**

[1] *Emergency Medicine, Department of Medical-Surgery Sciences and Translational Medicine, Sapienza University of Rome, Sant'Andrea Hospital, Via di Grottarossa 1035/1039, 00189 Rome, Italy*

[2] *Clinical and Molecular Medicine Department, Sapienza University of Rome, Sant'Andrea Hospital, 00189 Rome, Italy*

[3] *Institute of Biochemistry and Clinical Biochemistry, Catholic University of the Sacred Heart, 00168 Rome, Italy*

[4] *Division of Cardiology, Massachusetts General Hospital, Harvard Medical School, Boston, MA 02114, USA*

[5] *Department of Emergency Medicine, Massachusetts General Hospital, Harvard Medical School, Boston, MA 02114, USA*

Correspondence should be addressed to Salvatore Di Somma; salvatore.disomma@uniroma1.it

Introduction. Acute heart failure (AHF) is associated with a higher risk for the occurrence of rehospitalization and death. Galectin-3 (GAL3) is elevated in AHF patients and is an indicator in predicting short-term mortality. The total body water using bioimpedance vector analysis (BIVA) is able to identify mortality within AHF patients. The aim of this study was to evaluate the short- and long-term predictive value of GAL3, BIVA, and the combination of both in AHF patients in Emergency Department (ED). *Methods*. 205 ED patients with AHF were evaluated by testing for B type natriuretic peptide (BNP) and GAL3. The primary endpoint was death and rehospitalization at 30, 60, 90, and 180 days and 12 and 18 months. AHF patients were evaluated at the moment of ED arrival with clinical judgment and GAL3 and BIVA measurement. *Results*. GAL3 level was significantly higher in patients >71 years old, and with eGFR < 30 cc/min. The area under the curve (AUC) of GAL3 + BIVA, GAL3 and BIVA for death and rehospitalization both when considered in total and when considered serially for the follow-up period showed that the combination has a better prognostic value. Kaplan-Meier survival curve for GAL3 values >17.8 ng/mL shows significant survival difference. At multivariate Cox regression analysis GAL3 is an independent variable to predict death + rehospitalization with a value of 32.24 ng/mL at 30 days ($P < 0.005$). *Conclusion*. In patients admitted for AHF an early assessment of GAL3 and BIVA seems to be useful in identifying patients at high risk for death and rehospitalization at short and long term. Combining the biomarker and the device could be of great utility since they monitor the severity of two pathophysiological different mechanisms: heart fibrosis and fluid overload.

1. Introduction

In patients with acute heart failure (AHF), the occurrence of rehospitalization and death is very common [1, 2]. There is need for tools to immediately identify patients with AHF at high risk for short- and long-term mortality and readmission. Galectin-3 (GAL3) is a β-galactoside-binding lectin

overexpressed by macrophages during phagocytosis that has been shown to be elevated in patients with AHF representing a prognostic biomarker for future adverse events such as death and rehospitalization [3, 4]. The adverse outcome in patients with elevated circulating level of GAL3 has been linked with the presence of enhanced amount of the fibrosis of the heart [5]. Between patients that need to be hospitalized for

AHF the occurrence of body congestion is a common finding [6].

Recently, the assessment of total body water using bioimpedance vector analysis (BIVA) has been suggested to be useful for the differential diagnosis of dyspnea, identifying patients with fluid overload [7]. Moreover, within subjects referring to the Emergency Department (ED) for AHF, BIVA has been demonstrated to be able to identify people at high risk for short-term mortality [8, 9]. In consideration of the two different aspects of GAL3 and of BIVA (the first is a fibrosis marker, and the second is a dynamic marker of congestion), we decided to evaluate in this study the degree of congestion correlated to that of fibrosis in AHF patients alone or together for the prediction of events. So far no data are available on potential usefulness of combining GAL3, as a biomarker of heart fibrosis, and BIVA, as a device for detecting fluid overload in patients with AHF in order to identify subject at high risk for future adverse outcome. The aim of this study was to evaluate the short- and long-term predictive value of GAL3, BIVA, and the combination of both in patients with AHF at the moment of their hospital admission.

2. Materials and Methods

2.1. Study Design.
In a prospective, blinded international study, patients presenting to ED with AHF were evaluated by testing for B type natriuretic peptide (BNP) and GAL3. The primary endpoint was death and rehospitalization at 30, 60, 90, and 180 days and 12 and 18 months.

We enrolled 205 subjects from March 2012 to September 2013 at two tertiary care academic medical centers members of the Global Research on Acute Conditions Team (GREAT): Sant'Andrea Hospital (Rome, Italy) and the Massachusetts General Hospital (Boston, MA). All study procedures were approved by local institutional review boards. AHF patients were evaluated at the moment of ED arrival with clinical judgement and blood routine laboratory tests plus GAL3 and BIVA. Inclusion criteria included moderate or severely symptomatic AHF (classified on the basis of current guidelines [10]) requiring intensification of diuretic therapy [10]. Exclusion criteria included renal failure requiring current renal replacement therapy, ≥8 hours from the first dose of intravenous diuretic, and unwillingness or inability to participate in study procedures. At the moment of ED arrival, baseline demographics, vital signs, and results of physical examination were evaluated and recorded after informed consent was signed. The protocol was designed following the criteria of the Declaration of Helsinki and was approved by the ethical committee of each participating hospital. Peripheral venous blood was withdrawn and processed as noted below.

2.2. Blood Analysis.
Peripheral venous blood was withdrawn by each patient and put into tubes containing ethylenediaminetetraacetic acid or no anticoagulant and spun for 15 minutes; samples were immediately aliquoted to freezer tubes and frozen at −80° for biomarkers measurement following the completion of the trial. Samples were thawed for the first time for measurement of biomarkers. Biomarkers of myocardial stretch BNP (Alere Triage BNP, San Diego, CA), biomarkers of risk stratification of patients GAL3 (VIDAS, Biomerieux, Marcy l'Étoile, France), and biomarkers of renal function included blood urea nitrogen (BUN), serum creatinine, and estimated glomerular filtration rate (eGFR, estimated using the simplified modification of diet in renal disease equation [11]). Clinicians were blinded to GAL3 and BIVA results.

2.3. Galectin-3.
GAL3 (VIDAS, Biomerieux, Marcy l'Étoile, France) is a quantitative, one-step sandwich assay with fluorescence detection, designed for use with the VIDAS automated immunoassay system. Briefly the system measures GAL3 in human serum or plasma (200 μL) using the ELFA (enzyme-linked fluorescent assay) technique in 20 minutes. All stages of the assay are performed automatically by the instrument, calculating the concentration of GAL3 relative to a stored calibration curve and enabling patients to be assigned as low, intermediate, or high risk of GAL3 mediated HF. Correct assay performance and validation of results are ensured by analysis of the control sample included in the kit. Decisional cut-offs are represented by ≤17.8 ng/mL "low risk," 17.8–25.9 ng/mL "intermediate risk," and ≥25.9 ng/mL "high risk" [12]; the three risk categories have been previously defined for the BGM Galectin-3 microplate assay [13].

2.4. BIVA Assessment.
We used standard tetrapolar bioelectrical impedance electrodes at a frequency of 50 kHz (Akern Srl, Pontassieve, Florence, Italy). The BIVA measurement assessed at patients' ED arrival was performed at bedside, with the patient supine, without metal contacts, and with inferior limbs at 45° and superior limbs abducted at 30° to avoid skin contacts. Four skin electrodes were applied (two on the wrist and two on the ipsilateral ankle) maintaining a minimal interelectrode distance of 5 cm. The machine used an alternating current flux of 300 μA and an operating frequency of 50 kHz. The results were visualized in two ways: as a vector or as a BIVA-derived hydration percentage. The first method includes a direct impedance plot which measures resistance (Rz) and reactance (Xc) as a bivariate vector in a nomogram. Reference values adjusted for age, BMI, and gender are plotted as tolerance ellipses in the same coordinate system. Three tolerance ellipses are distinguished, corresponding to the 50th, 75th, and 95th vector percentiles of the healthy reference population. The major axis of this ellipse indexes hydration status and the minor axis reflects tissue mass. The second method involves a scale called a hydrograph (or hydrogram), which expresses the state of hydration as a percentage (HI). This value is calculated by an independently determined equation that uses the two components of BIVA, Rz and Xc. The normal value is 73.3% with tolerance between 72.7% and 74.3%, corresponding to the 50th percentile. On arrival at the ED, Rz and Xc were recorded, normalized by the subject's height, and graphically expressed on the Rz-Xc plane; furthermore, HI was also assessed [8, 14–17]. Clinicians were blinded to the results of BIVA.
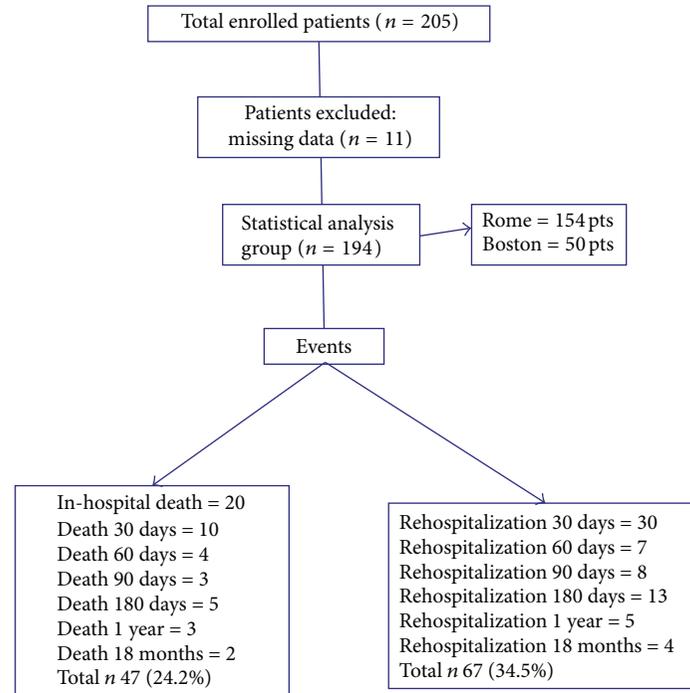
FIGURE 1: Flowchart of the study.

2.5. Follow-Up. In-hospital, 30-, 60-, 90-, and 180-day and 12- and 18-month follow-up events (deaths or rehospitalization) were recorded.

2.6. Statistical Analysis. Continuous variables were summarized as mean ± standard deviation (SD) if normally distributed and as median and interquartile range [IQR] if not normally distributed. Discrete variables are shown as percentage. Baseline variables of study participants for events (death + rehospitalization) and death were compared using Student's t-test for continuous variables or X_2 test for discrete variables if data were normally distributed; the Mann-Whitney U test was used for continuous variables and Fisher's exact test for discrete variables in the states of nonnormality. To determine the prognostic value of GAL3 and phase angle, the receiver operating characteristic (ROC) tests compared the results of GAL3 and phase angle and combination of both for predicting rehospitalization or death, expressed as area under the curve (AUC); the P value was obtained. Univariable comparisons between baseline characteristics were used to identify candidate variables for entry to a multivariable logistic regression model in order to select the variables most predictive of patients' outcomes; only those with a P value <0.05 were retained for multivariable modeling. Net reclassification index (NRI) analysis was used to improve the accuracy of the risk-prediction model for in-hospital mortality. All statistical analyses were performed using Medcalc version 12.1.4 (Medcalc Software, Mariakerke, Belgium) software. All P values are two-sided with a value of <0.05 considered significant.

3. Results

Figure 1 showed the flowchart of the study, 11 patients were excluded for missing data, total deaths in hospital and during 18-month follow-up were 47 (24.2%), and total rehospitalization during all follow-up period was 67 (34.5%). Patients' characteristics are showed in Table 1. At the moment of ED arrival compared to survivors there were no statistically significant differences for demographic data in patients with death or total adverse events (rehospitalization and death) observed in all periods of the study. Beta blockers use was higher in patients who survived. On the contrary, in patients who died, there was a significant increase of serum creatinine (sCr), blood urea nitrogen (BUN), and white blood cells (WBC). When considering the combination of death and rehospitalization during follow-up, there was significant increase of age, hypertension, diabetes mellitus, use of ACE inhibitors (ACEi), sCr, and BUN values in patients who develop events. Table 2 shows that, compared to survivors, GAL3 level at admission was significantly higher in both groups that died or that developed death + rehospitalization during follow-up. On the contrary, BNP value was not different within groups of patients who survived, died, or were rehospitalized. As for BIVA data, there was a significant increase of Xc in patients who died during follow-up compared to survivors (Table 2). Figure 2 shows the value of GAL3 subdivided in quartiles on the basis of age (a) and of eGFR (b). Figure 2(a) demonstrates that GAL3 level was significantly higher in patients within quartiles of age >71 years and in patients within quartiles of eGFR<30 mL/min/1.73 m^2 (Figure 2(b)). Table 3 shows the ROC curve analysis of GAL3,

TABLE 1: Baseline characteristics of study subjects as a function of the subsequent development of events (in-hospital death and rehospitalization and total death.

	Total (N = 194) n (%)	Events			Death		
		Yes (N = 88) n (%)	No (N = 106) n (%)	P	Yes (N = 47) n (%)	No (N = 147) n (%)	P value
Demographics							
Age (years) (mean, SD)	76.23 ± 10.84	78.23 ± 10.58	74.51 ± 10.92	0.01	80.09 ± 10.54	74.97 ± 10.74	0.08
Male	107 (56.1%)	48	59	0.37	24 (12.6%)	83 (43.6%)	0.41
Medical history							
Prior heart failure	104 (54.73%)	47	57	0.42	24 (12.63%)	80 (42.10%)	0.56
CKD	58 (30.52%)	28	30	0.42	16 (8.42%)	42 (22.10%)	0.54
Hypertension	149 (78.42%)	64	85	0.05	32 (16.84%)	117 (61.5%)	0.47
Myocardial infarction	63 (33.15%)	29	34	0.54	15 (7.89%)	48 (25.26%)	0.83
CAD	67 (35.26%)	28	39	0.22	11 (5.78%)	56 (29.47%)	0.50
COPD	52 (27.36%)	31	33	0.39	17 (8.94%)	47 (24.73%)	0.67
Atrial fibrillation	79 (41.57%)	37	42	0.51	19 (10.0%)	60 (31.57%)	0.85
Diabetes mellitus	86 (45.26%)	47	39	0.02	22 (11.5%)	64 (33.6%)	0.80
Prior medication							
ACE-i	54 (28.42%)	31	23	0.03	15 (7.89%)	39 (20.52%)	0.57
ARBs	26 (13.68%)	8	18	0.07	5 (2.63%)	21 (11.05%)	0.47
BB	115 (60.52%)	45	70	0.01	15 (7.89%)	100 (52.63%)	<0.001
Loop diuretic	124 (65.26%)	57	67	0.52	30 (15.78%)	94 (49.47%)	0.72
Nitrates	60 (31.57%)	25	25	0.29	13 (6.84%)	37 (19.47%)	0.84
Digoxin	20 (10.52%)	9	11	0.56	7 (3.68%)	13 (6.84%)	0.27
ASA	96 (50.52%)	43	53	0.45	18 (9.47%)	78 (41.05%)	0.43
NSAID	19 (10.0%)	11	8	0.19	2 (1.05%)	17 (8.94%)	0.12
Spironolactone	24 (12.63%)	13	20	0.27	7 (3.68%)	26 (13.68%)	0.58
Jugular venous distention	68 (35.78%)	31	37	0.52	17 (8.94%)	51 (26.84%)	0.87
Lower extremity edema	106 (55.78%)	46	60	0.22	21 (11.05%)	85 (44.73%)	0.77
Cough	39 (20.52%)	17	22	0.42	7 (3.68%)	32 (16.84%)	0.27
Orthopnea	136 (71.57%)	67	69	0.12	34 (17.89%)	102 (53.68%)	0.89
Paroxysmal nocturnal dyspnea	88 (46.31%)	46	42	0.08	26 (13.68%)	62 (32.63%)	0.15
Chest pain	40 (21.05%)	16	24	0.23	7 (3.68%)	33 (17.36%)	0.23
Hepatojugular reflux	41 (21.57%)	25	16	0.02	7 (14.21%)	14 (7.36%)	0.11
Murmur	84 (44.21%)	39	47	0.46	22 (11.57%)	64 (33.68%)	0.80
Rales	149 (78.42%)	72	77	0.19	42 (22.10)	107 (56.31%)	0.36
Wheezing	145 (76.31%)	21	24	0.54	9 (4.73%)	36 (18.94%)	0.39
Edema	115 (60.52%)	58	57	0.16	28 (14.73%)	87 (45.78%)	0.87
Interstitial edema	120 (63.15%)	59	61	0.18	34 (17.89%)	86 (45.26%)	0.13
Pleural effusions	99 (52.10%)	46	53	0.54	28 (14.73%)	71 (37.36%)	0.23

TABLE 1: Continued.

| | Total (N = 194) n (%) | Events | | | Death | | |
		Yes (N = 88) n (%)	No (N = 106) n (%)	P	Yes (N = 47) n (%)	No (N = 147) n (%)	P value
Heart rate	88.14 ± 24.70	88.32 ± 24.64	87.28 ± 25.06	0.77	93.66 ± 25.74	85.81 ± 24.26	0.59
SBP	146.94 ± 33.67	147.89 ± 34.53	147.46 ± 32.81	0.93	145.1 ± 33.0	148.5 ± 33.78	0.75
DBP	79.30 ± 17.64	79.26 ± 16.62	79.57 ± 18.56	0.90	78.55 ± 15.05	79.71 ± 18.45	0.31
sCr (mg/dL)	1.56 ± 1.09	1.73 ± 1.26	1.34 ± 0.81	0.01	1.99 ± 1.49	1.37 ± 0.8	0.001
BUN (mg/dL)	34.9 ± 21.5	39.21 ± 22.54	30.28 ± 18.52	0.003	44.0 ± 23.8	31.27 ± 18.09	0.005
eGFR	55.0 ± 28.5	50.99 ± 29.71	59.40 ± 25.68	0.03	45.48 ± 29.01	58.80 ± 26.76	0.48
Na (mE/L)	136.7 ± 64	135.97 ± 6.05	137.46 ± 4.93	0.62	134.26 ± 6.54	137.59 ± 4.88	0.16
Glucose	145 ± 70	151.94 ± 66.79	145.09 ± 74.60	0.51	159.6 ± 73.4	144.5 ± 70.0	0.55
WBC	9.8 ± 9.8	11.01 ± 11.77	9.27 ± 4.04	0.16	13.1 ± 15.6	9.05 ± 3.68	<0.001
HGB	11.9 ± 0	11.68 ± 2.02	12.15 ± 1.99	0.11	11.56 ± 2.09	12.05 ± 2.02	0.86
RDW	17.4 ± 0	16.79 ± 2.65	17.49 ± 16.13	0.68	17.23 ± 2.9	17.14 ± 13.65	0.61
BMI	28.95 ± 13.76	27.98 ± 8.32	29.28 ± 16.27	0.49	26.7 ± 4.02	29.3 ± 14.9	0.95

(a)

(b)
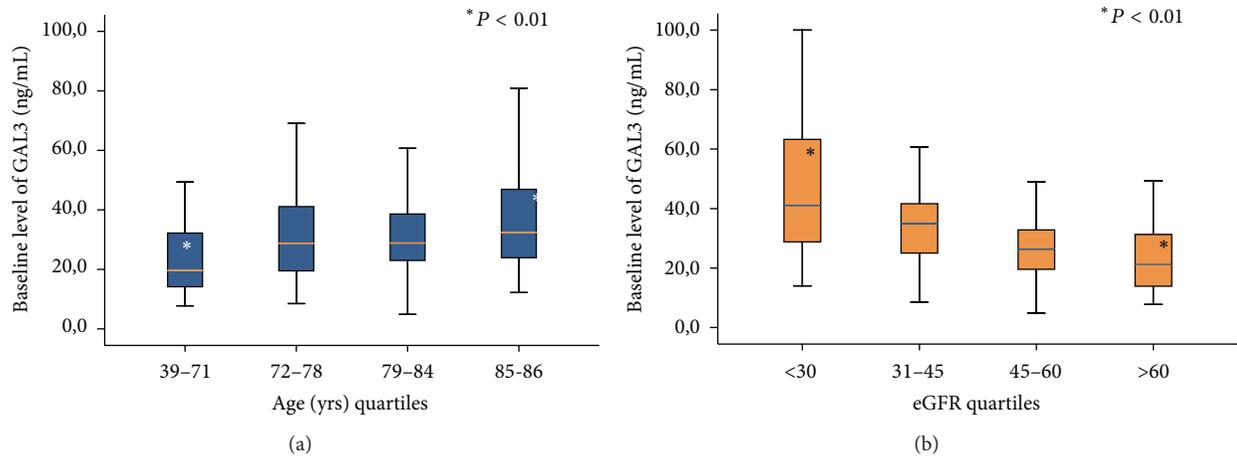
FIGURE 2: GAL3 levels increase proportionally with age quartiles (a) and decrease with eGFR quartiles (b).

TABLE 2: Baseline biomarkers as a function of the primary endpoint of events (in-hospital death and rehospitalization and death at 18-month follow-up) and death.

Variable (mean ± SD)	Total (N = 194)	Events (death + rehospitalization)		P	Death		P
		Yes (N = 88)	No (N = 106)		Yes (N = 47)	No (N = 147)	
GAL3 (ng/mL)	32.19 ± 19.03	37.15 ± 21.8	26.12 ± 13.6	<0.001	40.58 ± 23.09	28.16 ± 15.96	<0.001
BNP (pg/mL)	872.9 ± 1024.4	969.5 ± 1205.5	774.5 ± 837.1	0.91	1030.0 ± 1059.9	821.25 ± 1014.6	0.27
Hydration (%)	79.44 ± 6.55	80.75 ± 6.55	78.75 ± 6.66	0.75	80.62 ± 7.6	79.05 ± 6.19	0.11
Xc/H	34.8 ± 16.4	27.0 ± 14.2	27.35 ± 11.63	0.93	28.25 ± 26.85	17.07 ± 11.28	0.05
Rz/H	364.25 ± 136.8	363.73 ± 140.02	341.07 ± 120.88	0.21	386.05 ± 340.54	155.30 ± 119.68	0.28
Phase angle	4.4 ± 1.7	4.3 ± 1.7	4.7 ± 1.5	0.17	4.24 ± 2.09	4.62 ± 1.48	0.79

BIVA (phase angle), and GAL3 + phase angle for mortality and rehospitalization for 30, 60, 90, and 180 days and 12 and 18 months. Figure 3 shows the Kaplan-Meier survival curve for death (a) and for total events (death and rehospitalization) (b) on the basis of GAL3 values greater than 17.8 ng/mL, international cut-off [12]. It is evident that in patients with GAL3 >17.8 ng/mL there was a higher incidence of death or of all events (death and rehospitalization) during 18-month follow-up. Cox regression analysis demonstrated that GAL3 is an indipendent variable to predict death to predict death and rehospitalization with a value of 32.24 ng/mL at 30 days ($P < 0.005$). We constructed a clinical model based on variables suggested by the referee (age, sex, BNP, LVEF, and creatinine), using as decisional cut-off of the median values of our entire population. Each patient was classified at low or high risk for development of events on the basis of the positivity at the different predictive variables. The best predictive model in terms of sensitivity and specificity was obtained with positivity at 3 out of 5 variables (sensitivity 61.4%, specificity 61.8%, and accuracy 62%). The use of galectin-3 at a threshold of 17.8 combined to previously described clinical model was able to improve the global risk classification (NRI) of 18% (NRI for events +27%, NRI for no events −9%, $P = 0.021$). The use of galectin-3 and BIVA was able to get a NRI of 20% especially improving the

"no events" correct reclassification (NRI for events +16%, NRI for no events +4%, $P = 0.012$).

4. Discussion

Cardiac remodeling and congestion are crucial determinants of the clinical outcome of heart failure (HF) and are linked to disease progression and poor prognosis [18]. Recently it has been demonstrated that slowing or reversing the progression of remodeling could become a therapeutic goal of HF patients' management. Circulating plasma concentrations of BNP is currently the most commonly used biomarker in AHF and its level is generally increased in proportion to the severity of the myocardial stretch or overload [19]. However, the applicability of BNP is limited, since its levels substantially vary over the day, and is not related to the underlying cardiac disease process. Prognostic value of GAL3 when upregulated in hypertrophied hearts has been confirmed in a number of studies [2, 3, 20–25]. Data from our study strongly support the original research papers that showed how GAL3 could play an important role in the underlying structural heart disease processes. Elevated value of GAL3 is associated with heart failure progression due to increase of heart fibrosis leading to poor outcome in AHF patients.

TABLE 3: ROC curve analysis of GAL3, BIVA (phase angle), and GAL3 + phase angle for mortality and rehospitalization for 30, 60, and 90 days, 1 year, and 18 months.

	GAL3 + phase angle		GAL3		Phase angle	
	AUC	P	AUC	P	AUC	P
Rehospitalization						
30 days	0.526	ns	0.51	ns	0.52	ns
60 days	**0.625**	**0.003**	0.61	0.04	0.54	0.04
90 days	0.583	ns	0.57	ns	0.57	ns
180 days	**0.545**	**0.05**	0.54	ns	0.52	ns
12 months	0.52	ns	0.54	ns	0.53	ns
18 months	**0.620**	**0.04**	0.59	0.04	0.52	ns
Death						
30 days	**0.764**	**0.0001**	0.69	0.002	0.64	0.01
60 days	**0.754**	**0.0001**	0.68	0.0001	0.68	0.003
90 days	**0.667**	**0.005**	0.64	0.01	0.58	0.04
180 days	**0.841**	**0.0001**	0.67	0.006	0.79	0.0001
12 months	**0.833**	**0.0001**	0.72	0.002	0.79	0.0001
18 months	**0.863**	**0.0001**	0.73	0.0003	0.86	0.0001

TABLE 4: Multivariate Cox regression analysis GAL3 is an independent variable to predict death and rehospitalization with a value of 32.24 ng/mL at 30 days ($P < 0.005$).

Variables	Logistic regression			
	B	SE	Wald	P
GAL3	**0.671**	**0.370**	**3.290**	**0.05**
Phase angle	−1.462	0.773	3.574	<0.03
Hi	0.103	0.708	0.021	ns

From our results GAL3 value in patients who develop higher incidence of death and rehospitalization was independent risk factor with a cut-off of 32.24 ng/mL greater than the cut-off of 17.8 ng/mL that is currently accepted, Table 4 [12, 20–26]. Moreover GAL3 was statistically higher in patients who died ($P < 0.001$) and were rehospitalized compared to survivors ($P < 0.001$). Our results are also in agreement with van Kimmenade et al. who demonstrated that, elevated GAL3 levels in patients presenting to ED for AHF, GAL3 was the best independent predictor for 60-day mortality [4]. Furthermore our results are in the same directions with the ones from Shah et al. who demonstrated that in patients with AHF presenting to ED a value of GAL3 levels above the median value had higher incidence of mortality [3]. Our study is probably the first in which a long-term follow-up for mortality and rehospitalization has been studied in AHF patients in consideration of GAL3 levels measured in ED; furthermore, our follow-up study was serially conducted (30-, 60-, 90-, and 180-day and 12- and 18-month follow-up events (deaths or rehospitalization)). In literature there are very few data on short- and long-term follow-up but all these papers are not serially [3, 4, 27]. Recently published data from three large research trials from HF patients. They demonstrated that elevation of GAL3 levels was significantly predictive of rehospitalization of 30 days from discharge. Moreover those patients of elevation of GAL3 at the time of hospitalization were readmitted within 30 days at three times of rate of patients without GAL3 elevation and the increased risk of

hospitalization conferred by GAL3 elevation persisted at 60, 90, and 120 days in the study [28].

As described in literature GAL3 was able to identify those AHF patients at risk for short-term death or for the combination of death and readmission [4]; in our study GAL3 measured at the moment of ED arrivals predicts adverse events better than BNP. So we can consider that on the basis of this data BNP has not a real prognostic value at admission; our group already demonstrated this finding in the ITALIAN RED study [29]. However, we must underline the fact that BNP is internationally considered as the gold standard biomarker in any risk score of AHF patients.

We also analyzed the levels of GAL3 based on eGFR quartiles and we demonstrated that GAL3 levels were significantly higher in patients with reduced eGFR (<30 mL/min/1.73 m^2). O'Seaghdha et al. already demonstrated that high levels of GAL3 were associated with a rapid decline of eGFR and with a higher risk of incidence of chronic kidney disease (CKD) [30]. Findings from our study are also supported by a study from Tang et al. who recently demonstrated that high GAL3 levels are associated with a poor renal function [24]. As a consequence, the inverse relationship between GAL3 and renal function, which we observed in our AHF patients, leads to the suggestion that increased plasma GAL3 in AHF might be linked to renal dysfunction, and the ability of GAL3 to predict outcomes in HF might reflect the consequences of renal impairment [3, 24, 25]. Moreover, GAL3 levels were significantly higher in patients with age >71 years, too. This

(a)

(b) Kaplan-Meier GAL3 for all events (death + rehospitaliza-tion)
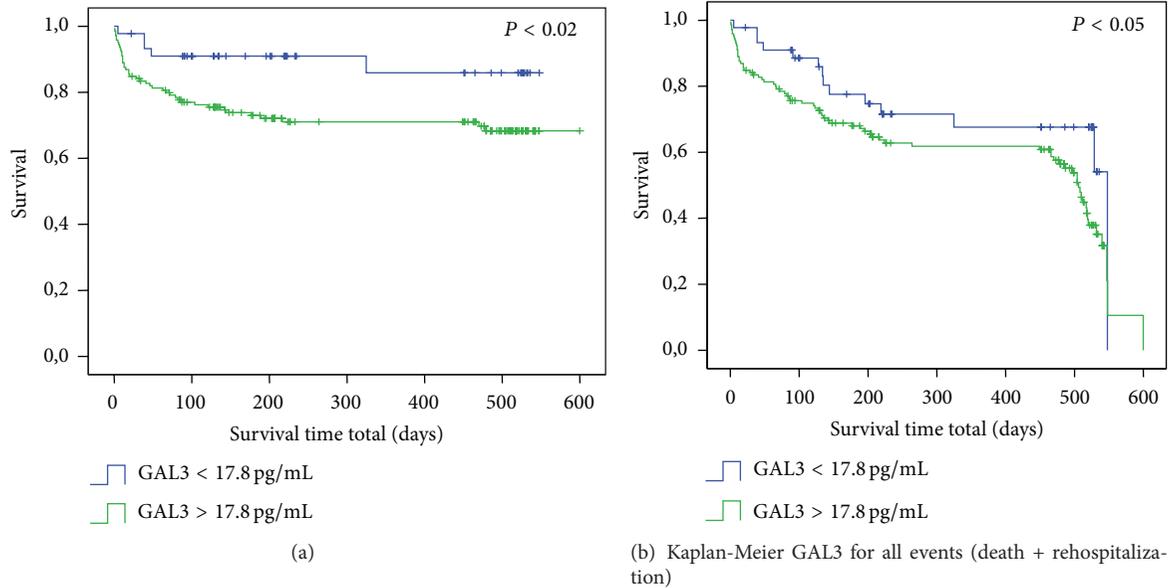
FIGURE 3: Kaplan-Meier for death (a) and events (b) on the basis of GAL3 values greater than 17.8 ng/mL.

suggests that in evaluating the value of GAL3 the physician should take into account the age of patients as confounding factor. This association of elevated GAL3 level and age should not be surprising; it is well known that heart fibrosis is a structural process related to aging. Other authors already found this relationship with GAL3 and age in the same cohort of patients [24]. We also found that BIVA had significant prognostic value for death for each considered follow-up time. This is not surprising and confirms previous study of our group, we also demonstrated additive value for AHF risk stratification of BIVA + BNP [8, 9]. The most important of our opinion results of our study is that the combination of BIVA + GAL3 increases the prognostic value for death and also for rehospitalization. It seems that the prognostic value of the combining of BIVA and GAL3 is of great significance since they mirror two different physiopathological aspects of HF. BIVA (phase angle) represents the degree of body fluid congestion, typical of AHF patients especially in the end stage of the disease; on the other hand, GAL3 value represents the level of fibrosis and the heart remodeling [31]. The combination of BIVA (phase angle) and GAL3 seems to have the better AUC compared to BIVA alone or GAL3 alone in predicting patients' adverse outcome. Nevertheless in our study multivariate Cox regression analysis showed that GAL3 is an independent variable more than BIVA variables to predict death and rehospitalization of value 32.24 ng/mL only at 30 days. These results strengthen the hypothesis that GAL3 could be considered a better predictive marker in comparison to BIVA and BNP when measured at admission in ED. More studies on larger population group are needed to confirm this hypothesis. When the survival Kaplan-Meier curve was made for GAL3, we found that, considering the cut-off of 17.8 ng/mL, those patients above this cut-off had a significant higher incidence of death and rehospitalization. This confirms the importance of cut-off of

GAL3 of 17.8 ng/mL representing an additive value to help physicians especially emergency physicians to individuate those patients of adverse outcomes.

5. Conclusion

In patients admitted for AHF an early assessment of GAL3 and BIVA seems to be useful in identifying patients at high risk for death and rehospitalization at short and long term. Combining the biomarker and the device could be of great utility since they are monitoring the severity of two patho-physiological different mechanisms underlining the severity of disease: heart fibrosis and fluid overload. GAL3 per se has the strongest independent predicting value for death and rehospitalization at 30 days with a cut-off of 32.24 ng/mL. The use of combining GAL3 and BIVA assessment, at the moment of AHF patients' presentation, could support decision making and different therapeutic approach.

Conflict of Interests

The authors declare that there is no conflict of interests regarding the publication of this paper.

Acknowledgment

References

[1] H. M. Krumholz, A. R. Merrill, E. M. Schone et al., "Patterns of hospital performance in acute myocardial infarction and

heart failure 30-day mortality and readmission," *Circulation: Cardiovascular Quality and Outcomes*, vol. 2, no. 5, pp. 407–413, 2009.

[2] A. S. Desai and L. W. Stevenson, "Rehospitalization for heart failure: predict or prevent?" *Circulation*, vol. 126, no. 4, pp. 501–506, 2012.

[3] R. V. Shah, A. A. Chen-Tournoux, M. H. Picard, R. R. van Kimmenade, and J. L. Januzzi, "Galectin-3, cardiac structure and function, and long-term mortality in patients with acutely decompensated heart failure," *European Journal of Heart Failure*, vol. 12, no. 8, pp. 826–832, 2010.

[4] R. R. van Kimmenade, J. L. Januzzi Jr., P. T. Ellinor et al., "Utility of amino-terminal pro-brain natriuretic peptide, galectin-3, and apelin for the evaluation of patients with acute heart failure," *Journal of the American College of Cardiology*, vol. 48, no. 6, pp. 1217–1224, 2006.

[5] E. López, V. del Pozo, T. Miguel et al., "Inhibition of chronic airway inflammation and remodeling by galectin-3 gene therapy in a murine model," *The Journal of Immunology*, vol. 176, no. 3, pp. 1943–1950, 2006.

[6] M. Gheorghiade, F. Follath, P. Ponikowski et al., "Assessing and grading congestion in acute heart failure: a scientific statement from the acute heart failure committee of the heart failure association of the European society of cardiology and endorsed by the European society of intensive care medicine," *European Journal of Heart Failure*, vol. 12, no. 5, pp. 423–433, 2010.

[7] A. Piccoli, M. Codognotto, V. Cianci et al., "Differentiation of cardiac and noncardiac dyspnea using bioelectrical impedance vector analysis (BIVA)," *Journal of Cardiac Failure*, vol. 18, no. 3, pp. 226–232, 2012.

[8] S. Di Somma, B. de Berardinis, C. Bongiovanni, R. Marino, E. Ferri, and B. Alfei, "Use of BNP and bioimpedance to drive therapy in heart failure patients," *Congestive Heart Failure*, vol. 16, no. supplement 1, pp. S56–S61, 2010.

[9] S. Di Somma, I. Lalle, L. Magrini et al., "Additive diagnostic and prognostic value of Bioelectrical Impedance Vector Analysis (BIVA) to brain natriuretic peptide "grey-zone" in patients with acute heart failure in the emergency department," *European Heart Journal: Acute Cardiovascular Care*, vol. 3, no. 2, pp. 167–175, 2014.

[10] J. J. McMurray, S. Adamopoulos, S. D. Anker et al., "ESC Guidelines for the diagnosis and treatment of acute and chronic heart failure 2012: the task force for the diagnosis and treatment of acute and chronic heart failure 2012 of the European Society of Cardiology. Developed in collaboration with the Heart Failure Association (HFA) of the ESC," *European Heart Journal*, vol. 33, no. 14, pp. 1787–1847, 2012.

[11] A. S. Levey, J. P. Bosch, J. B. Lewis, T. Greene, N. Rogers, and D. Roth, "A more accurate method to estimate glomerular filtration rate from serum creatinine: a new prediction equation. Modification of diet in Renal Disease Study Group," *Annals of Internal Medicine*, vol. 130, no. 6, pp. 461–470, 1999.

[12] P. A. McCullough, A. Olobatoke, and T. E. Vanhecke, "Galectin-3: a novel blood test for the evaluation and management of patients with heart failure," *Reviews in Cardiovascular Medicine*, vol. 12, no. 4, pp. 200–210, 2011.

[13] D. J. Whellan, C. M. O'Connor, K. L. Lee et al., "Heart failure and a controlled trial investigating outcomes of exercise training (HF-ACTION): design and rationale," *American Heart Journal*, vol. 153, no. 2, pp. 201–211, 2007.

[14] R. Valle, N. Aspromonte, L. Milani et al., "Optimizing fluid management in patients with acute decompensated heart failure (ADHF): the emerging role of combined measurement of body hydration status and brain natriuretic peptide (BNP) levels," *Heart Failure Reviews*, vol. 16, no. 6, pp. 519–529, 2011.

[15] R. F. Kushner, "Bioelectrical impedance analysis: a review of principles and applications," *Journal of the American College of Nutrition*, vol. 11, no. 2, pp. 199–209, 1992.

[16] A. Piccoli, "Bioelectric impedance vector distribution in peritoneal dialysis patients with different hydration status," *Kidney International*, vol. 65, no. 3, pp. 1050–1063, 2004.

[17] H. C. Lukaski, P. E. Johnson, W. W. Bolonchuk, and G. I. Lykken, "Assessment of fat-free mass using bioelectrical impedance measurements of the human body," *The American Journal of Clinical Nutrition*, vol. 41, no. 4, pp. 810–817, 1985.

[18] R. A. de Boer, L. Yu, and D. J. van Veldhuisen, "Galectin-3 in cardiac remodeling and heart failure," *Current Heart Failure Reports*, vol. 7, no. 1, pp. 1–8, 2010.

[19] A. Maisel, C. Mueller, K. Adams Jr. et al., "State of the art: using natriuretic peptide levels in clinical practice," *European Journal of Heart Failure*, vol. 10, no. 9, pp. 824–839, 2008.

[20] R. A. de Boer, A. A. Voors, P. Muntendam, W. H. van Gilst, and D. J. van Veldhuisen, "Galectin-3: a novel mediator of heart failure development and progression," *European Journal of Heart Failure*, vol. 11, no. 9, pp. 811–817, 2009.

[21] H. Milting, P. Ellinghaus, M. Seewald et al., "Plasma biomarkers of myocardial fibrosis and remodeling in terminal heart failure patients supported by mechanical circulatory support devices," *Journal of Heart and Lung Transplantation*, vol. 27, no. 6, pp. 589–596, 2008.

[22] R. A. de Boer, D. J. Lok, T. Jaarsma et al., "Predictive value of plasma galectin-3 levels in heart failure with reduced and preserved ejection fraction," *Annals of Medicine*, vol. 43, no. 1, pp. 60–68, 2011.

[23] M. Lainscak, A. P. Coletta, N. Sherwi, and J. G. Cleland, "Clinical trials update from the Heart Failure Society of America Meeting 2009: FAST, IMPROVE-HF, COACH galectin-3 substudy, HF-ACTION nuclear substudy, DAD-HF, and MARVEL-1," *European Journal of Heart Failure*, vol. 12, no. 2, pp. 193–196, 2010.

[24] W. H. Tang, K. Shrestha, Z. Shao et al., "Usefulness of plasma galectin-3 levels in systolic heart failure to predict renal insufficiency and survival," *American Journal of Cardiology*, vol. 108, no. 3, pp. 385–390, 2011.

[25] D. J. A. Lok, P. van der Meer, P. W. de la Porte et al., "Prognostic value of galectin-3, a novel marker of fibrosis,in patients with chronic heart failure: data from the DEAL-HF study," *Clinical Research in Cardiology*, vol. 99, no. 5, pp. 323–328, 2010.

[26] A. R. van der Velde, L. Gullestad, T. Ueland et al., "Prognostic value of changes in galectin-3 levels over time in patients with heart failure data from CORONA and COACH," *Circulation: Heart Failure*, vol. 6, no. 2, pp. 219–226, 2013.

[27] A. Bayes-Genis, M. de Antonio, J. Vila et al., "Head-to-head comparison of 2 myocardial fibrosis biomarkers for long-term heart failure risk stratification: ST2 versus galectin-3," *Journal of the American College of Cardiology*, vol. 63, no. 2, pp. 158–166, 2014.

[28] W. C. Meijers, J. L. Januzzi, C. deFilippi et al., "Elevated plasma galectin-3 is associated with near-term rehospitalization in heart failure: a pooled analysis of 3 clinical trials," *American Heart Journal*, vol. 167, no. 6, pp. 853.e4–860.e4, 2014.

[29] S. Di Somma, L. Magrini, V. Pittoni et al., "In-hospital percentage BNP reduction is highly predictive for adverse events in patients admitted for acute heart failure: the Italian RED Study," *Critical Care*, vol. 14, no. 3, article R116, 2010.

[30] C. M. O'Seaghdha, S. J. Hwang, J. E. Ho, R. S. Vasan, D. Levy, and C. S. Fox, "Elevated galectin-3 precedes the development of CKD," *Journal of the American Society of Nephrology*, vol. 24, no. 9, pp. 1470–1477, 2013.

[31] U. C. Sharma, S. Pokharel, T. J. van Brakel et al., "Galectin-3 marks activated macrophages in failure-prone hypertrophied hearts and contributes to cardiac dysfunction," *Circulation*, vol. 110, no. 19, pp. 3121–3128, 2004.

Research Article

Comparison of Commercial Genetic-Testing Services in Korea with 23andMe Service

Sollip Kim, Ki-Won Eom, Chong-Rae Cho, and Tae Hyun Um

Department of Laboratory Medicine, Ilsan Paik Hospital, Inje University College of Medicine,
Joowha-ro 170, Ilsanseo-gu, Goyang, Gyeonggi 411-706, Republic of Korea

Correspondence should be addressed to Tae Hyun Um; uthmd@hanmail.net

Introduction. Genetic testing services for disease prediction, drug responses, and traits are commercially available by several companies in Korea. However, there has been no evaluation study for the accuracy and usefulness of these services. We aimed to compare two genetic testing services popular in Korea with 23andMe service in the United States. *Materials and Methods*. We compared the results of two persons (one man and one woman) serviced by Hellogene Platinum (Theragen Bio Institute), DNAGPS Optimus (DNAlink), and 23andMe service. *Results*. Among 3 services, there were differences in the estimation of relative risks for the same disease. For lung cancer, the range of relative risk was from 0.9 to 2.09. These differences were thought to be due to the differences of applied single nucleotide polymorphisms (SNPs) in each service for the calculation of risk. Also, the algorithm and population database would have influence on the estimation of relative disease risks. The concordance rate of SNP calls between DNAGPS Optimus and 23andMe services was 100% (30/30). *Conclusions*. Our study showed differences in disease risk estimations among three services, although they gave good concordance rate for SNP calls. We realized that the genetic services need further evaluation and standardization, especially in disease risk estimation algorithm.

1. Introduction

Genetic testing services for disease prediction, drug responses, and personal traits are becoming available by several companies and getting more popular in Korea. These genetic services were based on the results of high-tech methods, such as microarray [1]. The analytical methods for detecting hundreds to thousands of single nucleotide polymorphisms (SNPs) are very complex multistep procedures, which are liable to error [1]. Such errors could be translated into a risk misclassification, which in turn could make an individual feel a false sense of security or unnecessary anxiety [1]. So, analytical accuracy and credibility for risk estimation algorithms should be evaluated for commercialized genetic services. Although previous studies showed that the concordance of SNP calls between 23andMe and Navigenics was 99.7–100%, there were some considerable differences in the calculated relative risk of diseases in those studies [1, 2]. Newly developed Korean services have not been evaluated for SNP genotype

accuracy and risk estimation of disease, yet. We aimed to compare Korean genetic services with 23andMe service for the evaluation.

2. Materials and Methods

This study was approved by the local institutional ethics committee (IRB number IB-3-1405-017). All subjects provided written informed consent. Schematic diagram of study design was shown in Figure 1. Samples were obtained from two volunteers, one healthy man (participant 1) and one healthy woman (participant 2). Samples were obtained with dedicated sample-collection kits according to each company's instruction. EDTA-anticoagulated blood samples were for Hellogene Platinum (Theragen Bio Institute, Suwon, South Korea) and DNAGPS Optimus (DNAlink, Seoul, South Korea), and saliva samples were for 23andMe (Mountain View, CA, USA).

Theragen Bio Institute used DNA microarrays SNP chip developed by themselves; DNAlink used DNA microarrays
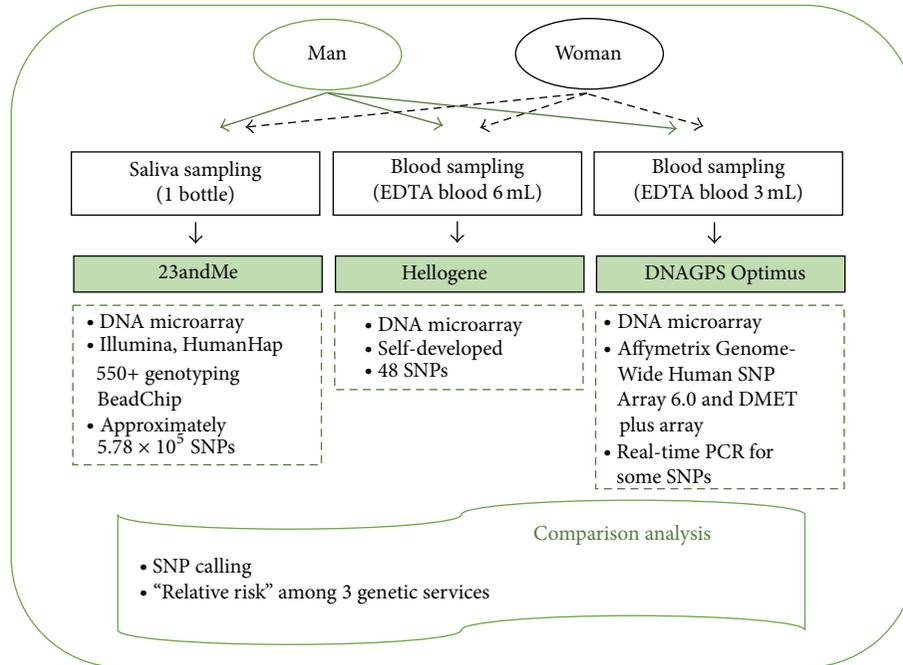
FIGURE 1: Schematic diagram of this study design.

from Affymetrix GeneChip (Genome-Wide Human SNP Array 6.0 and DMET plus array) for the most of SNPs. Real-time PCR with TaqMan probe was used for some SNPs. 23andMe used DNA microarrays from Illumina with the HumanHap 550+ Genotyping BeadChip (approximately 5.78×10^5 SNP) [1]. SNP call results and relative risks data for diseases were retrieved from formal customer reports of three services. The rs numbers of SNPs of DNAGPS Optimus and 23andMe were used for the evaluation of analytical SNP call concordance rate. But it was not available for Hellogene Platinum service because of proprietary concern of the manufacturer. The disease risk analysis of Korean services was known to be for the Korean population. For the 23andMe, we selected "Asian population" for the disease risk analysis through the 23andMe internet web page (https://www.23andme.com/).

3. Results

The numbers of SNPs used in each genetic service were shown in Table 1. All genetic services covered 16 disease categories. Mean 1.3 (range, 1-2) SNPs for each disease category were used in Hellogene Platinum service, while 3.7 (2–7) and 5.8 (1–15) SNPs were used in DNAGPS Optimus and in 23andMe service, respectively. Throughout 16 disease categories, 3 SNPs (rs9642880 for bladder cancer, rs1994090 for Parkinson's disease, and rs9939609 for obesity) were concurrently used in 3 services.

The comparison data of relative risks among 3 genetic services was shown in Table 2. The relative risks for several disease risk estimations were not concurred. For the lung cancer, its risk of participant 1 was very high in Hellogene

Platinum and DNAGPS Optimus but was low in 23andMe. And the risk for participant 2 was high in Hellogene Platinum but was relatively low in DNAGPS Optimus and 23andMe.

The SNP calls concordance rate between services were done for DANGPS Optimus and 23andMe, 100% (30/30).

4. Discussion

This study was the first investigational study on Korean commercial genetic services for disease risk estimation. Each genetic service was based on an association between a specific genetic variant and a particular disorder [3]. The risk estimation was based on the data of several genome-wide association studies (GWAS), which showed the odds ratios between disease developing risk and genetic variants (SNP) in the huge population of an ethnic group. Most of the genetic variants tested for GWAS are weak predictors, accounting for only a small fraction of the overall heritability of a trait or disease, with the relative risk conferred being less than two [4, 5]. Being common, all individuals are likely to carry one or more risk alleles [6]. In our study, the highest relative risk was only 2.41 and mean relative risk was 1.02 ± 0.46. Even when GWAS demonstrated a strong association, there may not be any clinical utility [6]. One cannot base treatment decisions on such genome information, because most genotype information has no bearing on treatment strategy so far [6]. Most important concern is that commercial genetic services' predictive value must be sufficient to meet the standards for clinical use [3]. The clinical utility of a genetic test should be an essential criterion for deciding to offer this test to a person or a group of persons [3]. We emphasize that genetic services must be evaluated for clinical

Table 1: The number of SNPs used for calculation of relative risk in three genetic services.

Category	The number of SNPs for all ethnic group (for Asian)			Number of overlapping SNPs among services	
	Hellogene Platinum	DNAGPS Optimus	23andMe		
Lung cancer	1 (1)	3 (2)	1 (0)	0	
Esophageal squamous cell cancer	2 (2)	5 (5)	1 (1)	2	(Hellogene and DNAGPS)
Colorectal caner	1 (1)	4 (3)	4 (2)	2	(DNAGPS and 23andMe)
Bladder cancer	1 (1)	3 (0)	6 (1) for male 7 (2) for female	1	(Three services)
Breast cancer (for female only)	1 (1)	5 (5)	8 (3)	1	(Hellogene and DNAGPS)
Atopic dermatitis	1 (1)	3 (1)	5 (1)	0	
Rheumatoid arthritis	1 (1)	4 (4)	9 (2)	1	(DNAGPS and 23andMe)
Systemic lupus erythematosus	1 (1)	3 (3)	6 (4)	0	
Psoriasis	2 (2)	4 (4)	3 (0)	1	(Hellogene and DNAGPS)
Diabetes mellitus, type 1	1 (1)	4 (0)	8 (0)	0	
Body mass index (obesity)	1 (1)	2 (2)	10 (0)	1 2	(Three services) (DNAGPS and 23andMe)
Atrial fibrillation	1 (1)	2 (0)	2 (0)	1	(Hellogene and DNAGPS)
Coronary artery disease	1 (1)	7 (4)	15 (0)	0	0
Parkinson's disease	2 (2)	4 (4)	10 (4)	1 1	(Three services) (Hellogene and 23andMe)
Narcolepsy	1 (1)	2 (1)	1 (0)	0	
Warfarin maintenance dose	1[†]	4[‡]	3[‡]	2	(DNAGPS and 23andMe)

[†] Warfarin dosing of Hellogene Platinum was based on *GGCX* gene genotyping results.
[‡] Warfarin dosing of DNAGPS Optimus and 23andMe was based on *CYP2C9* and *VKORC1* gene genotyping results.

Table 2: Comparison of relative risks among 3 genetic tests.

Category	Relative risk for participant 1 (man)			Relative risk for participant 2 (woman)		
	Hellogene Platinum	DNAGPS Optimus	23andMe	Hellogene Platinum	DNAGPS Optimus	23andMe
Lung cancer	2.09	1.97	0.8[*]	2.09	0.92	0.8[*]
Esophageal squamous cell carcinoma	1.25	2.41	1.21	0.72	0.52	0.8
Colorectal caner	1.36	0.73	1.1	0.98	0.97	1.1
Bladder cancer	0.77	0.8	Typical	0.77	0.9	Typical/lower
Breast cancer	NA	NA	NA	0.84	0.77	0.98
Atopic dermatitis	1.16	1.13	Typical	1.16	0.74	Lower
Rheumatoid arthritis	NA	NA	0.71	0.97	2.95	1.1
Systemic lupus erythematosus	NA	NA	NA	0.97	1.47	1.09
Psoriasis	0.97	0.46	0.87[*]	0.69	1.06	0.44[*]
Diabetes mellitus, type 1	0.77	0.97	0.08[*]	1.11	1.08	0.1[*]
Body mass index (obesity)	0.91		0.85[*]	0.91		0.83[*]
Atrial fibrillation	0.94	0.68	1.12[*]	0.94	1.39	1.93[*]
Coronary artery disease	1.06	0.51	0.78[*]	0.62	0.34	0.71[*]
Parkinson's disease	1.09	0.84	1.05	0.95	1.04	0.77
Narcolepsy	1.41	1.29	Lower[*]	1.41	1.29	Typical[*]
Warfarin maintenance dose	Normal dose	Moderate dose	Decreased dose	Normal dose	Increased dose	Slightly decreased dose

NA: not applicable.
[*] Relative risk in European. There was no Asian data.

utility just as other medical procedures. In Korea, all newly introduced medical procedure and health technology should be applied to clinical field after being thoroughly evaluated by new health technology assessment (nHTA) system.

The results offered by commercial genetic services could inform health-related decisions such as lifestyle modification and medication [7]. Therefore analytical accuracy is essential. In this study, the concordance rate of SNP calls between DNAGPS Optimus and 23andMe services was 100% (30/30). This may be regarded as high concordance. The discrepant call for same SNP could gave totally oppositive interpretation. Continuous proficiency analysis and on-site inspection would be necessary for the improvement of analytical performance and user confidence.

Although methodology of GWAS has been developed through decades by standardization of study protocol and statistical method, it still has several issues and limitations. Lack of well-defined case and control groups, insufficient sample size, control for multiple testing, and control for population stratification are common problems [8]. Therefore, selection of optimal SNPs from qualified GWAS study is very important for calculation of individual disease risk. In this study, the numbers of SNPs for calculation for disease risk were different in each genetic service. While mean 1.3 (range, 1-2) SNPs for risk calculation were used in Hellogene Platinum, mean 3.7 (range, 2–7) SNPs and 5.8 (range, 1–15) SNPs were used for DNAGPS Optimus and 23andMe, respectively (Table 1). Also, the results of GWAS for the same disorder could be different according to the ethnic group; consequently the relative risks of genetic services entail different results. For example, the genotype of *SNCA* gene rs356220 CT means the relative risk of 1.02 for European but 0.96 for Asian (Participant 1). The selection of appropriate population for GWAS is very important. Some diseases listed in Korean genetic tests did not have even Asian genotype information, needless to say Korean data. The information obtained from Korean population should be more gathered into database.

In this study, each institute used their own calculation method for disease risk estimation. This was not only due to the lack of consensus guideline for selection of SNPs for risk calculation, but also due to use of unpublished data, which is produced by each institute. It could make selection bias, consequently making huge miscalculation of disease risk. For example, the SNP calls of rs2274223 were the same between DNAGPS Optimus and 23andMe services, but risks for esophageal cancer were different (1.85 for DNAGPS Optimus versus 1.21 for 23andMe for participant 1). Methodology of risk calculation must be validated and standardized.

For proper evaluation, each genetic service must provide the accurate and sufficient information, which is essential for objective and scientific interpretation and consultation, to doctors and patients. This information includes at least gene names, SNP names (rs number), used published references for risk calculation, test method, risk calculation method, and performance characteristics of the tests as other clinical genetic tests. If there is an interpretation guideline for specific genetic tests, each institute must follow this. In this study, even though there has been an established interpretation guideline for warfarin dosing (http://www.warfarindosing.org/) [9–11], DNAGPS Optimus does not interpret the results properly; consequently the dosing results of DNAGPS were opposite to those of 23andMe. What is worse is that Hellogene tested inapposite gene (*GGCX* gene) for warfarin dosing. This problem could be caused by lack of participation of medical specialist when these genetic services were developed. The genetic services offering the disease risk are not a merely genetic test for research but a medical test for clinical use. Therefore, doctors, especially laboratory physician, should be involved in the development and validation process of genetic services. In a case of other medical genetic tests, laboratory physician has responsibility of the whole test procedure and interpretative report, because its influences for patients are quite huge.

Laws and institution or clinical practices must be made ahead of consideration of commercialization to protect the privacy of the individual's genetic profile, which is the most private information [12]. There is some debate over a person's right to refuse to know that some genetic information has been engaged [12]. For these reasons, US Food & Drug Administration (FDA) ordered the 23andMe to stop marketing its health-related genetic test kit to consumers in November 2013 [12].

In conclusion, our study showed good concordance for SNP calls but discouraging concordance for disease risk estimation among three genetic services. Although they were performed by different companies using different assay platforms, we realized that these genetic services need standardization of interpretation algorithm and detailed evaluation of clinical utility.

Conflict of Interests

The authors declare that they have no conflict of interests.

Acknowledgments

References

[1] K. Imai, L. J. Kricka, and P. Fortina, "Concordance study of 3 direct-to-consumer genetic-testing services," *Clinical Chemistry*, vol. 57, no. 3, pp. 518–521, 2011.

[2] P. C. Ng, S. S. Murray, S. Levy, and J. C. Venter, "An agenda for personalized medicine," *Nature*, vol. 461, no. 7265, pp. 724–726, 2009.

[3] P. Borry, "Statement of the ESHG on direct-to-consumer genetic testing for health-related purposes," *European Journal of Human Genetics*, vol. 18, no. 12, pp. 1271–1273, 2010.

[4] A. C. Sturm and K. Manickam, "Direct-to-consumer personal genomic testing: a case study and practical recommendations for 'genomic counseling'," *Journal of Genetic Counseling*, vol. 21, no. 3, pp. 402–412, 2012.

[5] C. C. Chung and S. J. Chanock, "Current status of genome-wide association studies in cancer," *Human Genetics*, vol. 130, no. 1, pp. 59–78, 2011.

[6] C. Li, "Personalized medicine—the promised land: are we there yet?" *Clinical Genetics*, vol. 79, no. 5, pp. 403–412, 2011.

[7] D. J. Kaufman, J. M. Bollinger, R. L. Dvoskin, and J. A. Scott, "Risky business: risk perception and the use of medical services among customers of DTC personal genetic testing," *Journal of Genetic Counseling*, vol. 21, no. 3, pp. 413–422, 2012.

[8] T. A. Pearson and T. A. Manolio, "How to interpret a genome-wide association study," *Journal of the American Medical Association*, vol. 299, no. 11, pp. 1335–1344, 2008.

[9] B. F. Gage, C. Eby, J. A. Johnson et al., "Use of pharmacogenetic and clinical factors to predict the therapeutic dose of warfarin," *Clinical Pharmacology and Therapeutics*, vol. 84, no. 3, pp. 326–331, 2008.

[10] T. E. Klein, R. B. Altman, N. Eriksson, B. F. Gage, S. E. Kimmel, M. T. Lee et al., "Estimation of the warfarin dose with clinical and pharmacogenetic data," *The New England Journal of Medicine*, vol. 360, pp. 753–764, 2009.

[11] M. R. McClain, G. E. Palomaki, M. Piper, and J. E. Haddow, "A Rapid-ACCE review of CYP2C9 and VKORC1 alleles testing to inform warfarin dosing in adults at elevated risk for thrombotic events to avoid serious bleeding," *Genetics in Medicine*, vol. 10, no. 2, pp. 89–98, 2008.

[12] M. Healy, "FDA wins high-profile support in consumer genetics kerfuffle," Los Angeles Times, March 2014, http://www.latimes.com/science/sciencenow/la-sci-sn-fda-consumer-genetics-20140313,0,3621735.story.

Research Article

Hematological and Biochemical Markers of Iron Status in a Male, Young, Physically Active Population

Lázaro Alessandro Soares Nunes,[1] Helena Zerlotti W. Grotto,[2] René Brenzikofer,[3] and Denise Vaz Macedo[4]

[1] *Faculty of Biomedical Sciences, Metrocamp College-IBMEC Group, 13035-270 Campinas, SP, Brazil*

[2] *Department of Clinical Pathology, School of Medical Sciences, State University of Campinas, 13083-881 Campinas, SP, Brazil*

[3] *Laboratory of Instrumentation for Biomechanics, Physical Education Institute, State University of Campinas, 13083-851 Campinas, SP, Brazil*

[4] *Laboratory of Exercise Biochemistry-LABEX, Biochemistry Department, Biology Institute, State University of Campinas, 13083-970 Campinas, SP, Brazil*

Correspondence should be addressed to Lázaro Alessandro Soares Nunes; lazaroalessandro@yahoo.com.br

The aim of this study was to establish reference intervals (RIs) for the hemogram and iron status biomarkers in a physically active population. The study population included male volunteers ($n = 150$) with an average age of 19 ± 1 years who had participated in a regular and controlled exercise program for four months. Blood samples were collected to determine hematological parameters using a Sysmex XE-5000 analyzer (Sysmex, Kobe, Japan). Iron, total iron-binding capacity (TIBC), transferrin saturation and ferritin, and high-sensitivity C-reactive protein (CRP) concentrations in serum samples were measured using commercial kits (Roche Diagnostics, GmbH, Mannheim, Germany) and a Roche/Hitachi 902 analyzer. The RIs were established using the RefVal program 4.1b. The leucocyte count, TIBC, and CRP and ferritin concentrations exhibited higher RIs compared with those in a nonphysically active population. Thirty volunteers (outliers) were removed from the reference population due to blood abnormalities. Among the outliers, 46% exhibited higher CRP concentrations and lower concentrations of iron and reticulocyte hemoglobin compared with the nonphysically active population ($P < 0.001$). Our results showed that it is important to establish RIs for certain laboratory parameters in a physically active population, especially for tests related to the inflammatory response and iron metabolism.

1. Introduction

The physical training undertaken by athletes results in different degrees of microtrauma to the muscle. This microtrauma is related to the acute inflammatory response, which promotes muscle repair and regeneration. This response involves the production, recruitment, and delivery of proteins (e.g., cytokines, immunoglobulins, and acute phase proteins) and cells (e.g., leukocytes) in the circulation [1]. Acute and chronic exercise training produce different effects on hematological parameters. After a single bout of exercise, there is a rapid and pronounced neutrophilia due to demargination caused by shear stress and catecholamines, followed by a second delayed increase due to the cortisol-induced release of neutrophils from the bone marrow [2, 3]. Whereas the numbers of monocytes and lymphocytes can increase during and immediately after an exercise bout, the lymphocyte count falls below preexercise levels during the early stages of recovery, returning to basal levels within 4 hours [4]. All of these numbers generally return to basal levels within 3–24 hours [5].

Exercise training can influence immune function, health, and performance. In general, exercise training with low-to-moderate volume and intensity, with gradual increases,

can enhance immune function and reduce the incidence of infections [3]. However, among highly trained and elite athletes, high-intensity training periods and strenuous physical exercise are associated with an increased susceptibility to upper respiratory tract infections (URTIs) [3, 6, 7]. Moreover, other factors, including lifestyle behaviors and nutritional status, can influence an athlete's immune function. Hence, monitoring an athlete's immune function through hematological parameters has become an important part of competition preparation [4].

Fully automated hematology analyzers have the capacity to quantify reticulocytes, the immature form of erythrocytes. The evaluation of immature red blood cell (RBC) parameters, including the number and hemoglobin content of reticulocytes, can be useful for monitoring positive adaptations to training or for identifying the use of prohibited substances to stimulate bone marrow production. Moreover, measuring hemoglobin concentration and reticulocyte parameters may be useful for diagnosing sports anemia, which can impair an athlete's performance. Persistent abnormalities in RBCs, hemoglobin concentration, and hematological indices can also indicate pathological conditions, such as deficits in iron, folic acid, or vitamin B12. Furthermore, other hematological abnormalities (thalassemia, sickle cell disease, and hereditary spherocytosis) can also alter an athlete's RBC profile [8, 9].

Athletic-induced iron deficiency is commonly detected in athletes, particularly those who engage in endurance sports. Iron is an essential component of hemoglobin, myoglobin, cytochromes, and other iron-containing proteins that participate in oxidative phosphorylation [10]. Additionally, macrophages can accumulate iron derived from RBCs, which is recycled by the reticuloendothelial system and thus participates in the immune defense against microbial pathogens [11]. In the bloodstream, iron is coupled to transferrin and can inhibit damage by reactive oxygen species (ROS) derived from Fenton's reaction [12]. In reticuloendothelial cells in the liver, spleen, and bone marrow, iron is stored as ferritin and hemosiderin [13].

To monitor immune function and iron status in athletes, it is important to understand the influence of exercise training on hematological and iron-related biochemical parameters. To increase the utility of these screening tests in physically active individuals, it is crucial to establish specific reference intervals in a physically active population, according to the International Federation of Clinical Chemistry (IFCC) rules. The aim of this study was to establish reference intervals for the hemogram, high-sensitivity C-reactive protein, and iron status biomarkers in young male individuals who had undergone 4 months of regular physical activity.

2. Materials and Methods

2.1. Participants. The study included five hundred ($n = 150$) healthy male volunteers with an average age of 19 ± 1 years. All the participants were in the first stage of physical and educational preparation for careers in the army. They were from different regions of the country, and, for one year, they had lived at the same place and had participated in the

same numbers of hours of sleeping, eating, exercising, and studying. The volunteers participated in a regular and strictly controlled exercise program, which consisted predominantly of aerobic activities (high volume and different submaximal intensities), such as running and swimming. They had exercised three hours daily for four months in 2011 (from February to May). They had trained five days per week, with two days of rest. This group constituted a highly uniform group of young, physically active individuals. The participants provided written formal consent for participation in the research. The participants completed a questionnaire concerning their use of medication, complaints of pain, and injuries caused by training. Were selected for the reference group only those with no history of tobaccoism or chronic inflammatory disease. Those who were using medications, had not trained in the last three days, exhibited different clinical conditions (injuries related to training, muscle pain complaints, shin splint, or flu), or were suspected of congenital disorders (thalassemia or sickle cell disease) were analyzed separately as outliers. This study was approved by the University Ethics Committee for Research with Humans (CAAE: 0200.0.146.000-08). All the study procedures were in accordance with the Declaration of Helsinki.

2.2. Blood Sampling and Analysis. All blood samples were collected after two days of rest to avoid the effects of hemodynamic variations and acute hemodilution that are induced by exercise [14]. The blood samples were collected under the following standardized conditions: 2.0 mL of total venous blood was collected in vacuum tubes containing EDTA/K3 to determine hematological parameters, and 8.0 mL was collected in tubes with a Vacuette (Greiner Bio-one, Brazil) gel separator to obtain serum for biochemical measurements. The blood samples were collected in the morning after 12 hours of fasting, with the subjects being in a seated position. All the samples were then transported to the laboratory at 4°C and were analyzed within 60 min after the blood collection. The hematological parameters were obtained with a Sysmex XE-5000 automated analyzer, which uses a polymethine dye specific for RNA/DNA to facilitate reticulocyte enumeration and determinations of degree of immaturity and hemoglobin content. The e-Check (Lot 1144) Sysmex 3 levels were used as an internal quality control and were performed in parallel with the hematological tests. The means and standard deviation derived from the control samples were used to calculate the coefficient of analytical variation (CV_A). The analyzed parameters and each respective CV_A were as follows: red blood cell count (RBC) ($CV_A = 0.7\%$); blood hemoglobin concentration (Hb) ($CV_A = 1.1\%$); hematocrit (Ht) ($CV_A = 1.0\%$); mean corpuscular volume (MCV) ($CV_A = 0.8\%$); erythrocyte distribution width (RDW) ($CV_A = 0.9\%$); mean corpuscular hemoglobin (MCH) ($CV_A = 1.0\%$); mean corpuscular hemoglobin concentration (MCHC) ($CV_A = 1.2\%$); reticulocyte count (Ret) ($CV_A = 3.7\%$); immature reticulocyte fraction (IRF) ($CV_A = 10.0\%$); reticulocyte hemoglobin equivalent (Ret-He) ($CV_A = 2.5\%$); white blood cell (WBC) ($CV_A = 2.2\%$), lymphocyte (Lymph) ($CV_A = 2.3\%$), neutrophil (Neut) ($CV_A = 3.0\%$), monocyte

TABLE 1: The reference intervals, confidence intervals, and outliers excluded by Horn's algorithm for hematological parameters in a male, young, physically active population.

Analyses	Reference interval 2.5th–97.5th	90% confidence interval		Subjects (n)	Outliers (n)
		2.5th	97.5th		
WBC (10^9/L)	5.0–10.8	4.9–5.2	10.4–11.7	119	1
Lymph (%)	15.0–48.0	14.0–19.0	43–53	119	1
Lymph (10^9/L)	1.3–3.7	1.2–1.4	3.3–4.1	119	1
Neut (%)	37.0–72.0	33.0- 41.0	67.0–76.0	120	—
Neut (10^9/L)	2.4–7.5	2.3–2.5	6.6–8.0	119	1
Mono (%)	7. 0–13.0	6.5–7.5	13.0–15.0	118	2
Mono (10^9/L)	0.4–1.4	0.3–0.5	1.1–1.5	118	2
Eo (%)	0.9–7.7	0.8–1.2	7.0–7.8	114	6
Eo (10^9/L)	0.05–0.55	0.04–0.08	0.53–0.87	118	2
Baso (%)	0.4–1.8	0.3–0.4	1.5–1.9	117	3
Baso (10^9/L)	0.02–0.11	0.01–0.03	0.11–0.15	120	—
PLT (10^9/L)	141–305	133–153	284–320	120	—
MPV (fL)	9.8–13.4	9.7–10.1	13.0–13.7	120	—
IPF (%)	2.0–10.4	1.7–2.2	9.9–11.8	119	1
RBC (10^{12}/L)	4.77–5.72	4.74–4.84	5.57–5.77	118	2
Ht (%)	40.6–47.4	39.4–41.0	46.6–48.9	120	—
Hb (g/L)	133–162	132–135	158–163	118	2
MCV (fL)	80.0–89.5	79.5–80.7	88.6–91.2	118	2
MCH (pg)	26–30.0	24–26	30–31	120	—
MCHC (g/L)	32–35	31–32	34–35	119	1
RDW (%)	12.4–14.9	12.4–12.7	14.7–15.2	119	1
RDW-SD (fL)	38–45	37–38	44–46	120	—
RET (%)	0.54–1.33	0.5-0.6	1.2–1.4	120	—
RET (10^9/L)	28–68	24–30	64–75	120	—
IRF (%)	3–14	2.7–3.6	11.5–15.0	119	1
Ret-He (pg)	32.2–39.2	31.6–33.0	38.5–39.4	119	1

(Mono) (CV_A = 6.2%), basophil (Baso) (CV_A = 2.5%), eosinophil (Eo) (CV_A = 7.5%); platelet (PLT) counts (CV_A = 2.6%); mean platelet volume (MPV) (CV_A = 1.0%); and immature platelet fraction (IPF) (CV_A = 5.6%). The biochemical measurements were conducted using commercial kits (Roche Diagnostics, GmbH, Mannheim, Germany) and a Roche/Hitachi 902 analyzer. Control serum was used to estimate the imprecision of the methods of biochemical analysis. The assays included the serum concentrations of iron (CV_A = 1.0%), ferritin (CV_A = 2.1%), and high-sensitivity C-reactive protein (h-CRP) (CV_A = 3.2%) as well as total iron-binding capacity (TIBC) (CV_A = 5.4%). The percent transferrin saturation (% TSAT) was calculated as follows: [iron/(TIBC)] × 100.

2.3. Statistical Analysis. The data were tested for Gaussian distribution using the Kolmogorov-Smirnov test. The Mann-Whitney test for nonparametric distribution was used to determine the differences between the high h-CRP (outliers) and normal h-CRP (reference individuals) groups. GraphPad Prism 6.0 for Mac OS X (GraphPad Software) was used to perform the statistical analyses and create the graphs. Values of $P < 0.05$ were considered significant. Reference intervals

were established according to the IFCC rules using Ref Val program 4.1 beta [15]. We calculated the nonparametric 2.5th and 97.5th percentiles, with their 90% confidence intervals (CIs), using a bootstrap methodology. Horn's algorithm was used to remove the outliers from the reference population [16].

3. Results

After the blood sample analyses, 22 individuals who exhibited abnormal blood results (leukocyte count > 12.0×10^9/L, hemoglobin concentration < 120 g/L, or C-reactive protein level > 15.0 mg/L) [17, 18] or different clinical conditions (injuries related to training, muscle pain complaints, shin splint, or flu) were classified as outliers and were removed from the reference interval calculation. Additionally, eight individuals with mild microcytosis and higher RBC numbers, which are characteristics of thalassemia, were identified using the Mentzer index [19] and were excluded from the reference population and also included as outliers. As such, 120 healthy, physically active individuals constituted the reference sample group (Table 1).

TABLE 2: The reference intervals, confidence intervals, and outliers excluded by Horn's algorithm for biochemical parameters in a male, young, physically active population.

Analyses	Reference interval 2.5th–97.5th	90% confidence interval		Subjects (n)	Outliers (n)
		2.5th	97.5th		
h-CRP (mg/L)	0.2–10.2	0.2–0.3	7.0–14.8	120	—
Iron (μmol/L)	8.4–28.8	8.2–8.9	27.5–31.6	119	1
TIBC (μmol/L)	43.8–64.5	43.1–45.0	63.1–68.9	120	—
%TSAT	19–45	19–20	43–46	119	1
Ferritin (μg/L)	47–331	41–53	264–436	119	1

(a)

(b)

(c)
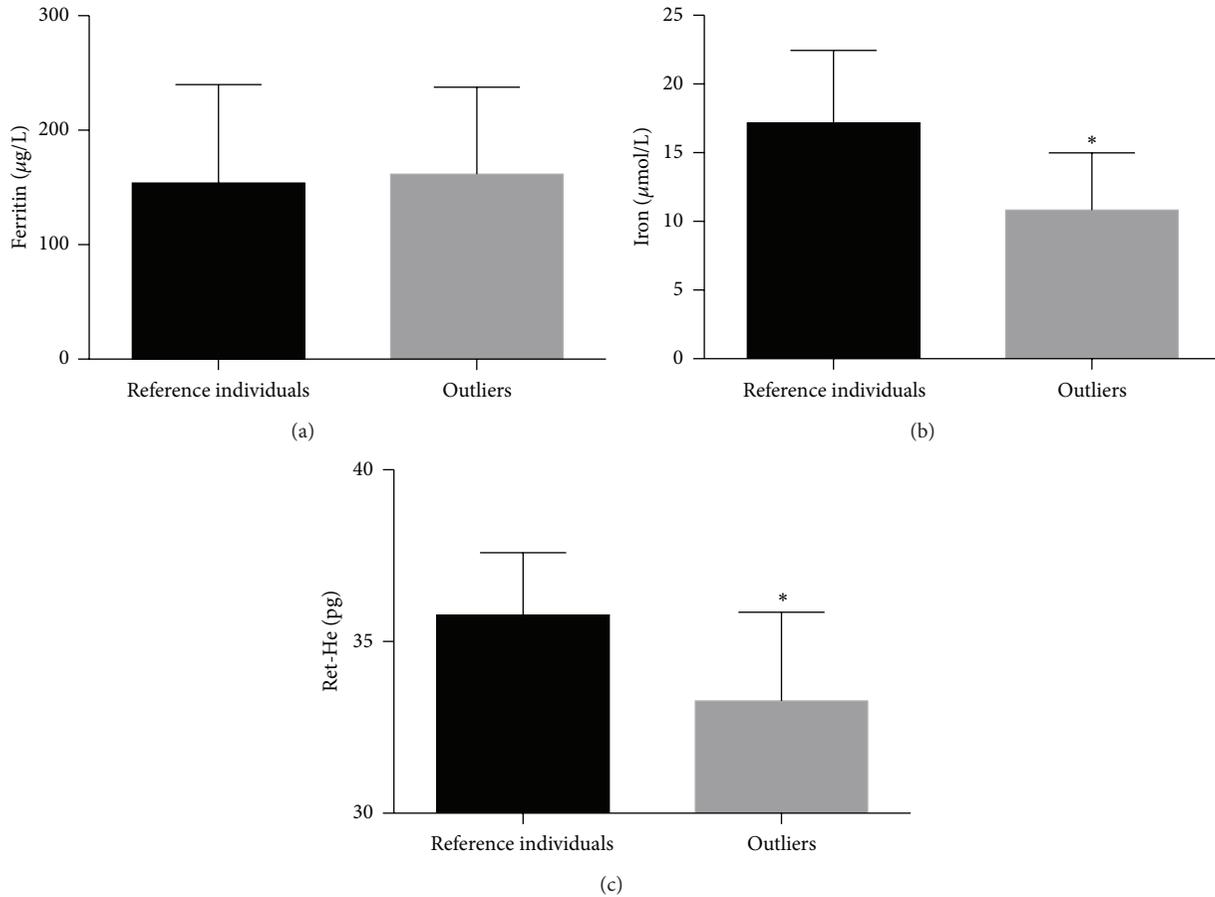
FIGURE 1: Ferritin (a), iron (b), and Ret-He (c) values in reference individuals (normal h-CRP) ($n = 119$) compared with outliers (higher h-CRP) ($n = 14$). The normal CRP reference range (<10.2 mg/L) was based on a reference population study. The graph shows the means ± standard deviation. $^{*}P < 0.001$.

Table 1 shows the reference intervals (2.5th and 97.5th percentiles) and the respective confidence intervals for the examined hematological parameters in male, young, physically active individuals after four months of regular and systematized training. The outliers detected by Horn's algorithm (indicated in Table 1) were removed from the reference interval calculation.

Table 2 shows the reference intervals and confidence intervals for iron status and acute phase proteins in male, young, physically active individuals.

In this study, 30 subjects were classified as outliers due to abnormal blood results and were excluded from the reference interval calculation. Moreover, 46% ($n = 14$) of the subjects classified as outliers presented CRP values above the reference intervals for physically active subjects. Figure 1 shows a comparison of the ferritin (a), iron (b), and Ret-He (c) values between the reference individuals (normal CRP concentrations) and outliers (higher CRP concentrations).

No differences in ferritin levels were observed between the normal and higher CRP groups (Figure 1(a)). The iron (Figure 1(b)) and Ret-He (Figure 1(c)) values were significantly lower in the higher CRP group compared with the reference group ($P < 0.001$).

4. Discussion

Previous studies from our group showed that different young, physically active individuals respond to four months of training stimulus similarly to athletes in terms of certain parameters in blood [17] and saliva [20], justifying the use of this young male trained population to establish reference intervals for sports medicine applications.

Exercise training appears to result in local and systemic imbalances in the anti-inflammatory, compared with the proinflammatory, status. This imbalance promotes tissue adaptation and protects the organism against the development of chronic inflammatory diseases and against the deleterious effects of overtraining, a condition in which systemic and chronic proinflammatory and prooxidant states appear to preponderate [21, 22]. In our population, we found slightly higher WBC and neutrophil counts in the lower percentile compared with healthy sedentary individuals (WBC = 3.5–9.8×10^9/L and Neut = 1.5–7.0×10^9/L) [23]. The 2.5th and 97.5th percentile monocyte counts (Table 1) were higher than those of a healthy, nonphysically active population (Mono = 0.2–0.64×10^9/L) [23], indicating the effects of training on this parameter. Blood monocytes are the main source of tissue macrophages recruited in response to exercise [24], and they participate in the repair, growth, and regeneration of muscles [25].

There is little published evidence suggesting clinical differences between the immune functions of sedentary and physically active subjects in the true resting state (i.e., more than 24 h after the last training session) [1]. In our study of physically active subjects, we found a slightly higher lymphocyte count compared with a nonphysically active population (lymphocytes = 1.0–2.9×10^9/L) [23].

The reference intervals for RBC parameters determined in our study did not differ from those in a nonphysically active population [23]. In sports medicine, mature and immature erythrocytes can be assessed to identify possible doping methods, such as the enhancement of oxygen transport by recombinant erythropoietin (rEPO) abuse. This indirect form of doping control was implemented by the World Anti-Doping Agency (WADA) through the hematological module of the athlete biological passport (ABP). As a part of the ABP, assessments of hemoglobin concentration and reticulocyte count allow the estimation of oxygen blood transport capacity and recent RBC production, respectively [26]. The reference intervals for reticulocyte count obtained in our study of physically active individuals were similar to those for a healthy nonphysically active population [23] and for athletes, including cyclists, swimmers, rugby players, tennis players, and soccer players [27–29].

The IRF in our population was relatively high compared with the general population (1.6–10.5%) using the same hematology analyzer [23]. The continuous stimulation of bone marrow due to accelerated iron metabolism, hypoxia, and exercise-induced hemolysis in athletes can partially explain this difference [8, 30]. Moreover, IRF can be a sensitive marker of erythropoietic activity in athletes undergoing altitude training or exposed to exogenous EPO stimuli [28].

Acute exercise bouts have been shown to promote an acute phase response, resulting in postexercise cytokine levels similar to those observed during sepsis or inflammatory disease. Strenuous exercise induces moderate increase in proinflammatory cytokines tumor necrosis factor α (TNF-α) and interleukin 1β [21, 31]. Interleukin-6 (IL-6) derived from the muscle cells can rise up to 100-fold during the exercise compared to preexercise levels [21]. CRP is the major acute phase protein associated with coronary events in apparently healthy subjects. Our CRP reference interval for physically active individuals (Table 2) was based on the 97.5th percentile. Other studies have found similar results for the 95th percentile in healthy, nonphysically active populations [32–34]. However, it is important to emphasize that these values are above the value (>3.0 mg/L) used to determine groups at high risk of cardiovascular disease, which is based on CRP [34]. Interleukin-6, which is produced in response to continuous training, can stimulate the synthesis of acute phase proteins by hepatocytes and can promote an elevated steady-state CRP concentration compared with healthy, nonphysically active subjects.

Iron, TIBC, and ferritin levels are traditional biomarkers for screening athletes during the training season [35]. Iron deficiency may have a negative impact on oxygen transport and immune defense, thus influencing athletic performance [36]. The main mechanisms of exercise-related iron loss in athletes include hemolysis, hematuria, sweating, gastrointestinal bleeding, and chronic inflammation [36]. Iron metabolism must be tightly regulated to supply iron as needed while avoiding the toxicity associated with iron excess. The main stimuli to regulate iron homeostasis are hypoxia, iron deficit, iron overload, and inflammation. In addition, iron metabolism is influenced by nutritional status, age, gender, bone marrow activity, and some pathological conditions such as bacterial infections [37]. Furthermore, recent reports have suggested that hepcidin, an iron-regulatory peptide hormone mainly produced in the liver, can regulate plasma iron concentrations in response to inflammation [38]. Hepcidin regulates iron concentration and tissue iron distribution via the inhibition of intestinal absorption, released by macrophages and iron mobilization from hepatic stores [39]. The primary mediator for the upregulation of hepcidin is IL-6 [40, 41]. Hepcidin levels increase 3–24 hours after exercise in response to IL-6, producing rapid decreases in the plasma iron concentration [40, 41]. The hepcidin synthesis decreases in iron deficiency, anaemia, and hypoxia [37]. The two last conditions are associated with increased erythropoiesis secondary to a rise of EPO secretion [42].

In our study, some subjects were classified as outliers due to high CRP concentrations and were excluded from the reference interval calculation. They had lower iron and hemoglobin reticulocyte concentrations (Ret-He), similar to those found in individuals with anemia of chronic disease (ACD). ACD results from the activation of the immune and inflammatory systems, resulting in the increased production of inflammatory cytokines that reduce the rate of iron mobilization from tissue stores [43]. The degree of hemoglobinization in reticulocytes is used to detect functional iron deficits and enables the early evaluation of bone marrow activity [44].

Ferritin levels, a biomarker of iron stores, did not differ between the higher and normal CRP groups (Figure 1(a)). Ferritin is an acute phase protein that is upregulated by tumor necrosis factor α (TNF-α) and interleukin 2 (IL-2), two proinflammatory cytokines produced during and after strenuous exercise [3, 45]. It is possible that the chronic inflammation state present in these subjects masked the changes in plasma ferritin levels. Although the results indicate a link between chronic inflammation and iron status parameters in these individuals, one limitation of this study was the lack of blood sample collection before the exercise program to identify the possibility of a prior inflammatory state. Thus, our comparisons were based on prior published studies conducted under specific conditions using different instruments. This limitation is particularly relevant for several parameters, such as monocytes, IRF, and reticulocytes [23]. Future investigations could verify this association in a larger sample including TNF-α, IL-2, and IL-6 results.

5. Conclusions

In conclusion, our results showed that it is important to consider exercise training when establishing reference intervals for several specific parameters, mainly those related to the inflammatory response. In addition, to avoid deficits in iron, an element that is crucial for an athlete's performance, it is important to monitor iron status using new hematological parameters and inflammatory biomarkers.

Conflict of Interests

The authors declare that there is no conflict of interests regarding the publication of this paper.

Acknowledgments

References

[1] N. P. Walsh, M. Gleeson, R. J. Shephard et al., "Position statement part one: immune function and exercise," *Exercise Immunology Review*, vol. 17, pp. 6–63, 2011.

[2] D. A. McCarthy, I. Macdonald, M. Grant et al., "Studies on the immediate and delayed leucocytosis elicited by brief (30-min) strenuous exercise," *European Journal of Applied Physiology and Occupational Physiology*, vol. 64, no. 6, pp. 513–517, 1992.

[3] M. Gleeson, "Immune function in sport and exercise," *Journal of Applied Physiology*, vol. 103, no. 2, pp. 693–699, 2007.

[4] M. W. Kakanis, J. Peake, E. W. Brenu et al., "The open window of susceptibility to infection after acute exercise in healthy young male elite athletes," *Exercise Immunology Review*, vol. 16, pp. 119–137, 2010.

[5] M. Gleeson, "Can nutrition limit exercise-induced immunodepression?" *Nutrition Reviews*, vol. 64, no. 3, pp. 119–131, 2006.

[6] C. Malm, "Susceptibility to infections in elite athletes: the S-curve," *Scandinavian Journal of Medicine and Science in Sports*, vol. 16, no. 1, pp. 4–6, 2006.

[7] S. Bermon, "Airway inflammation and upper respiratory tract infection in athletes: is there a link?" *Exercise Immunology Review*, vol. 13, pp. 6–14, 2007.

[8] R. D. Telford, G. J. Sly, A. G. Hahn, R. B. Cunningham, C. Bryant, and J. A. Smith, "Footstrike is the major cause of hemolysis during running," *Journal of Applied Physiology*, vol. 94, no. 1, pp. 38–42, 2003.

[9] K. W. Mercer and J. J. Densmore, "Hematologic disorders in the athlete," *Clinics in Sports Medicine*, vol. 24, no. 3, pp. 599–621, 2005.

[10] Y. Olaf Schumacher, A. Schmid, D. Grathwohl, D. Bültermann, and A. Berg, "Hematological indices and iron status in athletes of various sports and performances," *Medicine and Science in Sports and Exercise*, vol. 34, no. 5, pp. 869–875, 2002.

[11] S. Recalcati, M. Locati, E. Gammella, P. Invernizzi, and G. Cairo, "Iron levels in polarized macrophages: regulation of immunity and autoimmunity," *Autoimmunity Reviews*, vol. 11, no. 12, pp. 883–889, 2012.

[12] J. Finaud, G. Lac, and E. Filaire, "Oxidative stress: relationship with exercise and training," *Sports Medicine*, vol. 36, no. 4, pp. 327–358, 2006.

[13] R. Hinzmann, "Iron metabolism. From diagnosis to treatment and monitoring," *Sysmex Journal International*, vol. 13, no. 2, pp. 65–74, 2004.

[14] M. N. Sawka, V. A. Convertino, E. R. Eichner, S. M. Schnieder, and A. J. Young, "Blood volume: importance and adaptations to exercise training, environmental stresses, and trauma/sickness," *Medicine and Science in Sports and Exercise*, vol. 32, no. 2, pp. 332–348, 2000.

[15] H. E. Solberg, "The IFCC recommendation on estimation of reference intervals. The RefVal program," *Clinical Chemistry and Laboratory Medicine*, vol. 42, no. 7, pp. 710–714, 2004.

[16] P. S. Horn, L. Feng, Y. Li, and A. J. Pesce, "Effect of outliers and nonhealthy individuals on reference interval estimation," *Clinical Chemistry*, vol. 47, no. 12, pp. 2137–2145, 2001.

[17] L. A. S. Nunes, R. Brenzikofer, and D. V. Macedo, "Reference change values of blood analytes from physically active subjects," *European Journal of Applied Physiology*, vol. 110, no. 1, pp. 191–198, 2010.

[18] L. A. S. Nunes, F. L. Lazarim, F. Papaléo, R. Hohl, R. Brenzikofer, and D. V. Macedo, "Muscle damage and inflammatory biomarkers reference intervals from physically active population," *Clinical Chemistry*, vol. 57, supplement 10, p. A35, 2011.

[19] W. C. Mentzer Jr., "Differentiation of iron deficiency from thalassaemia trait," *The Lancet*, vol. 1, no. 7808, pp. 882–884, 1973.

[20] L. A. S. Nunes, R. Brenzikofer, and D. V. Macedo, "Reference intervals for saliva analytes collected by a standardized method in a physically active population," *Clinical Biochemistry*, vol. 44, no. 17-18, pp. 1440–1444, 2011.

[21] A. M. W. Petersen and B. K. Pedersen, "The anti-inflammatory effect of exercise," *Journal of Applied Physiology*, vol. 98, no. 4, pp. 1154–1162, 2005.

[22] M. Gleeson, N. C. Bishop, D. J. Stensel, M. R. Lindley, S. S. Mastana, and M. A. Nimmo, "The anti-inflammatory effects of exercise: mechanisms and implications for the prevention and treatment of disease," *Nature Reviews Immunology*, vol. 11, no. 9, pp. 607–610, 2011.

[23] J. Van den Bossche, K. Devreese, R. Malfait et al., "Reference intervals for a complete blood court determined on different automated haematology analysers: Abx Pentra 120 retic, Coulter Gen-S, Sysmex SE 9500, Abbott Cell Dyn 4000 and Bayer Advia 120," *Clinical Chemistry and Laboratory Medicine*, vol. 40, no. 1, pp. 69–73, 2002.

[24] S. Gordon and F. O. Martinez, "Alternative activation of macrophages: mechanism and functions," *Immunity*, vol. 32, no. 5, pp. 593–604, 2010.

[25] J. G. Tidball and M. Wehling-Henricks, "Macrophages promote muscle membrane repair and muscle fibre growth and regeneration during modified muscle loading in mice in vivo," *The Journal of Physiology*, vol. 578, no. 1, pp. 327–336, 2007.

[26] P. E. Sottas, N. Robinson, O. Rabin, and M. Saugy, "The athlete biological passport," *Clinical Chemistry*, vol. 57, no. 7, pp. 969–976, 2011.

[27] G. Banfi, "Reticulocytes in sports medicine," *Sports Medicine*, vol. 38, no. 3, pp. 187–211, 2008.

[28] V. S. Nadarajan, C. H. Ooi, P. Sthaneshwar, and M. W. Thompson, "The utility of immature reticulocyte fraction as an indicator of erythropoietic response to altitude training in elite cyclists," *International Journal of Laboratory Hematology*, vol. 32, no. 1, pp. 82–87, 2010.

[29] R. Milic, J. Martinovic, M. Dopsaj, and V. Dopsaj, "Haematological and iron-related parameters in male and female athletes according to different metabolic energy demands," *European Journal of Applied Physiology*, vol. 111, no. 3, pp. 449–458, 2011.

[30] G. Banfi, C. Lundby, P. Robach, and G. Lippi, "Seasonal variations of haematological parameters in athletes," *European Journal of Applied Physiology*, vol. 111, no. 1, pp. 9–16, 2011.

[31] N. Mathur and B. K. Pedersen, "Exercise as a mean to control low-grade systemic inflammation," *Mediators of Inflammation*, vol. 2008, Article ID 109502, 6 pages, 2008.

[32] E. J. Erlandsen and E. Randers, "Reference interval for serum C-reactive protein in healthy blood donors using the Dade Behring N Latex CRP mono assay," *Scandinavian Journal of Clinical and Laboratory Investigation*, vol. 60, no. 1, pp. 37–44, 2000.

[33] T. B. Ledue and N. Rifai, "Preanalytic and analytic sources of variations in C-reactive protein measurement: implications for cardiovascular disease risk assessment," *Clinical Chemistry*, vol. 49, no. 8, pp. 1258–1271, 2003.

[34] P. M. Ridker, "Clinical application of C-reactive protein for cardiovascular disease detection and prevention," *Circulation*, vol. 107, no. 3, pp. 363–369, 2003.

[35] K. E. Fallon, "The clinical utility of screening of biochemical parameters in elite athletes: analysis of 100 cases," *British Journal of Sports Medicine*, vol. 42, no. 5, pp. 334–337, 2008.

[36] P. Peeling, B. Dawson, C. Goodman, G. Landers, and D. Trinder, "Athletic induced iron deficiency: new insights into the role of inflammation, cytokines and hormones," *European Journal of Applied Physiology*, vol. 103, no. 4, pp. 381–391, 2008.

[37] N. C. Andrews and P. J. Schmidt, "Iron homeostasis," *Annual Review of Physiology*, vol. 69, pp. 69–85, 2007.

[38] P. Peeling, B. Dawson, C. Goodman et al., "Effects of exercise on hepcidin response and iron metabolism during recovery," *International Journal of Sport Nutrition and Exercise Metabolism*, vol. 19, no. 6, pp. 583–597, 2009.

[39] E. H. J. M. Kemna, H. Tjalsma, H. L. Willems, and D. W. Swinkels, "Hepcidin: from discovery to differential diagnosis," *Haematologica*, vol. 93, no. 1, pp. 90–97, 2008.

[40] E. Nemeth, S. Rivera, V. Gabayan et al., "IL-6 mediates hypoferremia of inflammation by inducing the synthesis of the iron regulatory hormone hepcidin," *The Journal of Clinical Investigation*, vol. 113, no. 9, pp. 1271–1276, 2004.

[41] E. Kemna, P. Pickkers, E. Nemeth, H. Van Der Hoeven, and D. Swinkels, "Time-course analysis of hepcidin, serum iron, and plasma cytokine levels in humans injected with LPS," *Blood*, vol. 106, no. 5, pp. 1864–1866, 2005.

[42] W. Jelkmann, "Regulation of erythropoietin production," *The Journal of Physiology*, vol. 589, no. 6, pp. 1251–1258, 2011.

[43] C. Thomas and L. Thomas, "Biochemical markers and hematologic indices in the diagnosis of functional iron deficiency," *Clinical Chemistry*, vol. 48, no. 7, pp. 1066–1076, 2002.

[44] L. Thomas, S. Franck, M. Messinger, J. Linssen, M. Thomé, and C. Thomas, "Reticulocyte hemoglobin measurement—comparison of two methods in the diagnosis of iron-restricted erythropoiesis," *Clinical Chemistry and Laboratory Medicine*, vol. 43, no. 11, pp. 1193–1202, 2005.

[45] S. Recalcati, P. Invernizzi, P. Arosio, and G. Cairo, "New functions for an iron storage protein: the role of ferritin in immunity and autoimmunity," *Journal of Autoimmunity*, vol. 30, no. 1-2, pp. 84–89, 2008.

Review Article

Current Approaches for Predicting a Lack of Response to Anti-EGFR Therapy in *KRAS* Wild-Type Patients

Tze-Kiong Er,[1,2] Chih-Chieh Chen,[3,4] Luis Bujanda,[5] and Marta Herreros-Villanueva[5]

[1] Division of Molecular Diagnostics, Department of Laboratory Medicine, Kaohsiung Medical University Hospital, Kaohsiung Medical University, 100 Shih-Chuan 1st Road, Kaohsiung 80708, Taiwan

[2] Translational Research Center, Kaohsiung Medical University Hospital, Kaohsiung Medical University, 100 Shih-Chuan 1st Road, Kaohsiung 80708, Taiwan

[3] Center for Lipid Biosciences, Kaohsiung Medical University Hospital, 100 Shih-Chuan 1st Road, Kaohsiung 80708, Taiwan

[4] Biomedical Technology and Device Research Laboratories, Industrial Technology Research Institute, No. 195, Section 4, Chung-Hsing Road, Chutung, Hsinchu 31040, Taiwan

[5] Department of Gastroenterology, Donostia Hospital, Biodonostia Institute, Center for Biomedical Research in Network for Hepatic and Digestives Diseases (CIBERehd), Centro de Investigación Biomédica en Red de Enfermedades Hepáticas y Digestivas (CIBERehd), University of Basque Country, 20014 San Sebastian, Spain

Correspondence should be addressed to Marta Herreros-Villanueva; martahvh1978@hotmail.com

Targeting epidermal growth factor receptor (EGFR) has been one of the most effective colorectal cancer strategies. Anti-EGFR antibodies function by binding to the extracellular domain of EGFR, preventing its activation, and ultimately providing clinical benefit. *KRAS* mutations in codons 12 and 13 are recognized prognostic and predictive biomarkers that should be analyzed at the clinic prior to the administration of anti-EGFR therapy. However, still an important fraction of *KRAS* wild-type patients do not respond to the treatment. The identification of additional genetic determinants of primary or secondary resistance to EGFR targeted therapy for further improving the selection of patients is urgent. Herein, we review the latest published literature highlighting the most important genes that may predict resistance to anti-EGFR monoclonal antibodies in colorectal cancer patients. According to the available findings, the evaluation of *BRAF*, *NRAS*, *PIK3CA*, and *PTEN* status could be the right strategy to select patients who are likely to respond to anti-EGFR therapies. In the future, the combination of those biomarkers will help establish consensus that can be introduced into clinical practice.

1. Introduction

With a global increasing incidence of more than one million cases annually and status as the third most common cancer, colorectal cancer (CRC) is a major health burden [1, 2]. Important progress has been made in the treatment of this disease since the introduction of new therapies that have improved patient survival even after metastasis development. Targeting epidermal growth factor receptor (EGFR) has been intensively pursued as a cancer strategy. In the clinical setting of CRC, the use of monoclonal antibodies to block EGFR has demonstrated important clinical benefit exhibiting antitumor activity as monotherapy or in combination with chemotherapy and/or radiation. In particular, the antibodies cetuximab (IMC-C225, Erbitux) and panitumumab (Vectibix) work by binding to the extracellular domain of EGFR and preventing its activation. Mechanistically, both antibodies prevent EGFR receptor activation and dimerization and ultimately induce receptor internalization and downregulation [3].

2. Structure of KRAS, NRAS, BRAF, and PIK3CA Proteins

KRAS, *NRAS*, or *BRAF* mutations can all activate the RAS-RAF-MAPK pathway, which is downstream from EGFR. The KRAS and NRAS hotspot mutation sites G12, G13, Q61, and A146 are indicated in Figures 1(a) and 1(b) showing as the red spheres. These mutations activate the oncogenic

(a) KRAS

(b) NRAS
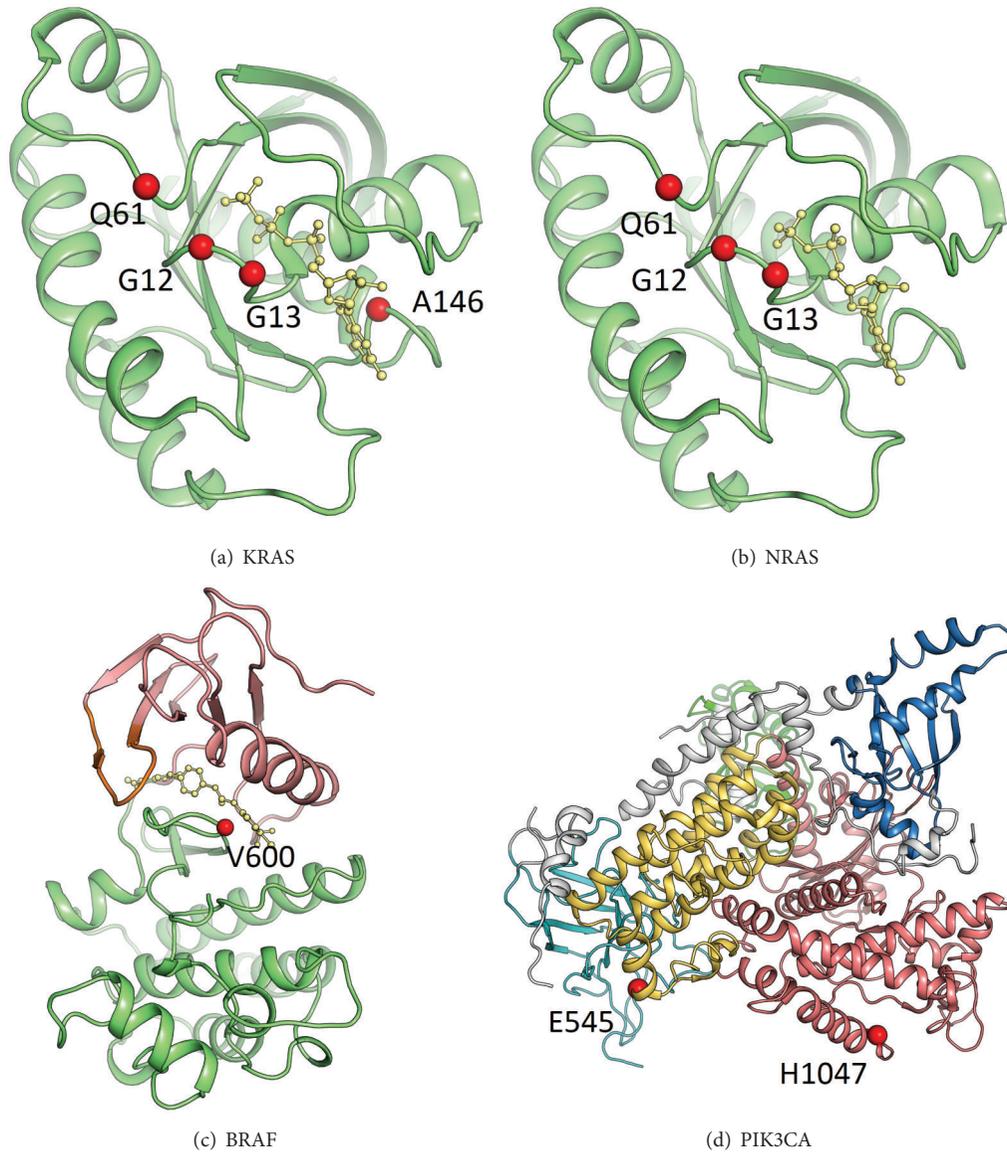
(c) BRAF

(d) PIK3CA

FIGURE 1: Downstream signaling proteins of EGFR: (a) KRAS, (b) NRAS, (c) BRAF, and (d) PIK3CA. The most frequent activating mutation sites are shown as red spheres.

properties of RAS proteins and it has been reported that they do so by inhibiting GTPase activity. The BRAF hotspot mutation, V600E, located at the A-loop is highlighted in red spheres (Figure 1(c)). This mutation may disrupt an inactive conformation of BRAF kinase. Therefore, *BRAF* V600E increases the kinase activity that provides cancer cells with both proliferation and survival signals and promotes them to become tumors in the model system. *PIK3CA* mutations activate the PI3 K-PTEN-AKT pathway, which is downstream from both the EGFR and the RAS-RAF-MAPK pathways. The PIK3CA mutations E545 and H1047 are located at the helical domain and kinase domain of the protein, respectively (Figure 1(d)). Studies showed that mutant E545 inhibits the activity of the catalytic subunit, because it interacts with L379 and A340 of the p85 nSH2 domain. The mutant H1047 has a direct effect on the conformation of the activation loop,

changing its interaction with phosphatidylinositol substrates. Notably, Smith et al. [4] found that exon 9, but not exon 20, mutations in *PIK3CA* were associated with *KRAS* mutations. Exon 9 mutations lie in the helical domain of protein and require interaction with GTP bound RAS. Moreover, exon 20 mutations lie in the kinase domain and require p85 binding but are independent of GTP bound RAS [5].

3. Potential Biomarkers for Anti-EGFR Therapy

3.1. KRAS. It is well known that *KRAS* mutation is the first described and most important factor contributing to anti-EGFR therapies [6]. *KRAS* mutations have been reported to be associated with a lack of response to cetuximab and panitumumab and/or poorer survival in chemorefractory

metastatic CRC patients in several independent studies [6–9]. The hypothesis is that *KRAS* mutation activates the RAS/MAPK signaling pathway downstream of EGFR independently of ligand binding to the receptor. Based on confirmed preclinical and clinical data, the European Medicines Agency and the U.S. Food and Drug Administration (FDA) have suggested that only *KRAS* wild-type patients should be candidates to receive cetuximab or panitumumab.

Although 40–60% of CRCs are *KRAS* wild-type [10, 11], the response rate to cetuximab in monotherapy is approximately 10% and does not exceed 23% even when combined with chemotherapy. A very recent hypothesis suggested that *KRAS* mutations may not be detected in initial disease because a small number of cells with *KRAS* mutations exist in the presence of a vast majority of wild-type *KRAS* cells. Diaz et al. found that 38% of patients whose tumors were initially *KRAS* wild-type developed *KRAS* mutations that were detectable in their sera after 5-6 months of treatment [12]. Recently, Custodio and Feliu indicated that, in addition to *KRAS*, there are signaling events/molecules downstream of EGFR that can become unregulated [13]. It is therefore necessary to identify the factors that contribute to anti-EGFR resistance in *KRAS* wild-type patients.

3.2. BRAF. The detection of *BRAF* mutations is currently included in some clinical laboratory protocols, although it has not been established as routine clinical practice. BRAF is a protein member of the *RAF* family (RAF1, BRAF, ARAF), also regulated by RAS binding.

BRAF encodes a serine-threonine protein kinase that is the most important downstream effector of activated KRAS [14]. Mutated BRAF activates a signaling cascade involving proteins in the mitogen-activated protein kinase system, resulting in cell proliferation [15]. Approximately 15% of CRCs have the *BRAF* mutation, and this is an indicator of poor prognosis regardless of the treatment or administration [16]. Most of the *BRAF* mutations associated with cancer are located in exons 11 and 15, coding for the kinase domain. The hotspot mutation is the T-to-A transversion at nucleotide 1796 that corresponds to the V600E mutation. This mutation is predisposed to the inhibition of apoptosis and also aids in increasing invasiveness [17]. It has also been suggested that *BRAF* mutation is a negative prognostic indicator in CRC [18] and a negative predictor of response to EGFR inhibitors, according to results from CRYSTAL, OPUS, and PICCOLO trials [19–21]. *BRAF* mutation was also associated with shorter progression-free survival (PFS) and overall survival (OS) [22, 23]. *KRAS* and *BRAF* mutations are mutually exclusive in CRC [24, 25]; therefore, the National Comprehensive Cancer Network (NCCN) suggests considering *BRAF* mutation testing when *KRAS* is wild-type [26]. Different studies demonstrated that *BRAF* mutation confers resistance to both cetuximab and panitumumab [25]. Specifically, *BRAF* is responsible for resistance when patients received anti-EGFR therapy in a second or subsequent round of treatment, as shown in several retrospective studies [10, 25, 27, 28]. In contrast, the predictive value of *BRAF* mutations in first line treatment has not been fully demonstrated [18, 29, 30]. A recent study conducted by Saridaki et al. showed lower PFS and OS in BRAF V600E mutated patients compared with wild-type (4.2 versus 11.1 months and 14.3 versus 35.0 months, resp.), although differences were not significantly significant [31]. Due to the poor prognosis of *BRAF* mutated patients and the lack of response to anti-EGFR therapy, rational therapeutic strategies have been directed toward selective RAF inhibitors. For instance, BRAF inhibitors used for melanoma have also been tested against CRC. However, very little clinical benefit was observed, suggesting that the biological behavior in melanoma and colorectal cancer can be different.

3.3. NRAS. KRAS and NRAS are highly homologous and closely related to KRAS [32]. Mutant *NRAS* has been reported to have an antiapoptotic function and promotes CRC in an inflammatory context [33]. Unlike *KRAS* mutations, which are commonly seen in CRC, *NRAS* mutations are found in approximately 3–5% of CRCs and occur most commonly in codon 61 rather than in codon 12 or 13 [13, 34]. *NRAS* mutations like *BRAF* mutations are mutually exclusive from *KRAS* mutations [26]. Because *KRAS* and *NRAS* mutations are mutually exclusive, *NRAS* mutation testing should be performed when *KRAS* is wild-type. To date, several studies demonstrated that the presence of *NRAS* mutations is associated with a lack of response to cetuximab therapy [21, 24]. Shen et al. showed that 4.19% (26/621) of tumors harbored an *NRAS* mutation and distant metastatic tumors had a higher *NRAS* mutation rate [34]. The authors recommended that *NRAS* mutation detection should be considered before anti-EGFR therapy, especially in *KRAS* wild-type tumors. Recently, Russo et al. found that *NRAS* mutations were identified almost exclusively in patients with rectal cancer and were more common in older patients [35]. They also showed that *NRAS* mutation was not associated with clinical outcomes. However, di Bartolomeo et al. indicated that *KRAS*/*NRAS* wild-type status was the most important predictor of efficacy in terms of PFS in a TEGAFOX-E (cetuximab, oxaliplatin, and oral uracil/ftorafur-UFT) phase II study [36]. Additionally, Douillard et al. reported that additional *RAS* mutations predicted a lack of response in patients with mCRC who received panitumumab-FOLFOX4 [37]. Most recently, Sclafani et al. showed that a significant proportion of *KRAS*/*BRAF* wild-type patients (17%) had *RAS* mutations beyond *KRAS* exons 2-3 (additional *KRAS* mutations in 10.2%, *NRAS* mutations in 6.8%) in retrospective analysis (EXPERT-C trial) [38]. They also found that the addition of cetuximab was associated with higher response; however, this was not statistically significant. Based on the published literature, *NRAS* mutation testing is required before initiating treatment with EGFR inhibitors. Notably, the Medicines and Healthcare Products Regulatory Agency (MHRA) indicates that the evidence of wild-type RAS status (at exons 2, 3, and 4 of KRAS and NRAS) is required before initiating treatment with panitumumab alone or in combination with other chemotherapy for metastatic colorectal cancer (mCRC). Genetic testing for *RAS* gene mutations (in *KRAS* and *NRAS*) beyond the routine analysis of *KRAS* exon 2 will become the standard for selecting patients for anti-EGFR therapy in near future.

3.4. PI3 K/PTEN/AKT. Several preclinical studies note the importance of the PI3 K/PTEN/AKT pathway in determining the sensitivity of CRC cell lines to cetuximab. *PI3KCA* mutations, present in 10–25% of CRCs [28, 39–41], have been reported to be "gain of function" mutations activating the PI3 K/AKT pathway. *PIK3CA* mutations, which are located in exon 9 or exon 20, can coincide with *KRAS* and *BRAF* mutations [42] and exert different oncogenic effects including resistance to anti-EGFR therapies. Although the role of the *PIK3CA* mutational status in the anti-EGFR response is still controversial, several published studies agree on the fact that there is a significant negative correlation between *PIK3CA* mutation in codon 20 and the response to anti-EGFR antibodies [39, 43]. In contrast, Prenen et al. [41] did not find this association, and Karapetis et al. concluded that, in chemotherapy-refractory colorectal cancer, neither *PIK3CA* mutation status nor PTEN expression was prognostic, or predictive of benefit from cetuximab [44]. Additionally, recent data suggest that *PIK3CA* exon 20 mutations are associated with poorer PFS, OS, and objective response to anti-EGFR antibodies, whereas patients with mutations in codon 9 are equally responsive to wild-type subjects [45]. Taking these data together, we can conclude that most published literature supports a role of *PIK3CA* exon 20 in predicting resistance to cetuximab and panitumumab, but further studies need to be performed to display clinical significance.

PTEN is a key tumor suppressor gene involved in PI3 K/AKT signaling. The loss of PTEN, by mutation, allelic loss, or epigenetic events results in the persistent activation of PI3K effectors [46, 47]. It has been shown that the loss of PTEN is present in 19–42% of CRCs and often coincides with *KRAS*, *BRAF*, and *PI3KCA* mutations [48]. Preclinical data have shown that PTEN loss confers resistance to cetuximab-induced apoptosis in CRC cell lines [49]. Jhawer et al. [49] also demonstrated that *PI3KCA* mutation and PTEN expression predict a poor response of colon cancer cells to cetuximab. Some groups suggested that the loss of PTEN protein expression is associated with nonresponsiveness to cetuximab [50]. Retrospective studies provided evidence that the loss of PTEN is associated with poorer response to cetuximab [50, 51]. In contrast, Razis et al. did not find association between PTEN protein expression and clinical outcomes in patients treated with cetuximab [52]. However, because there are contradictory results, principally due to protein expression interpretation, further prospective studies are needed to evaluate PTEN expression for its use in the clinical setting.

Although AKT phosphorylation has been correlated with the response to gefitinib [53], its association with the response to cetuximab has not been addressed. In contrast, some reports have shown that p-AKT can modulate the response to anti-EGFR antibodies [54]. In conclusion, there is no clear evidence useful to the clinical setting to support an improved response to anti-EGFR therapies based on AKT phosphorylation.

3.5. HER Family Members. Different preclinical data have suggested that the heterodimers of EGFR with other members of the HER family, such as HER2 and HER3, may affect anti-EGFR therapies. Wheeler et al. [55] analyzed resistance in lung cancer and observed that EGFR, HER2, HER3, and c-MET were highly activated in cetuximab-resistant clones derived from lung cancer cell lines. Their data demonstrated the dysregulation of EGFR internalization/degradation and the subsequent EGFR-dependent activation of HER2 and HER3. Furthermore, it appears that HER3 activity, which depends on EGFR and HER2, represents a critical step for cells to overcome cetuximab effects. Additionally, c-MET was highly phosphorylated in the absence of its ligand HGF. A recent paper has shown that the amplification of the MET protooncogene is associated with *de novo* and acquired resistance in wild-type tumors [56].

Large-scale retrospective analyses have been performed to strengthen the role of HER2 as a resistance biomarker in CRC. The frequency of HER2 amplification is similar to other genes such as BRAF and NRAS [42], and the evaluation of the HER2 gene by FISH may in fact be an additional useful test for the identification of mCRC patients who will benefit from anti-EGFR targeted therapies. Martin et al. [57] concluded that patients with an increased HER2 gene copy number show a worse response to anti-EGFR antibodies. In addition, a phase I clinical trial demonstrated that anti-HER2 therapy combined with cetuximab in refractory CRC was associated with antitumor activity, although the combination was not tolerable due to overlapping toxicities [58]. However, HER2 testing needs to be further investigated for future personalized medicine.

3.6. MicroRNAs. MicroRNA (miRNAs) are a class of endogenous, short (17–25 nucleotides), noncoding single-stranded RNAs involved in the posttranscriptional regulation of gene expression [59]. miRNA causes either the degradation or the inhibition of translation by binding imperfectly to the 3′-untranslated region of targeted mRNA [60]. Dysregulated miRNAs are associated with CRC development, progression, and therapeutic response [61]. Ragusa et al. demonstrated that the downregulation of members of the Let-7 family was a predictive marker of cetuximab sensitivity [62]. They also showed that miR-146b-3p and miR-486-5p were less abundant in *KRAS* wild-type compared with *KRAS*-mutated tumors. Similarly, two studies implicated the potential role of Let-7 family members in *KRAS* regulation and anti-EGFR therapy sensitivity in CRC [63, 64]. Additionally, Sebio et al. showed a LCS6 polymorphism in the 3′-UTR of KRAS, which is in a binding site for Let-7, may serve as a predictive marker of anti-EGFR treatment in *KRAS* wild-type and *BRAF* wild-type patients [65]. Meanwhile, Pichler et al. showed that low expression of miR-200a is associated with poor survival [66]. Furthermore, Cappuzzo et al. showed that patients highly expressing the miR-99a/Let-7c/miR-125b cluster showed longer PFS and longer OS than patients expressing low levels of the cluster in the *KRAS* wild-type population [61]. They thus concluded that the miR-99a/Let-7c/miR-125b signature may improve the selection of *KRAS* wild-type patients for anti-EGFR therapy. Recently, Pichler et al. indicated that the miR-181a expression level is associated with poor survival in patients with CRC and that miR-181a expression may predict PFS in EGFR targeted
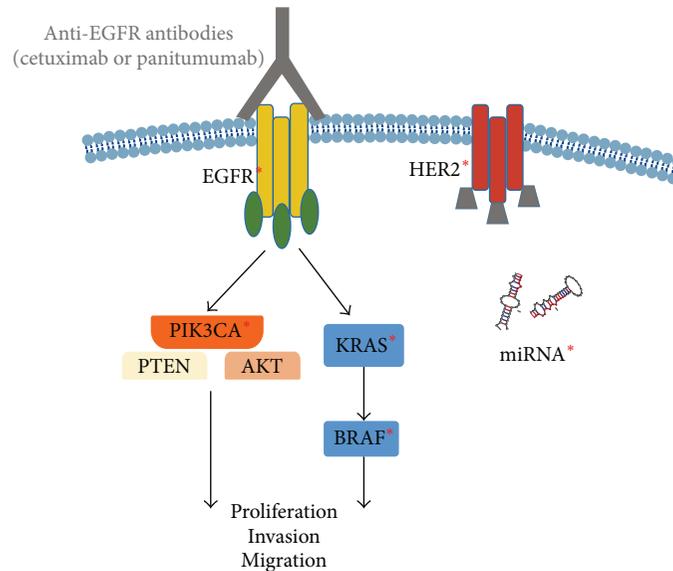
FIGURE 2: Signaling pathways implicated in the lack of response to anti-EGFR therapies. * indicates some receptors or downstream effectors which are responsible for anti-EGFR resistance when they are mutated or overexpressed.

therapy [67]. Based on these findings, miRNAs could be used as predictive biomarkers in selecting patients for anti-*EGFR* antibody therapy in the future.

4. Conclusion

According to the available data obtained during the last decade, it is clear that the evaluation of not only the *KRAS* mutational status but also *BRAF*, *NRAS*, *PIK3CA*, and *PTEN* alterations could be beneficial to the selection of patients who are likely to respond to anti-EGFR therapies (Figure 2). However, there are no guidelines or recommendations from the European group, United States-based group, or Canadian Expert group recommending the use of *BRAF*, *NRAS*, *PIK3CA*, PTEN, or AKT to select CRC patient for anti-EGFR antibody therapy [68]. Notably, the Evaluation of Genomic Applications in Practice and Prevention (EGAPP) Working Group (EWG) found insufficient evidence to recommend or discourage testing for mutations in BRAF V600E, NRAS, or PIK3CA and/or loss of PTEN or AKT protein. Therefore, the EWG discourages the use of these tests for deciding whether to introduce anti-EGFR therapy with cetuximab or panitumumab until more evidence supports improved clinical outcomes [69]. Moreover, a meta-analysis suggests that mutations in *KRAS* exons 3 and 4, *NRAS*, *BRAF*, *PIK3CA*, and nonfunctional PTEN predict resistance to anti-EGFR therapies [70] and concluded that these biomarkers should be implemented for prediction of clinical benefit from anti-EGFR antibodies in mCRC.

In the near future, a panel of multiple genes is likely to be analyzed simultaneously and used for selecting patients and predicting the efficacy of anti-EGFR therapy (Figure 3). A panel of these different mutations identifies a subgroup of mCRC patients with distinct biological behavior and response to treatments, including anti-EGFR antibodies. This
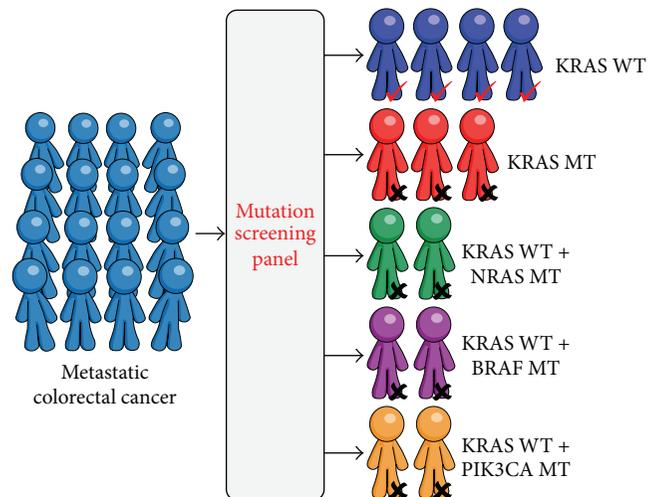
FIGURE 3: A panel of different genes will be a step forward in the "personalized medicine" of CRC patients for selecting patients and predicting efficacy of anti-EGFR therapy. *KRAS* WT: no mutations were detected in exons 2, 3, and 4.

panel will be a step forward in the "personalized medicine" treatment of CRC patients. In summary, the main molecular markers described in this review may enable an accurate selection of patients who will benefit from anti-EGFR therapy.

Conflict of Interests

The authors declare that there is no conflict of interests regarding the publication of this paper.

Authors' Contribution

Tze-Kiong Er and Chih-Chieh Chen contributed equally to this paper.

Acknowledgments

References

[1] R. Siegel, C. Desantis, K. Virgo et al., "Cancer treatment and survivorship statistics, 2012," *CA: A Cancer Journal for Clinicians*, vol. 62, no. 4, pp. 220–241, 2012.

[2] A. Walther, E. Johnstone, C. Swanton, R. Midgley, I. Tomlinson, and D. Kerr, "Genetic prognostic and predictive markers in colorectal cancer," *Nature Reviews Cancer*, vol. 9, no. 7, pp. 489–499, 2009.

[3] H. Sunada, B. E. Magun, J. Mendelsohn, and C. L. MacLeod, "Monoclonal antibody against epidermal growth factor receptor is internalized without stimulating receptor phosphorylation," *Proceedings of the National Academy of Sciences of the United States of America*, vol. 83, no. 11, pp. 3825–3829, 1986.

[4] C. G. Smith, D. Fisher, B. Claes et al., "Somatic profiling of the epidermal growth factor receptor pathway in tumors from patients with advanced colorectal cancer treated with chemotherapy ± cetuximab," *Clinical Cancer Research*, vol. 19, no. 15, pp. 4104–4113, 2013.

[5] L. Zhao and P. K. Vogt, "Helical domain and kinase domain mutations in p110α of phosphatidylinositol 3-kinase induce gain of function by different mechanisms," *Proceedings of the National Academy of Sciences of the United States of America*, vol. 105, no. 7, pp. 2652–2657, 2008.

[6] R. G. Amado, M. Wolf, M. Peeters et al., "Wild-type *KRAS* is required for panitumumab efficacy in patients with metastatic colorectal cancer," *Journal of Clinical Oncology*, vol. 26, no. 10, pp. 1626–1634, 2008.

[7] W. de Roock, H. Piessevaux, J. de Schutter et al., "*KRAS* wild-type state predicts survival and is associated to early radiological response in metastatic colorectal cancer treated with cetuximab," *Annals of Oncology*, vol. 19, no. 3, pp. 508–515, 2008.

[8] F. di Fiore, F. Blanchard, F. Charbonnier et al., "Clinical relevance of *KRAS* mutation detection in metastatic colorectal cancer treated by Cetuximab plus chemotherapy," *British Journal of Cancer*, vol. 96, no. 8, pp. 1166–1169, 2007.

[9] A. Lièvre, J.-B. Bachet, V. Boige et al., "*KRAS* mutations as an independent prognostic factor in patients with advanced colorectal cancer treated with cetuximab," *Journal of Clinical Oncology*, vol. 26, no. 3, pp. 374–379, 2008.

[10] M. Herreros-Villanueva, M. Rodrigo, M. Claver et al., "*KRAS*, *BRAF*, *EGFR* and *HER2* gene status in a Spanish population of colorectal cancer," *Molecular Biology Reports*, vol. 38, no. 2, pp. 1315–1320, 2011.

[11] C. S. Karapetis, S. Khambata-Ford, D. J. Jonker et al., "K-ras mutations and benefit from cetuximab in advanced colorectal cancer," *The New England Journal of Medicine*, vol. 359, no. 17, pp. 1757–1765, 2008.

[12] L. A. Diaz Jr., R. T. Williams, J. Wu et al., "The molecular evolution of acquired resistance to targeted *EGFR* blockade in colorectal cancers," *Nature*, vol. 486, no. 7404, pp. 537–540, 2012.

[13] A. Custodio and J. Feliu, "Prognostic and predictive biomarkers for epidermal growth factor receptor-targeted therapy in colorectal cancer: beyond *KRAS* mutations," *Critical Reviews in Oncology/Hematology*, vol. 85, no. 1, pp. 45–81, 2013.

[14] H. Rajagopalan, A. Bardelli, C. Lengauer, K. W. Kinzler, B. Vogelstein, and V. E. Velculescu, "*RAF/RAS* oncogenes and mismatch-repair status," *Nature*, vol. 418, no. 6901, p. 934, 2002.

[15] W. Kolch, "Meaningful relationships: the regulation of the Ras/Raf/MEK/ERK pathway by protein interactions," *Biochemical Journal*, vol. 351, no. 2, pp. 289–305, 2000.

[16] A. D. Roth, S. Tejpar, M. Delorenzi et al., "Prognostic role of *KRAS* and *BRAF* in stage II and III resected colon cancer: results of the translational study on the PETACC-3, EORTC 40993, SAKK 60-00 trial," *Journal of Clinical Oncology*, vol. 28, no. 3, pp. 466–474, 2010.

[17] P. Minoo, M. P. Moyer, and J. R. Jass, "Role of *BRAF*-V600E in the serrated pathway of colorectal tumourigenesis," *Journal of Pathology*, vol. 212, no. 2, pp. 124–133, 2007.

[18] E. van Cutsem, C.-H. Köhne, I. Láng et al., "Cetuximab plus irinotecan, fluorouracil, and leucovorin as first-line treatment for metastatic colorectal cancer: updated analysis of overall survival according to tumor *KRAS* and *BRAF* mutation status," *Journal of Clinical Oncology*, vol. 29, no. 15, pp. 2011–2019, 2011.

[19] E. van Cutsem, C.-H. Köhne, E. Hitre et al., "Cetuximab and chemotherapy as initial treatment for metastatic colorectal cancer," *The New England Journal of Medicine*, vol. 360, no. 14, pp. 1408–1417, 2009.

[20] C. Bokemeyer, I. Bondarenko, J. T. Hartmann et al., "Efficacy according to biomarker status of cetuximab plus FOLFOX-4 as first-line treatment for metastatic colorectal cancer: the OPUS study," *Annals of Oncology*, vol. 22, no. 7, pp. 1535–1546, 2011.

[21] M. T. Seymour, S. R. Brown, G. Middleton et al., "Panitumumab and irinotecan versus irinotecan alone for patients with *KRAS* wild-type, fluorouracil-resistant advanced colorectal cancer (PICCOLO): a prospectively stratified randomised trial," *The Lancet Oncology*, vol. 14, no. 8, pp. 749–759, 2013.

[22] F. Loupakis, A. Ruzzo, C. Cremolini et al., "*KRAS* codon 61, 146 and *BRAF* mutations predict resistance to cetuximab plus irinotecan in *KRAS* codon 12 and 13 wild-type metastatic colorectal cancer," *British Journal of Cancer*, vol. 101, no. 4, pp. 715–721, 2009.

[23] T. S. Maughan, R. A. Adams, C. G. Smith et al., "Addition of cetuximab to oxaliplatin-based first-line combination chemotherapy for treatment of advanced colorectal cancer: results of the randomised phase 3 MRC COIN trial," *The Lancet*, vol. 377, no. 9783, pp. 2103–2114, 2011.

[24] W. de Roock, B. Claes, D. Bernasconi et al., "Effects of *KRAS*, *BRAF*, *NRAS*, and *PIK3CA* mutations on the efficacy of cetuximab plus chemotherapy in chemotherapy-refractory metastatic colorectal cancer: a retrospective consortium analysis," *The Lancet Oncology*, vol. 11, no. 8, pp. 753–762, 2010.

[25] F. di Nicolantonio, M. Martini, F. Molinari et al., "Wild-type *BRAF* is required for response to panitumumab or cetuximab in metastatic colorectal cancer," *Journal of Clinical Oncology*, vol. 26, no. 35, pp. 5705–5712, 2008.

[26] X. Sagaert, "Prognostic biomarkers in colorectal cancer: where do we stand?" *Virchows Archiv*, vol. 464, no. 3, pp. 379–391, 2014.

[27] S. Benvenuti, A. Sartore-Bianchi, F. di Nicolantonio et al., "Oncogenic activation of the *RAS/RAF* signaling pathway impairs the response of metastatic colorectal cancers to anti-epidermal growth factor receptor antibody therapies," *Cancer Research*, vol. 67, no. 6, pp. 2643–2648, 2007.

[28] M. Herreros-Villanueva, N. Gomez-Manero, P. Muñiz, C. García-Girón, and M. J. Coma del Corral, "*PIK3CA* mutations in *KRAS* and *BRAF* wild type colorectal cancer patients. A study of Spanish population," *Molecular Biology Reports*, vol. 38, no. 2, pp. 1347–1351, 2011.

[29] J. Tol, M. Koopman, A. Cats et al., "Chemotherapy, bevacizumab, and cetuximab in metastatic colorectal cancer," *The New England Journal of Medicine*, vol. 360, no. 6, pp. 563–572, 2009.

[30] C. Bokemeyer, I. Bondarenko, J. T. Hartmann et al., "Efficacy according to biomarker status of cetuximab plus FOLFOX-4 as first-line treatment for metastatic colorectal cancer: the OPUS study," *Annals of Oncology*, vol. 22, no. 7, pp. 1535–1546, 2011.

[31] Z. Saridaki, M. Tzardi, M. Sfakianaki et al., "*BRAF*V600E mutation analysis in patients with metastatic colorectal cancer (mCRC) in daily clinical practice: correlations with clinical characteristics, and its impact on patients' outcome," *PLoS ONE*, vol. 8, Article ID e84604, 2013.

[32] J. Downward, "Targeting RAS signalling pathways in cancer therapy," *Nature Reviews Cancer*, vol. 3, no. 1, pp. 11–22, 2003.

[33] Y. Wang, S. Velho, E. Vakiani et al., "Mutant N-RAS protects colorectal cancer cells from stress-induced apoptosis and contributes to cancer development and progression," *Cancer Discovery*, vol. 3, no. 3, pp. 294–307, 2013.

[34] Y. Shen, J. Wang, X. Han et al., "Effectors of epidermal growth factor receptor pathway: the genetic profiling of *KRAS*, *BRAF*, *PIK3CA*, *NRAS* mutations in colorectal cancer characteristics and personalized medicine," *PLoS ONE*, vol. 8, no. 12, Article ID e81628, 2013.

[35] A. L. Russo, D. R. Borger, J. Szymonifka et al., "Mutational analysis and clinical correlation of metastatic colorectal cancer," *Cancer*, vol. 120, no. 10, pp. 1482–1490, 2014.

[36] M. di Bartolomeo, F. Pietrantonio, F. Perrone et al., "Lack of *KRAS*, *NRAS*, *BRAF* and TP53 mutations improves outcome of elderly metastatic colorectal cancer patients treated with cetuximab, oxaliplatin and UFT," *Targeted Oncology*, 2013.

[37] J. Y. Douillard, K. S. Oliner, S. Siena et al., "Panitumumab-FOLFOX4 treatment and RAS mutations in colorectal cancer," *The New England Journal of Medicine*, vol. 369, no. 11, pp. 1023–1034, 2013.

[38] F. Sclafani, D. Gonzalez, D. Cunningham et al., "RAS mutations and cetuximab in locally advanced rectal cancer: results of the EXPERT-C trial," *European Journal of Cancer*, vol. 50, no. 8, pp. 1430–1436, 2014.

[39] F. Perrone, A. Lampis, M. Orsenigo et al., "*PI3KCA/PTEN* deregulation contributes to impaired responses to cetuximab in metastatic colorectal cancer patients," *Annals of Oncology*, vol. 20, no. 1, pp. 84–90, 2009.

[40] K. Nosho, T. Kawasaki, M. Ohnishi et al., "*PIK3CA* mutation in colorectal cancer: relationship with genetic and epigenetic alterations," *Neoplasia*, vol. 10, no. 6, pp. 534–541, 2008.

[41] H. Prenen, J. de Schutter, B. Jacobs et al., "*PIK3CA* mutations are not a major determinant of resistance to the epidermal growth factor receptor inhibitor cetuximab in metastatic colorectal cancer," *Clinical Cancer Research*, vol. 15, no. 9, pp. 3184–3188, 2009.

[42] W. de Roock, B. Claes, D. Bernasconi et al., "Effects of *KRAS*, *BRAF*, *NRAS*, and *PIK3CA* mutations on the efficacy of cetuximab plus chemotherapy in chemotherapy-refractory metastatic colorectal cancer: a retrospective consortium analysis," *The Lancet Oncology*, vol. 11, no. 8, pp. 753–762, 2010.

[43] A. Sartore-Bianchi, M. Martini, F. Molinari et al., "*PIK3CA* mutations in colorectal cancer are associated with clinical resistance to *EGFR*-targeted monoclonal antibodies," *Cancer Research*, vol. 69, no. 5, pp. 1851–1857, 2009.

[44] C. S. Karapetis, D. Jonker, M. Daneshmand et al., "*PIK3CA*, *BRAF*, and *PTEN* status and benefit from cetuximab in the treatment of advanced colorectal cancer—results from NCIC CTG/AGITG CO.17," *Clinical Cancer Research*, vol. 20, no. 3, pp. 744–753, 2014.

[45] Z.-Y. Yang, X.-Y. Wu, Y.-F. Huang et al., "Promising biomarkers for predicting the outcomes of patients with *KRAS* wild-type metastatic colorectal cancer treated with anti-epidermal growth factor receptor monoclonal antibodies: a systematic review with meta-analysis," *International Journal of Cancer*, vol. 133, no. 8, pp. 1914–1925, 2013.

[46] M. Cully, H. You, A. J. Levine, and T. W. Mak, "Beyond *PTEN* mutations: the PI3K pathway as an integrator of multiple inputs during tumorigenesis," *Nature Reviews Cancer*, vol. 6, no. 3, pp. 184–192, 2006.

[47] A. di Cristofano and P. P. Pandolfi, "The multiple roles of *PTEN* in tumor suppression," *Cell*, vol. 100, no. 4, pp. 387–390, 2000.

[48] A. Sartore-Bianchi, F. di Nicolantonio, M. Nichelatti et al., "Multi-determinants analysis of molecular alterations for predicting clinical benefit to *EGFR*-targeted monoclonal antibodies in colorectal cancer," *PLoS ONE*, vol. 4, no. 10, Article ID e7287, 2009.

[49] M. Jhawer, S. Goel, A. J. Wilson et al., "*PIK3CA* mutation/*PTEN* expression status predicts response of colon cancer cells to the epidermal growth factor receptor inhibitor cetuximab," *Cancer Research*, vol. 68, no. 6, pp. 1953–1961, 2008.

[50] M. Frattini, P. Saletti, E. Romagnani et al., "*PTEN* loss of expression predicts cetuximab efficacy in metastatic colorectal cancer patients," *British Journal of Cancer*, vol. 97, no. 8, pp. 1139–1145, 2007.

[51] F. Loupakis, L. Pollina, I. Stasi et al., "*PTEN* expression and *KRAS* mutations on primary tumors and metastases in the prediction of benefit from cetuximab plus irinotecan for patients with metastatic colorectal cancer," *Journal of Clinical Oncology*, vol. 27, no. 16, pp. 2622–2629, 2009.

[52] E. Razis, E. Briasoulis, E. Vrettou et al., "Potential value of *PTEN* in predicting cetuximab response in colorectal cancer: an exploratory study," *BMC Cancer*, vol. 8, article 234, 2008.

[53] F. Cappuzzo, E. Magrini, G. L. Ceresoli et al., "Akt phosphorylation and gefitinib efficacy in patients with advanced non-small-cell lung cancer," *Journal of the National Cancer Institute*, vol. 96, no. 15, pp. 1133–1141, 2004.

[54] M. Scartozzi, R. Giampieri, E. Maccaroni et al., "Phosphorylated AKT and MAPK expression in primary tumours and in corresponding metastases and clinical outcome in colorectal cancer patients receiving irinotecan-cetuximab," *Journal of Translational Medicine*, vol. 10, no. 1, article 71, 2012.

[55] D. L. Wheeler, S. Huang, T. J. Kruser et al., "Mechanisms of acquired resistance to cetuximab: role of HER (ErbB) family members," *Oncogene*, vol. 27, no. 28, pp. 3944–3956, 2008.

[56] A. Bardelli, S. Corso, A. Bertotti et al., "Amplification of the MET receptor drives resistance to anti-*EGFR* therapies in colorectal cancer," *Cancer Discovery*, vol. 3, no. 6, pp. 658–673, 2013.

[57] V. Martin, L. Landi, F. Molinari et al., "*HER2* gene copy number status may influence clinical efficacy to anti-*EGFR* monoclonal antibodies in metastatic colorectal cancer patients," *British Journal of Cancer*, vol. 108, no. 3, pp. 668–675, 2013.

[58] D. A. Rubinson, H. S. Hochster, D. P. Ryan et al., "Multi-drug inhibition of the HER pathway in metastatic colorectal cancer: results of a phase I study of pertuzumab plus cetuximab in cetuximab-refractory patients," *Investigational New Drugs*, vol. 32, no. 1, pp. 113–122, 2014.

[59] D. P. Bartel, "MicroRNAs: target recognition and regulatory functions," *Cell*, vol. 136, no. 2, pp. 215–233, 2009.

[60] J. Raisch, A. Darfeuille-Michaud, and H. T. Nguyen, "Role of microRNAs in the immune system, inflammation and cancer," *World Journal of Gastroenterology*, vol. 19, no. 20, pp. 2985–2996, 2013.

[61] F. Cappuzzo, A. Sacconi, L. Landi et al., "MicroRNA signature in metastatic colorectal cancer patients treated with anti-*EGFR* monoclonal antibodies," *Clinical Colorectal Cancer*, vol. 13, no. 1, pp. 37–45.e4, 2014.

[62] M. Ragusa, A. Majorana, L. Statello et al., "Specific alterations of microRNA transcriptome and global network structure in colorectal carcinoma after cetuximab treatment," *Molecular Cancer Therapeutics*, vol. 9, no. 12, pp. 3396–3409, 2010.

[63] A. Ruzzo, F. Graziano, B. Vincenzi et al., "High let-7a microRNA levels in *KRAS*-mutated colorectal carcinomas may rescue anti-*EGFR* therapy effects in patients with chemotherapy-refractory metastatic disease," *The Oncologist*, vol. 17, no. 6, pp. 823–829, 2012.

[64] W. Zhang, T. Winder, Y. Ning et al., "A let-7 microRNA-binding site polymorphism in 3′-untranslated region of *KRAS* gene predicts response in wild-type *KRAS* patients with metastatic colorectal cancer treated with cetuximab monotherapy," *Annals of Oncology*, vol. 22, no. 1, pp. 104–109, 2011.

[65] A. Sebio, L. Paré, D. Páez et al., "The LCS6 polymorphism in the binding site of let-7 microRNA to the *KRAS* 3′-untranslated region: its role in the efficacy of anti-*EGFR*-based therapy in metastatic colorectal cancer patients," *Pharmacogenetics and Genomics*, vol. 23, no. 3, pp. 142–147, 2013.

[66] M. Pichler, A. L. Ress, E. Winter et al., "MiR-200a regulates epithelial to mesenchymal transition-related gene expression and determines prognosis in colorectal cancer patients," *British Journal of Cancer*, vol. 110, no. 6, pp. 1614–1621, 2014.

[67] M. Pichler, E. Winter, A. L. Ress et al., "miR-181a is associated with poor clinical outcome in patients with colorectal cancer treated with *EGFR* inhibitor," *Journal of Clinical Pathology*, vol. 67, no. 3, pp. 198–203, 2013.

[68] F. Aubin, S. Gill, R. Burkes et al., "Canadian expert group consensus recommendations: *KRAS* testing in colorectal cancer," *Current Oncology*, vol. 18, no. 4, pp. e180–e184, 2011.

[69] Evaluation of Genomic Applications in Practice and Prevention (EGAPP) Working Group, "Recommendations from the EGAPP Working Group: can testing of tumor tissue for mutations in *EGFR* pathway downstream effector genes in patients with metastatic colorectal cancer improve health outcomes by guiding decisions regarding anti-*EGFR* therapy?" *Genetics in Medicine*, vol. 15, no. 7, pp. 517–527, 2013.

[70] C. Therkildsen, T. K. Bergmann, T. Henrichsen-Schnack, S. Ladelund, and M. Nilbert, "The predictive value of *KRAS*, *NRAS*, *BRAF*, *PIK3CA* and *PTEN* for anti-*EGFR* treatment in metastatic colorectal cancer: a systematic review and meta-analysis," *Acta Oncologica*, 2014.

Research Article

Comparison of Quasispecies Diversity of HCV between Chronic Hepatitis C and Hepatocellular Carcinoma by Ultradeep Pyrosequencing

Chang-Wook Park,[1] Min-Chul Cho,[2] Keumrock Hwang,[3] Sun-Young Ko,[4] Heung-Bum Oh,[1] and Han Chu Lee[5]

[1] *Department of Laboratory Medicine, Asan Medical Center, University of Ulsan College of Medicine, 88 Olympic-ro 43-gil, Songpa-gu, Seoul 138-736, Republic of Korea*

[2] *Department of Laboratory Medicine, Gyeongsang National University Hospital and Gyeongsang National University School of Medicine, Jinju 660-701, Republic of Korea*

[3] *Department of Laboratory Medicine, Sure Quest Laboratory, Yongin 446-916, Republic of Korea*

[4] *Department of Laboratory Medicine, College of Medicine, Korea University, Seoul 136-705, Republic of Korea*

[5] *Department of Internal Medicine, Asan Medical Center, University of Ulsan College of Medicine, Seoul 138-736, Republic of Korea*

Correspondence should be addressed to Heung-Bum Oh; hboh@amc.seoul.kr

Backgrounds. Hepatitis C virus (HCV) exists as population of closely related genetic variants known as quasispecies. HCV quasispecies diversity is strongly influenced by host immune pressure on virus. Quasispecies diversity is expected to decline as host immune response to HCV decreases over natural course of progressing from chronic hepatitis C (CHC) to hepatocellular carcinoma (HCC). *Methods.* Ultradeep pyrosequencing (UDPS) was used to evaluate degree of quasispecies diversity in 49 patients infected with HCV including 26 with CHC and 23 with HCC. Whole structural protein of HCV genome was subjected to UDPS. *Results.* Shannon's indices for quasispecies diversity in HCV E1 were significantly lower in patients with HCC than in those with CHC. 14 amino acid positions differed significantly between two groups. Area under curve of ROC analysis for differentiating HCC from CHC was >0.8 for all of 14 amino acid positions. *Conclusion.* HCV quasispecies diversity as indicator of declining host immune functions was easily assessed by UDPS technology. Shannon's indices in 14 amino acid positions were found to differentiate between patients with CHC and those with HCC. Our data propose that degree of HCV quasispecies measured by UDPS might be useful to predict progression of HCC in chronic HCV patients.

1. Introduction

Hepatitis C virus (HCV) is an enveloped RNA virus [1]. HCV is capable of producing highly diverse variants, so called quasispecies, by initiating replications based on RNA-dependent, error-prone RNA polymerase [2, 3]. These HCV quasispecies are considered as one of the mechanisms by which HCV evades host immune pressure [4].

Nearly 80% of the patients with HCV infection progress to chronic HCV infection. Of those, 20% develop cirrhosis over a period of 20 years. The risk of developing hepatocellular carcinoma (HCC) increases by 5% per year in those with cirrhosis [5–7]. It is known that the progression of chronic hepatitis C to HCC is accompanied by anergy of host immune system [8]. These changes in host immune response to the virus also affect the diversity in HCV quasispecies.

A lower HCV quasispecies diversity has been expected in patients with HCC than those with chronic HCV infection. However, the results of earlier studies have not been consistent with this expectation [9, 10]. Divided results are

TABLE 1: Primer sequences for PCR amplification of HCV genome encoding structural proteins.

Region		Primer name	Primer sequence ($5' \to 3'$)
Core	1st	B1xL.1-AP1	GGGCGACACTCCACCATAG
		B1xR.1-AP1	GCCGGCRAARAGYAGCAYC
	2nd	B1xL.1-AP2	ACTCCCCTGTGAGGAACTAY
		B1xR.1-AP3	TGGGATCCGGAGYARCTG
E1/E2	1st	B1yL.1-AP1	TTCTGYTCCGCYATGTAYG
		B1yR.1-AP1	CACAAGRAAGGAGAGRANRC
	2nd	B1yL.1-AP3	GAACTGGTCRCCYACARCRG
		B1yR.1-AP2	GGACCACCARGTTCTCYARG

attributed to the fact that the numbers of samples and clones analyzed in cloning and sequencing analysis were not enough [9, 10] and that single stranded conformation polymorphism (SSCP) and heteroduplex tracking assays (HTA) used in those studies had technical shortfalls [11–15]. Also, investigated HCV positions varied among studies [9, 10].

The next generation sequencing (NGS) that allows massive parallel sequencing has been recently developed. Massive parallel sequencing allows a simultaneous sequencing by breaking the whole genome into numerous pieces, generating the results of hundreds of megabase sequences in a single sequencing run [16–18]. Using these technologies, ultradeep pyrosequencing (UDPS) has been used to detect various genetic variants by analyzing sequences from the same gene regions. This tool is very effective to detect variants of viral quasispecies [19–22]. UDPS of HCV quasispecies offers the same benefits as the analysis of several thousands of clones at a time, providing more accurate and sensitive results on quasispecies diversity. In this study, thus, UDPS was performed to investigate the degree of quasispecies diversity between the patients with chronic HCV infection and those with HCC in the whole HCV structural proteins.

2. Materials and Methods

2.1. Study Subjects. A total of 49 samples with HCV genotype 1b were included for this study. Among them, 26 patients had chronic HCV infection and 23 had HCV-induced hepatocellular carcinoma. *t*-tests were performed to evaluate differences between the two groups in demographic profile (age and gender), the quantity of HCV RNA, and biochemical profile (AST, ALT, albumin, platelet, bilirubin, and prothrombin time).

The quantity of HCV RNA was measured using a real-time PCR assay (Abbott Molecular Inc., Abbott Park, IL, USA) following the manufacturer's recommendations. HCV RNA level of all samples was over 1.0×10^4 IU/mL.

The study protocol was reviewed and approved by Asan Medical Center Institutional Review Board, Ethics reference number (2013-0643). According to the policy in our institutional review board, informed consent was waived since the remaining serum samples with which HCV genotyping tests were already completed and reported were utilized in this study, and all the patient information was kept anonymous and minimally used only for the study purpose.

The recommendations of the Declaration of Helsinki for biomedical research involving human subjects were followed.

2.2. PCR and UDPS. HCV RNA was isolated using QIAamp MinElute Virus Spin Kit (Qiagen Inc., Valencia, CA, USA) according to the manufacturer's recommendations. Obtained HCV RNA was synthesized to cDNA and then amplified twice to cover a 2 kb fragment of core and E1 and E2 regions using four primer pairs (Table 1). The primary PCR was performed with 5 μL of HCV cDNA and 20 μL of polymerase chain reaction reagent. Advantage 2 PCR kit (Clontech, Inc., CA, USA) was used as polymerase chain reaction solution, which contains 1x PCR buffer 40 mM Tricine-KOH (pH 8.7), 15 mM KOAc, 3.5 mM Mg(OAc)2, 3.75 μg/mL BSA, Tween 20 0.005%, 25 mM dNTP, 12.5 μM primer, and 1x Advantage 2 polymerase mix. PCR reactions started with predenaturation step at 95°C for 10 minutes, followed by denaturation at 95° for 30 seconds, annealing at 55.8°C for one minute, 25 cycles of extension at 72°C for one minute, and additional extension at 72°C for 10 minutes. The secondary PCR was performed with 5 μL of primary PCR and 45 μL of polymerase chain reaction solution. Composition of polymerase chain reaction reagent was the same as that of primary PCR. The secondary reactions also included predenaturation step at 95°C for 10 minutes, denaturation at 95° for 30 seconds, annealing at 55.8°C for one minute, 25 cycles of extension at 72°C for one minute, and additional extension at 72°C for 10 minutes.

PCR amplification yield was purified with AMPure beads (Beckman Coulter Inc., Brea, CA, USA). And UDPS was performed in a sequential order of library preparation based on GS FLX Titanium platform, emulsion PCR, and pyrosequencing. DNA library was quantified using RiboGreen (Invitrogen, Eugene, OR, USA). Each library was diluted to 2×10^6 molecules/μL, and the entire volume of 20 μL from each sample was used to make pooled library. Emulsion PCR was performed and particles were counted using Multisizer 3 Coulter Counter (Beckman Coulter Inc.). After this, pyrosequencing was performed on region 1/4 of a 70 mm × 75 mm Picotiter Plate (PTP) using GS FLX 454 Genome Sequencer according to the manufacturer's recommendations.

2.3. Analysis of Sequence Data Generated by UDPS. After UDPS, the standard strain of HCV was set to align each UDPS read to a sequence. The standard sequence of HCV was defined by aligning 388 whole genome sequences of HCV
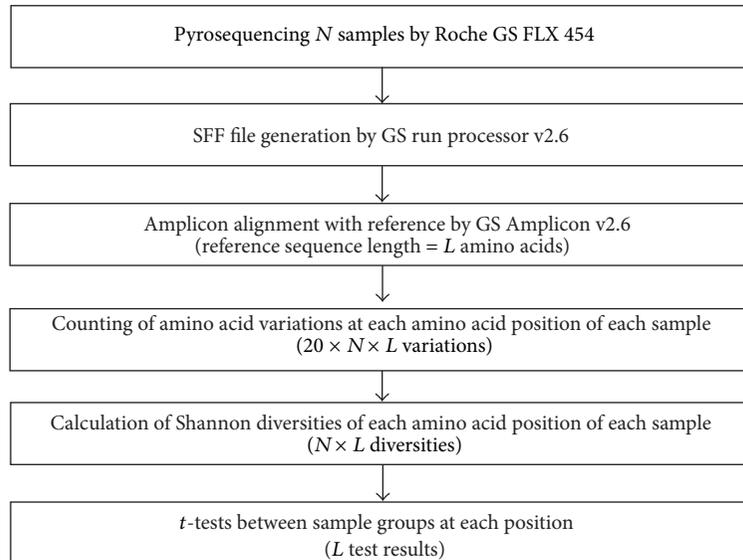
FIGURE 1: The workflow of UDPS data treatment and statistical process in this study.

genotype 1b, which were obtained from Los Alamos National Laboratory (http://hcv.lanl.gov). The standard sequence was applied when 70% or higher identical nucleotides were observed in a specific sequence position. If not, the standard sequence was marked with "N." If 70% or higher nucleotides were blank in a specific sequence position, the corresponding position was eliminated from the standard sequence. The standard amino acid sequence was deduced by replacing the sequence of protein production with the amino acids sequence in the standard sequence of HCV.

UDPS reads were aligned along with the standard sequence using Amplicon Variant Analyzer (AVA), supplied by the manufacturer. A sequence analysis program was developed to determine HCV quasispecies diversity. This analysis program is designed to store aligning reads in a database and evaluate the diversity of HCV quasispecies after calculating Shannon diversity index for the nucleotides and amino acids sequences, respectively.

The equation to calculate Shannon diversity index (H) for the nucleotides and amino acids sequences is as follows:

$$H = -\sum_{i}^{S} p_i \ln p_i \qquad (1)$$

in this equation, the summation from i to S is from 1 to 4 for nucleotide and from 1 to 20 for amino acid considering the number of nucleotide and amino acid, respectively. Thus, P_i represents proportion of each nucleotide and amino acid at each position.

t-test was also done for the nucleotides and amino acid positions to evaluate the differences in the HCV quasispecies diversity between the chronic HCV infection group and the hepatocellular carcinoma group. Bonferroni correction was used to verify statistical significance of the results of t-tests and corrected P value of less than 0.05 is considered significant. Receiver operating characteristic (ROC) curves were made for each nucleotide and amino acid sequence position showing significant differences between the two groups. Specificity and area under the curve (AUC) were calculated for the positions showing sensitivity of 90% or higher in the ROC curve. All the workflow including UDPS data treatment and statistical process is summarized in Figure 1.

3. Results

3.1. Study Subjects. A total of 26 patients in the chronic HCV infection group showed mean ± SD of 58 ± 13, 1.9 ± 1.6, 76.0 ± 71.1, 79.0 ± 71.1, 4.0 ± 0.4, 158 ± 75, 1.1 ± 0.4, and 97.5 ± 17.3, respectively, in age, the quantity of HCV RNA (×10^6 IU/mL), AST, ALT, albumin, platelet count (×10^3), bilirubin, and prothrombin time (%). A total of 26 patients in the HCC group exhibited 65 ± 9, 1.5 ± 2.7, 79.4 ± 40.0, 72.0 ± 58.0, 3.2 ± 0.5, 92 ± 38, 1.5 ± 0.7, and 74.4 ± 18.3 in the same categories. Significant differences were observed in age, albumin, platelet, bilirubin, and prothrombin time between the two groups ($P < 0.05$). But no significant differences were found in gender, HCV RNA quantity, AST, and ALT.

3.2. Results of UDPS. A total of 1,822,601 sequence reads were obtained from 49 samples using UDPS in the average number of sequence reads as 37,196 (range 4,996–94,180) per sample. Of those, UDPS sequence reads that can be aligned with standard sequence were 35,311 in average per sample, accounting for 94% of total reads (Figure 2(a)), and the average read length was 350 bp per each sample (Figure 2(b)).
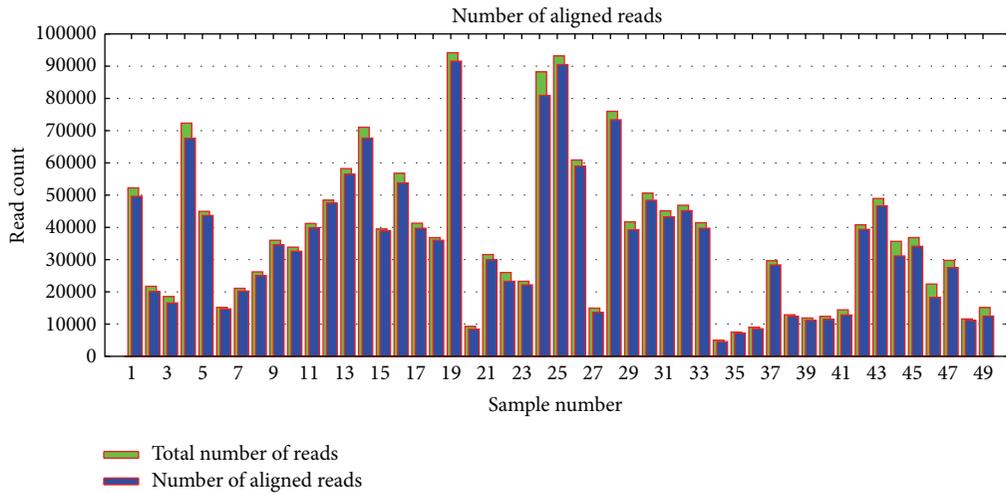
(a)
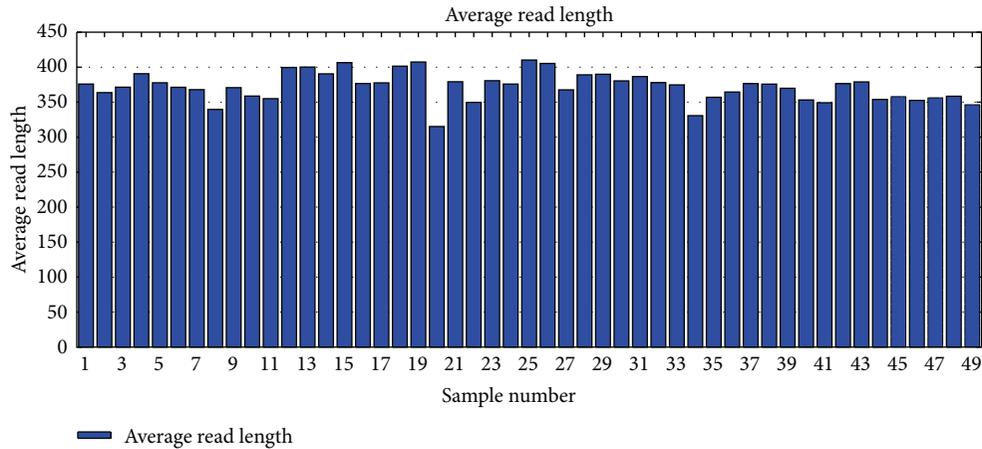
(b)
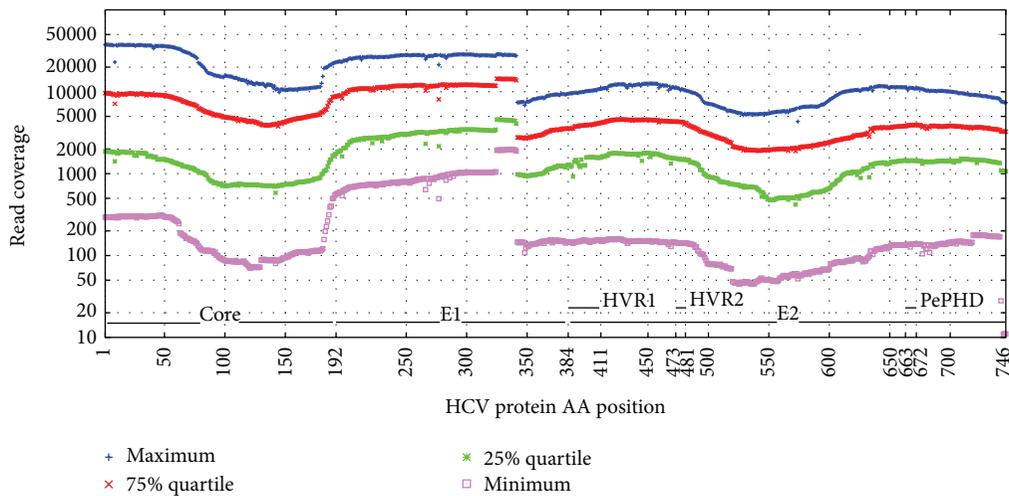
(c)

FIGURE 2: A summary of ultradeep pyrosequencing (UDPS) results. (a) Number of reads and aligned reads of each sample. (b) Average read length of each sample. (c) Hepatitis C virus (HCV) genome coverage by ultradeep pyrosequencing. The dots represent minimum, 25% quartile, 75% quartile, and maximum coverage of reads of samples at each amino acid position of HCV protein. HVR: hypervariable region.
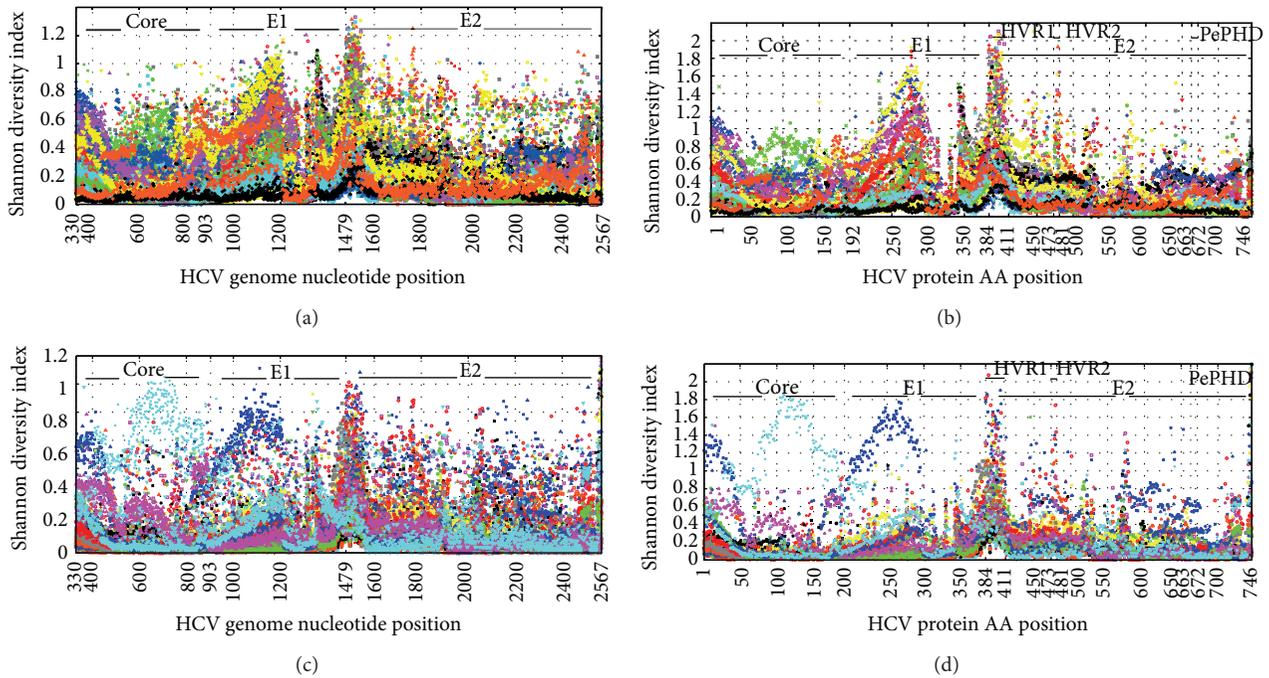
FIGURE 3: Hepatitis C virus (HCV) quasispecies diversity in the patients with chronic hepatitis C (CHC) and those with hepatocellular carcinoma (HCC) caused by HCV infection. (a) HCV quasispecies diversity of each nucleotide position in patients with CHC; (b) HCV quasispecies diversity of each amino acid position in patients with CHC; (c) HCV quasispecies diversity of each nucleotide position in patients with HCC caused by HCV infection; (d) HCV quasispecies diversity of each amino acid position in patients with HCC caused by HCV infection. HVR: hypervariable region; AA: amino acid.

The number of reads at each position in HCV genome (HCV genome coverage) was nearly 2,000 to 10,000 (Figure 2(c)).

3.3. HCV Quasispecies Diversity of the Patients with CHC and Those with HCC Caused by HCV Infection. The degree of HCV quasispecies diversity was analyzed for the whole structural protein of the HCV genome by calculating Shannon's diversity index for each of the nucleotides and amino acids sequence positions (Figure 3).

HCV quasispecies diversity of the HCV structural protein was significantly lower in the HCC group compared to the chronic HCV infection group. Especially, HCV quasispecies diversity has more significantly decreased at E1 position in the HCC group than the chronic HCV infection group (Figure 4).

A total of eight nucleotide positions showed statistically significant differences between the two groups (Table 2). Analysis of ROC curve for each of the eight significant nucleotide positions revealed that the chronic HCV infection group and the HCC group could be differentiated from each other in AUC value of 0.8 or higher (Figure 5(a)). In addition, a total of 14 amino acid positions exhibited statistically significant differences between the two groups (Table 3). Analysis of ROC curve for each of the 14 significant amino acid positions revealed that two groups could be

discriminated against each other in AUC value of 0.8 or higher (Figure 5(b)).

4. Discussion

It has been expected that the diversity of HCV quasispecies would be decreased with disease progression due to reduced immune response, while the diversity of HCV quasispecies is increased by active immune responses in early phase. However, previous study results have not been consistent with this expectation when HCV quasispecies diversity was measured by clone-based sequencing, SSCP, or HTA. Even though cloning and sequencing method of the quasispecies variants offers an advantage of identifying their whole characteristics, this approach is rather complicated, demanding, and costly. Therefore, the number of clones that can be obtained is limited. SSCP method also makes it difficult to optimize the experimental condition. Even more, the diversity of viral quasispecies was assessed depending only on a small number of SSCP bands ranging from 4 to 20 [11–14, 23]. HTA method is less expensive than the clone-based sequencing and offers higher sensitivity than SSCP. It is also easy to optimize experimental conditions. However, like SSCP, it does not enable researchers to identify the location of each variant and the proportion of variants [24].

(a)

(b)
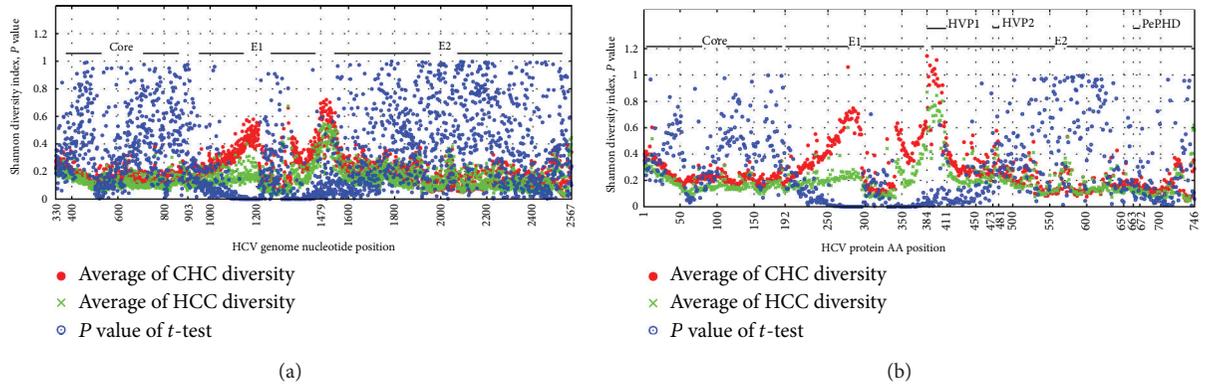
FIGURE 4: Comparison of HCV quasispecies diversity in chronic hepatitis C (CHC) and hepatocellular carcinoma (HCC) caused by HCV. Red dots represent the average Shannon diversity indices of the patients with CHC. Green dots represent the average Shannon diversity indices of the patients with HCC caused by HCV infection. And blue dots represent the corrected P value. (a) Comparison of HCV quasispecies diversity in each nucleotide position of HCV structural protein. (b) Comparison of HCV quasispecies diversity in each amino acid position of HCV structural protein.

TABLE 2: Eight nucleotide positions showing significantly different diversity between the patients with chronic hepatitis C (CHC) and those with hepatocellular carcinoma (HCC) caused by HCV infection.

Nucleotide position	Shannon diversity index		P value	AUC by ROC
	CHC (mean ± SD)	HCC (mean ± SD)		
1188	0.494 ± 0.250	0.174 ± 0.178	0.014	0.868
1200	0.504 ± 0.245	0.176 ± 0.200	0.014	0.88
1205	0.477 ± 0.212	0.186 ± 0.183	0.012	0.87
1213	0.392 ± 0.188	0.135 ± 0.167	0.017	0.871
1320	0.131 ± 0.058	0.048 ± 0.024	<0.001	0.936
1324	0.117 ± 0.041	0.056 ± 0.035	0.003	0.895
1327	0.121 ± 0.049	0.060 ± 0.035	0.009	0.885
1344	0.098 ± 0.042	0.044 ± 0.028	0.008	0.885

TABLE 3: Fourteen amino acid positions showing significantly different diversity between the patients with chronic hepatitis C (CHC) and those with hepatocellular carcinoma (HCC) caused by HCV infection.

Amino acid position	Shannon diversity index		P value	AUC by ROC
	CHC (mean ± SD)	HCC (mean ± SD)		
282	0.669 ± 0.403	0.220 ± 0.292	0.043	0.866
283	0.716 ± 0.419	0.247 ± 0.299	0.038	0.856
285	0.734 ± 0.415	0.251 ± 0.293	0.021	0.87
287	0.726 ± 0.375	0.264 ± 0.287	0.013	0.878
288	0.656 ± 0.377	0.234 ± 0.281	0.046	0.843
290	0.676 ± 0.356	0.225 ± 0.294	0.013	0.878
291	0.706 ± 0.377	0.254 ± 0.292	0.02	0.88
292	0.605 ± 0.313	0.224 ± 0.260	0.025	0.865
293	0.548 ± 0.286	0.220 ± 0.217	0.036	0.858
331	0.170 ± 0.067	0.081 ± 0.045	0.002	0.888
332	0.334 ± 0.194	0.116 ± 0.110	0.015	0.88
338	0.147 ± 0.062	0.076 ± 0.040	0.019	0.863
339	0.157 ± 0.061	0.081 ± 0.039	0.005	0.873
341	0.132 ± 0.060	0.068 ± 0.036	0.044	0.834
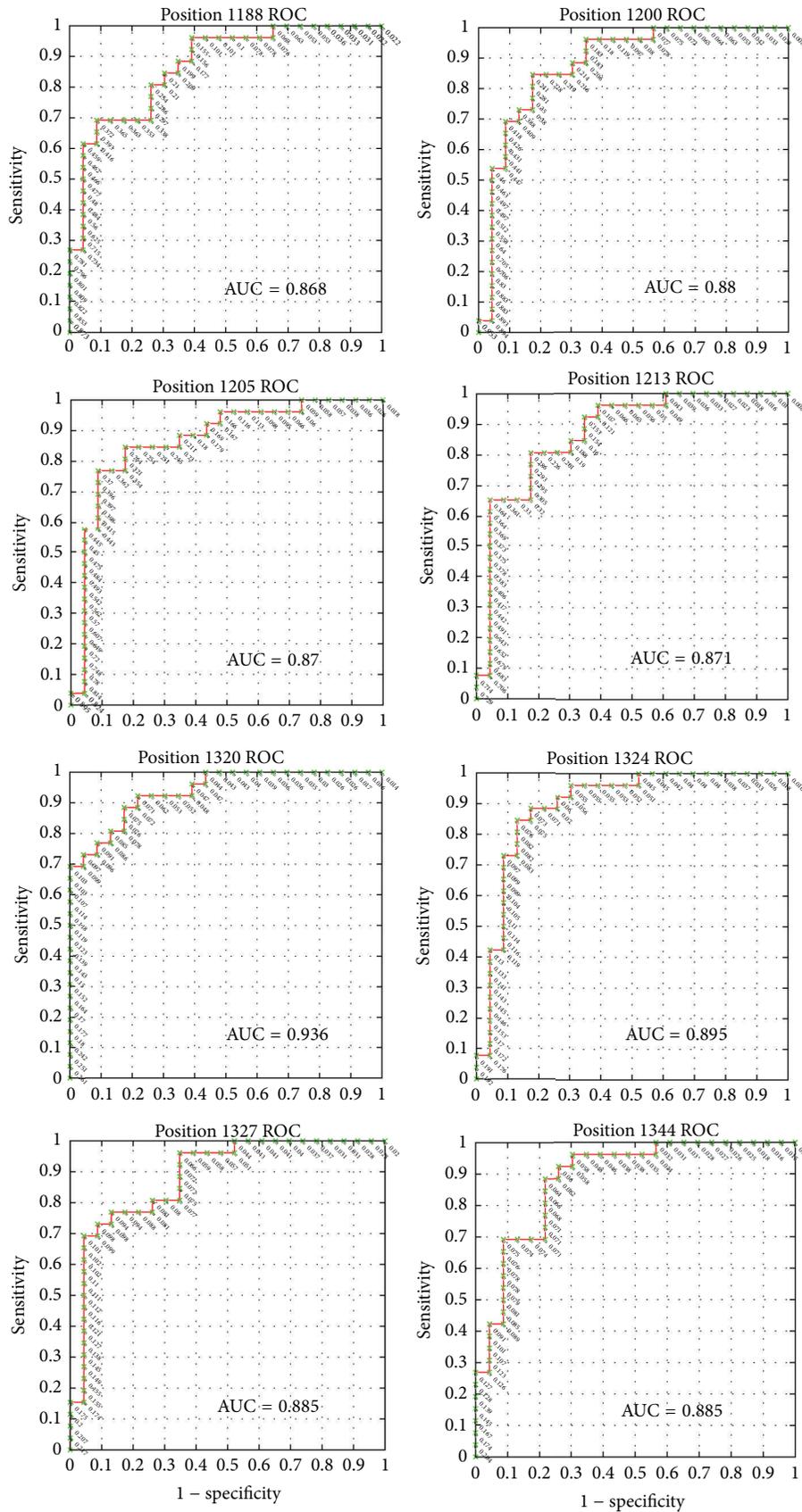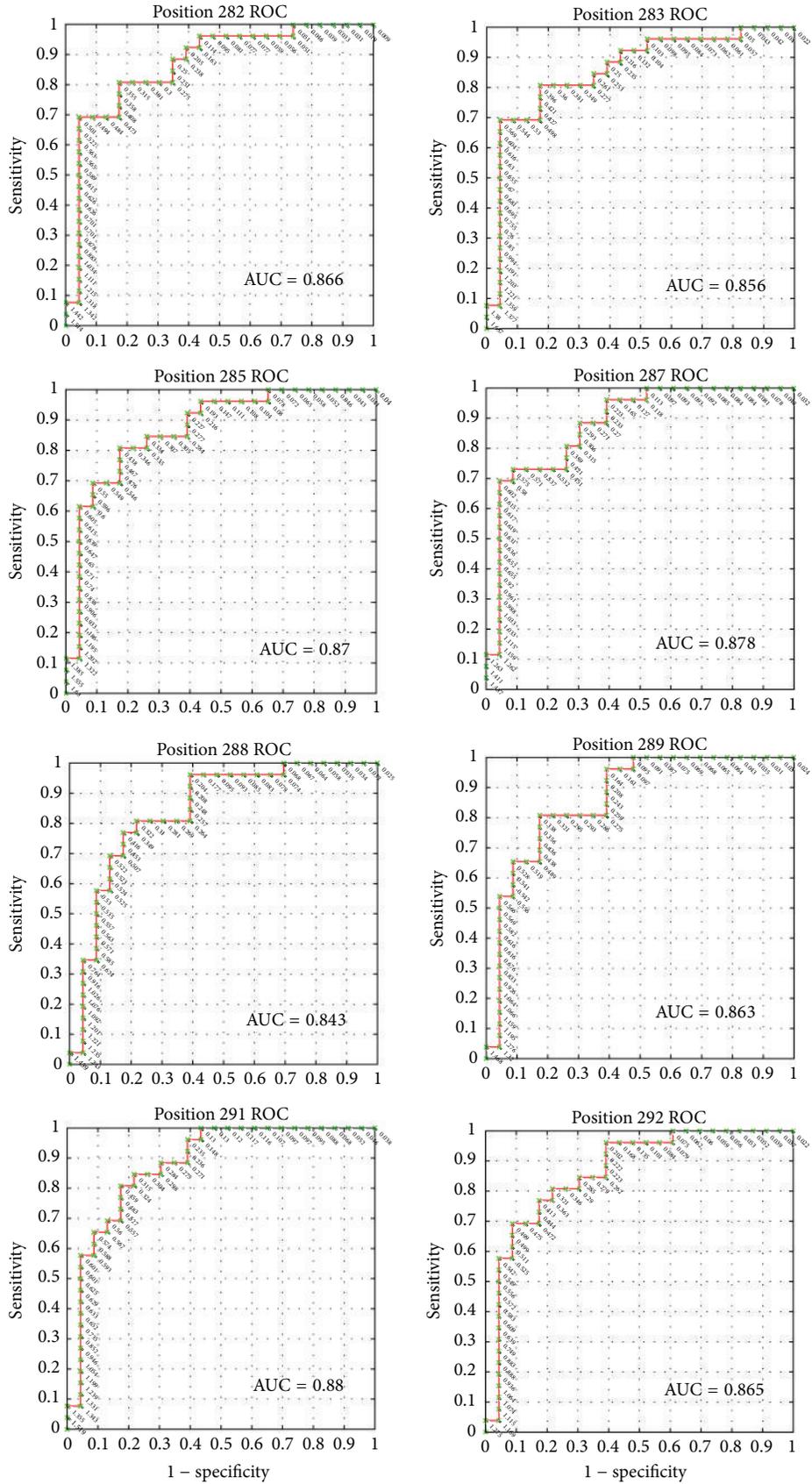
FIGURE 5: Continued.

(b) Continued

FIGURE 5: Continued.
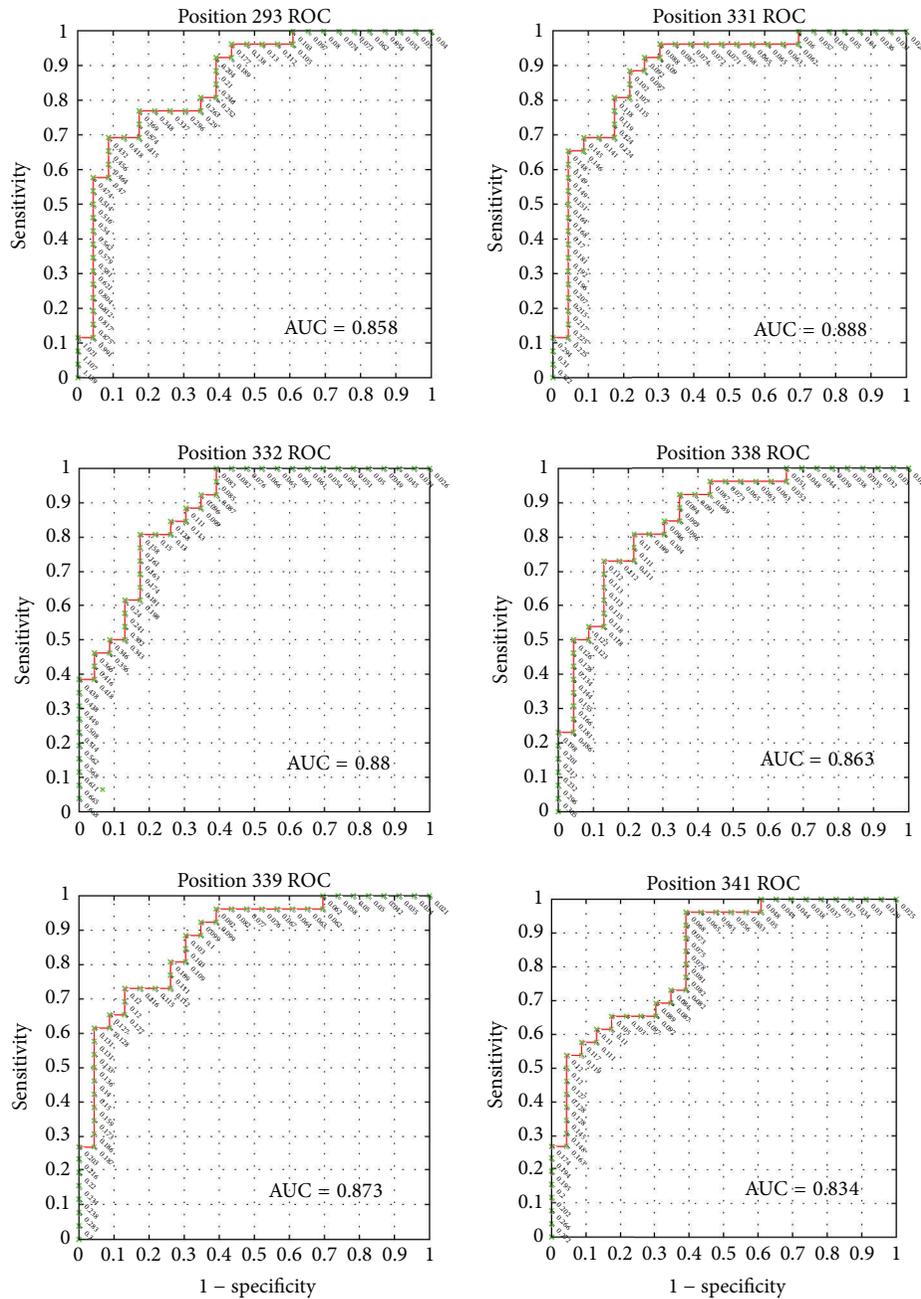
(b)

FIGURE 5: Receiver operating characteristic (ROC) curves of 8 nucleotide positions and 14 amino acid positions. (a) ROC curves of 8 nucleotide positions showing significantly different diversities between the patients with chronic hepatitis C and those with hepatocellular carcinoma caused by HCV infection. (b) ROC curves of 14 amino acid positions showing significantly different diversities between the patients with chronic hepatitis C without liver cirrhosis and those with hepatocellular carcinoma caused by HCV infection. AUC: area under the curve.

Newly developed UDPS method, on the contrary, is expected to overcome the pitfalls of above mentioned methods by enabling us to analyze simultaneously thousands of clonally amplified gene fragments. This improves the reliability of the results for the proportion of each variant and thus for the diversity measures. In this study, the average UDPS reads exceeded 2,000 for core and E1 and E2 proteins, which is much larger than those clones previously reported in other studies. Honda et al. analyzed 10 clones per sample. Hayashi et al. generated five clones per sample, Curran et al. 373 from 39 samples, and Qin et al. 767 clones from about 100 samples [9, 10, 25, 26]. Of those studies, Qin et al. who

analyzed the largest number of clones reported that HCV quasispecies diversity decreased over the natural course of HIV infection [9]. In the probabilistic view, approximately 250 clones should be generated per sample in order to include more than 99% of clones, each of which comprises more than 2% of total clones. In our study, more than 2,000 clones were analyzed, which implies that almost all types of clones present in serum were included in the analysis.

Host's humoral immune system attacks or neutralizes viral envelope proteins, which make the envelope hypervariable in the process of escaping the host immunity. Most of recent studies [9, 10] mainly focused on the analysis of HCV quasispecies diversity on E2 since this region has been known to harbor the most severe variations. However, this study analyzed a wide range of structural proteins, including core and E1 and E2, and found unexpectedly that E1 diversities rather than E2 were lower in the HCC group than that of chronic HCV infection group. An interesting finding was that all amino acid positions showing statistical differences between the two groups matched well with cytotoxic T-cell epitopes, which was claimed by Yusim et al. [27]. The fact that host immune response to HCV decreases irrespective of decreased diversity in T-cell epitope supports the idea that cytotoxic T-cells specific to HCV are more anergic in HCC than in chronic hepatitis C. And our findings could imply that the loss of cytotoxic T lymphocyte response may play an important role in carcinogenesis of HCC by HCV.

HCC can occur in HCV infection only after liver cirrhosis stage, the advanced fibrotic stage. Thus, it is recommended to perform surveillance for the occurrence of HCC since surgical treatment is only available for those with small-sized cancer and early stage. Currently, abdominal ultrasound and *alpha* fetoprotein (AFP) tests are recommended for patients with cirrhosis every six months [28]. However, AFP is known to be less sensitive and to have low positive predictive value especially in viral hepatocellular carcinoma. The diagnostic sensitivity of AFP is estimated at only 25% in those with tumor size of 3 cm or smaller, the resectable size, and nearly 50% in those with 3 cm or larger and specificity range from 76% to 96% [29, 30]. Therefore, new serum markers are actively being investigated and introduced for HCC detection [31]. Des-r-carboxyprothrombin (DCP) called PIVKA-II is one of the widely used additional markers for hepatocellular carcinoma. However, serum DCP level increases only in 50% to 60% of patients with hepatocellular carcinoma. The change in DCP value is less significant in patients with early hepatocellular carcinomas because only 15% to 30% of patients showed elevated DCP value [32]. DCP sensitivity ranged from 48% to 62%, and DCP specificity was reported in a range of 81 to 92%. Thus, it is known that DCP's diagnostic value as a hepatocellular carcinoma marker is similar to that of AFP [33]. In addition, a-l-fucosidase, r-glutamyl transferase, glypican-3, and squamous cell carcinoma antigen are used as a marker. However, no specific marker is satisfactory in terms of sensitivity and specificity. The next generation sequencing (NGS) is being increasingly used in clinical laboratories. Thus, Shannon's diversity index for 14 amino acid positions which show >0.8 area under curve of the ROC curve could be feasible as one of the new biomarkers in predicting the progression of hepatocellular carcinoma in chronic HCV patients.

In conclusion, this study found a significant decrease of HCV quasispecies diversity in the E1 region in patients with HCV-induced HCC. 14 amino acid positions were identified where patients with HCC could be differentiated from those with chronic HCV infection. These amino acid positions were matched with cytotoxic T-cell epitopes, which reinforces earlier findings that HCV-specific T-cells become anergic over the natural courses of chronic HCV infection. Our data also propose that the degree of HCV quasispecies diversity measured by UDPS might provide useful information to predict the progression of hepatocellular carcinoma in chronic HCV patients.

Conflict of Interests

The authors declare that there is no conflict of interests regarding the publication of this paper.

Acknowledgment

References

[1] M. A. Joyce and D. L. J. Tyrrell, "The cell biology of hepatitis C virus," *Microbes and Infection*, vol. 12, no. 4, pp. 263–271, 2010.

[2] S. L. Fishman and A. D. Branch, "The quasispecies nature and biological implications of the hepatitis C virus," *Infection, Genetics and Evolution*, vol. 9, no. 6, pp. 1158–1167, 2009.

[3] C. Argentini, D. Genovese, S. Dettori, and M. Rapicetta, "HCV genetic variability: from quasispecies evolution to genotype classification," *Future Microbiology*, vol. 4, no. 3, pp. 359–373, 2009.

[4] P. Farci, A. Shimoda, A. Coiana et al., "The outcome of acute hepatitis C predicted by the evolution of the viral quasispecies," *Science*, vol. 288, no. 5464, pp. 339–344, 2000.

[5] D. Amarapurkar, "Natural history of hepatitis C virus infection," *Journal of Gastroenterology and Hepatology*, vol. 15, supplement, pp. E105–E110, 2000.

[6] A. Alberti, L. Chemello, and L. Benvegnù, "Natural history of hepatitis C," *Journal of Hepatology*, vol. 31, supplement 1, pp. 17–24, 1999.

[7] L. B. Seeff, "Natural history of chronic hepatitis C," *Hepatology*, vol. 36, no. 5, pp. S35–S46, 2002.

[8] D. G. Bowen and C. M. Walker, "Adaptive immune responses in acute and chronic hepatitis C virus infection," *Nature*, vol. 436, no. 7053, pp. 946–952, 2005.

[9] H. Qin, N. J. Shire, E. D. Keenan et al., "HCV quasispecies evolution: association with progression to end-stage liver disease in hemophiliacs infected with HCV or HCV/HIV," *Blood*, vol. 105, no. 2, pp. 533–541, 2005.

[10] M. Honda, S. Kaneko, A. Sakai, M. Unoura, S. Murakami, and K. Kobayashi, "Degree of diversity of hepatitis C virus quasispecies and progression of liver disease," *Hepatology*, vol. 20, no. 5, pp. 1144–1151, 1994.

[11] M. Naito, N. Hayashi, T. Moribe et al., "Hepatitis C viral quasispecies in hepatitis C virus carriers with normal liver enzymes and patients with type C chronic liver disease," *Hepatology*, vol. 22, no. 2, pp. 407–412, 1995.

[12] J. M. Pawlotsky, M. Pellerin, M. Bouvier et al., "Genetic complexity of the hypervariable region 1 (HVR1) of hepatitis C virus (HCV): influence on the characteristics of the infection and responses to interferon alfa therapy in patients with chronic hepatitis C," *Journal of Medical Virology*, vol. 54, pp. 256–264, 1998.

[13] F.-X. López-Labrador, S. Ampurdaǹs, M. Giménez-Barcons et al., "Relationship of the genomic complexity of hepatitis C virus with liver disease severity and response to interferon in patients with chronic HCV genotype 1b interferon," *Hepatology*, vol. 29, no. 3, pp. 897–903, 1999.

[14] K. Koizumi, N. Enomoto, M. Kurosaki et al., "Diversity of quasispecies in various disease stages of chronic hepatitis C virus infection and its significance in interferon treatment," *Hepatology*, vol. 22, no. 1, pp. 30–35, 1995.

[15] D. G. Sullivan, D. Bruden, H. Deubner et al., "Hepatitis C virus dynamics during natural infection are associated with long-term histological outcome of chronic hepatitis C disease," *Journal of Infectious Diseases*, vol. 196, no. 2, pp. 239–248, 2007.

[16] J. Shendure and H. Ji, "Next-generation DNA sequencing," *Nature Biotechnology*, vol. 26, no. 10, pp. 1135–1145, 2008.

[17] K. V. Voelkerding, S. A. Dames, and J. D. Durtschi, "Next-generation sequencing:from basic research to diagnostics," *Clinical Chemistry*, vol. 55, no. 4, pp. 641–658, 2009.

[18] M. L. Metzker, "Sequencing technologies—the next generation," *Nature Reviews Genetics*, vol. 11, no. 1, pp. 31–46, 2010.

[19] M. Solmone, D. Vincenti, M. C. F. Prosperi, A. Bruselles, G. Ippolito, and M. R. Capobianchi, "Use of massively parallel ultradeep pyrosequencing to characterize the genetic diversity of hepatitis B virus in drug-resistant and drug-naive patients and to detect minor variants in reverse transcriptase and hepatitis B S antigen," *Journal of Virology*, vol. 83, no. 4, pp. 1718–1726, 2009.

[20] S. Margeridon-Thermet, N. S. Shulman, A. Ahmed et al., "Ultra-deep pyrosequencing of hepatitis b virus quasispecies from nucleoside and nucleotide reverse-transcriptase inhibitor (NRTI)-treated patients and NRTI-naive patients," *Journal of Infectious Diseases*, vol. 199, no. 9, pp. 1275–1285, 2009.

[21] V. Varghese, R. Shahriar, S.-Y. Rhee et al., "Minority variants associated with transmitted and acquired HIV-1 nonnucleoside reverse transcriptase inhibitor resistance: implications for the use of second-generation nonnucleoside reverse transcriptase inhibitors," *Journal of Acquired Immune Deficiency Syndromes*, vol. 52, no. 3, pp. 309–315, 2009.

[22] C. Hedskog, M. Mild, J. Jernberg et al., "Dynamics of HIV-1 quasispecies during antiviral treatment dissected using ultra-deep pyrosequencing," *PLoS ONE*, vol. 5, no. 7, Article ID e11345, 2010.

[23] N. Yuki, N. Hayashi, T. Moribe et al., "Relation of disease activity during chronic hepatitis C infection to complexity of hypervariable region 1 quasispecies," *Hepatology*, vol. 25, no. 2, pp. 439–444, 1997.

[24] K. L. Barlow, J. Green, and J. P. Clewley, "Viral genome characterisation by the heteroduplex mobility and heteroduplex tracking assays," *Reviews in Medical Virology*, vol. 10, pp. 321–335, 2000.

[25] J. Hayashi, Y. Kishihara, K. Yamaji et al., "Hepatitis C viral quasispecies and liver damage in patients with chronic hepatitis C virus infection," *Hepatology*, vol. 25, no. 3, pp. 697–701, 1997.

[26] R. Curran, C. L. Jameson, J. K. Craggs et al., "Evolutionary trends of the first hypervariable region of the hepatitis C virus E2 protein in individuals with differing liver disease severity," *Journal of General Virology*, vol. 83, no. 1, pp. 11–23, 2002.

[27] K. Yusim, R. Richardson, N. Tao et al., "Los Alamos hepatitis C immunology database," *Applied Bioinformatics*, vol. 4, no. 4, pp. 217–225, 2005.

[28] J. Bruix and M. Sherman, "Management of hepatocellular carcinoma," *Hepatology*, vol. 42, no. 5, pp. 1208–1236, 2005.

[29] M. Soresi, C. Magliarisi, P. Campagna et al., "Usefulness of alpha-fetoprotein in the diagnosis of hepatocellular carcinoma," *Anticancer Research*, vol. 23, no. 2, pp. 1747–1753, 2003.

[30] F. Trevisani, P. E. D'Intino, A. M. Morselli-Labate et al., "Serum α-fetoprotein for diagnosis of hepatocellular carcinoma in patients with chronic liver disease: influence of HBsAg and anti-HCV status," *Journal of Hepatology*, vol. 34, no. 4, pp. 570–575, 2001.

[31] M. Gambarin-Gelwan, D. C. Wolf, R. Shapiro, M. E. Schwartz, and A. D. Min, "Sensitivity of commonly available screening tests in detecting hepatocellular carcinoma in cirrhotic patients undergoing liver transplantation," *American Journal of Gastroenterology*, vol. 95, no. 6, pp. 1535–1538, 2000.

[32] I. C. Weitz and H. A. Liebman, "Des-γ-carboxy (abnormal) prothrombin and hepatocellular carcinoma: a critical review," *Hepatology*, vol. 18, no. 4, pp. 990–997, 1993.

[33] T. Nakagawa, T. Seki, T. Shiro et al., "Clinicopathologic significance of protein induced vitamin K absence or antagonist II and α-fetoprotein in hepatocellular carcinoma," *International Journal of Oncology*, vol. 14, no. 2, pp. 281–286, 1999.

Research Article

Misidentification of *Candida guilliermondii* as *C. famata* among Strains Isolated from Blood Cultures by the VITEK 2 System

Si Hyun Kim,[1,2] Jeong Hwan Shin,[1,2] Jeong Ha Mok,[3,4] Shine Young Kim,[5] Sae Am Song,[1] Hye Ran Kim,[1] Joong-Ki Kook,[6] Young-Hyo Chang,[7] Il Kwon Bae,[8] and Kwangha Lee[3,4,9]

[1] *Department of Laboratory Medicine, Inje University College of Medicine, Busan 614-735, Republic of Korea*

[2] *Paik Institute for Clinical Research, Inje University College of Medicine, Busan 614-735, Republic of Korea*

[3] *Department of Internal Medicine, Pusan National University School of Medicine, Busan 602-739, Republic of Korea*

[4] *Biomedical Research Institute, Pusan National University School of Medicine, Busan 602-739, Republic of Korea*

[5] *Department of Laboratory Medicine, Pusan National University School of Medicine, Busan 602-739, Republic of Korea*

[6] *Department of Oral Biochemistry, School of Dentistry, Chosun University, Gwangju 501-759, Republic of Korea*

[7] *Korean Collection for Type Cultures, Biological Resource Center, KRIBB, Daejeon 305-806, Republic of Korea*

[8] *Department of Dental Hygiene, College of Medical and Life Science, Silla University, Busan 617-736, Republic of Korea*

[9] *Department of Internal Medicine, Pusan National University Hospital, 179, Gudeok-ro, Seo-gu, Busan 602-739, Republic of Korea*

Correspondence should be addressed to Kwangha Lee; jubilate@pusan.ac.kr

Introduction. The aim of this study was to differentiate between *Candida famata* and *Candida guilliermondii* correctly by using matrix-assisted laser desorption/ionization-time of flight mass spectrometry (MALDI-TOF MS) and gene sequencing. *Methods*. Twenty-eight *Candida* strains from blood cultures that had been identified as *C. famata* ($N = 25$), *C. famata*/*C. guilliermondii* ($N = 2$), and *C. guilliermondii* ($N = 1$) by the VITEK 2 system using the YST ID card were included. We identified these strains by MALDI-TOF MS and gene sequencing using the 28S rRNA and *ITS* genes and compared the results with those obtained by the VITEK 2 system. *Results*. All 28 isolates were finally identified as *C. guilliermondii*. Sequencing analysis of the 28S rRNA gene showed 99.80%–100% similarity with *C. guilliermondii* for all 28 strains. The *ITS* gene sequencing of the strains showed 98.34%–100% homology with *C. guilliermondii*. By MALDI-TOF, we could correctly identify 21 (75%) of 28 *C. guilliermondii* isolates. *Conclusion*. We should suspect misidentification when *C. famata* is reported by the VITEK 2 system, and we always should keep in mind the possibility of misidentification of any organism when an uncommon species is reported.

1. Introduction

Bloodstream infections caused by *Candida* species have increased significantly over recent decades and are associated with high rates of morbidity and mortality [1, 2]. A rapid and accurate identification of *Candida* species is of great importance to the selection of appropriate antifungal agents and for appropriate patient management [3].

We have faced an increase in *Candida famata* isolation from blood cultures with the use of the VITEK 2 system in the clinical laboratory. This organism usually is found on natural substrates and has been reported as a rare pathogen of human beings [4–7]. *Candida famata* and *C. guilliermondii* are extremely difficult to differentiate by phenotypic features [8, 9], so we need to determine whether the recent increase of *C. famata* in the blood is true or reflects an error by the identification system because of the organism's similarity in biochemical characteristics to other *Candida* spp.

The aim of this study was to identify these strains correctly using matrix-assisted laser desorption/ionization-time of flight mass spectrometry (MALDI-TOF MS) and 28S rRNA and *ITS* gene sequencing.

2. Materials and Methods

2.1. Strains. Twenty-eight nonduplicated *Candida* strains identified as *C. famata* ($N = 25$), *C. famata/C. guilliermondii* ($N = 2$), or *Candida guilliermondii* ($N = 1$) by the VITEK 2 system using the YST-ID card were included. All 28 strains were collected from blood culture at Inje University Busan Paik Hospital in the Republic of Korea between January 2007 and December 2008. We selected 25 nonduplicated strains identified as *C. famata* (identification scores 92%–95%) and 2 nonduplicated strains showing a result of *C. famata/C. guilliermondii* (50%/50%) by the VITEK system. We selected these strains to achieve even distribution throughout the isolation period and the admission ward. One *Candida guilliermondii* isolate (97%) was used as a control. All isolates were stored in skim milk at $-80°C$ until testing.

2.2. Phenotypic Characterization. Fungal culture and identification were performed by standard procedures in a clinical microbiology laboratory. Yeast-form fungi were identified according to conventional biochemical laboratory methods by the VITEK 2 system using YST-ID. All procedures were done according to the manufacturer's instruction. We repeated the identification procedures twice using the same YST-ID for all strains.

2.3. MALDI-TOF MS Analysis. We identified all strains with MALDI-TOF MS using MALDI Biotyper. MALDI-TOF analyzes the unique protein spectra produced by extracts of microbial cells. First, α-cyano-4-hydroxycinnamic acid (HCCA portioned, number 255344, Bruker Daltonik GmbH, Bremen, Germany) was prepared as the MALDI matrix for Bruker MALDI Biotyper measurements. Colonies were transferred to a steel target, namely, MSP 96 polished steel (Bruker Daltonics), and overlaid with $1 \mu L$ of matrix solution directly after drying. The extraction steps were done as follows. Briefly, samples were prepared using formic acid and acetonitrile after alcohol treatment, and then $1 \mu L$ of extract supernatant fluid was used for analysis. Spectra were automatically concentrated on a maximum of 240 shots by MBT autoX and then compared with the Bruker Daltonics database using the MALDI Biotyper RTC software. We repeated test with extraction method if no result was obtained.

2.4. Gene Sequencing. All *Candida* strains were identified by polymerase chain reaction (PCR) and by direct sequencing of the 28S rRNA and *ITS* genes. The fungal genomic DNA collected from a single colony of an overnight culture was extracted with InstaGene Matrix kit (Bio-Rad Laboratories, Hercules, CA USA) according to the manufacturer's recommendation.

The *ITS* gene was amplified using the universal fungal primers ITS1 ($5'$-TCC GTA GGT GAA CCT GCG G-$3'$) and ITS4 ($5'$-TCC TCC GCT TAT TGA TAT GC-$3'$). The 28S rRNA gene was amplified with the primers D1/D2-F ($5'$-GCA TAT CAA TAA GCG GAG GAA AAG-$3'$) and D1/D2-R ($5'$-GGT CCG TGT TTC AAG ACG G-$3'$) as

previously described [10]. The primers for sequencing were the same as those for PCR amplification. Both strands of the purified DNA from the PCR were sequenced directly with a Big Dye Terminator Cycle Sequencing kit (Applied Biosystems, Foster City, CA) and the ABI PRISM 3130 genetic analyzer (Applied Biosystems). The sequences were compared with those of the type and reference strains to confirm species identification using NCBI (a genome database of the National Center for Biotechnology Information). Phylogenetic analyses were performed for the 28S rRNA and *ITS* using the neighbor-joining method with MEGA version 4.

3. Results

All 28 isolates were finally identified as *C. guilliermondii*, although 27 had been reported as *C. famata* ($N = 25$) or *C. famata/C. guilliermondii* ($N = 2$) by the VITEK 2 system using the YST-ID card. There was no true *C. famata* strain. Thus, we could confirm that *C. famata* is a rare cause of fungemia, its diagnosis being attributable to the misidentification of *C. guilliermondii* as *C. famata* by the VITEK 2 system.

The MALDI-TOF MS method was valuable for identification of *C. guilliermondii*. We could correctly identify 21 *C. guilliermondii* isolates that had been identified as *C. famata* ($N = 18$), *C. famata/C. guilliermondii* ($N = 2$), or *C. guilliermondii* ($N = 1$) by VITEK 2. Two strains showed a score of more than 2.0 by the Bruker MALDI Biotyper, whereas the scores of 19 strains were between 1.7 and 1.99. The remaining seven isolates could not be identified to the species level even though we retested and used the extraction method. They showed scores of less than 1.7, and we defined the result as no identification (Table 1).

The final correct identification could be acquired from the use of 28S rRNA and *ITS* sequencing. We compared the analyzed sequences from the clinical isolates with those of type and reference strains obtained from the NCBI database. By using 28S rRNA gene sequencing, all the 28 isolates were clearly identified as *C. guilliermondii* with a similarity between 99.80% and 100%, and these strains also showed close similarity to *C. carpophila* (99.65%–99.82%) and *C. caribbica* (99.30%–99.47%). For *ITS* sequencing, all 28 isolates were first identified as *C. guilliermondii*, showing similarity between 98.34% and 100%. However, the similarity with *C. caribbica* was also very high (99.03%–99.23%). To differentiate these closely related species, we constructed a phylogenetic tree using the neighbor-joining method with MEGA version 4. By this method, all strains were clustered with *C. guilliermondii*, and these were obviously distinguished from *C. famata* by both genes. For the phylogenetic tree of the 28S rRNA gene, *C. guilliermondii* strains were clearly differentiated from *C. caribbica*, but not from *C. carpophila* (Figure 1). When using the *ITS* sequence, all isolates were clustered as one group with *C. guilliermondii*, and this group was separated from *C. caribbica* and *C. carpophila* (Figure 2).

Table 1: VITEK 2 system, MALDI-TOF MS, and sequencing results for 28 *Candida* strains.

Strain	VITEK 2		MALDI-TOF MS		Sequencing			
	Identification	Score	Identification	Score	ID (28S gene)	Similarity	ID (*ITS* gene)	Similarity
M07-1257	*C. guilliermondii*	97%	*C. guilliermondii*	1.791	*C. guilliermondii*	100%	*C. guilliermondii*	100%
M07-1410	*C. famata*	95%	*C. guilliermondii*	1.782	*C. guilliermondii*	100%	*C. guilliermondii*	99.81%
M07-1525	*C. famata*	95%	*C. guilliermondii*	1.882	*C. guilliermondii*	100%	*C. guilliermondii*	99.81%
M07-1575	*C. famata*	95%	No ID*	1.682	*C. guilliermondii*	100%	*C. guilliermondii*	99.81%
M07-1586	*C. famata*	95%	*C. guilliermondii*	1.878	*C. guilliermondii*	100%	*C. guilliermondii*	98.34%
M07-1601	*C. famata*	93%	*C. guilliermondii*	1.951	*C. guilliermondii*	100%	*C. guilliermondii*	99.81%
M07-1627	*C. famata*	95%	*C. guilliermondii*	1.864	*C. guilliermondii*	100%	*C. guilliermondii*	99.81%
M07-1639	*C. famata*	95%	No ID*	1.700	*C. guilliermondii*	100%	*C. guilliermondii*	99.81%
M08-0109	*C. famata*	95%	*C. guilliermondii*	1.832	*C. guilliermondii*	100%	*C. guilliermondii*	99.81%
M08-0121	*C. famata*	95%	*C. guilliermondii*	1.951	*C. guilliermondii*	100%	*C. guilliermondii*	99.81%
M08-0160	*C. famata*	95%	*C. guilliermondii*	1.917	*C. guilliermondii*	100%	*C. guilliermondii*	99.81%
M08-0197	*C. famata*	95%	*C. guilliermondii*	1.719	*C. guilliermondii*	100%	*C. guilliermondii*	99.63%
M08-0217	*C. famata*	95%	*C. guilliermondii*	1.892	*C. guilliermondii*	100%	*C. guilliermondii*	99.81%
M08-0227	*C. famata*	95%	*C. guilliermondii*	1.726	*C. guilliermondii*	99.80%	*C. guilliermondii*	99.81%
M08-0296	*C. famata*	95%	*C. guilliermondii*	1.872	*C. guilliermondii*	100%	*C. guilliermondii*	99.81%
M08-0328	*C. famata*/*C. guilliermondii*	50%/50%	*C. guilliermondii*	2.068	*C. guilliermondii*	100%	*C. guilliermondii*	99.81%
M08-1839	*C. famata*	92%	No ID*	1.615	*C. guilliermondii*	100%	*C. guilliermondii*	99.81%
M08-1847	*C. famata*	95%	No ID*	1.492	*C. guilliermondii*	100%	*C. guilliermondii*	99.81%
M08-1848	*C. famata*	95%	*C. guilliermondii*	1.825	*C. guilliermondii*	99.80%	*C. guilliermondii*	99.81%
M08-1849	*C. famata*	95%	No ID*	1.394	*C. guilliermondii*	100%	*C. guilliermondii*	99.81%
M08-1850	*C. famata*	95%	*C. guilliermondii*	2.030	*C. guilliermondii*	100%	*C. guilliermondii*	99.81%
M08-1851*	*C. famata*/*C. guilliermondii*	50%/50%	*C. guilliermondii*	1.992	*C. guilliermondii*	100%	*C. guilliermondii*	99.81%
M08-1852	*C. famata*	95%	No ID*	1.649	*C. guilliermondii*	100%	*C. guilliermondii*	99.81%
M08-1854	*C. famata*	95%	*C. guilliermondii*	1.883	*C. guilliermondii*	99.80%	*C. guilliermondii*	99.81%
M08-1855	*C. famata*	95%	No ID*	1.637	*C. guilliermondii*	99.80%	*C. guilliermondii*	99.81%
M08-1857	*C. famata*	95%	*C. guilliermondii*	1.854	*C. guilliermondii*	100%	*C. guilliermondii*	99.81%
M08-1876	*C. famata*	95%	*C. guilliermondii*	1.722	*C. guilliermondii*	100%	*C. guilliermondii*	99.81%
M08-1898	*C. famata*	92%	*C. guilliermondii*	1.939	*C. guilliermondii*	100%	*C. guilliermondii*	99.81%

*No ID: not reliable identification.
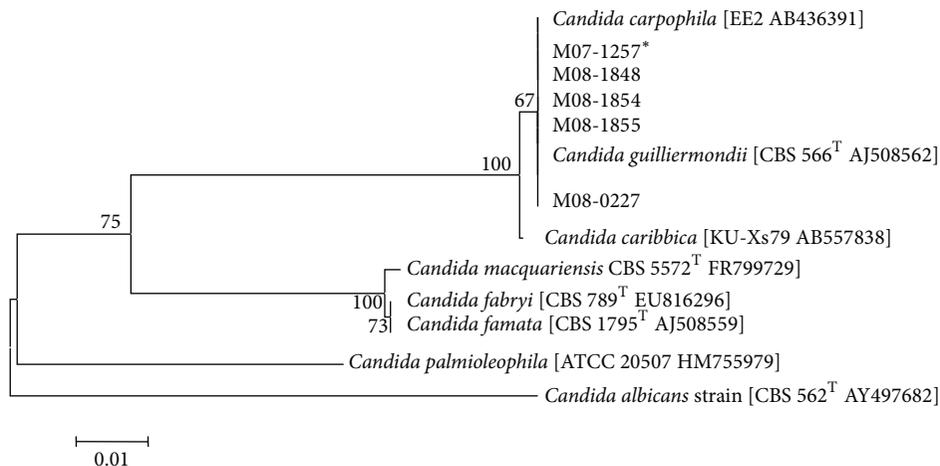
Figure 1: Phylogenetic analysis using the neighbor-joining method based on the 28S rDNA gene sequence for 28 clinical isolates and type and reference strains. The scale bar represents the distance between strains. *M07-1257 represents other strains that have 100% sequence similarity to purported 21 *C. famata*, 1 *C. guilliermondii*, and 2 *C. famata*/*C. guilliermondii* strains.
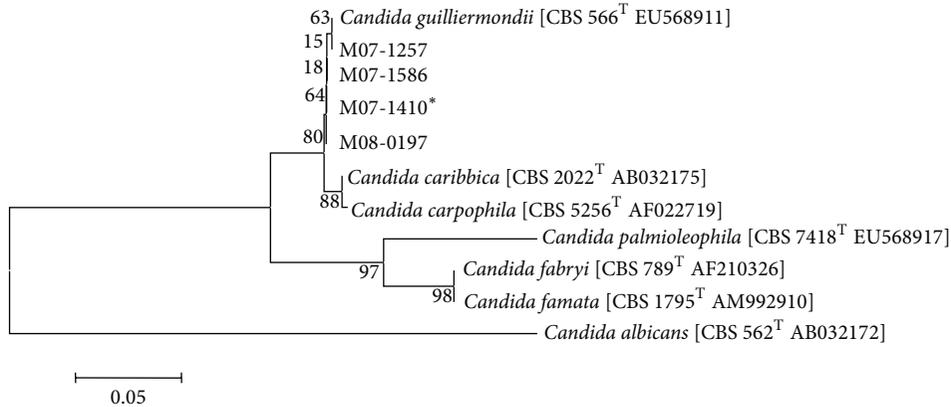
FIGURE 2: Phylogenetic analysis using the neighbor-joining method based on the *ITS* sequence for 28 clinical isolates and type and reference strains. The scale bar represents the distance between strains. *M07-1410 represents strains that have 100% sequence similarity to the purported 21 *C. famata*, 1 *C. guilliermondii*, and 2 *C. famata*/*C. guilliermondii* strains.

4. Discussion

Candida species are the fourth most common cause of nosocomial bloodstream infections [11]. *Candida albicans* is still the most common species isolated from human beings; however, the frequency of non-*albicans Candida* species is increasing as a major cause of catheter-related bloodstream infections especially [12].

Candida famata is a rare cause of invasive infection. This strain was described as *Torula candida* after being discovered in Japan [13]. It then was called *Torulopsis famata* and *Debaryomyces hansenii* and finally defined as *C. famata*. It occupies the human skin, vagina, and oral cavity as a colonizing organism, so it has been considered a contaminant even though it has been isolated from clinical specimens [13, 14].

However, there are several reports concerning invasive candidiasis caused by *C. famata*, and it should be considered an important opportunistic pathogen. The most important disease caused by *C. famata* is intravenous catheter-associated candidemia in immunocompromised patients, as described by St.-Germain and Laverdiere [7] in a bone marrow transplant patient. It also has been detected in patients with endophthalmitis with chronic intraocular inflammation [15], candidemia with aplastic anemia, and central catheterization [13] and fatal peritonitis in a patient undergoing continuous ambulatory peritoneal dialysis [16].

In clinical laboratories, most bacteria and yeasts are routinely identified by biochemical characteristics using a commercial kit or automated identification system such as API and VITEK. Renneberg et al. [17] reported evaluation by the Staph ID 32 and StaphZym systems for coagulase-negative staphylococci showing a high rate of misidentification. This phenomenon is obvious when some species have high similarity in biochemical reactions. Misidentification also is possible for *Candida* species when commercial kits such as API 20C are used for identification [10]. *Candida famata* is very similar in biochemical characteristics to *C.*

guilliermondii and *C. caribbica*. Desnos-Ollivier et al. [9] reported that several *C. famata* strains identified by API 32C were *C. guilliermondii*, *C. haemulonii*, *C. lusitaniae*, and *C. palmioleophila* when gene sequencing was done. More recently, there was an interesting report of misidentification of *C. parapsilosis* as *C. famata* in vertebral osteomyelitis [18]. The authors of that paper asserted the importance of this problem because of differences in antifungal susceptibility [3], especially the fact that the resistance rate to fluconazole and amphotericin B is high in *C. guilliermondii*. Similar misidentification can be seen in the identification of mold-form fungi [19]. We agree with their recommendation concerning the importance of using many molecular techniques for diagnosis of infectious diseases to overcome the limits of conventional methods [20, 21].

The VITEK 2 system is one of the most common automated identification systems using a colorimetric identification card of YST. In previous reports, it was noted to be of high sensitivity and specificity greater than 95% for common *Candida* species isolated from clinical specimens compared with molecular methods [22, 23]. On the other hand, the identification rates for *C. parapsilosis* by the VITEK 2 system were reported to be as low as 71.7%, although it can be improved to 93.3% by examining the morphologic features on cornmeal agar plates [23].

At first, we reported the results as *C. famata* for 25 strains because the identification scores were high (identification scores: 92%–95%) by the VITEK 2 system. However, the isolation of *C. famata* by the VITEK 2 system has increased in our clinical microbiology laboratory, and this is unusual for us. So we assumed either the possibility of a change in the distribution of *Candida* species isolated from blood culture or some error in identification by the VITEK 2 system. We tried to identify these isolates correctly using MALDI-TOF MS and 28S rRNA and *ITS* gene sequencing analysis, and we finally confirmed the misidentification by the VITEK 2 System of *C. guilliermondii* as *C. famata* in clinical isolates from blood culture.

Many microbes show similar patterns of biochemical reactions, and we have difficulty in identification. Broad-range PCR and gene sequencing is a good tool for the correct identification of fungi, and 28S rRNA and *ITS* are well known as useful regions for identification of fungi [24]. This technique allows more accurate identification of *Candida* species based on differences in the rRNA [25, 26]. In this study, all isolates were identified as *C. guilliermondii* using the 28S rRNA and *ITS* genes. We found that the 28S rRNA gene could not discriminate between *C. guilliermondii* and *C. carpophila* because of the high similarity of their sequences. However, these regions could distinguish between *C. famata* and *C. guilliermondii*.

In recent years, MALDI-TOF MS was introduced as a technique for molecular identification [27]. This technique has a profound advantage of rapid identification to the species level within a few minutes. We evaluated its ability to correctly identify *C. guilliermondii*. We analyzed these 28 *Candida* strains according to the recommendations of the manufacturers. Among the 28 *Candida* species, two isolates showed a score of more than 2.0 and were *C. guilliermondii*. Nineteen isolates gave a result of *C. guilliermondii*, but the scores were between 1.7 and 2.0. We got nonreliable results for 7 strains even though we retested after extraction. Stevenson et al. [28] evaluated the clinical usefulness of MALDI-TOF MS for the identification of yeasts by their own library using 109 reference and type strains. They could identify isolates correctly to the species level in 192 (97.5%) of 197 isolates with 100% correct identification of all 15 *C. guilliermondii*. Lacroix et al. [29] compared two MALDI-TOF MS systems, Andromas and Bruker MaldiBiotyper, with conventional identification methods using 1383 clinical *Candida* isolates. The correct identification rates of the two MALDI-TOF MS systems (98.2%) were higher than those of conventional methods (96.5%) by comparison with sequencing results. Bruker MaldiBiotyper recommends that a score greater than 2.0 be identified to the species level and to the genus level if the values are greater than 1.70 but lower than 2.0. It gives "Not reliable identification" if the values are lower than 1.70. However, only 2 strains were higher than 2.0 in this study, so we would recommend a cutoff value of 1.7 to identify *C. guilliermondii*.

In conclusion, we confirmed the misidentification of *C. guilliermondii* as *C. famata* by the VITEK 2 YST system. We now suspect misidentification when *C. famata* is reported by the VITEK 2 system, and we always keep in mind the possibility of misidentification when an uncommon species is reported.

Conflict of Interests

The authors declare that there is no conflict of interests regarding the publication of this paper.

Authors' Contribution

Si Hyun Kim and Jeong Hwan Shin contributed equally to this work.

References

[1] R. P. Wenzel, "Nosocomial candidemia: risk factors and attributable mortality," *Clinical Infectious Diseases*, vol. 20, no. 6, pp. 1531–1534, 1995.

[2] E. J. Won, J. H. Shin, W. K. Lee et al., "Distribution of yeast and mold species isolated from clinical specimens at 12 hospitals in Korea during 2011," *Annals of Clinical Microbiology*, vol. 16, no. 2, pp. 92–100, 2013.

[3] P. E. Verweij, I. M. Breuker, A. J. M. M. Rijs, and J. F. G. M. Meis, "Comparative study of seven commercial yeast identification systems," *Journal of Clinical Pathology*, vol. 52, no. 4, pp. 271–273, 1999.

[4] D. Wagner, A. Sander, H. Bertz, J. Finke, and W. V. Kern, "Breakthrough invasive infection due to *Debaryomyces hansenii* (teleomorph *Candida famata*) and *Scopulariopsis brevicaulis* in a stem cell transplant patient receiving liposomal amphotericin B and caspofungin for suspected aspergillosis," *Infection*, vol. 33, no. 5-6, pp. 397–400, 2005.

[5] J. A. Barnett, R. W. payne, and D. Yarrow, *Yeasts: characteristics and Identification*, Cambridge University Press, Cambridge, UK, 3rd edition, 2000.

[6] A. J. Gupta, H. Mi, C. Wroe, B. Jaques, and D. Talbot, "Fatal *Candida famata* peritonitis complicating sclerosing peritonitis in a peritoneal dialysis patient," *Nephrology Dialysis Transplantation*, vol. 21, no. 7, pp. 2036–2037, 2006.

[7] G. St.-Germain and M. Laverdiere, "Torulopsis candida, a new opportunistic pathogen," *Journal of Clinical Microbiology*, vol. 24, no. 5, pp. 884–885, 1986.

[8] A. Nishikawa, T. Sugita, and T. Shinoda, "Differentiation between *Debaryomyces hansenii/Candida famata* complex and *Candida guilliermondii* by polymerase chain reaction," *FEMS Immunology and Medical Microbiology*, vol. 19, no. 2, pp. 125–129, 1997.

[9] M. Desnos-Ollivier, M. Ragon, V. Robert, D. Raoux, J.-C. Gantier, and F. Dromer, "Debaryomyces hansenii (*Candida famata*), a rare human fungal pathogen often misidentified as *Pichia guilliermondii* (*Candida guilliermondii*)," *Journal of Clinical Microbiology*, vol. 46, no. 10, pp. 3237–3242, 2008.

[10] J. Xu, B. C. Millar, J. E. Moore et al., "Comparison of API20C with molecular identification of *Candida* spp isolated from bloodstream infections," *Journal of Clinical Pathology*, vol. 55, no. 10, pp. 774–777, 2002.

[11] M. B. Edmond, S. E. Wallace, D. K. McClish, M. A. Pfaller, R. N. Jones, and R. P. Wenzel, "Nosocomial bloodstream infections in United States hospitals: a three-year analysis," *Clinical Infectious Diseases*, vol. 29, no. 2, pp. 239–244, 1999.

[12] M.-K. Lee, D. Yong, M. Kim, M.-N. Kim, and K. Lee, "Species distribution and antifungal susceptibilities of yeast clinical isolates from three hospitals in Korea, 2001 to 2007," *Korean Journal of Laboratory Medicine*, vol. 30, no. 4, pp. 364–372, 2010.

[13] A. Nishikawa, H. Tomomatsu, T. Sugita, R. Ikeda, and T. Shinoda, "Taxonomic position of clinical isolates of *Candida famata*," *Journal of Medical and Veterinary Mycology*, vol. 34, no. 6, pp. 411–419, 1996.

[14] Y. F. Ngeow and T. S. Soo-Hoo, "Incidence and distribution of vaginal yeasts in Malaysian women," *Mycoses*, vol. 32, no. 11, pp. 563–567, 1989.

[15] N. A. Rao, A. V. Nerenberg, and D. J. Forster, "Torulopsis candida (*Candida famata*) endophthalmitis simulating *Propionibacterium acnes* syndrome," *Archives of Ophthalmology*, vol. 109, no. 12, pp. 1718–1721, 1991.

[16] G. Quindos, F. Cabrera, M. D. C. Arilla et al., "Fatal *Candida famata* peritonitis in a patient undergoing continuous ambulatory peritoneal dialysis who was treated with fluconazole," *Clinical Infectious Diseases*, vol. 18, no. 4, pp. 658–660, 1994.

[17] J. Renneberg, K. Rieneck, and E. Gutschik, "Evaluation of Staph ID 32 system and Staph-Zym system for identification of coagulase-negative staphylococci," *Journal of Clinical Microbiology*, vol. 33, no. 5, pp. 1150–1153, 1995.

[18] M. J. Burton, P. Shah, and E. Swiatlo, "Misidentification of candida parapsilosis as *C famata* in a clinical case of vertebral osteomyelitis," *American Journal of the Medical Sciences*, vol. 341, no. 1, pp. 71–73, 2011.

[19] H. J. Huh, J. H. Lee, K. S. Park et al., "A case of misidentification of *Aspergillus versicolor* complex as *Scopulariopsis* species isolated from a homograft," *Annals of Clinical Microbiology*, vol. 16, no. 2, pp. 105–109, 2013.

[20] S. H. Kim, H. S. Jeong, Y. H. Kim et al., "Evaluation of DNA extraction methods and their clinical application for direct detection of causative bacteria in continuous ambulatory peritoneal dialysis culture fluids from patients with peritonitis by using broad-range PCR," *Annals of Laboratory Medicine*, vol. 32, no. 2, pp. 119–125, 2012.

[21] M. Kim, M. J. Kwon, H.-S. Chung et al., "Evaluation of matrix-assisted laser desorption ionization-time of flight mass spectrometry for identification of aerobic bacteria in a clinical microbiology laboratory," *Korean Journal of Clinical Microbiology.*, vol. 15, no. 2, pp. 60–66, 2012.

[22] M. Sanguinetti, R. Porta, M. Sali et al., "Evaluation of VITEK 2 and RapID Yeast plus systems for yeast species identification: experience at a large clinical microbiology laboratory," *Journal of Clinical Microbiology*, vol. 45, no. 4, pp. 1343–1346, 2007.

[23] G. Valenza, J. Strasen, F. Schäfer, M. Frosch, O. Kurzai, and M. Abele-Horn, "Evaluation of new colorimetric Vitek 2 yeast identification card by use of different source media," *Journal of Clinical Microbiology*, vol. 46, no. 11, pp. 3784–3787, 2008.

[24] P. C. Iwen, A. G. Freifeld, T. A. Bruening, and S. H. Hinrichs, "Use of a panfungal PCR assay for detection of fungal pathogens in a commercial blood culture system," *Journal of Clinical Microbiology*, vol. 42, no. 5, pp. 2292–2293, 2004.

[25] T. J. Lott, R. J. Kuykendall, and E. Reiss, "Nucleotide sequence analysis of the 5.8S rDNA and adjacent ITS2 region of *Candida albicans* and related species," *Yeast*, vol. 9, no. 11, pp. 1199–1206, 1993.

[26] J.-H. Jang, J. H. Lee, C.-S. Ki, and N. Y. Lee, "Identification of clinical mold isolates by sequence analysis of the internal transcribed spacer region, ribosomal large-subunit D1/D2, and β-tubulin," *Annals of Laboratory Medicine*, vol. 32, no. 2, pp. 126–132, 2012.

[27] A. Bizzini and G. Greub, "Matrix-assisted laser desorption ionization time-of-flight mass spectrometry, a revolution in clinical microbial identification," *Clinical Microbiology and Infection*, vol. 16, no. 11, pp. 1614–1619, 2010.

[28] L. G. Stevenson, S. K. Drake, Y. R. Shea, A. M. Zelazny, and P. R. Murray, "Evaluation of matrix-assisted laser desorption ionization—time of flight mass spectrometry for identification of clinically important yeast species," *Journal of Clinical Microbiology*, vol. 48, no. 10, pp. 3482–3486, 2010.

[29] C. Lacroix, A. Gicquel, B. Sendid et al., "Evaluation of two matrix-assisted laser desorption ionization-time of flight mass spectrometry (MALDI-TOF MS) systems for the identification of *Candida* species," *Clinical Microbiology and Infection*, vol. 20, pp. 153–158, 2013.

Review Article

Laboratory Markers of Ventricular Arrhythmia Risk in Renal Failure

Ioana Mozos

Department of Functional Sciences, "Victor Babes" University of Medicine and Pharmacy, T. Vladimirescu Street 14, 300173 Timisoara, Romania

Correspondence should be addressed to Ioana Mozos; ioanamozos@yahoo.de

Sudden cardiac death continues to be a major public health problem. Ventricular arrhythmia is a main cause of sudden cardiac death. The present review addresses the links between renal function tests, several laboratory markers, and ventricular arrhythmia risk in patients with renal disease, undergoing or not hemodialysis or renal transplant, focusing on recent clinical studies. Therapy of hypokalemia, hypocalcemia, and hypomagnesemia should be an emergency and performed simultaneously under electrocardiographic monitoring in patients with renal failure. Serum phosphates and iron, PTH level, renal function, hemoglobin and hematocrit, pH, inflammatory markers, proteinuria and microalbuminuria, and osmolarity should be monitored, besides standard 12-lead ECG, in order to prevent ventricular arrhythmia and sudden cardiac death.

1. Introduction

Cardiovascular diseases continue to be the leading mortality cause worldwide. Cardiac and renal diseases frequently coexist and significantly increase mortality, morbidity, and the complexity and cost of care [1]. Cardiovascular diseases and complications are the major causes of death in patients with chronic kidney disease and on dialysis [2–4]. Impaired renal function is associated with worse clinical outcomes in patients with myocardial infarction, heart failure, and left ventricular systolic dysfunction [5, 6]. Syndromes describing the interaction between heart and kidney have been defined as cardiorenal syndromes to indicate the bidirectional nature of the various syndromes [1]. The incidence of the cardiorenal syndrome has increased due to the enhanced longevity of the population. Patients survive more years with cardiac or renal dysfunction [7].

Sudden cardiac death is an unexpected death from a cardiovascular cause with or without structural heart disease [8]. It is very often caused by ventricular arrhythmia.

The present review will address the links between renal function tests, several laboratory markers, and ventricular arrhythmia risk in patients with renal disease, undergoing or not hemodialysis or renal transplant, focusing on recent clinical studies.

2. Electrocardiographic Predictors of Ventricular Arrhythmia and Sudden Cardiac Death

Several electrocardiographic (ECG) methods can be used to assess ventricular arrhythmia risk, including measurement of the QT interval, Tpeak-Tend interval [9], and QT dispersion on the standard 12-lead ECG. The QT interval is the electrocardiographic expression of ventricular depolarization and repolarization and, if prolonged, a predictor of fatal ventricular arrhythmias and sudden cardiac death [10, 11]. QT dispersion, the range of interlead differences of the QT interval, was considered as an index of spatial inhomogeneity of repolarization duration [12]. It can be calculated as the difference between the longest and the shortest QT interval in all measurable leads. Despite simplicity, the measurement methodology and normal values have not been standardized and the sensitivity and specificity of abnormal values were low [13]. No superior alternative to the noninvasive methods has been found; thus, the data on QT dispersion should be further considered [14].

Signal averaged ECG (SA-ECG) is a method used to detect late ventricular potentials (LVPs), averaging approximately 300 ECG cycles, in order to detect late ventricular potentials, by minimizing the noise level [15]. LVPs are

low amplitude, high frequency waveforms, appearing in the terminal part of the QRS complex [16]. LVPs are present, if, according to an international convention, at least 2 of the following 3 criteria are positive: SAECG-QRS duration >120 ms, low amplitude signal (LAS40; the duration of the terminal part of the QRS complex with an amplitude below $40 \mu V$) >38 ms, and root mean square signal amplitude of the last 40 ms of the signal (RMS40) <20 μV [17].

Heart rate variability (HRV), recorded by continuous electrocardiography over a 24-hour period, is a noninvasive measure of autonomic dysfunction and a risk factor for cardiovascular disease [18]. Decreased heart rate variability is an independent risk factor for sudden cardiac death [19].

3. Renal Function

Recently, even a slight impaired kidney function has been associated with cardiovascular disease [20].

Several observational studies have demonstrated an association between moderate kidney dysfunction and sudden cardiac death in people with cardiovascular disease [21–23]. It was difficult to conclude whether kidney dysfunction is an independent predictor of sudden cardiac death.

Significant correlations and associations were obtained between signal averaged electrocardiography criteria and *serum creatinine* and *estimated glomerular filtration rate* (Modification of Diet in Renal Disease equation, Cockroft-Gault equation, and Salazar-Corcoran equation for obese patients) in hypertensive patients [24]. Despite the high prevalence of signal averaged electrocardiography abnormalities in patients with left ventricular hypertrophy, the later was not a sensitive or specific predictor for late ventricular potentials or abnormal signal averaged ECGs in the study of Mozos et al. [24].

Mild-to-moderate kidney dysfunction, assessed by the estimated glomerular filtration rate, is associated with a significant elevated risk of ventricular fibrillation in acute ST elevation myocardial infarction [25].

Several other new markers of renal function have been described, including neutrophil gelatinase associated lipocalin (NGAL), predicting mortality in heart failure patients, with and without chronic kidney disease [26], and adverse cardiac events in ST segment elevation myocardial infarction patients treated with primary percutaneous coronary intervention [27]. NGAL is a glycoprotein released by the damaged renal tubular cells and a marker of clinical and subclinical acute kidney injury [27] and in-hospital mortality in the emergency department, enabling clinicians to distinguish between chronic and early reversible kidney damage and to identify patients needing renal replacement therapy [28]. No study addressed yet the relation between NGAL and ventricular arrhythmia risk. A link could exist, considering that NGAL is expressed in endothelial cells, smooth muscle cells, and macrophages in atherosclerotic plaques and may be involved in the development of atherosclerosis via endothelial dysfunction, inflammation and matrix degradation, and plaque instability [27], and NGAL is an earlier marker of acute kidney injury than serum creatinine [28]. NGAL could

be an important biomarker for mirroring acute cardiac diseases, kidney damage and arrhythmias.

"Culprit" biomarkers including soluble ST2 and Galectin 3, reflecting cardiac and renal fibrosis, could also be linked to an increased arrhythmia risk. Galectins are a family of soluble beta-galactoside-binding lectins that play regulatory roles in inflammation, immunity, and cancer [29]. Galectin 3 was associated with fibrogenesis in the heart, kidney, and liver. A role for Galectin 3 in the pathophysiology of heart failure has been demonstrated, related to its stimulatory effect on macrophage migration, fibroblast proliferation, and the development of fibrosis [29]. In the kidneys, Gal 3 protects renal tubules from chronic injury by limiting apoptosis and it may be an important factor in matrix turnover and fibrosis attenuation [30]. Soluble ST2 is part of the interleukin 1 receptor family, and binding of interleukin 33 to soluble ST2 reduces binding to ST2 receptors, enabling cardiac fibrosis and hypertrophy [31]. Elevated soluble ST2 concentrations were predictive of sudden cardiac death in patients with chronic heart failure and may have an impact on clinical decision-making [32]. ST2 is a biomarker enabling identifying patients with low survival benefit from implantable cardioverter defibrillator therapy [33].

4. Renal Disease

Progressive renal disease is associated, from the earliest stages, with increased QT interval duration and dispersion and with an increased risk of cardiovascular death, especially sudden death. A stepwise increase in mortality for each stage of chronic kidney disease was found [34]. QTc prolongation and torsade de pointes are associated with end stage renal disease and they can cause sudden cardiac death [35].

It has also been reported that left ventricular mass is increased from the earliest stages of renal disease (near normal renal function), linked to increased QT interval and dispersion, and with minor rhythm abnormalities, providing a link with the high risk of sudden death in this population too [35]. Besides left ventricular hypertrophy, systolic and diastolic dysfunction, interstitial fibrosis, and autonomic neuropathy were found among patients with end stage renal disease [36, 37].

The risk of sudden cardiac death is dependent on the severity of chronic kidney disease [3]. A 10 mL/min reduction in *creatinine clearance* was associated with an increased risk of sudden cardiac death in a retrospective study of patients undergoing implantable cardioverter defibrillator (ICD) implantation for primary prevention of sudden cardiac death [38]. Hager et al. compared death at 1 year in 958 patients with chronic kidney disease, who had undergone ICD placement, and concluded that the mortality rate at 1 year increases with worsening chronic kidney disease and if left ventricular dysfunction was present [3].

Cystatin C, a cysteine protease inhibitor, produced by all nucleated cells, released into the bloodstream, undergoes glomerular filtration, and metabolization in the proximal tube [39]. It is considered a potential endogenous filtration marker and estimates the glomerular filtration rate better

than serum creatinine [39]. Impaired kidney function, assessed by cystatin C, is independently associated with sudden cardiac death risk among elderly persons without clinical cardiovascular disease [40]. Participants meeting the definition of "preclinical kidney disease" (an estimated GFR >60 mL/min per 1.73 m^2) had also an elevated risk of sudden cardiac death, equivalent to participants with chronic kidney disease [40]. Cystatin C levels and the corresponding cystatin-based eGFR estimates better the risk of sudden cardiac death among elderly persons than creatinine, considering that creatinine is an insensitive measure of kidney function in elderly persons [40, 41]. It should also be mentioned that elevated cystatin C concentrations also capture preclinical kidney disease [40].

Sudden cardiac death may be a direct result of kidney dysfunction. An increased prevalence of left ventricular hypertrophy and systolic and diastolic dysfunction were found among patients with kidney disease, including those with elevated cystatin C concentrations, which could explain the increased risk of sudden cardiac death [37]. Autonomic dysfunction, myocyte dysfunction, altered electrolyte metabolism, and cardiac fibrosis may also contribute to arrhythmic risk in patients with kidney dysfunction [40].

Electrolyte imbalances are common in patients with acute and chronic renal failure, especially hyperkalemia and hypocalcemia. Electrolyte disorders can alter cardiac ionic currents kinetics and can generate or facilitate cardiac arrhythmias [42]. Potassium, calcium, sodium, and magnesium play a role in the genesis of experimental arrhythmias; however, in the clinical setting, only altered potassium concentration is responsible for the majority of arrhythmias [43].

Hyperkalemia appears in patients with acute renal failure due to impaired renal excretion associated with oliguria or anuria, transmineralization, or due to cellular damage. It occurs late in chronic kidney disease, at significant reductions of the glomerular filtration rates, but is a common potentially fatal complication [44]. There are several other additional causes of hyperkalemia in patients with chronic kidney disease, including high dietary potassium intake relative to the residual renal function, an extracellular shift of potassium caused by the metabolic acidosis, and therapy with renin-angiotensin-aldosterone system blockers that inhibit renal potassium excretion [45]. Hyperkalemia reduces the resting membrane potential, slows conduction velocity, increases the rate of depolarization and repolarization due to increased membrane permeability for potassium, and shortens action potential duration [42, 45, 46]. Additional electrolyte disturbances in renal patients may influence the cardiac membrane potential [45]. The ECG manifestations of hyperkalemia include tall, "tented," peaked, narrow-based T waves, decreased amplitude of the R wave, delayed atrioventricular and intraventricular conduction delay with prolonged PR interval and widened QRS complex, blending of the QRS complex into the T wave (the sine wave), ST segment depression, QT interval shortening, decreased amplitude or disappearance of the P wave, accelerated junctional rhythm, ventricular tachycardia and fibrillation, and asystole [42, 43, 47]. Thus, hyperkalemia can induce deadly cardiac arrhythmias [47]. In patients with acutely elevated serum potassium levels due to potassium intoxication or renal failure, a pseudomyocardial infarction pattern may appear: ST segment elevation, secondary to derangements in myocyte repolarization, and lowering of serum potassium level by hemodialysis were associated with return of the electrocardiogram toward normal [48]. The thresholds of serum potassium, above which changes in the ECG are manifest, differ from patient to patient [44]. Patients with chronic kidney disease or chronic hyperkalemia may develop compensatory mechanisms, enabling restoring of the myocardial membrane potential to normal [49], which could explain normal ECGs despite very high serum potassium (>9 mmol/L) [50]. The ECG cannot reliably be used to exclude the presence of hyperkalemia or to monitor therapy designed to reduce serum potassium [50].

Loss of glomerular filtration rate explains why hyperkalemia is one of the most common reasons for emergency dialysis [44]. Green et al. demonstrated in a study of 145 patients with ESRD that hyperkalemia was not significantly predictive of T wave tenting, especially in older patients, considering that T wave amplitude decreases with age, and in diabetic patients [44]. On the other hand, in the absence of a baseline ECG for comparison, one cannot determine whether T wave tenting is due to an associated coronary heart disease, left ventricular hypertrophy, and acidosis or due to hyperkalemia [44, 51]. Dreyfuss et al. reported a positive correlation between the amplitude of the T wave in V2 and the arterial concentration of H$^+$ and a negative correlation with the arterial total CO_2 content [51].

Hyperkalemic events in patients without chronic kidney disease were associated with higher mortality than in patients with chronic kidney disease, due to an adaptive response that leads to a new increased steady state serum potassium level and an increased gut potassium excretion [45]. The reduced sensitivity to cardiac complications due to hyperkalemia in patients with chronic kidney disease is due to chronic hyperkalemia, which is better tolerated. An inverse relationship was found between the severity (stage) of chronic kidney disease and mortality after a hyperkalemic event [45].

Hypocalcemia, most frequently seen in chronic renal failure, appears due to hyperphosphatemia and reduced renal hydroxylation of vitamin D, with impaired calcium absorption, and causes secondary hyperparathyroidism. Hypocalcemia results in decreased contractility, increased excitability, and prolonged QT intervals and T wave alterations [42, 52].

Hypocalcemia is usually associated with other electrolyte abnormalities in chronic renal failure. The combination of hyperkalemia and hypocalcemia has a cumulative effect on the atrioventricular and intraventricular conduction and facilitates ventricular fibrillation [42]. A previous study found an inverse relationship between serum calcium and the T wave amplitude, hypothesizing that, in this case, hypercalcemia was cardioprotective from the effects of hyperkalemia and masked the hyperkalemic ECG changes [53].

Voiculescu et al. analyzed 68 patients with chronic renal failure and found a prolonged QT interval in 11.8% of the patients [54]. QT prolongation correlated with the number of years of renal failure, serum concentrations of potassium, and calcium and diastolic blood pressure but was not dependent

on the level of serum magnesium, phosphates, hemoglobin or bicarbonate, and the type of renal substitution (hemodialysis or continuous ambulatory peritoneal dialysis) [54]. During the follow up of 3.8 months, no cases of sudden cardiac death and no significant arrhythmia incidence were detected [54].

Magnesium, the second most abundant intracellular cation after potassium, is usually ignored outside critical care. Prevalence of hypomagnesemia in hospitalized patients is approximately 20% [55], and critical serum magnesium level is associated with seizures and life-threatening arrhythmias [56]. In the presence of low calcium concentrations, magnesium deficiency prolongs the action potential plateau [42]. Patients with acute myocardial infarction and hypomagnesemia have higher mortality due to ventricular arrhythmias secondary to a lower threshold for depolarization [57]. Patients with renal failure develop *hypermagnesemia* due to an impaired renal excretion. Low magnesium can appear due to an excessive urinary loss: diuresis due to alcohol; glycosuria in diabetes mellitus and diuretics [56]; therapy with nephrotoxic drugs including cisplatin and amphotericin B; use of bisphosphonates, cyclosporine, malabsorption, or malnutrition; formation of insoluble complexes with phosphorus; shifts from the extracellular to the intracellular fluid (due to acidosis, insulin); transdermal losses [55, 56]. Patients with *hypomagnesemia* had a higher mortality than those with normal levels of magnesium [55]. Considering that magnesium is required for cellular function, its deficiency will probably contribute to organ system failure [55]. Severe hypomagnesemia is often accompanied by hypocalcemia and hypokalemia, and both are refractory to therapy until magnesium has been repleted [55]. The contribution of hypomagnesemia is difficult to ascertain for ventricular arrhythmias, considering the associated electrolyte abnormalities, and clinicians, very often, fail to measure magnesium.

Foglia et al. reported prolonged QT intervals in primary renal hypokalemia-hypomagnesemia, confirming that potassium and magnesium depletion prolong the duration of the action potential of the cardiomyocyte [58]. The altered ventricular repolarization is, especially, linked to their concentration gradient across the cardiomyocyte membrane [58]. On the other hand, continuous ambulatory electrocardiography and exercise testing failed to detect clinically relevant arrhythmias in patients with renal hypokalemia [58–60].

Lower values of heart rate variability were found in patients with chronic renal failure [61]. Lower heart rate variability was significantly associated with older age, female gender, diabetes, higher heart rate, C-reactive protein and phosphorus, lower serum albumin, higher high-density lipoprotein, and stage 5 chronic kidney disease in patients with nondialysis chronic kidney disease [18]. C-reactive protein is a known cardiovascular risk factor, and autonomic function may be impaired due to inflammation [62].

Hyperphosphatemia, highly prevalent among patients with end stage renal disease, especially if higher than 6.5 mg/dL, contributes to cardiac mortality, including sudden death [63]. The relative risk of sudden death in patients with hyperphosphatemia was strongly associated with elevated calcium-phosphate product and elevated serum parathyroid

hormone levels [63]. It is speculated that elevated phosphates may increase vascular calcification and smooth muscle proliferation and may impair myocardial perfusion [63].

Bonato et al. evaluated 111 chronic kidney disease patients, using 24-hour electrocardiogram, echocardiogram, and laboratory parameters [64]. Ventricular arrhythmia was found in 35% of the patients and was associated with age, increased *hemoglobin* level, and reduced ejection fraction [64].

A relationship was described between PTH level and sudden cardiac death, probably due to arrhythmia. The correlation between heart rate variability parameters and PTH serum level indicated the impaired autonomic function in patients with chronic renal failure [61]. Probably PTH has a role in the development of uremic cardiomyopathy, suggested by the correlations between PTH level and left ventricular hypertrophy in chronic renal failure [61].

Proteinuria is a marker of renal injury, detected earlier than the decline in glomerular filtration rate, and an independent risk factor for cardiovascular morbidity and mortality [65]. Microalbuminuria was related to prolonged QT interval, left ventricular hypertrophy, and ST-T changes in hypertensive patients, emphasizing the need of ECG monitoring and followup in patients with microalbuminuria [66]. High albumin excretion was related to left ventricular hypertrophy independent of age, blood pressure, diabetes, race, serum creatinine, or smoking, suggesting parallel cardiac damage and albuminuria [67]. Microalbuminuria was also independently associated with electrocardiographic markers of myocardial ischemia [68]. Urinary protein excretion reflects not only localized subclinical renal disease but also a generalized vascular endothelial dysfunction, and proteinuria was associated with inflammatory markers, including elevated C-reactive protein, fibrinogen, and asymmetric dimethylarginine (which causes endothelial dysfunction through inhibition of nitric oxide production), and also with circulating von Willebrand factor, soluble vascular cell adhesion molecule, and vascular endothelial growth factor [65]. Besides inflammation and endothelial dysfunction, thrombogenic factors may also link proteinuria and cardiovascular disease, including tissue plasminogen activator [65]. Proteinuria was also associated with insulin resistance and higher plasma insulin levels and altered lipid profile [69].

Iron overload in hemodialysis patients causes oxidative toxicity and may precipitate arrhythmias [70]. The high iron stores in patients with chronic ambulatory peritoneal dialysis patients were associated with higher QT dispersion [70]. Patients with QT dispersion longer than 65 ms had higher levels of serum ferritin and transferrin saturation than other patients undergoing chronic ambulatory peritoneal dialysis [70].

Patients with end stage renal disease have several factors which could predispose to the development of ventricular arrhythmia, including structural remodeling: myocardial fibrosis, left ventricular hypertrophy, the uremic cardiomyopathy, deposition of calcium, iron and aluminium within the heart tissue, endothelial dysfunction and vascular calcification; electrophysiological remodeling: slowing of conduction velocity, repolarization heterogeneities; pathophysiological triggers: ischemia, increased sympathetic activity, and

inflammation; and dialytic triggers: electrolyte shifts, acid-base balance alterations, and hypotension [8, 42, 62, 64, 71]. The mentioned morphological changes could represent the substrate of the delayed and fractionated electrical conduction, enabling the appearance of late ventricular potentials [72]. Laboratory data, including serum electrolytes, especially potassium and calcium, pH, inflammatory markers, serum iron, proteinuria, hemoglobin, phosphates, and cystatin C, should be monitored, besides ECG QT intervals and T and R wave amplitude, in patients with end stage renal disease.

Cardioverter defibrillator implantation has been shown to reduce the risk of sudden cardiac death in patients with chronic kidney disease, in several randomized controlled trials. Many of those trials excluded patients on hemodialysis or with advanced chronic kidney disease [34]. The chronic kidney disease stage should be considered when an ICD should be implanted. On the other hand, chronic kidney disease modifies the efficacy of the ICD and sudden cardiac death is not necessarily a result of ventricular arrhythmia [34]. Hyperkalemia can augment T wave amplitude large enough to be detected by an ICD and deliver inappropriate ICD shocks [73]. Serum potassium should be monitored in ICD recipients with renal dysfunction and treated with angiotensin-converting enzyme inhibitors or angiotensin II receptor blockers, in order to prevent inappropriate ICD deliveries [73].

5. Hemodialysis

Cardiac disease and sudden cardiac death are increased in patients undergoing dialysis [74, 75]. Sudden cardiac death is responsible for about a third of total mortality among dialysis patients and is due to autonomic nervous system dysfunction and increased sympathetic activity, in particular [76]. Several electrocardiographic abnormalities were found in patients with chronic kidney disease undergoing a regular hemodialysis program, including QT interval prolongation and signs of left ventricular hypertrophy [77, 78].

Hemodialysis (HD) prolongs QTc in end stage renal disease patients, mainly related to rapid changes in electrolyte plasma concentrations. Important increases in QT interval and QT dispersion were found in both pre- and post-HD to levels only comparable to those recorded following myocardial infarction. However, the impact on QTc dispersion is less important in the absence of significant coexisting cardiac disease [77]. Patients on HD had longer QTd than patients on continuous ambulatory peritoneal dialysis, difference due to the higher *serum calcium* level [52]. QT and QTc dispersion were higher in patients who underwent hemodialysis, as well, in another study including 19 uremic patients. QTc dispersion positively and directly correlated with serum phosphates, and negatively to the calcium/phosphate ratio [79].

Patients, in whom a dialysis session determines an increase in QTc, started initially with significantly lower K and higher ionized calcium levels and displayed a greater reduction in calcium following dialysis [77]. Pre-HD plasma calcium appears to be the major determinant of QTc changes in HD patients. Thus, manipulation of plasma calcium through dialysate calcium may prove an effective mechanism to limit the arrhythmogenicity of a haemodialysis session, which may be important in dialysis subjects with known cardiac disease. Changes in ventricular repolarization duration associated with HD largely depend on the concentrations of calcium and potassium in the dialysis bath [80]. Similar results were obtained by Di Iorio et al., as the QT interval was significantly longer in patients with dialysate that contained the lowest concentrations of calcium and *potassium* and the highest concentration of *bicarbonate* [81].

The prevalence of late ventricular potentials in patients undergoing hemodialysis varied from study to study: 25% [72] versus 11% [52], and 7% continuous ambulatory peritoneal dialysis patients had positive late potentials. The differences were due to patient selection criteria and timing of SA-ECG after HD [52]. Signal averaged ECG parameters improved with HD due to fluid removal [82]. A prolongation of the SA-QRS duration after HD could be, probably, due to widening of the initial portion of the QRS, related to the acute reduction in serum potassium due to a generalized slowing of conduction in the myocardial fibers [72]. There was no relationship between SA-QRS duration prolongation and dialysis-induced changes in *serum sodium* and calcium or body weight changes [72]. LAS40 increased significantly postdialysis, correlated also with the changes of potassium [83].

Patients with end stage renal disease have tolerance for hyperkalemia, with less evident cardiac and neuromuscular consequences than in those with normal renal function [53]. No typical ECG changes of the T wave amplitude were found in HD patients with a high predialysis serum potassium concentration [53]. The tolerance to hyperkalemia is also explained by the slow rate of increase in serum potassium compared to the general population after excessive potassium ingestion [84].

Potassium level after HD is a very vulnerable point in arrhythmogenesis, considering that hypokalemia (<4 mEq/L), an insufficient decrease of potassium by hemodialysis or hyperkalemia (>5.6 mEq/L), are arrhythmogenic factors [83, 85, 86]. Hypokalemia contributes to reduced survival of cardiac patients and increased incidence of arrhythmic death [87]. Hypokalemia-induced arrhythmogenicity is due to slowed conduction, prolonged ventricular repolarization, and action potential duration associated with shortening of the effective refractory period enabling reentry, abnormal pacemaker activity, and early and delayed afterdepolarizations [87]. Checherita et al. evaluated the association of potassium level changes and arrhythmia in predialyzed and dialyzed patients and demonstrated that hypokalemia is a stronger risk factor than hyperkalemia for arrhythmia in chronic kidney disease patients [86].

As already mentioned, hypocalcemia prolongs the QT interval. QT dispersion increased with the use of low calcium-containing dialysate [88] and low calcium levels due to citrate anticoagulation are related to increased arrhythmic risk [89].

Using a low *magnesium* dialysate bath in 22 hemodynamically stable patients on maintenance hemodialysis without preexisting advanced cardiac disease did not significantly change QTc and QT dispersion [90].

Heart rate variability decreases in chronic HD patients, and the decrease is more important in diabetic uremic patients [19]. The changes of serum electrolytes and bicarbonate during HD did not affect heart rate variability [19]. On the other hand, depressed heart rate variability was associated with a higher risk of progression to end stage renal disease and suggested that autonomic dysfunction may lead to kidney damage [91].

Kyriakidis et al. concluded, in a study including 25 hemodialysis patients for chronic renal failure and undergoing Holter ECG monitoring for a continuous 48-hour period, that hemodialysis had no influence on type or frequency of arrhythmia, because they found only benign atrial arrhythmias and no complex ventricular arrhythmias [92]. The most important limitation of the mentioned study is the low number of patients.

Bignotto et al. found prolonged QT intervals in half of 179 patients on dialysis, a condition that was linked to left ventricular hypertrophy, presence of left bundle branch block, longer dialysis therapy period, older age, higher percentage of catheter use, and low body mass index [78].

Predialysis *hematocrit*, *oxygen content*, *serum urea*, and *osmolarity* were significantly different in chronic renal failure patients with and without arrhythmias and postdialysis serum phosphorus and osmolarity [93].

The adverse cardiomyopathic and vasculopathic milieu in chronic kidney disease favors the occurrence of supraventricular and ventricular arrhythmias, conduction abnormalities, and sudden cardiac death, exacerbated by electrolyte shifts, volume and acid-base balance shifts, blood pressure changes, diabetes mellitus and myocardial ischemia as comorbidities, sympathetic overactivity, inflammation, iron deposition and the deposition of calcium and aluminium salts in the heart tissue, impaired baroreflex sensitivity, and obstructive sleep apnea [72, 75, 94]. Changes of QT intervals during hemodialysis depend both on electrolyte and bicarbonate concentrations in the dialysate [81].

6. Kidney Transplantation

The risk of cardiovascular death is reduced in the renal transplant patients compared with those on dialysis, but still significantly greater than that of the general population [4]. Cardiovascular mortality in kidney transplant recipients is still high, especially in the first year of transplantation, and ventricular arrhythmia is one of the etiologies of sudden cardiac death [95]. Longer length on dialysis contributes to a greater prevalence of cardiovascular complications among kidney transplant recipients, especially from deceased donors [96]. The renal transplantation procedure may disturb the repolarization process, despite optimal hemodynamic or metabolic status [97].

Normalization of electrolytes and the acid-base status from a uremic state to the normal kidney function after successful kidney transplantation decreases the prolonged QT interval [98].

7. Conclusions

Ventricular arrhythmia and sudden cardiac death risk are increased in patients with renal failure, although not all studies have demonstrated it. Even mild reductions in kidney function can alter the electrophysiological properties of the myocardium and increase the risk of ventricular arrhythmias and sudden cardiac death.

The present review emphasizes important factors for the safety of patients with chronic kidney disease and enables multiple links between cardiology and nephrology departments and clinical laboratory, overcoming barriers, motivating nephrologists to consider cardiologists' opinion and laboratory data in order to prevent sudden cardiac death in end stage renal disease. All patients with kidney disease should be screened for cardiovascular disease.

Therapy of hypokalemia, hypocalcemia, and hypomagnesemia should be an emergency and performed simultaneously, under electrocardiographic monitoring in patients with renal failure, and sympathetic activity, serum phosphates and iron, PTH level, renal function, hemoglobin and hematocrit, pH, inflammatory markers, proteinuria and microalbuminuria, and osmolarity should be monitored, besides standard 12-lead ECG in order to prevent ventricular arrhythmia and sudden cardiac death. The relationship between new bystander biomarkers of renal function, including NGAL, and ventricular arrhythmia and sudden cardiac death should be assessed. Soluble ST2 and Galectin 3, biomarkers reflecting renal and cardiac fibrosis, could also be associated with an increased arrhythmia risk.

Electrocardiograms are low cost diagnostic tools for renal therapy centers, and nephrologists must consider QT interval, associated laboratory conditions, nutritional status, and QT interval prolonging drugs in their patients.

Conflict of Interests

The author declares that there is no conflict of interests regarding the publication of this paper.

References

[1] C. Ronco, P. McCullough, S. D. Anker et al., "Cardio-renal syndromes: report from the consensus conference of the acute dialysis quality initiative," *European Heart Journal*, vol. 31, no. 6, pp. 703–711, 2010.

[2] D. Polak-Jonkisz, K. Laszki-Szczachor, L. Purzyc et al., "Usefulness of body surface potential mapping for early identification of the intraventricular conduction disorders in young patients with chronic kidney disease," *Journal of Electrocardiology*, vol. 42, no. 2, pp. 165–171, 2009.

[3] C. S. Hager, S. Jain, J. Blackwell, B. Culp, J. Song, and C. D. Chiles, "Effect of renal function on survival after implantable cardioverter defibrillator placement," *American Journal of Cardiology*, vol. 106, no. 9, pp. 1297–1300, 2010.

[4] H. Pilmore, G. Dogra, M. Roberts et al., "Cardiovascular disease in patients with chronic kidney disease," *Nephrology*, vol. 19, no. 1, pp. 3–10, 2014.

[5] M. P. Tokmakova, H. Skali, S. Kenchaiah et al., "Chronic kidney disease, cardiovascular risk, and response to angiotensin-converting enzyme inhibition after myocardial infarction: the Survival and Ventricular Enlargement (SAVE) study," *Circulation*, vol. 110, no. 24, pp. 3667–3673, 2004.

[6] H. Clark, H. Krum, and I. Hopper, "Worsening renal function during renin-angiotensin-aldosterone system inhibitor initiation and long-term outcomes in patients with left ventricular systolic dysfunction," *European Journal of Heart Failure*, vol. 16, no. 1, pp. 41–48, 2014.

[7] F. D. De Castro, P. Castro Chaves, and A. F. Lette-Moreira, "Sindrome cardiorrenal e suas implicacoes fisiopatologicas," *Revista Portuguesa de Cardiologia*, vol. 29, no. 10, pp. 1535–1554, 2010.

[8] I. R. Whitman, H. I. Feldman, and R. Deo, "CKD and sudden cardiac death: epidemiology, mechanisms, and therapeutic approaches," *Journal of the American Society of Nephrology*, vol. 23, pp. 1029–1039, 2012.

[9] P. Gupta, C. Patel, H. Patel et al., "Tp-e/QT ratio as an index of arrhythmogenesis," *Journal of Electrocardiology*, vol. 41, no. 6, pp. 567–574, 2008.

[10] S. M. Al-Khatib, N. M. Allen LaPointe, J. M. Kramer, and R. M. Califf, "What clinicians should know about the QT interval," *Journal of the American Medical Association*, vol. 289, no. 16, pp. 2120–2127, 2003.

[11] P. M. Rautaharju, B. Surawicz, and L. S. Gettes, "AHA/ACCF/HRS recommendations for the standardization and interpretation of the electrocardiogram: part IV: the ST segment, T and U waves, and the QT interval A scientific statement from the american heart association electrocardiography and arrhythmias committee, council on clinical cardiology; the american college of cardiology foundation; and the heart rhythm society endorsed by the international society for computerized," *Journal of the American College of Cardiology*, vol. 53, no. 11, pp. 982–991, 2009.

[12] C. P. Day, J. M. McComb, and R. W. F. Campbell, "QT dispersion: an indication of arrhythmia risk in patients with long QT intervals," *British Heart Journal*, vol. 63, no. 6, pp. 342–344, 1990.

[13] B. Surawicz, "Will QT dispersion play a role in clinical decision-making?" *Journal of Cardiovascular Electrophysiology*, vol. 7, no. 8, pp. 777–784, 1996.

[14] M. Malik and V. Batchvarov, *QT Dispersion*, Futura Publishing, New York, NY, USA, 2000.

[15] I. Mozos, C. Serban, and R. Mihaescu, "Late ventricular potentials in cardiac and extracardiac diseases," in *Cardiac Arrythmias-New Considerations*, F. R. Breijo-Marquez, Ed., In Tech, 2012.

[16] P. R. B. Barbosa, M. O. D. Sousa, E. C. Barbosa, A. D. S. Bomfim, P. Ginefra, and J. Nadal, "Analysis of the prevalence of ventricular late potentials in the late phase of myocardial infarction based on the site of infarction," *Arquivos Brasileiros de Cardiologia*, vol. 78, no. 4, pp. 352–363, 2002.

[17] J. J. Goldberger, M. E. Cain, S. H. Hohnloser et al., "American heart association/American college of cardiology foundation/heart rhythm society scientific statement on noninvasive risk stratification techniques for identifying patients at risk for sudden cardiac death. A scientific statement from the American heart association council on clinical cardiology committee on electrocardiography and arrhythmias and council on epidemiology and prevention," *Heart Rhythm*, vol. 5, no. 10, pp. e1–e21, 2008.

[18] P. Chandra, R. L. Sands, B. W. Gillespie et al., "Predictors of heart rate variability and its prognostic significance in chronic kidney disease," *Nephrology Dialysis Transplantation*, vol. 27, no. 2, pp. 700–709, 2012.

[19] M. H. Sipahioglu, I. Kocyigit, A. Unal et al., "Effect of serum electrolyte and bicarbonate concentration changes during hemodialysis sessions on heart rate variability," *Journal of Nephrology*, vol. 25, no. 6, pp. 1067–1074, 2012.

[20] P. Kes, D. Milicic, and N. Basic-Jukic, "How to motivate nephrologists to think more "cardiac" and cardiologists to think more "renal"?" *Acta Medica Croatica*, vol. 65, no. 3, pp. 85–89, 2011.

[21] I. Goldenberg, A. J. Moss, S. McNitt et al., "Relations among renal function, risk of sudden cardiac death, and benefit of the implanted cardiac defibrillator in patients with ischemic left ventricular dysfunction," *American Journal of Cardiology*, vol. 98, no. 4, pp. 485–490, 2006.

[22] L. A. Saxon, M. R. Bristow, J. Boehmer et al., "Predictors of sudden cardiac death and appropriate shock in the comparison of medical therapy, pacing, and defibrillation in heart failure (COMPANION) trial," *Circulation*, vol. 114, no. 25, pp. 2766–2772, 2006.

[23] R. Deo, C. L. Wassel Fyr, L. F. Fried et al., "Kidney dysfunction and fatal cardiovascular disease-an association independent of atherosclerotic events: results from the Health, Aging, and Body Composition (Health ABC) study," *American Heart Journal*, vol. 155, no. 1, pp. 62–68, 2008.

[24] I. Mozos, M. Hancu, and L. Susan, "Signal averaged electrocardiography and renal function in hypertensive patients," in *Latest Advances in Biology, Environment and Ecology*, R. Raducanu, N. Mastorakis, R. Neck, V. Niola, and K. L. Ng, Eds., WSEAS Press, 2012.

[25] D. Dalal, J. S. S. G. De Jong, F. V. Y. Tjong et al., "Mild-to-moderate kidney dysfunction and the risk of sudden cardiac death in the setting of acute myocardial infarction," *Heart Rhythm*, vol. 9, no. 4, pp. 540–545, 2012.

[26] V. M. Van Deursen, K. Damman, A. A. Voors et al., "Prognostic value of plasma NGAL for mortality in heart failure patients," *Circulation: Heart Failure*, vol. 7, no. 1, pp. 35–42, 2014.

[27] S. Lindberg, S. H. Pedersen, R. Mogelvang et al., "Prognostic utility of neutrophil gelatinase-associated lipocalin in predicting mortality and cardiovascular events in patients with ST-segment elevation myocardial infarction treated with primary percutaneous coronary intervention," *Journal of the American College of Cardiology*, vol. 60, pp. 339–345, 2012.

[28] S. Di Somma, L. Magrini, B. De Berardinis et al., "Additive value of blood neutrophil gelatinase associated lipocalin to clinical judgement in acute kidney injury diagnosis and mortality prediction in patients hospitalized from the emergency department," *Critical Care*, vol. 17, article R29, 2013.

[29] R. A. De Boer, A. A. Voors, P. Muntendam, W. H. Van Gilst, and D. J. Van Veldhuisen, "Galectin-3: a novel mediator of heart failure development and progression," *European Journal of Heart Failure*, vol. 11, no. 9, pp. 811–817, 2009.

[30] D. M. Okamura, K. Pasichnyk, J. M. Lopez-Guisa et al., "Galectin-3 preserves renal tubules and modulates extracellular matrix remodeling in progressive fibrosis," *American Journal of Physiology: Renal Physiology*, vol. 300, no. 1, pp. F245–F253, 2011.

[31] A. H. B. Wu, "Biomarkers beyond the natriuretic peptides for chronic heart failure: galectin-3 and soluble ST2," *The Journal of the International Federation of Clinical Chemistry and Laboratory Medicine*, vol. 23, no. 3, 2012.

[32] D. A. Pascual-Figal, J. Ordoñez-Llanos, P. L. Tornel et al., "Soluble ST2 for predicting sudden cardiac death in patients with chronic heart failure and left ventricular systolic dysfunction," *Journal of the American College of Cardiology*, vol. 54, no. 23, pp. 2174–2179, 2009.

[33] P. A. Scott, P. A. Townsend, L. L. Ng et al., "Defining potential to benefit from implantable cardioverter defibrillator therapy: the role of biomarkers," *Europace*, vol. 13, no. 10, pp. 1419–1427, 2011.

[34] J. M. Hoffmeister, N. A. M. Estes, and A. C. Garlitski, "Prevention of sudden cardiac death in patients with chronic kidney disease: risk and benefits of the implantable cardioverter defibrillator," *Journal of Interventional Cardiac Electrophysiology*, vol. 35, no. 2, pp. 227–234, 2012.

[35] S. Patanè, F. Marte, G. Di Bella, A. Currò, and S. Coglitore, "QT interval prolongation, torsade de pointes and renal disease," *International Journal of Cardiology*, vol. 130, no. 2, pp. e71–e73, 2008.

[36] I. Karayaylali, M. San, G. Kudaiberdieva et al., "Heart rate variability, left ventricular functions, and cardiac autonomic neuropathy in patients undergoing chronic hemodialysis," *Renal Failure*, vol. 25, no. 5, pp. 845–853, 2003.

[37] J. H. Ix, M. G. Shlipak, G. M. Chertow, S. Ali, N. B. Schiller, and M. A. Whooley, "Cystatin C, left ventricular hypertrophy, and diastolic dysfunction: data from the heart and soul study," *Journal of Cardiac Failure*, vol. 12, no. 8, pp. 601–607, 2006.

[38] P. S. Cuculich, J. M. Sánchez, R. Kerzner et al., "Poor prognosis for patients with chronic kidney disease despite ICD therapy for the primary prevention of sudden death," *Pacing and Clinical Electrophysiology*, vol. 30, no. 2, pp. 207–213, 2007.

[39] R. Mihaescu, C. Serban, S. Dragan et al., "Diabetes and renal disease," in *Diseases of Renal Parenchyma*, M. Sahay, Ed., In Tech, 2012.

[40] R. Deo, N. Sotoodehnia, R. Katz et al., "Cystatin C and sudden cardiac death risk in the elderly," *Circulation: Cardiovascular Quality and Outcomes*, vol. 3, no. 2, pp. 159–164, 2010.

[41] M. G. Shlipak, L. F. Fried, M. Cushman et al., "Cardiovascular mortality risk in chronic kidney disease: comparison of traditional and novel risk factors," *Journal of the American Medical Association*, vol. 293, no. 14, pp. 1737–1745, 2005.

[42] N. El-Sherif and G. Turitto, "Electrolyte disorders and arrhythmogenesis," *Cardiology Journal*, vol. 18, no. 3, pp. 233–245, 2011.

[43] C. Fisch, "Relation of electrolyte disturbances to cardiac arrhythmias," *Circulation*, vol. 47, no. 2, pp. 408–419, 1973.

[44] D. Green, H. D. Green, D. I. New, and P. A. Kalra, "The clinical significance of hyperkalaemia-associated repolarization abnormalities in end-stage renal disease," *Nephrology Dialysis Transplantation*, vol. 28, pp. 99–105, 2013.

[45] L. M. Einhorn, M. Zhan, V. D. Hsu et al., "The frequency of hyperkalemia and its significance in chronic kidney disease," *Archives of Internal Medicine*, vol. 169, no. 12, pp. 1156–1162, 2009.

[46] K. Greenspan, C. Wunsch, and C. Fisch, "T wave of normo- and hyperkalemic canine heart: effect of vagal stimulation," *The American Journal of Physiology*, vol. 208, pp. 954–958, 1965.

[47] W. A. Parham, A. A. Mehdirad, K. M. Biermann, and C. S. Fredman, "Hyperkalemia revisited," *Texas Heart Institute Journal*, vol. 33, no. 1, pp. 40–47, 2006.

[48] E. A. Gelzayd and D. Holzman, "Electrocardiographic changes of hyperkalemia simulating acute myocardial infarction. Report of a case," *Diseases of the Chest*, vol. 51, no. 2, pp. 211–212, 1967.

[49] D. Kaji and T. Khan, "Na-K pump in chronic renal failure," *American Journal of Physiology*, vol. 252, pp. F785–F793, 1987.

[50] H. M. Szerlip, J. Weiss, and I. Singer, "Profound hyperkalemia without electrocardiographic manifestations," *American Journal of Kidney Diseases*, vol. 7, no. 6, pp. 461–465, 1986.

[51] D. Dreyfuss, G. Jondeau, R. Couturier, J. Rahmani, P. Assayag, and F. Coste, "Tall T waves during metabolic acidosis without hyperkalemia: a prospective study," *Critical Care Medicine*, vol. 17, no. 5, pp. 404–408, 1989.

[52] A. Yildiz, V. Akkaya, S. Sahin et al., "QT dispersion and signal-averaged electrocardiogram in hemodialysis and CAPD patients," *Peritoneal Dialysis International*, vol. 21, no. 2, pp. 186–192, 2001.

[53] S. Aslam, E. A. Friedman, and O. Ifudu, "Electrocardiography is unreliable in detecting potentially lethal hyperkalaemia in haemodialysis patients," *Nephrology Dialysis Transplantation*, vol. 17, no. 9, pp. 1639–1642, 2002.

[54] M. Voiculescu, C. Ionescu, and G. Ismail, "Frequency and prognostic significance of QT prolongation in chronic renal failure patients," *Romanian Journal of Internal Medicine*, vol. 44, no. 4, pp. 407–417, 2006.

[55] F. Wolf and A. Hilewitz, "Hypomagnesaemia in patients hospitalized in internal medicine is associated with increased mortality," *International Journal of Clinical Practice*, vol. 68, no. 1, pp. 111–116, 2014.

[56] D. R. Mouw, R. A. Latessa, and E. J. Sullo, "What are the causes of hypomagnesemia?" *Journal of Family Practice*, vol. 54, no. 2, pp. 156–178, 2005.

[57] J. M. Topf and P. T. Murray, "Hypomagnesemia and hypermagnesemia," *Reviews in Endocrine and Metabolic Disorders*, vol. 4, no. 2, pp. 195–206, 2003.

[58] P. E. G. Foglia, A. Bettinelli, C. Tosetto et al., "Cardiac work up in primary renal hypokalaemia-hypomagnesaemia (Gitelmam syndrome)," *Nephrology Dialysis Transplantation*, vol. 19, no. 6, pp. 1398–1402, 2004.

[59] C. Blomstrom-Lundqvist, K. Caidahl, S. B. Olsson, and A. Rudin, "Electrocardiographic findings and frequency of arrhythmias in Bartter's syndrome," *British Heart Journal*, vol. 61, no. 3, pp. 274–279, 1989.

[60] R. Scognamiglio, A. Semplicini, and L. A. Calo, "Myocardial function in Bartter's and Gitelman's syndrome," *Kidney International*, vol. 64, pp. 366–367, 2003.

[61] M. Wanic-Kossowska, P. Guzik, P. Lehman, and S. Czekalski, "Heart rate variability in patients with chronic renal failure treated by hemodialysis," *Polskie Archiwum Medycyny Wewnetrznej*, vol. 114, no. 3, pp. 855–861, 2005.

[62] R. Lampert, J. D. Bremner, S. Su et al., "Decreased heart rate variability is associated with higher levels of inflammation in middle-aged men," *American Heart Journal*, vol. 156, no. 4, pp. 759e1–759e7, 2008.

[63] S. K. Ganesh, A. G. Stack, N. W. Levin, T. Hulbert-Shearon, and F. K. Port, "Association of elevated serum PO4, Ca × PO4 product, and parathyroid hormone with cardiac mortality risk in chronic hemodialysis patients," *Journal of the American Society of Nephrology*, vol. 12, no. 10, pp. 2131–2138, 2001.

[64] F. O. Bonato, M. M. Lemos, J. L. Cassiolato, and M. E. Canziani, "Prevalence of ventricular arrhythmia and its associated factors in nondialysed chronic kidney disease patients," *PLoS ONE*, vol. 8, no. 6, Article ID e66036, 2013.

[65] G. Currie and C. Delles, "Proteinuria and its relation to cardiovascular disease," *International Journal of Nephrology and Renovascular Disease*, vol. 7, pp. 13–24, 2013.

[66] O. Busari, G. Opadijo, T. Olarewaju, A. Omotoso, and A. Jimoh, "Electrocardiographic correlates of microalbuminuria in adult Nigerians with essential hypertension," *Cardiology Journal*, vol. 17, no. 3, pp. 281–287, 2010.

[67] K. Wachtell, M. H. Olsen, B. Dahlöf et al., "Microalbuminuria in hypertensive patients with electrocardiographic left ventricular hypertrophy: the LIFE study," *Journal of Hypertension*, vol. 20, no. 3, pp. 405–412, 2002.

[68] G. F. H. Diercks, A. J. Van Boven, H. L. Hillege et al., "Microalbuminuria is independently associated with ischaemic electrocardiographic abnormalities in a large non-diabetic population: the PREVEND (Prevention of REnal and Vascular ENdstage Disease) study," *European Heart Journal*, vol. 21, no. 23, pp. 1922–1927, 2000.

[69] L. Mykkänen, D. J. Zaccaro, L. E. Wagenknecht, D. C. Robbins, M. Gabriel, and S. M. Haffner, "Microalbuminuria is associated with insulin resistance in nondiabetic subjects: the insulin resistance atherosclerosis study," *Diabetes*, vol. 47, no. 5, pp. 793–800, 1998.

[70] N. Bavbek, H. Yilmaz, H. K. Erdemli et al., "Correlations between iron stores and QTc dispersion in chronic ambulatory peritoneal dialysis patients," *Renal Failure*, vol. 36, no. 2, pp. 187–190, 2014.

[71] B. Franczyk-Skora, A. Gluba, M. Banach et al., "Prevention of sudden cardiac death in patients with chronic kidney disease," *BMC Nephrology*, vol. 13, article 162, 2012.

[72] M.-A. Morales, C. Gremigni, P. Dattolo et al., "Signal-averaged ECG abnormalities in haemodialysis patients. Role of dialysis," *Nephrology Dialysis Transplantation*, vol. 13, no. 3, pp. 668–673, 1998.

[73] Y. Hosaka, M. Chinushi, K. Iijima, A. Sanada, H. Furushima, and Y. Aizawa, "Correlation between surface and intracardiac electrocardiogram in a patient with inappropriate defibrillation shocks due to hyperkalemia," *Internal Medicine*, vol. 48, no. 13, pp. 1153–1156, 2009.

[74] C. A. Herzog, J. M. Mangrum, and R. Passman, "Sudden cardiac death and dialysis patients," *Seminars in Dialysis*, vol. 21, no. 4, pp. 300–307, 2008.

[75] M. K. Shamseddin and P. S. Parfrey, "Sudden cardiac death in chronic kidney disease: epidemiology and prevention," *Nature Reviews Nephrology*, vol. 7, no. 3, pp. 145–154, 2011.

[76] O. Vonend, L. C. Rump, and E. Ritz, "Sympathetic overactivity—the cinderella of cardiovascular risk factors in dialysis patients," *Seminars in Dialysis*, vol. 21, no. 4, pp. 326–330, 2008.

[77] A. Covic, M. Diaconita, P. Gusbeth-Tatomir et al., "Haemodialysis increases QTc interval but not QTc dispersion in ESRD patients without manifest cardiac disease," *Nephrology Dialysis Transplantation*, vol. 17, no. 12, pp. 2170–2177, 2002.

[78] L. H. Bignotto, M. E. Kallas, R. J. T. Djouki et al., "Electrocardiographic findings in chronic hemodialysis patients," *Jornal Brasileiro de Nefrologia*, vol. 34, no. 3, pp. 235–242, 2012.

[79] F. Milone, S. Urso, M. Garozzo, A. M. Memeo, G. Volpe, and G. Battaglia, "Risk of arrhythmias in hemodialysis patients vs healthy people," *Giornale Italiano di Nefrologia*, vol. 21, pp. S241–S246, 2004.

[80] S. Genovesi, C. Dossi, M. R. Viganò et al., "Electrolyte concentration during haemodialysis and QT interval prolongation in uraemic patients," *Europace*, vol. 10, no. 6, pp. 771–777, 2008.

[81] B. Di Iorio, S. Torraca, C. Piscopo et al., "Dialysate bath and QTc interval in patients on chronic maintenance hemodialysis: pilot study of single dialysis effects," *Journal of Nephrology*, vol. 25, no. 5, pp. 653–660, 2012.

[82] I. Girgis, G. Contreras, S. Chakko et al., "Effect of hemodialysis on the signal-averaged electrocardiogram," *American Journal of Kidney Diseases*, vol. 34, no. 6, pp. 1105–1113, 1999.

[83] H. Ichikawa, Y. Nagake, and H. Makino, "Signal averaged electrocardiography (SAECG) in patients on hemodialysis," *Journal of Medicine*, vol. 28, no. 3-4, pp. 229–243, 1997.

[84] P. P. Frohnert, E. R. Giuliani, M. Friedberg, W. J. Johnson, and W. N. Tauxe, "Statistical investigation of correlations between serum potassium levels and electrocardiographic findings in patients on intermittent hemodialysis therapy," *Circulation*, vol. 41, no. 4, pp. 667–676, 1970.

[85] C. P. Kovesdy, D. L. Regidor, R. Mehrotra et al., "Serum and dialysate potassium concentrations and survival in hemodialysis patients," *Clinical Journal of the American Society of Nephrology*, vol. 2, no. 5, pp. 999–1007, 2007.

[86] I. A. Checherita, C. David, V. Diaconu, A. Ciocalteu, and I. Lascar, "Potassium level changes—arrhythmia contributing factor in chronic kidney disease patients," *Romanian Journal of Morphology and Embryology*, vol. 52, supplement 3, pp. 1047–1050, 2011.

[87] O. E. Osadchii, "Mechanisms of hypokalemia-induced ventricular arrhythmogenicity," *Fundamental and Clinical Pharmacology*, vol. 24, no. 5, pp. 547–559, 2010.

[88] S. E. Näppi, V. K. Virtanen, H. H. T. Saha, J. T. Mustonen, and A. I. Pasternack, "QT(c) dispersion increases during hemodialysis with low-calcium dialysate," *Kidney International*, vol. 57, no. 5, pp. 2117–2122, 2000.

[89] J. W. Lohr, S. Slusher, and D. Diederich, "Safety of regional citrate hemodialysis in acute renal failure," *American Journal of Kidney Diseases*, vol. 13, no. 2, pp. 104–107, 1989.

[90] F. Afshinnia, H. Doshi, and P. S. Rao, "The effect of different dialysate magnesium concentrations on QTc dispersion in hemodialysis patients," *Renal Failure*, vol. 34, no. 4, pp. 408–412, 2012.

[91] P. Melillo, R. Izzo, N. De Luca, and L. Pecchia, "Heart rate variability and renal organ damage in hypertensive patients," *Conference proceedings: IEEE Engineering in Medicine and Biology Society*, vol. 2012, pp. 3825–3828, 2012.

[92] M. Kyriakidis, S. Voudiclaris, and D. Kremastinos, "Cardiac arrhythmias in chronic renal failure? Holter monitoring during dialysis and everyday activity at home," *Nephron*, vol. 38, no. 1, pp. 26–29, 1984.

[93] O. M. Shapira and Y. Bar-Khayim, "ECG changes and cardiac arrhythmias in chronic renal failure patients on hemodialysis," *Journal of Electrocardiology*, vol. 25, no. 4, pp. 273–279, 1992.

[94] J. Dubrava, J. Fekete, and A. Lehotska, "Relation of ventricular late potentials and intradialytic changes in serum electrolytes, ultrafiltration, left ventricular ejection fraction and left ventricular mass index in haemodialysis patients," *Bratislavske Lekarske Listy*, vol. 104, no. 12, pp. 388–392, 2003.

[95] A. P. Marcassi, D. C. Yasbek, J. O. M. Pestana et al., "Ventricular arrhythmia in incident kidney transplant recipients: prevalence and associated factors," *Transplant International*, vol. 24, no. 1, pp. 67–72, 2011.

[96] D. C. Yazbek, A. B. de Carvalho, C. S. Barros et al., "Cardiovascular disease in early kidney transplantation: comparison between living and deceased donor recipients," *Transplantation Proceedings*, vol. 44, no. 10, pp. 3001–3006, 2012.

[97] M. Zukowski, J. Biernawska, K. Kotfis et al., "Factors influencing QTc interval prolongation during kidney transplantation," *Annals of Transplantation*, vol. 16, no. 2, pp. 43–49, 2011.

[98] A. Monfared and A. J. Ghods, "Improvement of maximum corrected QT and corrected QT dispersion in electrocardiography after kidney transplantation," *Iranian Journal of Kidney Diseases*, vol. 2, no. 2, pp. 95–98, 2008.

Research Article

Evaluation of Assays for Measurement of Serum (Anti)oxidants in Hemodialysis Patients

Tatjana Ruskovska,[1] Eugene H. J. M. Jansen,[2] and Risto Antarorov[3]

[1] *Faculty of Medical Sciences, Goce Delcev University, 2000 Stip, Macedonia*
[2] *National Institute for Public Health and the Environment, 3721 MA, Bilthoven, The Netherlands*
[3] *General City Hospital, 1000 Skopje, Macedonia*

Correspondence should be addressed to Tatjana Ruskovska; tatjana.ruskovska@ugd.edu.mk

Background. Various biomarkers and assays have been used for assessment of (anti)oxidant status in hemodialysis patients, including those intended for measurement of serum total (anti)oxidants, most often as a part of panel biomarkers. *Methods.* Serum (anti)oxidant status was measured in 32 chronically hemodialyzed patients and in 47 healthy persons, using two oxidations and three antioxidant assays. *Results.* The patients before the hemodialysis session have had higher values of total oxidants in comparison to the healthy persons, with a further increase during the hemodialysis. These findings were confirmed with both oxidation assays, but they differ in the percentage of increase and the statistical significance. All three antioxidant assays showed significantly higher values of the total serum antioxidants in the patients before the hemodialysis session in comparison to the healthy persons, and their significant decrease during the hemodialysis. However, the assays differ in the percentage of decrease, its statistical significance, and the correlations with uric acid. *Conclusion.* The variability of results of total (anti)oxidants which are obtained using different assays should be taken into account when interpreting data from clinical studies of oxidative stress, especially in complex pathologies such as chronic hemodialysis.

1. Introduction

Oxidative stress, as a state of substantial prooxidant imbalance between oxidants and antioxidants within the cells and tissues, leads to an oxidative damage of proteins, lipids, and DNA. As such, the oxidative stress implies numerous noncommunicable diseases, including end-stage renal disease [1]. Accumulation of uremic toxins [2], bioincompatibility of the dialyzer's membrane [3], depletion of low molecular antioxidants, in the first place ascorbic acid, during the hemodialysis session [4], and excessive and indiscriminate use of intravenous iron preparations [5] have been described as the main factors which cause oxidative stress in the chronically hemodialyzed patients. There is a large body of evidence that the prooxidant state of the chronically hemodialyzed patients is associated with cardiovascular disease [6–8], renal anemia [9, 10], and mineral and bone disorders [11], which largely contribute to their increased morbidity and mortality.

Although the oxidative stress in chronically hemodialyzed patients has been extensively studied, there is no consensus about the use of (anti)oxidant status biomarkers and assays. Thus, different biomarkers and assays and various combinations of them have been used in different clinical studies. Among others, the assays for measurement of the levels of total oxidants [12] and total antioxidants [13] in serum/plasma have been used in many studies. However, using these assays, sometimes different [14, 15] or even opposite findings are reported [16, 17], especially for the total serum antioxidants. These inconsistent data in the literature could be a result of many factors like variations in the process of hemodialysis itself and/or influence of the analytical factors, that is, the methods used.

Therefore, the aim of this study was to conduct a comparative analysis of some of the assays for quantification of the total oxidants and the total antioxidants in serum samples from chronically hemodialyzed patients both before and after

the single hemodialysis session and in a group of healthy persons. More specifically, we have evaluated two commercial assays for determining the serum oxidants, as well as two commercial assays and one in-house assay for measurement of total serum antioxidants. We focused primarily on commercial assays because of the less variability in preparation of reagents and standards, which enables generation of more accurate and precise results.

2. Materials and Methods

2.1. Samples. Serum samples from 32 chronically hemodialyzed patients and 47 healthy persons were analyzed in this study.

The samples from the chronically hemodialyzed patients who were on hemodialysis treatment for more than 1 year and who were treated with a protocol of three hemodialysis sessions a week were obtained from the Department of Hemodialysis at Military Hospital in Skopje. The mean age of the patients was 61 ± 10 years (range 38–78 years). Blood for analysis was drawn immediately before and after the second hemodialysis session within the week in blood collecting tubes (Sarstedt) containing clot activator. Before the hemodialysis blood was drawn after an overnight fasting. The serum was separated with standard centrifugation procedure and immediately divided in portions which were kept tightly closed at $-70°C$ until analysis [18].

The results obtained from the hemodialyzed patients were compared to those from 47 healthy persons (mean age: 25 ± 3 years), candidates for military service. They were physically and mentally healthy, without any chronic or acute disease, as confirmed with their clinical presentation at the day of blood sampling and the results from the standard medical examinations. They did not report use of any antioxidants and supplements. Fasting blood samples, drawn at about 9:00–9:30 am, were obtained during the scheduled standard systematic medical examination. After the centrifugation, the sera were aliquoted in portions which were kept tightly closed at $-70°C$ until analysis.

The Command of the Military Medical Center in Skopje approved this study, as stated in the document N number 07-1756/1 from the Army mail 2990/80, Army of Republic of Macedonia.

2.2. Assays. Within this study the following assays have been evaluated: the reactive oxygen metabolites (ROM), test kit d-ROM from Diacron [19] (Grosseto, Italy); the total oxidant status (TOS), test kit from Rel Assay Diagnostics [20] (Gaziantep, Turkey); the ferric reducing ability of plasma (FRAP), an in-house assay; the total antioxidant status (TAS), test kit from Rel Assay Diagnostics; and the biological antioxidant potential (BAP), test kit from Diacron. We have also measured the serum concentrations of uric acid using the method with uricase, with a dedicated test kit, on the autoanalyzer LX20-Pro (Beckman-Coulter).

2.2.1. Oxidation Assays. The d-ROM assay is intended for measurement of the concentration of total hydroperoxides

in serum or heparin plasma. The method was first described by Alberti et al. in 2000 [21]. It is based on the following principle. *In vitro*, in an acidic buffered solution (pH = 4.8), the iron ions are released from the serum (plasma) proteins and catalyze the reaction of transformation of hydroperoxides into alkoxyl and peroxyl radicals, which further react with the chromogen N,N-diethyl-p-phenylenediamine. The concentration of the colored complex is directly proportional to the concentration of the hydroperoxides which are present in the sample. The absorbance is measured at 505 nm, and the results are expressed in CARR U. One CARR U corresponds to 0.08 mg/100 mL H_2O_2. The characteristics of the assay were evaluated and validated by Verde et al. in 2002 [22], who report that the assay is reliable even in patients with hyposideremic anemia. In our study the assay has been automated on the autoanalyzer LX20-Pro (Beckman-Coulter).

The TOS assay, developed by Erel in 2005 [23], is intended for measurement of the level of oxidant molecules in various biological samples. The assay is based on the principle of oxidation of the ferrous ion-chelator complex to ferric ion with the oxidants which are present in the sample. The ferric ion further forms a colored complex with a chromogen, and the color intensity is directly proportional to the level of total oxidants. The absorbance is measured at 530 nm. The assay is calibrated with hydrogen peroxide and the results are expressed in μmol H_2O_2 Eq/L. We have performed this assay in microtiter plates.

2.2.2. Antioxidant Assays. The FRAP, TAS, and BAP assays are intended for direct measurement of the total antioxidant activity of the sample.

The in-house FRAP assay is a modification of the original method of Benzie and Strain [24]. The method is based on the principle of reduction of the ferric-tripyridyltriazine complex to the ferrous form with the antioxidants which are present in the sample. The increase of absorbance is measured at 593 nm, in a kinetic mode. In a modified method we have used an end-point approach with incubation of exactly 8 minutes. The absorbance has been measured at 600 nm on a microplate autoanalyzer ChemWell [25]. A freshly prepared standard solution of $FeSO_4$ has been used for calibration of the assay. The results are expressed in μmol/L $FeSO_4$.

The TAS assay, developed by Erel in 2004 [26], is based on the principle of reduction of the dark blue-green colored 2,2'-azino-bis(3-ethylbenzothiazoline-6-sulphonic acid) (ABTS) radical to its colorless reduced form with the antioxidants which are present in the sample. The change of the absorbance is measured at 660 nm. The assay is calibrated with a stable antioxidant standard solution, vitamin E analog—Trolox Equivalent. The results are expressed in μmol/L (μmol Trolox Equivalent/L). We have automated this assay on the autoanalyzer LX20-Pro (Beckman-Coulter).

The BAP assay is based on the ability of a colored solution which contains ferric ions bound to a chromogenic substrate (a thiocyanate derived compound) to decolor upon reduction of ferric to ferrous ions. The absorbance is measured at 505 nm, and the results are expressed as μEq/L (μEq ferric ions reducing antioxidants/L). Notably, there is no scientific

paper which describes validation and verification of the characteristics of this assay. This information is available from the manufacturer of the reagent kit [27]. In our study the assay was automated on the autoanalyzer LX20-Pro (Beckman-Coulter).

All analyses have been run within one analytical series.

2.3. Statistical Analysis. The results from measurements are expressed as mean ± standard deviation. The distribution of the data was assessed with Kolmogorov-Smirnov test, using Statistica 7 software.

The data which are normally distributed were processed with Microsoft Excel software. The statistical significance was calculated with Student's *t*-test (paired, two-sample equal variance or two-sample unequal variance, as appropriate).

For the data which are not normally distributed, the Wilcoxon matched pairs test or the Mann-Whitney *U* test was used, as appropriate (Statistica 7 software).

The difference between means was considered as statistically significant when it was $P < 0.05$.

The statistical significance of the coefficients of correlation was assessed according to the number of subjects within the group, using a statistical table [28].

3. Results

3.1. Oxidation Assays. The results from both of the oxidation assays (d-ROM and TOS) show an increase of the concentration of serum oxidants as a result of the single hemodialysis session. However, there is a difference between the assays with regard to the percentage and the statistical significance of the increase. More precisely, we have measured serum ROM concentrations of 428 ± 120 CARR U before and 463 ± 120 CARR U immediately after the hemodialysis session, which is a statistically significant increase for 8.2% ($P < 0.025$). In contrast, as measured with the TOS assay, the percentage of the increase has been much higher (22.4%), but the difference between the values obtained before (2.46 ± 1.86 μmol H_2O_2 Eq/L) and after (3.01 ± 2.38 μmol H_2O_2 Eq/L) the single hemodialysis session was not statistically significant ($P > 0.05$). Coefficients of correlation between d-ROM and TOS before and after the single hemodialysis session were −0.083 and 0.160, respectively ($P > 0.05$ for both comparisons).

We have also compared the results for serum oxidants of the patients on hemodialysis and the healthy persons and obtained consistent conclusions.

Namely, both ROM (408 ± 92 CARR U) and TOS (2.01 ± 0.81 μmol H_2O_2 Eq/L) levels were lower in the healthy persons in comparison to the patients before the hemodialysis session, but the differences were not statistically significant ($P > 0.05$ for both comparisons). However, the increased values of ROM and TOS after the single hemodialysis session were significantly different from those measured in the healthy persons ($P = 0.023$ for ROM; $P = 0.029$ for TOS).

The results from the oxidation assays are presented in Figure 1. For better visual presentation the results of the TOS assay are multiplied by 100.
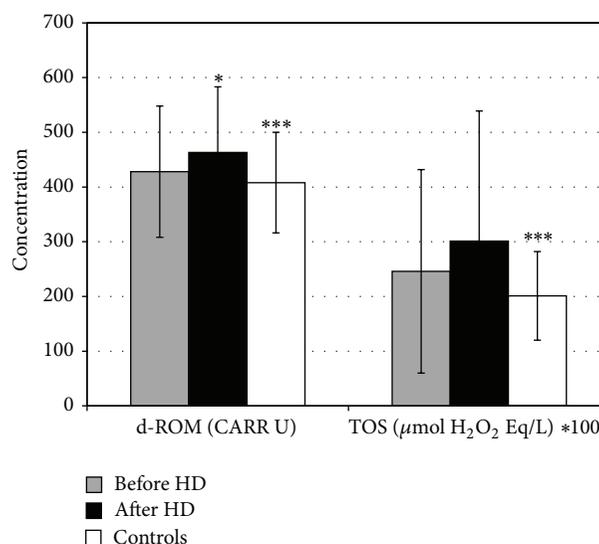
Figure 1: Serum oxidants in patients on chronic hemodialysis and healthy persons. *Statistically significant difference between patients before and after the single hemodialysis session. ***Statistically significant difference between patients after hemodialysis and healthy persons.

3.2. Antioxidant Assays. Before the hemodialysis session, very high values of FRAP in the patients (1758 ± 320 μmol/L), compared to the healthy persons (1378 ± 159 μmol/L), were measured and this difference was highly statistically significant ($P < 0.001$). However, measured immediately after the hemodialysis, the values of FRAP significantly dropped to 1080 ± 162 μmol/L, or on average, for 38.6%, which was again highly statistically significant in comparison to the values before the hemodialysis and to those of the healthy persons ($P < 0.001$ for both comparisons).

Similarly, TAS significantly decreased from 2300 ± 380 μmol/L before the hemodialysis to 1490 ± 240 μmol/L after the hemodialysis session ($P < 0.001$). The percentage of the decrease of TAS (35.2%) was almost identical to that of the FRAP assay. The group of healthy persons have had TAS values of 1550 ± 150 μmol/L, which were significantly lower than those measured in the hemodialyzed patients before the hemodialysis ($P < 0.001$). However, the decline of the TAS values during the hemodialysis session was not so pronounced as to reach a statistical significance in comparison to the healthy persons.

General conclusions which are withdrawn from the BAP assay are the same as those of the FRAP assay. Exceptions are the percentage of the BAP decrease as a result of the single hemodialysis session and the levels of statistical significance of the differences between the healthy subjects and the hemodialysis patients both before and after the single hemodialysis session. More precisely, in the hemodialyzed patients we have measured 2592 ± 239 μEq/L of BAP before and 2265 ± 268 μEq/L after the hemodialysis ($P < 0.001$), which is a decrease for only 12.6%. BAP values of the healthy persons were 2442 ± 149 μEq/L and were significantly

TABLE 1: Coefficients of correlation between FRAP, TAS, and BAP assays, both before and after the single hemodialysis session.

|		TAS		BAP	
		Before HD	After HD	Before HD	After HD
FRAP	Before HD	0.903**		0.527**	
	After HD		0.805**		0.259[ns]
TAS	Before HD			0.575**	
	After HD				0.668**

[ns]Nonsignificant.
**$P < 0.01$.
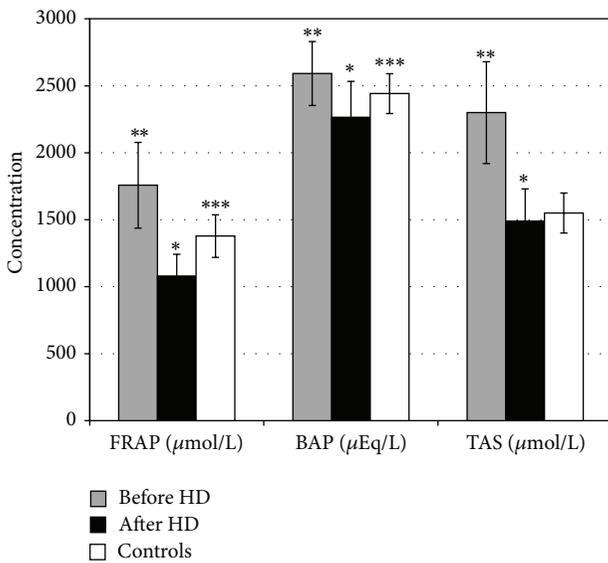
FIGURE 2: Serum antioxidants in patients on chronic hemodialysis and healthy persons. *Statistically significant difference between patients before and after the single hemodialysis session. **Statistically significant difference between patients before hemodialysis and healthy persons. ***Statistically significant difference between patients after hemodialysis and healthy persons.

different from the values of hemodialyzed patients before and after the hemodialysis ($P < 0.01$ for both comparisons).

The graphic presentation of the results obtained from the antioxidant assays is given in Figure 2. The coefficients of correlation between these assays, both before and after the single hemodialysis session, are given in Table 1.

The serum concentrations of uric acid in the hemodialyzed patients before the hemodialysis session (320 ± 62 μmol/L) were not significantly different from those measured in the healthy persons (303 ± 56 μmol/L), $P > 0.05$. However, during the hemodialysis session, the serum uric acid concentrations decreased to 84 ± 30 μmol/L, which is, on average, a decrease for 73.8%, and which is highly statistically significant in comparison to the values before the hemodialysis and to those of the healthy persons ($P < 0.001$ for both comparisons).

Moreover, the serum uric acid concentrations significantly correlated with FRAP, TAS, and BAP in the hemodialyzed

TABLE 2: Correlation coefficients of uric acid versus FRAP, TAS, and BAP.

Correlation coefficients	Before hemodialysis	After hemodialysis	Healthy persons
Uric acid versus FRAP	0.547**	0.430*	0.875**
Uric acid versus TAS	0.662**	0.521**	0.930**
Uric acid versus BAP	0.410*	0.385*	0.366*

*$P < 0.05$.
**$P < 0.01$.

patients, both before and after the hemodialysis session, as well as in the healthy persons (results shown in Table 2).

4. Discussion

4.1. Oxidation Assays. Two assays, for measurement of the serum oxidants (d-ROM and TOS), were evaluated in this study. These assays are based on completely different principles. Therefore, it was not surprising that the coefficients of correlation between them, both before and after the single hemodialysis session, were not statistically significant. However, the analysis of the results demonstrated that the conclusions which are withdrawn from both assays are generally consistent, yet with some differences.

It has been shown with both of the oxidation assays that before the hemodialysis session the patients had higher concentrations of serum oxidants than the healthy persons, but the difference was not statistically significant.

In other clinical studies, using the d-ROM assay [14, 29], higher values of serum oxidants were also found in hemodialyzed patients in comparison to healthy persons. Notably, in both studies the difference between the patients and the healthy persons was statistically significant, but the P values were above 0.025, indicating small differences between the groups. However, in another study [30] the difference of the ROM concentrations between hemodialyzed patients and healthy persons was more pronounced.

It has been also shown with both of the oxidation assays that there was an increase in the concentrations of serum oxidants during the hemodialysis session, leading to a statistically significant difference between the hemodialyzed patients and the healthy subjects.

Others, using the d-ROM assay, have also found a significant increase of ROM levels during the single hemodialysis session [14], but there is also a different finding [15].

To the best of our knowledge, the levels of serum oxidants in hemodialyzed patients have not been measured before with the TOS assay from Rel Assay Diagnostics.

Altogether, although not specific for a particular oxidant or oxidation mechanism and based on completely different principles, the d-ROM and TOS assays in this study consistently reflected the oxidation state of the hemodialyzed patients, which are slightly increased oxidation in comparison to the healthy subjects and further increase during the

TABLE 3: Relative contributions of individual plasma antioxidants to total FRAP and TAS values (data from literature).

	Estimated % contribution to total FRAP	Estimated % contribution to total TAS
Uric acid	60	33
Protein	10	53
Bilirubin	5	2
Ascorbic acid	15	5
α-Tocopherol	5	2
Others	5	5

single hemodialysis session. However, assessing the increase of serum oxidants during the single hemodialysis session, we found an inconsistence between these two assays with regard to the percentage of the increase and its statistical significance, which warrants caution in the interpretation of the results.

4.2. Antioxidant Assays. After the introduction of the concept of oxidative stress as an imbalance between the molecules with prooxidant and antioxidant activity, a number of methods for measurement of total nonenzymatic plasma antioxidant activity have been published. There is almost no disease or condition where the total nonenzymatic plasma antioxidant activity has not been assessed. However, the intention to relate *directly* the levels of total antioxidants in food with the total plasma antioxidant activity is not justified because of the known ADME (absorption, distribution, metabolism, and elimination) effects of the human body on the nutritional antioxidants [31]. In addition, it is also not justifiable to relate the values of the total plasma antioxidant activity, directly and in an indiscriminate manner, with the state of good health. The chronically hemodialyzed patients are such an example. Still, the total antioxidant assays remain a useful tool for oxidative stress research, in carefully designed clinical studies, as members of panel biomarkers and always in correlation with other clinical data.

Three photometric assays for direct measurement of the total antioxidant activity (FRAP, TAS, and BAP) have been evaluated in this study, all of them based on different principles. Namely, the FRAP and BAP assays are based on the principle of reduction of ferric to ferrous ions but with use of different complexes, while the TAS assay is based on the principle of reduction of ABTS radical. All three assays are nonspecific and are intended for measurement of various antioxidants which are present in the sample. Relative contributions of the most common plasma antioxidants to the values of FRAP [24] and TAS [26] are given in Table 3. The manufacturer does not provide such data for the BAP assay, but referring to the FRAP assay which also uses the principle of reduction of ferric ions presents data from experiments with uric acid, bilirubin, ascorbic acid, and α-tocopherol [27]. Since hyperbilirubinemia is not an issue in the patients included in this study (data not shown) and proteins are nondialyzable molecules, we focus on uric acid

and its correlations with the total antioxidant status assays, both before and after a single hemodialysis session.

When the FRAP, TAS, and BAP assays were applied on the same sets of serum samples from hemodialyzed patients and healthy subjects, the results generally reflected the same trends, although there were also some differences. In addition, all three assays correlated significantly with each other both before and after the single hemodialysis session, with exception of the correlation between the FRAP and BAP assays after the hemodialysis session.

Before the hemodialysis session the patients had significantly higher levels of total antioxidants in comparison to the healthy persons, which has been demonstrated with all three assays.

This, at a first glance paradoxical finding, is in accordance with the results from other studies where the total antioxidant status was measured with the FRAP assay [32, 33]. However, there are also some opposite findings [34]. To the best of our knowledge, the BAP assay from Diacron has not been used before for a parallel measurement of total antioxidants in hemodialyzed patients and healthy persons. There is also no information that the TAS assay from Rel Assay Diagnostics had been applied on serum samples from hemodialyzed patients. However, an assay based on the ABTS reduction principle has been used before [35] and the authors report higher levels of total antioxidants in chronically hemodialyzed patients in comparison to healthy persons.

The high levels of total serum antioxidants in the hemodialyzed patients before the single hemodialysis session have been attributed to the abundance of small molecules with reductive properties, mostly the uric acid [36, 37]. However, we did not find that the slightly higher serum uric acid concentrations of the patients before the hemodialysis session were significantly different from those measured in the healthy subjects. As such, it appears that the uric acid is not a primary cause of the remarkably high levels of total antioxidants in the predialyzed patients and that other molecules with ability to reduce the ferric ions or the ABTS radicals substantially contribute to their levels.

In contrast to our (and others') results, there are also findings of lower levels of total serum antioxidants in chronically hemodialyzed patients before the hemodialysis session in comparison to healthy subjects [38, 39]. Notably, in these clinical studies were used completely different methods (in which hydroxyl radical is generated) than those evaluated in our study [40, 41].

All three antioxidant assays have shown that there was a highly significant decrease of the content of total serum antioxidants during the single hemodialysis session.

This is a common finding of many clinical studies [15, 42] which is explained with depletion of the low molecular antioxidants through the dialyzer's membrane. However, there are also some opposite findings [43].

The percentage of decrease of the levels of antioxidants during the hemodialysis session was rather high and almost identical when measured with the FRAP and TAS assays (38.6% and 35.2%, resp.) but almost three times lower when measured with the BAP assay (12.6%). This finding could possibly be explained with the fact that the coefficient of

correlation between the BAP and the uric acid is the lowest in comparison to all other coefficients of correlation of the uric acid (Table 2). In addition, the lowest correlation between BAP and uric acid could mean that the BAP assay reflects better the presence of antioxidants other than the uric acid, with possible beneficial health effects. In this context, a recent study demonstrated that hemodialysis patients with higher BAP values have better survival rate [44].

Serum total antioxidants were lower in the postdialyzed patients than in the healthy subjects, which has been demonstrated by all three assays.

This difference was statistically significant for the FRAP and BAP assays only (iron reduction principle) but not for TAS assay (ABTS reduction principle). Once more this finding emphasizes the influence of different assays on the final conclusions which are withdrawn for the same sets of clinical samples.

5. Conclusion

Conducting this comparative analysis of some of the total (anti)oxidant assays, using the same sets of serum samples from chronically hemodialyzed patients and healthy subjects, we demonstrate that even with a tight control of all preanalytical and analytical variables (such as identical treatment of all samples, automation of most of the assays, and analysis within the same analytical series), different assays intended for measurement of the same complex "analyte," being the total (anti)oxidants, occasionally lead to different conclusions. However, we did not get any opposite results. Discussing our findings, we highlight data from the literature about the levels of total (anti)oxidants in chronically hemodialyzed patients that are sometimes inconsistent and even opposite, which warrants careful evaluation of the results obtained from laboratory measurements.

It is noteworthy that all assays which are evaluated in this study, and many similar ones, are not specific for a particular (anti)oxidant. Besides, they have been used in many clinical studies, individually or more often as a part of panel biomarkers, and together with other clinical findings, thus contributing to get a more complete insight of the changes of the (anti)oxidant status as a result of a specific treatment or condition. Therefore, the variability of measurements should be taken into account in interpretation of data from clinical trials. This study highlights the importance of this issue in hemodialysis patients.

Abbreviations

ROM: Reactive oxygen metabolites
CARR U: Carratelli units
TOS: Total oxidant status
FRAP: Ferric reducing ability of plasma
TAS: Total antioxidant status
BAP: Biological antioxidant potential
ABTS: 2,2′-azino-bis(3-ethylbenzothiazoline-6-sulphonic acid).

References

[1] M. J. Puchades, G. Saez, M. C. Muñoz et al., "Study of oxidative stress in patients with advanced renal disease and undergoing either hemodialysis or peritoneal dialysis," *Clinical Nephrology*, vol. 80, no. 3, pp. 177–186, 2013.

[2] N. Jourde-Chiche, L. Dou, C. Cerini, F. Dignat-George, and P. Brunet, "Vascular incompetence in dialysis patients—protein-bound uremic toxins and endothelial dysfunction," *Seminars in Dialysis*, vol. 24, no. 3, pp. 327–337, 2011.

[3] G. J. Dahe, R. S. Teotia, S. S. Kadam, and J. R. Bellare, "The biocompatibility and separation performance of antioxidative polysulfone/vitamin E TPGS composite hollow fiber membranes," *Biomaterials*, vol. 32, no. 2, pp. 352–365, 2011.

[4] X. F. Shi, F. Ding, Q. Y. Zhu et al., "Use of ascorbate-rich dialysate to attenuate oxidative stress in maintenance hemodialysis patients," *Renal Failure*, vol. 27, no. 2, pp. 213–219, 2005.

[5] N. D. Vaziri, "Understanding iron: promoting its safe use in patients with chronic kidney failure treated by hemodialysis," *The American Journal of Kidney Diseases*, vol. 61, no. 6, pp. 992–1000, 2013.

[6] M. Bossola, C. Vulpio, L. Colacicco, D. Scribano, C. Zuppi, and L. Tazza, "Reactive oxygen metabolites (ROMs) are associated with cardiovascular disease in chronic hemodialysis patients," *Clinical Chemistry and Laboratory Medicine*, vol. 50, no. 8, pp. 1447–1453, 2012.

[7] H. Honda, M. Ueda, S. Kojima et al., "Oxidized high-density lipoprotein as a risk factor for cardiovascular events in prevalent hemodialysis patients," *Atherosclerosis*, vol. 220, no. 2, pp. 493–501, 2012.

[8] E. Ari, Y. Kaya, H. Demir et al., "Oxidative DNA damage correlates with carotid artery atherosclerosis in hemodialysis patients," *Hemodialysis International*, vol. 15, no. 4, pp. 453–459, 2011.

[9] G. Celik, M. Yöntem, M. Bilge, M. Cilo, and M. Ünaldi, "The relationship between the antioxidant system and anaemia in haemodialysis patients," *Journal of International Medical Research*, vol. 39, no. 5, pp. 1954–1960, 2011.

[10] A. Rusu, F. Rusu, D. Zalutchi, A. Muresan, M. G. Caprioara, and I. Kacso, "The influence of vitamin E supplementation on erythropoietin responsiveness in chronic hemodialysis patients with low levels of erythrocyte superoxide dismutase," *International Urology and Nephrology*, vol. 45, no. 2, pp. 495–501, 2013.

[11] H. Tanaka, H. Komaba, M. Koizumi, T. Kakuta, and M. Fukagawa, "Role of uremic toxins and oxidative stress in the development of chronic kidney disease-mineral and bone disorder," *Journal of Renal Nutrition*, vol. 22, no. 1, pp. 98–101, 2012.

[12] S. Suvakov, T. Damjanovic, A. Stefanovic et al., "*Glutathione S-transferase A1, M1, P1* and *T1* null or low-activity genotypes are associated with enhanced oxidative damage among haemodialysis patients," *Nephrology Dialysis Transplantation*, vol. 28, no. 1, pp. 202–212, 2013.

[13] M. Muñoz-Cortés, C. Cabré, D. Villa et al., "Oxidative stress and other risk factors for white matter lesions in chronic hemodialysis patients," *Clinical Nephrology*, vol. 80, no. 3, pp. 187–197, 2013.

[14] G. Gerardi, M. Usberti, G. Martini et al., "Plasma total antioxidant capacity in hemodialyzed patients and its relationships to other biomarkers of oxidative stress and lipid peroxidation," *Clinical Chemistry and Laboratory Medicine*, vol. 40, no. 2, pp. 104–110, 2002.

[15] K. Nakayama, H. Terawaki, M. Nakayama, M. Iwabuchi, T. Sato, and S. Ito, "Reduction of serum antioxidative capacity during hemodialysis," *Clinical and Experimental Nephrology*, vol. 11, no. 3, pp. 218–224, 2007.

[16] F. Montazerifar, M. Hashemi, M. Karajibani, and M. Dikshit, "Hemodialysis alters lipid profiles, total antioxidant capacity, and vitamins A, E, and C concentrations in humans.," *Journal of Medicinal Food*, vol. 13, no. 6, pp. 1490–1493, 2010.

[17] E. S. Namiduru, M. Tarakcioglu, O. Tiryaki, and C. Usalan, "Evaluation of oxidative and nitrosative stress in hemodialysis patients," *Minerva Medica*, vol. 101, no. 5, pp. 305–310, 2010.

[18] E. H. Jansen, P. K. Beekhof, J. W. Cremers, D. Viezeliene, V. Muzakova, and J. Skalicky, "Long-term stability of parameters of antioxidant status in human serum," *Free Radical Research*, vol. 47, no. 6-7, pp. 535–540, 2013.

[19] Diacron, 2012, http://www.diacron.com/.

[20] Rel Assay Diagnostics, http://www.relassay.com/.

[21] A. Alberti, L. Bolognini, D. Macciantelli, and M. Caratelli, "The radical cation of *N,N*-diethl-*para*-phenylendiamine: a possible indicator of oxidative stress in biological samples," *Research on Chemical Intermediates*, vol. 26, no. 3, pp. 253–267, 2000.

[22] V. Verde, V. Fogliano, A. Ritieni, G. Maiani, F. Morisco, and N. Caporaso, "Use of N,N-dimethyl-p-phenylenediamine to evaluate the oxidative status of human plasma," *Free Radical Research*, vol. 36, no. 8, pp. 869–873, 2002.

[23] O. Erel, "A new automated colorimetric method for measuring total oxidant status," *Clinical Biochemistry*, vol. 38, no. 12, pp. 1103–1111, 2005.

[24] I. F. F. Benzie and J. J. Strain, "The ferric reducing ability of plasma (FRAP) as a measure of "antioxidant power": the FRAP assay," *Analytical Biochemistry*, vol. 239, no. 1, pp. 70–76, 1996.

[25] E. H. Jansen and T. Ruskovska, "Comparative analysis of serum (anti)oxidative status parameters in healthy persons," *International Journal of Molecular Sciences*, vol. 14, no. 3, pp. 6106–6115, 2013.

[26] O. Erel, "A novel automated direct measurement method for total antioxidant capacity using a new generation, more stable ABTS radical cation," *Clinical Biochemistry*, vol. 37, no. 4, pp. 277–285, 2004.

[27] "The BAP test and the global assessement of oxidative stress in clinical practice," Release 4.1, 2010, http://www.medial.cz/data/files/medial/download/prospekty/HaD/2010_4_1_BAP_TEST_PRESENTATION.pdf.

[28] P. B. Dodatak, *Osnovne Statisticke Metode Za Nematematicare*, Manualia Universitatis Studiorum Zagrabiensis, SNL, Zagreb, Croatia, 2nd edition, 1985.

[29] E. Samouilidou, E. Grapsa, A. Karpouza, and A. Lagouranis, "Reactive oxygen metabolites: a link between oxidative stress and inflammation in patients on hemodialysis," *Blood Purification*, vol. 25, no. 2, pp. 175–178, 2007.

[30] S. Coaccioli, M. L. Standoli, R. Biondi et al., "Open comparison study of oxidative stress markers between patients with chronic renal failure in conservative therapy and patients in haemodialysis," *Clinica Terapeutica*, vol. 161, no. 5, pp. 435–439, 2010.

[31] A. Pompella, H. Sies, R. Wacker et al., "The use of "total antioxidant capacity" as surrogate marker for food quality and its impact on health is to be discouraged," *Nutrition*, 2014.

[32] J. Rysz, R. A. Stolarek, A. Pedzik, M. Nowicki, and D. Nowak, "Serum antioxidant capacity is preserved in peritoneal dialysis contrary to its robust depletion after hemodialysis and hemodiafiltration sessions," *Therapeutic Apheresis and Dialysis*, vol. 14, no. 2, pp. 209–217, 2010.

[33] U. R. Kuppusamy, M. Indran, T. Ahmad, S. W. Wong, S. Y. Tan, and A. A. Mahmood, "Comparison of oxidative damage in Malaysian end-stage renal disease patients with or without non-insulin-dependent diabetes mellitus," *Clinica Chimica Acta*, vol. 351, no. 1-2, pp. 197–201, 2005.

[34] A. Khaira, S. Mahajan, A. Kumar et al., "Endothelial function and oxidative stress in chronic kidney disease of varying severity and the effect of acute hemodialysis," *Renal Failure*, vol. 33, no. 4, pp. 411–417, 2011.

[35] P. Castilla, R. Echarri, A. Dávalos et al., "Concentrated red grape juice exerts antioxidant, hypolipidemic, and antiinflammatory effects in both hemodialysis patients and healthy subjects," *The American Journal of Clinical Nutrition*, vol. 84, no. 1, pp. 252–262, 2006.

[36] C. Erdoğan, Y. Unlüçerçi, A. Türkmen, A. Kuru, O. Cetin, and S. Bekpinar, "The evaluation of oxidative stress in patients with chronic renal failure," *Clinica Chimica Acta*, vol. 322, no. 1-2, pp. 157–161, 2002.

[37] P. Jackson, C. M. Loughrey, J. H. Lightbody, P. T. McNamee, and I. S. Young, "Effect of hemodialysis on total antioxidant capacity and serum antioxidants in patients with chronic renal failure," *Clinical Chemistry*, vol. 41, no. 8, part 1, pp. 1135–1138, 1995.

[38] M. Horoz, C. Bolukbas, F. F. Bolukbas et al., "Oxidative stress in hepatitis C infected end-stage renal disease subjects," *BMC Infectious Diseases*, vol. 6, article 114, 2006.

[39] Z. M. Dimitrijevic, T. P. Cvetkovic, V. M. Djordjevic et al., "How the duration period of erythropoietin treatment influences the oxidative status of hemodialysis patients," *International Journal of Medical Sciences*, vol. 9, no. 9, pp. 808–815, 2012.

[40] O. Erel, "A novel automated method to measure total antioxidant response against potent free radical reactions," *Clinical Biochemistry*, vol. 37, no. 2, pp. 112–119, 2004.

[41] D. Koracevic, G. Koracevic, V. Djordjevic, S. Andrejevic, and V. Cosic, "Method for the measurement of antioxidant activity in human fluids," *Journal of Clinical Pathology*, vol. 54, no. 5, pp. 356–361, 2001.

[42] C. Carollo, R. Lo Presti, and G. Caimi, "Leukocyte activation markers and oxidative status in chronic kidney disease," *Minerva Urologica e Nefrologica*, vol. 65, no. 1, pp. 69–76, 2013.

[43] A. A. Nassiri, M. S. Hakemi, M. Soulati, M. Marashian, K. Rahbar, and F. Azizi, "Effects of heparin and dalteparin on oxidative stress during hemodialysis in patients with end-stage

renal disease," *Iranian Journal of Kidney Diseases*, vol. 3, no. 3, pp. 162–167, 2009.

[44] T. Ishii, T. Ohtake, K. Okamoto et al., "Serum biological antioxidant potential predicts the prognosis of hemodialysis patients," *Nephron Clinical Practice* , vol. 117, no. 3, pp. c230–c236, 2011.

Research Article
Total and Free Serum Sialic Acid Concentration in Liver Diseases

Ewa Gruszewska,[1] Bogdan Cylwik,[2] Anatol Panasiuk,[3] Maciej Szmitkowski,[1] Robert Flisiak,[3] and Lech Chrostek[1]

[1] *Department of Biochemical Diagnostics, Medical University of Bialystok, Waszyngtona 15A Street, 15-269 Bialystok, Poland*
[2] *Department of Pediatric Laboratory Diagnostics, Medical University of Bialystok, Waszyngtona 17 Street, 15-269 Bialystok, Poland*
[3] *Department of Infectious Diseases and Hepatology, Medical University of Bialystok, Zurawia 15 Street, 15-540 Bialystok, Poland*

Correspondence should be addressed to Ewa Gruszewska; gr_ewa@interia.pl

Background. The objective of this study was to compare the levels of total (TSA) and free (FSA) sialic acid in acute and chronic liver diseases. *Materials and Methods.* The serum TSA and FSA levels were determined in 278 patients suffering from acute and chronic liver diseases of different etiologies. TSA was estimated by enzymatic method and FSA by the thiobarbituric method modified by Skoza and Mohos. *Results.* There were no significant differences in the serum TSA concentration between liver diseases of different etiologies, although in most of the liver diseases the mean TSA level was significantly lower than that in the control group. In contrast to TSA, the concentration of FSA appears to differ between liver diseases. In toxic hepatitis it was higher than that in nonalcoholic cirrhosis. However, neither of them differs between alcoholic and nonalcoholic cirrhosis or between liver tumors and tumors with cirrhosis. *Conclusions.* We conclude that the changes in concentrations of TSA and FSA during the same liver diseases indicate significant disturbances in sialylation of serum glycoproteins.

1. Introduction

Most of the serum proteins are glycoproteins, in which glycans are terminated with sialic acid residues [1–3]. In liver diseases, the changes in the concentration of sialylated glycoproteins in the blood have been reported [4, 5]. These changes should affect the concentration of total sialic acid (TSA). On the other hand, it is well known that the changes in protein glycosylation play an important role in the pathogenesis and progression of liver diseases [1, 2, 6, 7]. Because the most common disturbances in glycosylation rely on the increase of enzymatic activity that cuts off sialic acid residues from serum glycoproteins and/or on the decrease of enzymatic activity that binds sugar residues to oligosaccharide chains, these processes may result in increase of free sialic acid (FSA) concentration in the blood [6, 8].

The aim of this study was to assess the changes in the sialylation of serum glycoproteins by measuring total (TSA) and free sialic acid (FSA) concentration in the sera of patients suffering from acute and chronic liver diseases.

2. Materials and Methods

2.1. Subjects. The tested group consisted of 278 patients (99 females and 179 males) who were admitted to the Department of Infectious Diseases and Hepatology of University Hospital of Bialystok. The patients were divided into subgroups according to the diagnosis of liver diseases: 54 had alcoholic cirrhosis (AC), 34 nonalcoholic cirrhosis (NAC), 23 chronic nonviral hepatitis (CH), 32 toxic hepatitis (TH), 20 chronic viral hepatitis C (HCV), 17 chronic viral hepatitis B (HBV), 14 autoimmune hepatitis (AIH), 15 acute hepatitis B (AHB), 16 primary biliary cirrhosis (PBC), 14 fatty liver (FL), 24 primary liver cancer (HCC), and 15 primary liver cancer and cirrhosis (HCC + C). The diagnosis

was performed on the basis of signs and symptoms of the disease, physical and clinical exam (ultrasonography and fine-needle biopsy in justified cases), and biochemical liver panel known as liver function tests (AST, ALT, and GGT). The diagnosis of viral hepatitis was supported by serological tests (HBsAg and anti-HCV). The causes of nonalcoholic liver cirrhosis were as follows: HBV-14, HCV-9, and unidentified factors-12. The toxic hepatitis was caused by alcohol abuse in 22 cases and drugs abuse in 10 cases. To confirm the diagnosis of primary biliary cirrhosis we performed the mitochondrial antibody test (AMA).

2.2. Controls.

The control group consisted of 50 healthy subjects (18 females and 32 males) recruited from hospital workers. All subjects (healthy and sick) gave their consent to participate in the studies. The study was approved by the Bioethical Committee of the Medical University of Bialystok.

2.3. Sample Collection.

Blood samples were taken by peripheral vein puncture once after admission and before treatment. The sera were separated by centrifugation at $1500 \times$g for 10 min at room temperature and stored at -86°C until analysis.

2.4. TSA Assay.

TSA concentration in the serum was measured on the Microplate Fluorescence Reader FL600 (Bio-Tek, USA) according to the enzymatic method (EnzyChrom Sialic Acid Assay Kit, BioAssay System, Hayward, USA) using the colorimetric procedure. Each determination in a single sample was performed three times. The samples should be pretreated in hydrolysis procedure, in which neuraminidase released the N-acetylneuraminic acid (NANA) from glycol-inkages. In the next step the NANA is decomposed into N-acetylmannosamine and pyruvic acid in the presence of aldolase. Then the pyruvate is oxidized by pyruvate oxidase to acetyl phosphate, carbon dioxide, and hydrogen peroxide. In the last step, peroxidases and hydrogen peroxide convert 4-aminoantipyrine and N-ethyl-N-2-hydroxyethyl-3-toluidine to red coloured derivative. Briefly, to $20\,\mu$L of serum was added $80\,\mu$L of hydrolyzing reagent. This mixture was incubated in a water bath at 80°C for 60 minutes. After that the tubes were cooled to room temperature. Next, $20\,\mu$L of neutralizing reagent was added to the reaction mixtures and the tubes were centrifuged for 5 minutes at 14,000 rpm at room temperature. After that, the samples were applied to a 96-well microplate in the ratio $10\,\mu$L of sample and $90\,\mu$L of working reagent, which includes N-acetylneuraminic acid aldolase, pyruvate oxidase, hydrogen peroxide, colored indicator, and a buffer. The microplate was incubated at room temperature for 60 minutes. The colour intensity of the reaction product at 570 nm is directly proportional to sialic acid concentration in the sample. The TSA concentration was read from standard curve (0; 0.3; 0.6; and 1.0 mM/L stock solution).

2.5. FSA Assay.

FSA was determined using the thiobarbituric method of Skoza and Mohos [9]. Each determination in a single sample was performed three times. All reagents were from Sigma-Aldrich Chemie GmbH. Briefly, to $100\,\mu$L

of serum was added $250\,\mu$L of periodic reagent (0.025 N periodic acid in 0.125 N sulfuric acid) and then it was mixed and incubated for 30 minutes at 37°C. The incubation was stopped by adding $200\,\mu$L of the sodium arsenite (2% sodium arsenite in 0.22 M hydrochloric acid). After disappearance of yellow color derived from the released iodine, the 1.5 mL of thiobarbituric acid (0.1 M, pH 9.0) was added to a reaction mixture. Next, tubes were placed in boiling water for 7.5 minutes. Immediately after that, the tubes were transferred to an ice bath and left for 10 minutes. To each tube 1.5 mL of sulfoxide dimethyl was added. Measurements were performed at 549 nm using quartz cuvettes on the spectrophotometer Shimadzu UV-1202 (Shimadzu Europa GmbH, Duisburg, Germany). The amount of FSA was calculated from the following equation:

$$
\begin{aligned}
\mu\text{mol of FSA} &= V \times \frac{\text{OD}_{549}}{68} \\
&= 3.55 \times \frac{\text{OD}_{549}}{68} = 0.0522 \times \text{OD}_{549},
\end{aligned}
\tag{1}
$$

where V is the final volume of the solution and OD_{549} is the optical density at 549 nm [10].

2.6. Other Laboratory Assays.

For characteristics of patients the following tests were performed: alanine aminotransferase (ALT), aspartate aminotransferase (AST), gamma glutamyltransferase (GGT), carbohydrate-deficient transferrin (CDT), prothrombin time (PT), and mean corpuscular volume (MCV). Almost all of biochemical tests (ALT, AST, and GGT) were done on the Architect c8000 system (Abbott Laboratories, Abbott Park, IL, USA) using the kits from Abbott Diagnostics (Wiesbaden, Germany). The CDT values were assayed by immunonephelometry using N-Latex CDT test (Siemens Healthcare Diagnostics, Marburg, Germany) on BN II System (Siemens Healthcare Diagnostics, USA). MCV was measured using a hematological analyzer ADVIA 120 (Bayer, Tarrytown, USA) and prothrombin time on the STA Compact Hemostasis Analyzer (Diagnostica Stago, France).

2.7. Statistical Analysis.

Significance of differences between groups (tested and control) was evaluated by Mann-Whitney U test. To test the hypothesis about differences in concentration of TSA and FSA in liver diseases of different etiology, ANOVA rank Kruskal-Wallis test was performed. Because the chance of finding one or more significant differences in 12 tested groups was 45.96% (Bonferroni correction factor), we performed the nonparametric multiple comparison test (post hoc test for Kruskal-Wallis) to ascertain which of the intermediate medians are significantly different. $P < 0.05$ was considered statistically significant.

3. Results

Table 1 presents laboratory tests performed for characteristics of patients with liver diseases. In most of liver diseases the mean values of MCV, PT, AST, ALT, and GGT were significantly higher than those in the control group. There were no

TABLE 1: The laboratory characteristics of patients with liver diseases and controls.

	MCV (fL)	PT (sec)	ALT (IU/L)	AST (IU/L)	GGT (IU/L)	CDT (mg/L)
C	88 80.2–94	12.45 11.7–13.8	16.5 8–39	23 14–39	21.5 8–46	43.3 26.8–61
FL	89.3 82–99	10.85* 10.2–15.6	75.5* 20–337	43* 29–136	63* 34–171	—
AC	98.2* 78–118.2	15* 7.2–31.7	32* 8–435	82* 23–1574	206* 12–2126	37.9 20.4–75.9
NAC	92* 61.1–108	14.45* 10.3–27.6	29.5* 6–115	46 13–146	58* 12–327	38.75 21.8–57.6
PBC	94* 86–105.8	14.2 9.9–20.3	31* 15–493	73* 35–245	142* 6–336	43.8 23.7–58.4
TH	99.1* 80.3–120	14.7 11–31.4	50* 7–302	60* 23–382	216* 9–4050	44.3 21.8–82.4
CH	89.6 77–97.7	12 9.8–17	72* 12–925	52* 16–674	44* 5–105	41.9 29.5–72.3
HCV	89.5* 85–102.1	12.2 10.1–15.5	60* 19–551	48* 19–236	75* 3–898	48.7 27.9–77.8
HBV	94.8* 84.9–97.4	13.1 11–14.5	62* 28–412	52* 27–378	53* 9–221	37.2 20.4–51.9
AIH	92* 87–94	13.2 9.7–20.6	141* 63–916	160* 58–460	232* 111–561	50.5 27–70.73
HCC	90.9 76–104.4	12.65 11–16.6	43* 6–194	84* 30–304	182* 81–1175	39.7 24.4–102
HCC + C	96.8* 85–98	17.6* 12.4–20	20.5 6–119	79* 35–195	141* 53–554	46 25–76.6
AHB	86.6 78.3–90	13.8 11.8–14.5	831.5* 726–1774	680.5* 125–1972	231* 168–453	—

Data are median and ranges. MCV: mean corpuscular volume, PT: prothrombin time, ALT: alanine aminotransferase, AST: aspartate aminotransferase, GGT: gamma glutamyltransferase, CDT: carbohydrate-deficient transferrin, C: controls, FL: fatty liver, AC: alcoholic cirrhosis, NAC: nonalcoholic cirrhosis, PBC: primary biliary cirrhosis, TH: toxic hepatitis, CH: chronic nonviral hepatitis, HCV: chronic viral hepatitis C, HBV: chronic viral hepatitis B, AIH: autoimmune hepatitis, HCC: primary liver cancer, HCC + C: primary liver cancer and cirrhosis, and AHB: acute hepatitis B.
*Significant differences in comparison to the control group.

significant differences in the serum values of CDT between liver diseases and control group.

There were no significant differences in the serum TSA concentration between liver diseases of different etiologies ($P = 0.143$; ANOVA rank Kruskal-Wallis), but in most of the liver diseases the mean TSA levels were significantly different than in the control group. Further analysis revealed that the mean TSA concentration in nonalcoholic cirrhosis (NAC), primary biliary cirrhosis (PBC), chronic nonviral hepatitis (CH), chronic viral hepatitis C (HCV) and B (HBV), primary liver cancer and cirrhosis (HCC + C), and acute hepatitis B (AHB) was significantly decreased when compared with the control group ($P < 0.001$; $P = 0.044$; $P < 0.001$; $P = 0.020$; $P = 0.024$; $P < 0.001$; $P < 0.001$, resp.) (Figure 1(a)).

The mean serum concentration of FSA appears to be different between liver diseases of different etiologies ($P = 0.015$; ANOVA rank Kruskal-Wallis test). Post hoc analysis for Kruskal-Wallis test indicated that the mean value of FSA for the toxic hepatitis (TH) was significantly higher than the mean value for nonalcoholic cirrhosis (NAC) ($P = 0.022$). The serum concentration of FSA in patients with toxic hepatitis (TH) and in patients with alcoholic cirrhosis (AC)

was significantly increased when compared to the control group ($P < 0.001$; $P = 0.010$, resp.) (Figure 1(b)).

4. Discussion

In our study we have measured the serum concentrations of TSA and FSA in liver diseases. Generally, we detected decreased levels of TSA in hepatitis of different etiology, cirrhosis, and liver cancer. Our results are similar to the results of Matsuzaki and coworkers which indicated that the serum level of TSA in patients with compensated cirrhosis was significantly lower than that in the control group and it was decreased further in those with decompensated cirrhosis [11]. The level of TSA in chronic hepatitis appeared to be similar to the level in the control group [11]. Though there were differences in TSA concentration in comparison to the controls, we did not find differences between liver diseases.

Interestingly, we did not observe the changes in TSA concentrations in patients with alcoholic cirrhosis. In our opinion, this fact may be the result of two opposing mechanisms. At first, the cirrhosis (nonalcoholic) causes the decrease of TSA concentration; secondly, alcohol abuse causes the

(a)

(b)
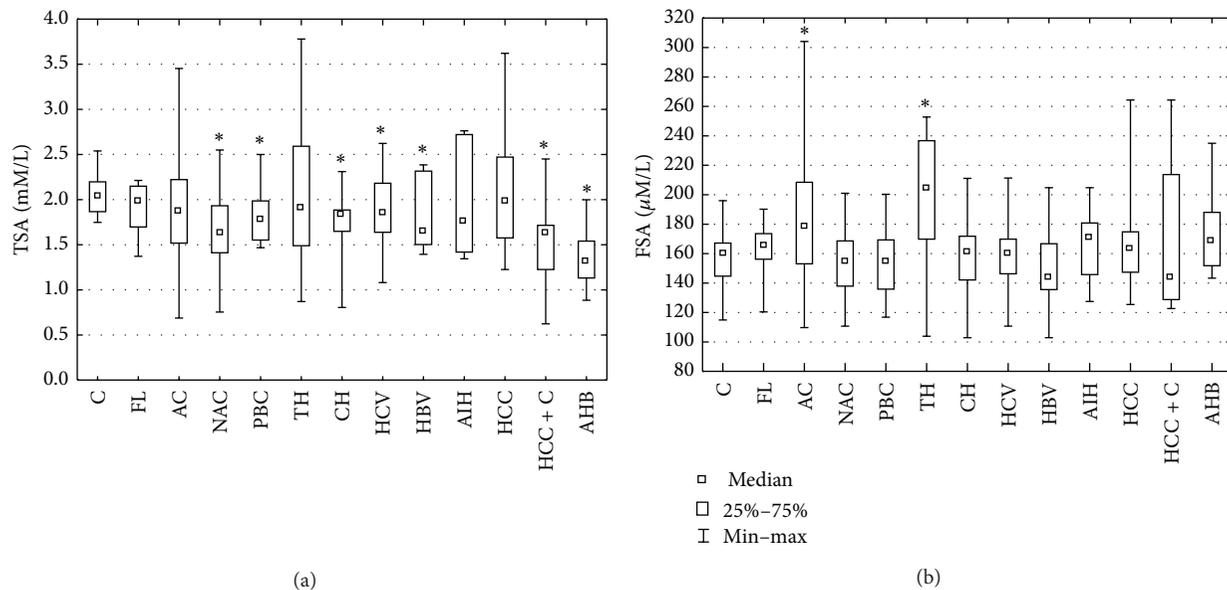
FIGURE 1: TSA (a) and FSA (b) concentrations in the sera of patients with liver diseases of different etiology. Results are presented as median and range. *Significant difference in comparison to controls. C: controls, FL: fatty liver, AC: alcoholic cirrhosis, NAC: nonalcoholic cirrhosis, PBC: primary biliary cirrhosis, TH: toxic hepatitis, CH: chronic nonviral hepatitis, HCV: chronic viral hepatitis C, HBV: chronic viral hepatitis B, AIH: autoimmune hepatitis, HCC: primary liver cancer, HCC + C: primary liver cancer and cirrhosis, and AHB: acute hepatitis B.

increase of TSA level [12–14]. The proof for the first argument may be the study of Stefenelli et al. who showed significantly lower TSA values in chronic liver diseases (among other cirrhoses) in comparison to malignant and noninflammatory diseases [15]. Matsuzaki et al. also point out that serum TSA concentrations in patients with compensated cirrhosis were significantly lower than in the control subjects and were decreased further in patients with decompensation [11]. In contrast, Arif and coworkers reported higher level of SA in advanced and terminal stages of disease but normal level in early ones [5]. They suggested that these results are related to aberration in carbohydrate structure of fibrinogen, which contains 0.6% of sialic acid, because both, fibrinogen and sialic acid, are the acute-phase reactants. These data confirmed that the unchanged concentration of total sialic acid in alcohol cirrhosis is the result of two factors: liver damage by cirrhosis and alcohol.

Similarly to the patients with nonalcoholic cirrhosis the total sialic concentration was also significantly decreased in patients suffering from liver cancer accompanied by cirrhosis in comparison to the control group. However, in patients with liver cancers without cirrhosis the TSA concentrations were slightly decreased, near normal. This can be explained by intensity of glycosylation disturbances during malignant diseases. There are many reports certifying the changes of sialic acid concentration in the course of malignant transformation [16, 17]. Besides, Stefenelli et al. confirmed that cases with extensive liver cirrhosis are characterised by continuous decline in the serum sialic acid level, especially in very severe cases with complications [15].

In our study we have also shown that FSA concentrations were significantly higher in toxic hepatitis than in

nonalcoholic cirrhosis. This difference can be explained by the pathogenesis of toxic hepatitis due to excessive consumption of alcohol in about 70% of patients. We suggest that differences in FSA concentration between these diseases are the result of aberrant glycosylation in alcohol abusers. Additional confirmation of this hypothesis is the comparisons of FSA concentrations in patients with alcoholic and nonalcoholic cirrhosis. The concentration of FSA in alcoholic cirrhosis was significantly higher than in controls while in nonalcoholic cirrhosis the FSA level was the same as in the control group. Therefore, in the current literature there are reports showing the aberrations of glycosylations in liver diseases, but the exact mechanisms of these changes in each liver disease are not known or they are not clearly explained. In our study we tried to explain these mechanisms by the measurements of total and free serum sialic acid concentrations. Also, in the present literature there is no information about behavior of the FSA concentrations in nonalcoholic liver disease or whether there are differences in relation to alcoholic liver disease. We suggest that the FSA serum concentration can be useful in the differential diagnosis of liver diseases, especially between toxic hepatitis and nonalcoholic cirrhosis. The causes of the changes in FSA concentration may be the alterations in glycosylation of glycoproteins in the liver diseases. These can rely on the increased desialylation, fucosylation, and branching and increased amounts of bisecting N-acetylglucosamine (GlcNAc) [6]. These changes may be explained by the alterations in the activity of enzymes, especially glycosyltransferases. These alterations occur in all liver diseases but with different intensities. The most important alterations observed in alcoholic liver

disease are desialylation of transferrin and also haptoglobin, alpha 1-antitrypsin, and ceruloplasmin [6, 18]. In fatty liver diseases there is accumulation of apolipoprotein-B with increased amounts of bisecting GlcNAc and the increased accumulation of apolipoprotein A-1. In viral liver diseases there is increase in the fucosylation of alpha 1-antitrypsin, alpha 1-acid glycoprotein, and haptoglobin [6]. In liver cancer the majority of aberrations are the changes in the activity of N-acetylglucosaminyltransferase III (GnT-III) and N-acetylglucosaminyltransferase V (GnT-V), which respond to formation of branching and addition of bisecting GlcNAc [6].

In our previous study, we have described TSA and FSA in alcoholic and nonalcoholic cirrhosis and chronic viral hepatitis [19]. In the present study, we extended these subgroups and added other liver diseases, in particular, toxic hepatitis, liver cancers, and acute liver disease. This comparison more clearly revealed that the levels of TSA do not change between liver diseases, although almost in all cases they were lower than in healthy people. In the previous study TSA was diminished only in nonalcoholic cirrhosis [19]. However, the concentration of FSA was different not only between cirrhosis and chronic hepatitis but also between cirrhosis and toxic hepatitis. This suggests that in the course of most of the liver diseases the sialylation of proteins plays a significant role.

5. Conclusions

We suggest that the changes in the concentration of TSA and FSA in some liver diseases confirm the presence of significant aberrations in the sialylation of serum glycoproteins in these diseases.

Conflict of Interests

The authors declare that there is no conflict of interests regarding the publication of this paper.

References

[1] R. Schauer and J. P. Kamerling, "Chemistry and biochemistry of sialic acids," in *Glycoproteins II*, J. Montreuil, J. F. G. Vliegenthart, and H. Schacter, Eds., pp. 243–402, Elsevier, Amsterdam, The Netherlands, 1997.

[2] R. Schauer, S. Kelm, G. Reuter et al., "Biochemistry and role of sialic acid," in *Biology of the Sialic Acid*, A. Rosenberg, Ed., pp. 7–47, Plenum Press, New York, NY, USA, 1995.

[3] H. Lis and N. Sharon, "Protein glycosylation: structural and functional aspects," *European Journal of Biochemistry*, vol. 218, no. 1, pp. 1–27, 1993.

[4] P. Sillanaukee, M. Pönniö, and I. P. Jääskeläinen, "Occurrence of sialic acids in healthy humans and different disorders," *European Journal of Clinical Investigation*, vol. 29, no. 5, pp. 413–425, 1999.

[5] S. Arif, N.-U. Haq, R. Hanif, A. S. Khan, J.-U. Rehman, and T. A. Mufti, "Variations of serum sialic acid level in liver cirrhosis," *Journal of Ayub Medical College Abbottabad*, vol. 17, no. 3, pp. 54–57, 2005.

[6] B. Blomme, C. van Steenkiste, N. Callewaert, and H. van Vlierberghe, "Alteration of protein glycosylation in liver diseases," *Journal of Hepatology*, vol. 50, no. 3, pp. 592–603, 2009.

[7] C. Traving and R. Schauer, "Structure, function and metabolism of sialic acids," *Cellular and Molecular Life Sciences*, vol. 54, no. 12, pp. 1330–1349, 1998.

[8] L. Chrostek, B. Cylwik, W. Korcz et al., "Serum free sialic acid as a marker of alcohol abuse," *Alcoholism: Clinical and Experimental Research*, vol. 31, no. 6, pp. 996–1001, 2007.

[9] L. Skoza and S. Mohos, "Stable thiobarbituric acid chromophore with dimethyl sulphoxide. Application to sialic acid assay in analytical de O acetylation," *Biochemical Journal*, vol. 159, no. 3, pp. 457–462, 1976.

[10] L. Warren, "The thiobarbituric acid assay of sialic acids," *The Journal of biological chemistry*, vol. 234, no. 8, pp. 1971–1975, 1959.

[11] S. Matsuzaki, M. Itakura, K. Iwamura, and H. Kamiguchi, "Serum sialic acid levels in liver cirrhosis and liver cancer," *The Japanese Journal of Gastroenterology*, vol. 78, no. 12, pp. 2395–2401, 1981.

[12] M. Pönniö, H. Alho, P. Heinälä, S. T. Nikkari, and P. Sillanaukee, "Serum and saliva levels of sialic acid are elevated in alcoholics," *Alcoholism: Clinical and Experimental Research*, vol. 23, no. 6, pp. 1060–1064, 1999.

[13] J. Romppanen, K. Punnonen, P. Anttila, T. Jakobsson, J. Blake, and O. Niemelä, "Serum sialic acid as a marker of alcohol consumption: effect of liver disease and heavy drinking," *Alcoholism: Clinical and Experimental Research*, vol. 26, no. 8, pp. 1234–1238, 2002.

[14] P. Sillanaukee, M. Pönniö, and K. Seppä, "Sialic acid: new potential marker of alcohol abuse," *Alcoholism: Clinical and Experimental Research*, vol. 23, no. 6, pp. 1039–1043, 1999.

[15] N. Stefenelli, H. Klotz, A. Engel, and P. Bauer, "Serum sialic acid in malignant tumors, bacterial infections, and chronic liver diseases," *Journal of Cancer Research and Clinical Oncology*, vol. 109, no. 1, pp. 55–59, 1985.

[16] A. Lagana, B. Pardo-Martinez, A. Marino, G. Fago, and M. Bizzarri, "Determination of serum total lipid and free N-acetylneuraminic acid in genitourinary malignancies by fluorimetric high performance liquid chromatography. Relevance of free N-acetylneuraminic acid as tumour marker," *Clinica Chimica Acta*, vol. 243, no. 2, pp. 165–179, 1995.

[17] E. W. Mabry and R. Carubelli, "Sialic acid in human cancer," *Experientia*, vol. 28, no. 2, pp. 182–183, 1972.

[18] M. Tsutsumi, J.-S. Wang, and A. Takada, "Microheterogeneity of serum glycoproteins in alcoholics: is desialo-transferrin the marker of chronic alcohol drinking or alcoholic liver injury?" *Alcoholism: Clinical and Experimental Research*, vol. 18, no. 2, pp. 392–397, 1994.

[19] B. Cylwik, L. Chrostek, A. Panasiuk, and M. Szmitkowski, "Serum total and free sialic acid in patients with chronic liver disease," *Clinical Chemistry and Laboratory Medicine*, vol. 48, no. 1, pp. 137–139, 2010.

Research Article

Relationship between Serum Total Cholesterol Level and Serum Biochemical Bone Turnover Markers in Healthy Pre- and Postmenopausal Women

Tae-Dong Jeong,[1] Woochang Lee,[1] Sung-Eun Choi,[1] Jae Seung Kim,[2] Hong-Kyu Kim,[3] Sung Jin Bae,[3] Sail Chun,[1] and Won-Ki Min[1]

[1] *Department of Laboratory Medicine, University of Ulsan College of Medicine and Asan Medical Center, 88 Olympic-ro 43-gil, Songpa-gu, Seoul 138-736, Republic of Korea*

[2] *Department of Nuclear Medicine, University of Ulsan College of Medicine and Asan Medical Center, 88 Olympic-ro 43-gil, Songpa-gu, Seoul 138-736, Republic of Korea*

[3] *The Health Screening and Promotion Center, University of Ulsan College of Medicine and Asan Medical Center, 88 Olympic-ro 43-gil, Songpa-gu, Seoul 138-736, Republic of Korea*

Correspondence should be addressed to Woochang Lee; wlee1@amc.seoul.kr

Background. The presence of common risk factors suggests that there is a relationship between osteoporosis and cardiovascular disease, possibly via dyslipidemia and inflammation. We investigated the relationships among the lipid profile, the inflammation marker high-sensitivity C-reactive protein (hsCRP), bone turnover markers, and bone mineral density (BMD) to assess the correlation between osteoporosis and cardiovascular disease and identify factors predicting osteoporosis. *Methods.* The study included 759 Korean women older than 20 years of age. The BMD, serum lipid profile, and levels of hsCRP, cross-linked C-terminal peptide (CTX), and osteocalcin were measured. We compared the serum biomarkers between groups with normal and low BMD and assessed the correlations between the levels of bone turnover markers and the lipid profile and hsCRP level. *Results.* The concentrations of CTX, osteocalcin, and total cholesterol were significantly higher in the low BMD group than in the normal BMD group in premenopausal women group. However, hsCRP was not correlated with these parameters. Multivariate logistic regression analysis revealed that TC (OR, 1.647; 95% CI, 1.190–2.279) and osteocalcin (OR, 1.044; 95% CI, 1.002–1.088) had an increased risk of low BMD in premenopausal women. *Conclusions.* These results indicate that total cholesterol concentration is correlated with the levels of bone turnover markers, suggesting that it might predict osteoporosis in premenopausal women.

1. Introduction

Osteoporosis and cardiovascular disease cause increased morbidity and mortality in elderly females. Several epidemiological studies have demonstrated that these two conditions are closely related [1–3], suggesting a possible link in the pathogenesis of osteoporosis and cardiovascular disease. The most plausible concept is that a common underlying mechanism triggers both osteoporosis and cardiovascular disease by affecting bone and blood vessels simultaneously. The most likely contributing factor is lipid levels.

A high total cholesterol (TC) concentration is related to the risk of cardiovascular disease. Lipid levels are also used to assess the risk of coronary heart disease, as cutoffs indicating that the commencement of treatment is appropriate and as goals in patient outcomes [4, 5]. In addition, high level of high-density lipoprotein (HDL) cholesterol is a protective factor for coronary heart disease, while an increased triglyceride level is an important component of metabolic syndrome [5]. It has been well documented that the atherogenic lipid profile is considered a key indicator reflecting the risk of cardiovascular disease [4, 5].

A possible association between lipid profile and osteoporosis has also been investigated. Some researchers have demonstrated that an atherogenic lipid profile is associated with a lower bone mineral density (BMD) [6–9]. However, other reports have found no relationship between the lipid profile and the BMD [10, 11].

Apart from the lipid levels, a possible role for inflammation has also been suggested in both conditions. Increased level of high-sensitivity C-reactive protein (hsCRP) is tightly correlated with an increased incidence of coronary heart disease in healthy individuals [12, 13]. Meanwhile, it has been reported that the relationship between hsCRP and osteoporosis suggests that a high hsCRP level is associated with low BMD [14].

In this study, we aim to investigate the association among lipid profiles, hsCRP, and bone turnover markers (BTMs) in healthy pre- and postmenopausal women to identify possible biomarkers that might predict osteoporosis.

2. Materials and Methods

2.1. Subjects. The study population consisted of 759 Korean women older than 20 years of age who visited the Health Promotion Center of Asan Medical Center, Seoul, Korea, from January 2006 to December 2008, and in whom BMD and serum BTMs were measured. A self-administered questionnaire explored their medical, medication, and behavioral history. The height and weight of each subject were measured, while the subjects were dressed in light clothing without shoes, and the body mass index (BMI, kg/m^2) was calculated. Following an overnight fasting, venous blood was drawn from each subject for laboratory tests. Women were excluded if they had undergone a hysterectomy or if they had taken drugs such as HMG-CoA reductase, estrogen, or bisphosphonate, which could affect lipid levels and BMD.

2.2. Biochemical Measurements. The concentrations of TC, calcium, alkaline phosphatase, phosphorus, triglyceride, and HDL cholesterol were measured by colorimetric methods using a Toshiba 200FR automated analyzer (Toshiba Medical Systems, Tokyo, Japan). The serum hsCRP concentration was determined using the CRP immunoturbidimetric method (Roche Diagnostics, Basel, Switzerland) on a COBAS Integra 800 analyzer (Roche Diagnostics). The serum concentrations of CTX and osteocalcin were measured using a chemiluminescence immunoassay (Roche Diagnostics) on an Elecsys 2010 automated analyzer (Roche Diagnostics).

2.3. BMD Measurements. The BMD (g/cm^2) was measured at the nondominant femoral neck and the anterior-posterior lumbar spine (L1–L4) using dual energy X-ray absorptiometry (Prodigy Advance with ver. 11.4 software; GE Lunar, Madison, WI, USA). The *in vivo* precision of the machine was 0.60% for the femoral neck and 0.66% for the lumbar spine. Each T-score was calculated using inbuilt software, and a mean ± SD of BMD was established with reference to data for healthy young women from northeastern Asia. According to the World Health Organization (WHO) definitions, osteopenia was diagnosed in the range (−2.5 SD < T-score <

−1.0 SD) and osteoporosis was considered present when the T-score was ≤−2.5 SD at any site.

2.4. Statistical Analysis. The measurements for pre- and postmenopausal women were compared using Student's *t*-test, except for hsCRP level, which had a positively skewed distribution. The values of this parameter were compared using the Mann-Whitney *U*-test, and the data were logarithmically transformed for use in further analyses. The concentrations of biochemical markers and BTMs were compared between two groups with different BMD statuses (normal and low BMD) using Student's *t*-test. Univariate logistic regression analyses were performed and a backward stepwise multiple logistic regression analysis considering all variables was then conducted to assess the independent association of the BMD with other independent variables. Odds ratios (OR) and 95% confidence interval (CI) were calculated. All statistical analyses were performed using SPSS ver. 19 (SPSS, Chicago, IL, USA). *P* values < 0.05 were considered statistically significant.

3. Results

3.1. Baseline Characteristics. The characteristics of the study subjects were summarized in Table 1. The mean ages of the pre- and postmenopausal women were 43.6 ± 6.3 and 57.5 ± 6.7 years, respectively. All of the following were significantly higher in postmenopausal women: BMI, hsCRP, calcium, alkaline phosphatase, phosphorus, CTX, osteocalcin, TC, and triglyceride.

3.2. BTMs and Biochemical Markers by BMD Status. We categorized subjects based on BMD status (using the WHO definition) into three groups: normal, with osteopenia, and with osteoporosis. Among the 759 studied subjects, 425 women were normal, 287 had osteopenia, and 47 had osteoporosis. Owing to the small number of subjects with osteoporosis, we combined the osteopenia and osteoporosis groups into the "low BMD" group to give a total of 334 subjects and compared the marker levels between normal and low BMD groups. The CTX and osteocalcin levels were significantly higher in low BMD group than that of normal group (both *P* < 0.001; Figure 1), as were TC and hsCRP (both *P* < 0.05; Figure 1), whereas triglycerides and HDL cholesterol did not differ significantly between these two groups.

In a stratified analysis by menopausal status, both CTX and osteocalcin levels showed similar results (Figure 2). However, no statistical significance was found on hsCRP between normal and low BMD groups (Figure 2).

3.3. Stepwise Multivariate Logistic Regression Analysis. Multivariate logistic regression analysis revealed that the BMI (OR, 0.817; 95% CI, 0.756–0.884), TC (OR, 1.647; 95% CI, 1.190–2.279), and osteocalcin (OR, 1.044; 95% CI, 1.002–1.088) had an increased risk of low BMD in premenopausal women (Table 2). On the other hand, the age (OR, 1.094; 95% CI, 1.064–1.126), BMI (OR, 0.882; 95% CI, 0.826–0.942), and TC (OR, 0.649; 95% CI, 0.521–0.809) were statistically significant in postmenopausal women (Table 2).

TABLE 1: Clinical characteristics of the subjects based on menopausal status.

Variable	Premenopausal ($n = 319$)	Postmenopausal ($n = 440$)	P value
Age (years)	43.6 ± 6.3	57.5 ± 6.7	<0.001
Height (cm)	159.3 ± 5.4	156.2 ± 5.2	<0.001
Weight (kg)	56.0 ± 8.0	56.8 ± 7.3	NS
BMI (kg/m^2)	22.1 ± 2.9	23.3 ± 2.9	<0.001
Spine T-score	0.17 ± 1.18	-0.93 ± 1.27	<0.001
Femur T-score	-0.02 ± 0.92	-0.68 ± 0.94	<0.001
Calcium (mmol/L)	2.26 ± 0.09	2.31 ± 0.08	<0.001
ALP (U/L)	50.1 ± 14.1	66.6 ± 21.8	<0.001
Phosphorus (mmol/L)	1.16 ± 0.16	1.24 ± 0.17	<0.001
Total cholesterol (mmol/L)	4.75 ± 0.78	5.15 ± 0.81	<0.001
Triglycerides (mmol/L)	1.03 ± 0.52	1.19 ± 0.59	<0.001
HDL-C (mmol/L)	1.64 ± 0.40	1.58 ± 0.38	<0.05
hsCRP (mg/L) (median and interquartile range)	0.39 (0.26–0.73)	0.59 (0.36–1.21)	<0.001[*]
CTX (μg/L)	309 ± 172	546 ± 265	<0.001
Osteocalcin (μg/L)	15.40 ± 6.00	21.69 ± 8.58	<0.001

ALP: alkaline phosphatase; BMI: body mass index; CTX: cross-linked C-terminal telopeptide; HDL-C: high density lipoprotein cholesterol; NS: not significant; TC: total cholesterol. Values are expressed as means ± standard deviations if not otherwise specified. [*]Analyzed using the Mann-Whitney U-test.

TABLE 2: Stepwise multiple logistic regression analysis to assess the association between bone mineral density as a dependent variable and other covariables based on menopausal status.

Variable	Odds ratio	95% confidential interval	P value
Premenopause			
BMI	0.817	0.756–0.884	0.001
TC	1.647	1.190–2.279	<0.05
Osteocalcin	1.044	1.002–1.088	<0.05
Postmenopause			
Age	1.094	1.064–1.126	<0.001
BMI	0.882	0.826–0.942	<0.001
TC	0.649	0.521–0.809	<0.001
CTX	1.001	1.000–1.002	<0.05

Analyzed independent variables: age, BMI, TC, hsCRP, CTX, and osteocalcin.
See Table 1.

4. Discussion

We found that the TC levels were significantly higher in the low BMD group compared to the normal BMD group in premenopausal women and were also positively correlated with the serum concentrations of CTX and osteocalcin. These results suggest that the pathogenesis of osteoporosis is related to cholesterol metabolism. An atherogenic lipid profile is thought to be associated with osteoporosis. It has been speculated that oxidized lipid is the common trigger of atherosclerosis and osteoporosis. Oxidized lipid stimulates atherosclerosis by promoting mineralization of the arterial wall and can cause osteoporosis by reducing bone mineralization and inhibiting osteoblast differentiation [15]. Our findings do support the previous research in premenopausal group. With our results, on the other hand, higher serum TC levels are associated with higher BMD in postmenopausal women. This result is quite opposite compared to the data of premenopausal group in our study; however, this finding is consistent with the previous study although its pathophysiology is still unclear [9].

Hormone-replacement therapy prevents cardiovascular disease by reducing the level of low-density lipoprotein (LDL) cholesterol and inhibits osteoporosis in postmenopausal women [16]. The use of statins is associated with an increase in BMD and a reduction in fracture risk, indicating that statins have anabolic effects on bone metabolism [17–20]. These findings provide further evidence of the relationship between lipid levels and osteoporosis.

The importance of other lipid markers and the levels of HDL cholesterol and triglyceride, with respect to BMD, has been debated [6, 9, 11, 21]. Here, we show that none of these parameters were correlated with biochemical markers of bone turnover and no differences in levels were noted between the two BMD groups, indicating that the serum levels of HDL cholesterol and triglyceride may not be directly related to bone metabolism.

Biochemical BTMs offer a dynamic measure of bone metabolism. BTMs arereleased into the circulation during bone formation or resorption and respond more rapidly and profoundly to changes in bone turnover than the BMD. In addition, BTMs are easily measured in the blood or urine and are increasingly assessed in clinical settings. Both osteocalcin and CTX are well documented, sensitive, and specific biomarkers for bone metabolism [22]. In particular,

(a)

(b)

(c)

(d)
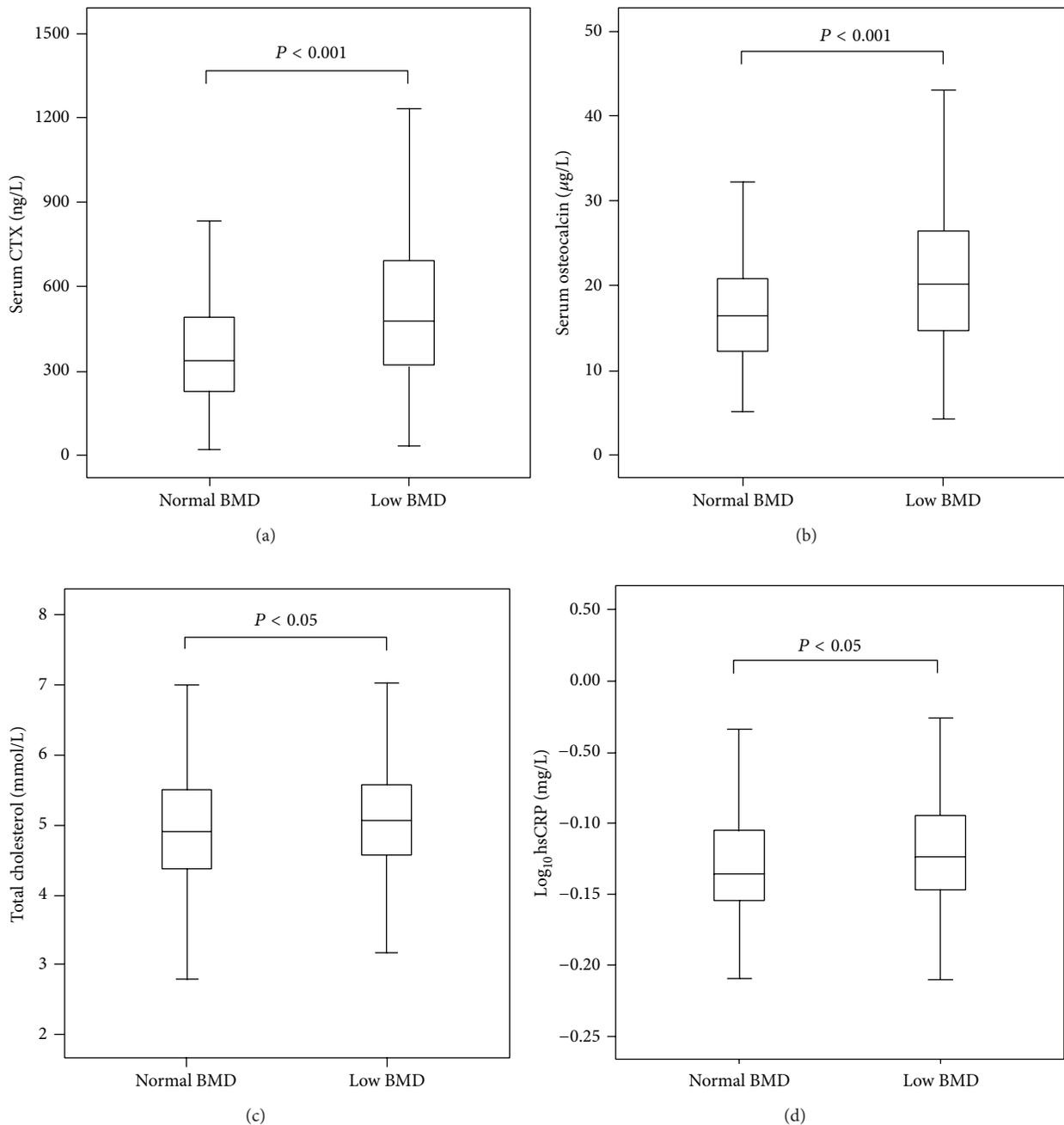
FIGURE 1: Serum CTX (a) osteocalcin, (b) total cholesterol, (c) log$_{10}$hsCRP, and (d) concentrations in normal and low BMD subjects. The low BMD group was defined as those with osteopenia or osteoporosis as defined by the WHO classification. There were significant differences in the serum CTX ($P < 0.001$), osteocalcin ($P < 0.001$), and log$_{10}$hsCRP ($P < 0.05$) levels between normal and low BMD groups. CTX, cross-linked C-terminal telopeptide; hsCRP, high sensitivity C-reactive protein.

osteocalcin has several and complex biological functions. Osteocalcin plays a role in the regulation of bone mineralization and also regulates osteoblast and osteoclast activity [23]. In addition, osteocalcin was known to be related to energy metabolism [24].

The hsCRP concentration showed no correlations with BTM levels. hsCRP is the most sensitive marker for detecting subclinical inflammation, so this finding is inconsistent with

the previous report [25]. Despite the absence of any perceived correlation, we cannot exclude a possible relationship between inflammation and osteoporosis. Several groups have provided evidence of a relationship between inflammation and osteoporosis. The incidence of osteoporosis is increased in individuals with inflammatory diseases [26–31]. It is possible that although hsCRP is a sensitive marker of inflammation, the dynamic hsCRP range in healthy individuals is

(a)

(b)

(c)

(d)

Premenopause
Postmenopause

Premenopause
Postmenopause
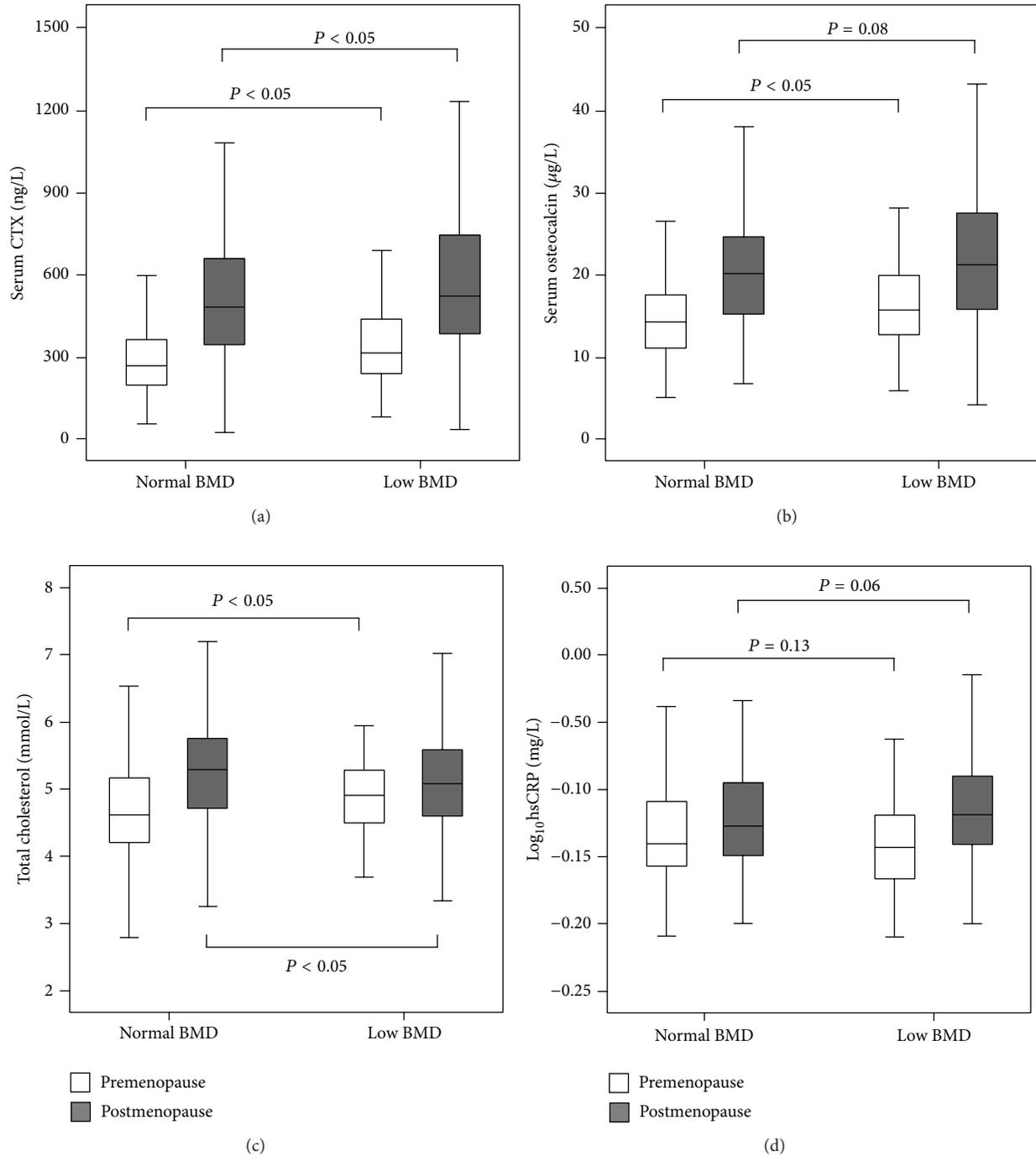
FIGURE 2: Serum CTX (a) osteocalcin, (b) total cholesterol, (c) $\log_{10}$hsCRP, and (d) concentrations in normal and low BMD subjects based on menopausal status. The low BMD group was defined as those with osteopenia or osteoporosis as defined by the WHO classification. CTX, cross-linked C-terminal telopeptide; hsCRP, high sensitivity C-reactive protein.

too narrow to reflect changes in bone turnover. Therefore, despite a possible relationship between inflammation and osteoporosis, the hsCRP level might not be a useful marker for investigating bone metabolism or for predicting the development of osteoporosis.

Our study has several limitations. This is a cross-sectional analysis with no prospective follow-up of patients. And

we have no information on the incidence of fracture and the ultimate clinical endpoint of osteoporosis. More well-controlled prospective studies would be needed to elucidate the relationship between candidate serum markers and the risk of osteoporosis.

In conclusion, our results indicate that a high TC level is associated with low BMD and atherosclerosis, suggesting

that dyslipidemia is the common mechanism triggering osteoporosis and atherosclerosis in premenopausal women. However, the changes in the level of the inflammation marker hsCRP were not sufficiently prominent to be useful as a predictor of osteoporosis, despite the suggested association of inflammation with osteoporosis.

Conflict of Interests

The authors declare that there is no conflict of interests regarding the publication of this paper.

References

[1] G. N. Farhat, A. B. Newman, K. Sutton-Tyrrell et al., "The association of bone mineral density measures with incident cardiovascular disease in older adults," *Osteoporosis International*, vol. 18, no. 7, pp. 999–1008, 2007.

[2] J. R. Shaffer, C. M. Kammerer, D. L. Rainwater et al., "Decreased bone mineral density is correlated with increased subclinical atherosclerosis in older, but not younger, Mexican American women and men: the San Antonio family osteoporosis Study," *Calcified Tissue International*, vol. 81, no. 6, pp. 430–441, 2007.

[3] L. B. Tanko, C. Christiansen, D. A. Cox, M. J. Geiger, M. A. McNabb, and S. R. Cummings, "Relationship between osteoporosis and cardiovascular disease in postmenopausal women," *Journal of Bone and Mineral Research*, vol. 20, no. 11, pp. 1912–1920, 2005.

[4] Anonymous, "Executive summary of the third report of the National Cholesterol Education Program (NCEP) expert panel on detection, evaluation, and treatment of high blood cholesterol in adults (adult treatment panel III)," *Journal of the American Medical Association*, vol. 285, no. 19, pp. 2486–2497, 2001.

[5] Anonymous, "Third report of the National Cholesterol Education Program (NCEP) expert panel on detection, evaluation, and treatment of high blood cholesterol in adults (adult treatment panel III) final report," *Circulation*, vol. 106, no. 25, pp. 3143–3421, 2002.

[6] T. Yamaguchi, T. Sugimoto, S. Yano et al., "Plasma lipids and osteoporosis in postmenopausal women," *Endocrine Journal*, vol. 49, no. 2, pp. 211–217, 2002.

[7] S. Lekamwasam, T. Weerarathna, M. Rodrigo, W. K. Arachchi, and D. Munidasa, "Osteoporosis and cardiovascular risk among premenopausal women in Sri Lanka," *Journal of Clinical Densitometry*, vol. 12, no. 2, pp. 245–250, 2009.

[8] P. D. Broulik and J. Kapitola, "Interrelations between body weight, cigarette smoking and spine mineral density in osteoporotic Czech women," *Endocrine Regulations*, vol. 27, no. 2, pp. 57–60, 1993.

[9] R. A. Brownbill and J. Z. Ilich, "Lipid profile and bone paradox: higher serum lipids are associated with higher bone mineral density in postmenopausal women," *Journal of Women's Health*, vol. 15, no. 3, pp. 261–270, 2006.

[10] E. J. Samelson, L. A. Cupples, M. T. Hannan et al., "Long-term effects of serum cholesterol on bone mineral density in women and men: the Framingham Osteoporosis Study," *Bone*, vol. 34, no. 3, pp. 557–561, 2004.

[11] D. H. Solomon, J. Avorn, C. F. Canning, and P. S. Wang, "Lipid levels and bone mineral density," *The American Journal of Medicine*, vol. 118, no. 12, pp. 1414–e5, 2005.

[12] S. S. Bassuk, N. Rifai, and P. M. Ridker, "High-sensitivity C-reactive protein: clinical importance," *Current Problems in Cardiology*, vol. 29, no. 8, pp. 439–493, 2004.

[13] M. A. Albert and P. M. Ridker, "The role of C-reactive protein in cardiovascular disease risk," *Current Cardiology Reports*, vol. 1, no. 2, pp. 99–104, 1999.

[14] J.-M. Koh, Y.-H. Khang, C.-H. Jung et al., "Higher circulating hsCRP levels are associated with lower bone mineral density in healthy pre- and postmenopausal women: evidence for a link between systemic inflammation and osteoporosis," *Osteoporosis International*, vol. 16, no. 10, pp. 1263–1271, 2005.

[15] F. Parhami, A. D. Morrow, J. Balucan et al., "Lipid oxidation products have opposite effects on calcifying vascular cell and bone cell differentiation. A possible explanation for the paradox of arterial calcification in osteoporotic patients," *Arteriosclerosis, Thrombosis, and Vascular Biology*, vol. 17, no. 4, pp. 680–687, 1997.

[16] M. Boschetti, U. Goglia, C. Teti et al., "Replacement therapy and cardiovascular diseases," *Journal of Endocrinological Investigation*, vol. 31, no. 9, pp. 85–90, 2008.

[17] D. H. Solomon, J. S. Finkelstein, P. S. Wang, and J. Avorn, "Statin lipid-lowering drugs and bone mineral density," *Pharmacoepidemiology and Drug Safety*, vol. 14, no. 4, pp. 219–226, 2005.

[18] Q. O. Tang, G. T. Tran, Z. Gamie et al., "Statins: under investigation for increasing bone mineral density and augmenting fracture healing," *Expert Opinion on Investigational Drugs*, vol. 17, no. 10, pp. 1435–1463, 2008.

[19] L. Rejnmark, M. L. Olsen, S. P. Johnsen, P. Vestergaard, H. Sørensen, and L. Mosekilde, "Hip fracture risk in statin users—a population-based Danish case-control study," *Osteoporosis International*, vol. 15, no. 6, pp. 452–458, 2004.

[20] G. Lupattelli, A. M. Scarponi, G. Vaudo et al., "Simvastatin increases bone mineral density in hypercholesterolemic postmenopausal women," *Metabolism: Clinical and Experimental*, vol. 53, no. 6, pp. 744–748, 2004.

[21] P. J. Buizert, N. M. Van Schoor, P. Lips, D. J. H. Deeg, and E. M. Eekhoff, "Lipid levels: a link between cardiovascular disease and osteoporosis?" *Journal of Bone and Mineral Research*, vol. 24, no. 6, pp. 1103–1109, 2009.

[22] R. Eastell and R. A. Hannon, "Biomarkers of bone health and osteoporosis risk," *Proceedings of the Nutrition Society*, vol. 67, no. 2, pp. 157–162, 2008.

[23] A. Neve, A. Corrado, and F. P. Cantatore, "Osteocalcin: skeletal and extra-skeletal effects," *Journal of Cellular Physiology*, vol. 228, no. 6, pp. 1149–1153, 2013.

[24] S. L. Booth, A. Centi, S. R. Smith et al., "The role of osteocalcin in human glucose metabolism: marker or mediator?" *Nature Reviews Endocrinology*, vol. 9, no. 1, pp. 43–55, 2013.

[25] B.-J. Kim, Y. M. Yu, E. N. Kim, Y.-E. Chung, J.-M. Koh, and G. S. Kim, "Relationship between serum hsCRP concentration and biochemical bone turnover markers in healthy pre- and postmenopausal women," *Clinical Endocrinology*, vol. 67, no. 1, pp. 152–158, 2007.

[26] H. P. Bhattoa, P. Bettembuk, A. Balogh, G. Szegedi, and E. Kiss, "Bone mineral density in women with systemic lupus erythematosus," *Clinical Rheumatology*, vol. 21, no. 2, pp. 135–141, 2002.

[27] S. Uaratanawong, U. Deesomchoke, S. Lertmaharit, and S. Uaratanawong, "Bone mineral density in premenopausal women with systemic lupus erythematosus," *Journal of Rheumatology*, vol. 30, no. 11, pp. 2365–2368, 2003.

[28] H. Kroger, R. Honkanen, S. Saarikoski, and E. Alhava, "Decreased axial bone mineral density in perimenopausal women with rheumatoid arthritis: a population based study," *Annals of the Rheumatic Diseases*, vol. 53, no. 1, pp. 18–23, 1994.

[29] J.-B. Jun, K.-B. Joo, M.-Y. Her et al., "Femoral bone mineral density is associated with vertebral fractures in patients with ankylosing spondylitis: a cross-sectional study," *Journal of Rheumatology*, vol. 33, no. 8, pp. 1637–1641, 2006.

[30] T. E. Van Dyke and C. N. Serhan, "Resolution of inflammation: a new paradigm for the pathogenesis of periodontal diseases," *Journal of Dental Research*, vol. 82, no. 2, pp. 82–90, 2003.

[31] M. Paganelli, C. Albanese, O. Borrelli et al., "Inflammation is the main determinant of low bone mineral density in pediatric inflammatory bowel disease," *Inflammatory Bowel Diseases*, vol. 13, no. 4, pp. 416–423, 2007.

Review Article

Platelet Function Tests: A Review of Progresses in Clinical Application

Jae-Lim Choi, Shuhua Li, and Jin-Yeong Han

Department of Laboratory Medicine, Dong-A University College of Medicine, 1,3-Ga, Dongdaesin-dong,
Seo-gu, Busan 602-715, Republic of Korea

Correspondence should be addressed to Jin-Yeong Han; jyhan@dau.ac.kr

The major goal of traditional platelet function tests has been to screen and diagnose patients who present with bleeding problems. However, as the central role of platelets implicated in the etiology of arterial thrombotic diseases such as myocardial infarction and stroke became widely known, platelet function tests are now being promoted to monitor the efficacy of antiplatelet drugs and also to potentially identify patients at increased risk of thrombosis. Beyond hemostasis and thrombosis, an increasing number of studies indicate that platelets play an integral role in intercellular communication, are mediators of inflammation, and have immunomodulatory activity. As new potential biomarkers and technologies arrive at the horizon, platelet functions testing appears to take on a new aspect. This review article discusses currently available clinical application of platelet function tests, placing emphasis on essential characteristics.

1. Introduction

Platelets are small, anucleated cytoplasmic bodies circulating in blood stream. These cellular fragments are derived from megakaryocytes in the bone marrow. In steady state, megakaryocytopoiesis supplies about 10^{11} platelets per day with a new turnover every 8-9 days. This process is influenced by various environmental changes and platelets normally circulate at concentrations of 150–400×10^9/L [1, 2].

Resting platelets appear small discoid cells (2–$4\,\mu$m by $0.5\,\mu$m), facilitating their margination toward the vessel wall, where they can constantly survey the integrity of the vascular endothelium. Platelets contain three major types of granules: α-granules, dense bodies, and lysosomes. α-Granules are the most abundant granules in platelets and are rapidly exocytosed upon activation to enhance hemostasis and inflammation. Dense bodies contain adenine nucleotides (ADP and ATP) and serotonin which induce platelet aggregation, vasoconstriction, cytokine production, and modulators of inflammation. Lysosomes contain glycohydrolases and proteases that can aid in pathogen clearance, breakdown of extracellular matrix, and contribute to the clearance of platelet thrombi and degradation of heparin [1–3].

The normal vascular endothelium produces potent platelet inhibitors such as nitric oxide, prostacyclin, and natural ADPase. Once subendothelial components including collagen, fibronectin, laminin, or von Willebrand factor (vWF) become exposed upon vessel wall injury, platelets undergo a highly regulated series of functional reactions like adhesion, spreading, release reaction, aggregation, procoagulant activity, microparticle formation, and subsequently clot retraction. Adhesion is mediated by the interaction between the glycoprotein (GP) Ib/V/IX receptor complex on the platelet surface to vWF and GP VI and GP Ia to collagen at the sites of vascular injury [3–5].

Multiple pathways bring to platelet activation such as collagen, ADP, thromboxane A2, epinephrine, serotonin, and thrombin. The cumulative action of these activators results in recruitment of platelets from the circulation and several distinct manifestations of platelet activation including platelet shape change, expression of P-selectin, soluble CD40 ligand and platelet procoagulant activity, and conversion of GP

TABLE 1: Major platelet function tests and their clinical applications.

Name of test	Principle	Clinical applications
Platelet aggregometry	Platelet aggregation to a panel of agonists	Diagnosis of inherited and acquired platelet defects
PFA-100/200	High shear platelet adhesion and aggregation	Detection of inherited and acquired platelet defects, monitoring antiplatelet drugs
Flow cytometry	Measurement of platelet GP, secretion, MP, and activation markers by fluorescence	Diagnosis of platelet GP defects, platelet release, PMP, platelet activation markers, monitoring antiplatelet drugs
Impact	Measurement of platelet adhesion and aggregation under high shear	Detection of inherited and acquired platelet defects, monitoring antiplatelet drugs
Thrombelastography (TEG/ROTEM)	Monitoring rate and quality of clot formation	Prediction of surgical bleeding, aid to blood product usage, monitoring antiplatelet drugs
VerifyNow	Platelet aggregation	Monitoring antiplatelet drugs
Multiplate	Platelet aggregation	Monitoring antiplatelet drugs
VASP-P	Flow cytometry with phosphoprotein-phosphorylation	Monitoring P2Y12 receptor activity
Microparticles	Flow cytometry with calibrated beads	Platelet activation markers, intercellular communication

PFA: platelet function analyzer; GP: glycoprotein; MP: microparticles; PMP: platelet-derived microparticles; TEG: thrombelastography; ROTEM: rotational thrombelastometry; VASP-P: phosphorylation of vasodilator-stimulated phosphoprotein-phosphorylation.

IIb/IIIa into an active form. GP IIb/IIIa is the central platelet receptor mediating platelet aggregation. Only the activated GP IIb/IIIa complex is able to bind soluble plasma fibrinogen leading to ultimate aggregation and further spreading of the stimulated platelets along the site of injury. Therefore, aggregation is critically dependent on G-protein coupled receptors and is mediated by bridges between fibrinogen/vWF (under high shear) and the activated GP IIb/IIIa complexes on adjacent, stimulated cells [1–6]. The exposure of anionic phospholipids, mainly phosphatidylserine, provides a surface upon which platelets can support thrombin. Thrombin, the key enzyme of the coagulation cascade and the most potent platelet agonist, acts by cleaving protease-activated surface receptor. The resulting thrombin burst leads to further activation and local recruitment of platelets into the vicinity and inclusion of leukocytes via their receptors for P-selectin. After the clot has been formed, the activated platelets rearrange and contract their intracellular actin/myosin cytoskeleton, which results in clot retraction.

Most platelet function tests have been traditionally used for the diagnosis and management of patients presenting with bleeding problems. In contrast to coagulation defects, where screening tests such as prothrombin time (PT) or activated partial thromboplastin time (aPTT) are more standardized and fully automated, platelet function tests are still labor intensive and time-consuming and require special equipment and experts of specialized laboratories. The laboratory identification of hemostasis defects including platelet function disorders now involves a multistep process. Because platelets are implicated in atherothrombosis as well, newer and existing platelet function tests are increasingly used for monitoring the efficacy of antiplatelet drugs, with the aim of predicting the adverse events such as bleeding or thrombosis in arterial thrombotic diseases. This review article discusses currently available clinical application of platelet function tests, placing emphasis on essential characteristics.

2. Platelet Function Testing

When investigating platelet function disorders, a stepwise process is required, and collaboration between clinical and laboratory personnel is important to obtain a detailed history. A review of recent and regular medications is also required. Then laboratory testing is initiated, which begins with a full blood count, often in conjunction with a blood film examination, particularly if the hematology analyzer gives abnormal platelet flags regarding the platelet count, mean platelet volume (MPV), or platelet distribution width (PDW). Many laboratories are utilizing the panel of screening tests when a patient presents with a clinical suspicion of defects in hemostasis. If the screening tests are all normal but the clinical indication is strong for platelet defects, it is imperative that a complete diagnostic workup is still performed. If appropriate, a complex panel of specialized tests including platelet aggregometry, a measure of platelet release, flow cytometry, platelet microRNAs (miRNA), genetic studies, and analysis of signal transduction pathways will be done. Table 1 provides a summary of currently available platelet function tests with their clinical utility [2, 7–10].

2.1. Platelet Aggregometry. Light transmission aggregometry (LTA) is regarded as the gold standard of platelet function testing and is still the most used test for the identification and diagnosis of platelet function defects. Platelet rich plasma (PRP) is stirred within a cuvette located between a light source and a detector. After addition of a various panel of agonists, such as collagen, ADP, thrombin, ristocetin, epinephrine, and arachidonic acid, the platelets aggregate and light transmission increases. Thrombin is a potent platelet agonist. But thrombin cleaves fibrinogen and leads clot formation. It is a difficult agonist to use for platelet aggregation testing. Instead of thrombin, thrombin receptor activating peptide (TRAP) is used for thrombin receptors. The platelet

aggregation pattern is thought as a primary response to an exogenous agonist, followed by a secondary response to the release of dense granule contents. This biphasic response can be masked if high concentrations of agonists are added. Parameters measured include the rate or slope of aggregation (%/min) and the maximal amplitude (%) or percentage of aggregation after a fixed period of time, usually 6–10 min [7–12].

Traditional LTA remains the most useful technique for diagnosing a wide variety of platelet defects. The main disadvantage of LTA is the use of PRP instead of the whole blood under relatively low shear conditions, and, in the absence of red and white cells, it does not accurately simulate primary hemostasis. It also requires large sample volume and is time-consuming and there are many preanalytical and analytical variables that affect the LTA results. The LTA technique is not standardized, despite the fact that guidelines have been published. Recent recommendations from the Platelet Physiology Subcommittee of the Scientific and Standardization Committee (SSC) of the International Society on Thrombosis and Haemostasis (ISTH) are available [13–15]. Alternative methods including whole blood aggregometry or lumiaggregometry have been introduced, but the majority of these techniques have not been widely adopted and failed to provide additional diagnostic information.

The limitations of conventional LTA assay triggered the development of new, easier-to-use platelet function tests. The most widely used test today is the platelet function analyzer- (PFA-) 100 and PFA-200 devices (Siemens, Marburg, Germany), which is considered to be a surrogate in vitro bleeding time. The instrument monitors the drop in flow rate, and the time required to obtain full occlusion of the aperture is reported as closure time (CT), up to a maximum of 300 seconds. This global platelet function test is easy to use, automated, and rapid and mimics several characteristics of physiologic platelet function, because it is a high shear system and the whole blood is used instead of PRP. Clinical applications have been recently reviewed, and they include screening for von Willebrand disease (vWD) and its treatment monitoring, identification of inherited and acquired platelet defects, monitoring antiplatelet therapy, and assessment of surgical bleeding risk [16, 17]. However, the CT is influenced by platelet count and hematocrit, and they would have poor specificity for any particular disorder. Thus, normal PFA CT results can be used with some confidence to exclude severe vWD or severe platelet dysfunction but would not exclude a possible mild vWF deficiency or mild platelet disorder. Any presumptive platelet function defect detected by abnormal CT needs to be confirmed by more specific tests.

2.2. Flow Cytometry. Whole blood flow cytometry is a powerful and popular laboratory technique for the assessment of platelet function and activation. Although flow cytometry requires sophisticated equipment, requires available monoclonal antibodies, and is not well-standardized, it has several advantages including small volume of whole blood and independence of platelet count. The most commonly used routine flow cytometry tests are the quantification of the basal platelet GP receptor status and the determination of the platelet granule composition. Flow cytometer can quantify GP IIb/IIIa deficiencies in Glanzmann's thrombasthenia and GP Ib/IX/V in Bernard-Soulier syndrome. It has also been devised to measure dense granules using mepacrine uptake and release [2, 7–12]. Flow cytometry allows the analysis of individual platelet functional capability and the measurement of the expression of platelet activation markers on individual platelets as well as the quantitation of associates between platelets and other blood cells.

The most common platelet activation markers assessed by flow cytometry are P-selectin expression on the platelet surface (as a marker of α-granule secretion), the conformational change of GP IIb/IIIa into its active state (measured with monoclonal antibody PAC-1), platelet-leukocyte conjugates, microparticle examination, exposure of anionic, negatively charged phospholipids on the platelet surface (procoagulant activity), and phosphorylation of vasodilator-stimulated phosphoprotein-phosphorylation (VASP-P) (Bio-Cytex, Marseille, France), as a marker of P2Y12 receptor activation-dependent signaling [18–20]. Many laboratories have measured a variety of different platelet activation markers and shown that they are elevated in various clinical conditions such as unstable angina, acute myocardial infarction, preeclampsia, peripheral vascular disease, and cerebrovascular ischemia.

2.3. Other Point-of-Care Testing (POCT). Platelet function tests are increasingly proposed as perioperative tools to aid in prediction of bleeding or for monitoring the efficacy of various types of prohemostatic therapies. As increasing numbers of patients are being treated with antiplatelet drugs, there is also an associated increased risk of bleeding. Traditional LTA still has an important role in the evaluation of platelet disorders, but it cannot easily be performed in the acute care conditions. The growing clinical need coupled with the development of new, simpler POCT machines has resulted in a tendency of platelet function tests to be done away from specialized clinical hemostasis laboratories. This review focuses on the clinical utility of two representative instruments: impact cone and plate analyzer (DiaMed, Cressier, Switzerland) [2, 18, 19] and thrombelastography (TEG) (Hemoscope, Niles, IL, USA) [7–10, 21, 22] in more detail, and the others are referred to below in the section of monitoring antiplatelet therapy.

The impact cone was originally designed to monitor platelet adhesion to a polystyrene plate. The instrument contains a microscope and performs staining and image analysis of the platelets that adhere and aggregate under a high shear rate of 1,800/sec. The results are reported as the percentage of the surface covered by platelets (surface coverage) and the average size of the adherent particles. The adhesion is dependent on vWF, fibrinogen binding, and platelets GP Ib and IIb/IIIa. The assay is fully automated, simple, and rapid to use, requiring small whole blood. Emerging data suggest that the impact cone can detect numerous platelet defects and vWD and could also be potentially used as a screening

method. But the fully automated version of impact cone has limited use and therefore further studies are required [2, 7–10, 18, 19].

TEG and rotational thrombelastometry (ROTEM) (Pentapharm GmbH, Munich, Germany) measure the physical properties of forming clots by the use of an oscillating cup that holds whole blood samples. TEG provides various data related to fibrin formation, clot development, the ultimate strength, and stability of fibrin clot as well as fibrinolysis. The particular advantages of TEG/ROTEM are to provide a complete profile of clot formation and allow for interactions between whole blood elements, including platelets and the coagulation system. Unlike other specific platelet function tests, these instruments have traditionally been used within surgical and anesthesiology departments for determining the risk of bleeding and as a guide for transfusion requirements. There is interlaboratory variation and it is a time-consuming analysis (at least 30 min) [7–10, 21, 22].

3. Monitoring Antiplatelet Therapy

As combined antiplatelet regimens become more widely used and newer agents offer more potent antiplatelet effects, it will become increasingly important to be able to optimize the risk-to-benefit ratio in individual patients. Modern antiplatelet therapy based on the inhibition of three major platelet activation pathways, (1) cyclooxygenase-1 inhibition resulting in a reduction of thromboxane A_2, (2) P2Y12 (ADP) inhibition, and (3) GP IIb/IIIa receptor blockade, is a cornerstone in the successful treatment [23–25]. Although dual therapy with aspirin and clopidogrel has proven to positively influence outcome in patients with acute coronary syndrome and, after percutaneous coronary interventions (PCI), a considerable variation in individual response to antiplatelet therapy assessed by different techniques can be observed [23–27]. These findings may be explained by the different testing populations but may primarily be a result of interassay variations such as different sensitivities, differences in platelet activation techniques, and variations in type of activators and their concentrations.

In the past decade, compelling evidence from numerous observational studies has emerged demonstrating a strong association between high platelet reactivity (HPR) to ADP and post-PCI ischemic events, especially stent thrombosis. In 2010, the Food and Drug Administration (FDA) added a boxed warning to clopidogrel to alert prescribers to the possibilities of CYP genetic polymorphisms that can result in poor metabolism and poor clopidogrel responsiveness [28]. The American Heart Association/the American College of Cardiology Foundation and the European Society of Cardiology guidelines issued a class IIb recommendation for platelet function testing to facilitate the choice of P2Y12 inhibitor in selected, high-risk patients undergoing PCI, although routine testing is not recommended (class III). Recently they updated the consensus document and proposed updated cutoff values for HPR and low platelet reactivity (LPR) to ADP that might be used in future investigations of personalized antiplatelet therapy. LPR to ADP is suggested to be associated with a

higher risk of bleeding. Therefore, they proposed a therapeutic window concept for P2Y12 inhibitor therapy [29–31].

The most widely used platelet function assays, VerifyNow P2Y12 assay (Accumetrics, San Diego, CA, USA) and, at present, Multiplate analyzer (H. Hoffmann-La Roche Ltd., Basel, Switzerland) and VASP assay, have overcome many of the technical and methodological limitations of the previous assays, including conventional LTA. Thus, at the present time, HPR and LPR in the setting of PCI have been defined by the receiver-operator characteristic (ROC) curve analyses using the following criteria, respectively: (1) >208 and <85 P2Y12 reaction units (PRU) by VerifyNow P2Y12 assay, (2) >50% and <16% platelet reactivity index (PRI) by VASP-P, and (3) >46 and <19 arbitrary aggregation units (AU) in response to ADP by Multiplate analyzer [29–31]. However, there are no large-scale clinical studies to date demonstrating that the adjustment of antiplatelet therapy based on any of these cut points improves clinical outcome. Currently, platelet function testing may be considered in determining an antiplatelet strategy in patients with a history of stent thrombosis and in patients prior to undergoing high-risk PCI [32–34].

4. Platelet-Derived Microparticles (PMP)

Circulating microparticles (MP) are defined as small and anucleoid phospholipid vesicles, approximately 0.1–1.0 μm in diameter, and derived from different cell types such as platelets, erythrocytes, leukocytes, endothelial cells, and vascular smooth muscle cells [35]. MP are distinguished from exosomes, which are smaller vesicles (40–100 nm) derived from endoplasmic membranes and apoptotic bodies that are larger particles (>1.5 μm) and contain nuclear components. MP carry surface proteins and include cytoplasmic materials of the parental cells, while MP membrane includes negatively charged phospholipids, mainly phosphatidylserine, thus, responsible for the exertion of microparticle-mediated biological effects [36, 37].

Under steady-state conditions, MP originating from platelet and megakaryocytes are the most abundant microparticles, constituting up to 70–90% of all MP in circulation [38]. PMP levels show gender-specific differences, with increased numbers in women as compared with men, which is further modulated by the menstruation cycle. Increases in PMP levels are observed with aging, during pregnancy, and after exercise, leading to a concomitant increase of hemostatic potential. About 25% of the procoagulant activity of stimulated platelet suspensions is associated with MP released upon platelet activation and their surface may be approximately 50–100 times more procoagulant than the surface of activated platelet per se. Low amounts of PMP are continuously shed from platelets, but this process is highly accelerated after platelet activation or intensive physical activity.

The thrombogenic properties of PMP have been confirmed in experimental studies and high PMP levels are strongly associated with different thrombotic conditions. PMP were also significantly increased in patients with acute

pulmonary embolism and were the main source of procoagulant MP. For example, in valvular atrial fibrillation, which carries a very high risk of thromboembolism, the numbers of PMP were more than threefold. Elevated PMP levels are associated with other disease states including heparin-induced thrombocytopenia, arterial thrombosis, idiopathic thrombocytopenic purpura, thrombotic thrombocytopenia, sickle cell disease, uremia, malignancy, and rheumatoid arthritis. PMP have also been implicated in the pathogenesis of atherosclerosis as well as the regulation of angiogenesis [39–43].

A number of studies indicate that MP contribute to intercellular communication. Recent studies provided now a rationale for the concept of MP as vehicles for intercellular exchange of biological signals and information. Although the physiological significance of PMP may have been overlooked for many years, ongoing research works suggest that these tiny blebs may play an important role in the transport and delivery of bioactive molecules and signals throughout the body. MP may affect target cells either by stimulating directly via surface-expressed ligands or by transferring surface receptors from one cell to the other. Because MP engulf cytoplasm during their formation, they acquire proteins and RNA that originate from the cytosol of the parent cell. An increasing body of evidence suggests that, after attachment or fusion with target cells, MP deliver cytoplasmic proteins and RNA to recipient cells. This process can be mediated either through receptor-ligand interactions or through internalization by recipient cells via endocytosis. Although antigens found on the surface of MP and the cargo of MP resemble those of their parental cells, MP represent more than just a miniature version of the specific cell of origin [35–38].

Several laboratory methods for analysis of PMP have been published, and the most widely used method today is flow cytometry. Although there are a large number of publications on PMP, the lack of standardization makes the comparison of results between studies difficult. A previous ISTH Vascular Biology Subcommittee survey showed that about 75% of laboratories use flow cytometry to quantitate MP in clinical samples. However, a wide variety of preanalytic and analytic variables have been reported in the literature, resulting in a broad range of PMP values in platelet-free plasma of healthy subjects [44–46]. Three ISTH SSC (Vascular Biology, Disseminated Intravascular Coagulation, and Haemostasis and Malignancy) have initiated a project aiming at standardization of the enumeration of cellular MP by flow cytometer. This strategy is based on the use of fluorescent calibrated submicrometer beads, Megamix beads (BioCytex, Marseille, France), which allow the MP analysis to be reproducible.

5. Platelet MicroRNAs (miRNA)

miRNA is a small (21–23 nucleotides) noncoding RNA regulating approximately 60% of the mammalian protein coding genes at least in part by translational repression [47]. Although platelets lack a nucleus or genomic DNA, they are able to translate inherited mRNA into protein. In addition to inherited functional translation machinery, for example,

rough endoplasmic reticulum, ribosomes, and small amount of poly(A) RNA from parent megakaryocytes, the presence of a strong correlation between platelet transcriptome and proteomic profile supports de novo translational capabilities of platelets and suggests the possibility of posttranscriptional regulation of gene expression within platelets. Interestingly, platelets inherit essential miRNA processing proteins in addition to miRNA transcripts originated from their parent megakaryocytes [47–49].

Activated platelets, as discussed above, release MP rich in growth factors or variety of effecter proteins that may exert extracellular effects. A recent report of miRNA recovery from plasma MP indicates that PMP may probably deliver platelet miRNA at the site action in cardiovascular system. Moreover, platelets-secreting miRNA may contribute to the plasma miRNA pool, which has become a great attraction for scientists searching novel biomarkers associated with various pathologic conditions [49–51]. Microarray screening revealed that miR-126, miR-197, miR-223, miR-24, and miR-21 are among the most highly expressed miRNAs in platelets and PMP. Their circulating levels actually correlated with PMP as quantified by flow cytometry. Levels of miR-340 and miR-624 were found to be significantly elevated in platelets from patients who suffer from premature coronary artery disease. Similarly, miR-28 overexpression was observed in platelets obtained from myeloproliferative neoplasms [51].

The presence of more than 750 of the roughly 2,000 known human miRNAs in platelets is quite interesting. miRNA has an established role in hematopoiesis and megakaryocytopoiesis; therefore, platelet miRNAs appear to be useful biomarkers and tools for understanding mechanisms of megakaryocyte and platelet gene expression. Because mRNA translation is the only mechanism for new protein synthesis in circulating platelets, it is expected that platelet miRNA plays a role in health and disorders of hemostasis and thrombosis.

6. Conclusions

Most platelet function tests have traditionally been used for the diagnosis and management of patients presenting with bleeding problems. In contrast to coagulation defects, where screening tests such as PT or aPTT are more standardized and fully automated, platelet function tests are still labor intensive and time-consuming and require special equipment and experts of specialized laboratories. The laboratory identification of hemostasis defects including platelet function disorders now involves a multistep process. Because platelets are implicated in atherothrombosis as well, newer and existing platelet function tests are increasingly used for monitoring the efficacy of antiplatelet drugs, with the aim of predicting the adverse events such as bleeding or thrombosis in arterial thrombotic diseases.

Many laboratories are utilizing the panel of screening tests when a patient presents with a clinical suspicion of defects in hemostasis. If the screening tests are all normal but the clinical indication is strong for platelet defects, it is imperative that a complete diagnostic workup is still

performed. If appropriate, a complex panel of specialized tests including platelet aggregometry, a measure of platelet release, flow cytometry, PMP, platelet miRNA, genetic studies, and analysis of signal transduction pathways will be done. Beyond hemostasis and thrombosis, an increasing number of studies indicate that platelets play an integral role in intercellular communication, are mediators of inflammation, and have immunomodulatory activity. As new potential biomarkers and technologies arrive at the horizon, platelet functions testing appears to take on a new aspect.

Conflict of Interests

The authors declare that there is no conflict of interests regarding the publication of this paper.

Acknowledgments

References

[1] S. S. Smyth, S. Whiteheart, J. E. Italiano Jr., and B. S. Coller, "Platelet morphology, biochemistry, and function," in *Williams Hematology*, chapter 114, pp. 1735–1814, 2010.

[2] P. Harrison and D. Keeling, "Platelet assays and platelet dysfunction," in *Laboratory Hematology Practice*, chapter 37, pp. 480–491, 2012.

[3] C. N. Jenne, R. Urrutia, and P. Kubes, "Platelets: bridging hemostasis, inflammation, and immunity," *International Journal of Laboratory Hematology*, vol. 35, no. 3, pp. 254–261, 2013.

[4] L. K. Jennings, "Mechanisms of platelet activation: need for new strategies to protect against platelet-mediated atherothrombosis," *Thrombosis and Haemostasis*, vol. 102, no. 2, pp. 248–257, 2009.

[5] K. J. Clemetson, "Platelets and primary haemostasis," *Thrombosis Research*, vol. 129, no. 3, pp. 220–224, 2012.

[6] R. Abbate, G. Cioni, I. Ricci, M. Miranda, and A. M. Gori, "Thrombosis and Acute coronary syndrome," *Thrombosis Research*, vol. 129, no. 3, pp. 235–240, 2012.

[7] P. Harrison, "Testing platelet function," *Hematology/Oncology Clinics of North America*, vol. 27, no. 3, pp. 411–441, 2013.

[8] R. Pakala and R. Waksman, "Currently available methods for platelet function analysis: advantages and disadvantages," *Cardiovascular Revascularization Medicine*, vol. 16, no. 36, pp. 4041–4051, 2010.

[9] C. K. Hofer, A. Zollinger, and M. T. Ganter, "Perioperative assessment of platelet function in patients under antiplatelet therapy," *Expert Review of Medical Devices*, vol. 7, no. 5, pp. 625–637, 2010.

[10] S. M. Picker, "In-vitro assessment of platelet function," *Transfusion and Apheresis Science*, vol. 44, no. 3, pp. 305–319, 2011.

[11] E. J. Favaloro, G. Lippi, and M. Franchini, "Contemporary platelet function testing," *Clinical Chemistry and Laboratory Medicine*, vol. 48, no. 5, pp. 579–598, 2010.

[12] B. E. Kehrel and M. F. Brodde, "State of the art in platelet function testing," *Transfusion Medicine and Hemotherapy*, vol. 40, no. 2, pp. 73–86, 2013.

[13] M. Cattaneo, C. P. Hayward, K. A. Moffat, M. T. Pugliano, Y. Liu, and A. D. Michelson, "Results of a worldwide survey on the assessment of platelet function by light transmission aggregometry: a report from the platelet physiology subcommittee of the SSC of the ISTH," *Journal of Thrombosis and Haemostasis*, vol. 7, no. 6, p. 1029, 2009.

[14] B. B. Dawood, G. C. Lowe, M. Lordkipanidze et al., "Evaluation of participants with suspected heritable platelet function disorders including recommendation and validation of a streamlined agonist panel," *Blood*, vol. 120, no. 25, pp. 5041–5049, 2012.

[15] M. Cattaneo, C. Cerletti, P. Harrison et al., "Recommendations for the standardization of light transmission aggregometry: a consensus of the working party form the platelet physiology subcommittee of SSC/ISTH," *Journal of Thrombosis and Haemostasis*, vol. 11, pp. 1183–1189, 2013.

[16] C. P. M. Hayward, P. Harrison, M. Cattaneo, T. L. Ortel, and A. K. Rao, "Platelet function analyzer (PFA)-100® closure time in the evaluation of platelet disorders and platelet function," *Journal of Thrombosis and Haemostasis*, vol. 4, no. 2, pp. 312–319, 2006.

[17] E. J. Favaloro, "Clinical utility of the PFA-100," *Seminars in Thrombosis and Hemostasis*, vol. 34, no. 8, pp. 709–733, 2008.

[18] C. D. Williams, G. Cherala, and V. Serebruany, "Application of platelet function testing to the bedside," *Thrombosis and Haemostasis*, vol. 103, no. 1, pp. 29–33, 2010.

[19] N. Hezard, A. Tessier-Marteau, and L. Macchi, "New insight in antiplatelet therapy monitoring in cardiovascular patients: from aspirin to thienopyridine," *Cardiovascular and Hematological Disorders-Drug Targets*, vol. 10, no. 3, pp. 224–233, 2010.

[20] J. R. Dahlen, M. J. Price, H. Parise, and P. A. Gurbel, "Evaluating the clinical usefulness of platelet function testing: considerations for the proper application and interpretation of performance measures," *Thrombosis and Haemostasis*, vol. 109, no. 5, pp. 808–816, 2013.

[21] A. Afshari, A. Wikkelsø, A. M. Møller, J. Brok, and J. Wetterslev, "Thrombelastography (TEG) or thrombelastometry (ROTEM) to monitor haematotherapy versus usual care in patients with massive transfusion," *Cochrane Database of Systematic Reviews*, vol. 3, pp. 1–90, 2011.

[22] B. Kim, M. L. Quan, R. Y. Goh et al., "Comparison of prolonged prothrombin and activated partial thromboplastin time results with thrombeastograph parameters," *Laboratory Medicine*, vol. 44, no. 4, pp. 319–323, 2013.

[23] S. L. Close, "Pharmacogenetics and pharmacogenomics of thienopyridines: clinically relevant?" *Fundamental and Clinical Pharmacology*, vol. 26, no. 1, pp. 19–26, 2012.

[24] W. O. Tobin, J. A. Kinsella, T. Coughlan et al., "High on-treatment platelet reactivity on commonly prescribed antiplatelet agents following transient ischaemic attack or ischaemic stroke: results from the Trinity Antiplatelet Responsiveness (TRAP) study," *European Journal of Neurology*, vol. 20, no. 2, pp. 344–352, 2013.

[25] D. Capodanno, J. L. Ferreiro, and D. J. Angiolillo, "Antiplatelet therapy: new pharmacological agents and changing paradigms," *Journal of Thrombosis and Haemostasis*, vol. 11, supplement 1, pp. 316–329, 2013.

[26] K. S. Woo, B. R. Kim, J. E. Kim et al., "Detemination of the prevalence of aspirin and clopidogrel resistances in patients

with coronary artery disease by using various platelet-function tests," *Korean Journal of Laboratory Medicine*, vol. 30, no. 5, pp. 460–468, 2010.

[27] K. E. Kim, K. S. Woo, R. Y. Goh et al., "Comparison of laboratory detection methods of aspirin resistance in coronary artery disease patients," *International Journal of Laboratory Hematology*, vol. 32, no. 1, pp. 50–55, 2010.

[28] K. J. Smock, P. J. Saunders, G. M. Rodgers, and V. Johari, "Laboratory evaluation of clopidogrel responsiveness by platelet function and genetic methods," *American Journal of Hematology*, vol. 86, no. 12, pp. 1032–1034, 2011.

[29] L. Bonello, U. S. Tantry, R. Marcucci et al., "Consensus and future directions on the definition of high on-treatment platelet reactivity to adenosine diphosphate," *Journal of the American College of Cardiology*, vol. 56, no. 12, pp. 919–933, 2010.

[30] D. Aradi, R. F. Storey, A. Komocsi et al., "Expert position paper on the role of platelet function testing in patients undergoing percutaneous coronary intervention," *European Heart Journal*, vol. 35, no. 4, pp. 209–215, 2014.

[31] U. S. Tantry, L. Bonello, D. Aradi et al., "Consensus and update on the definition of on-treatment platelet reactivity to adenosine diphosphate associated with ischemia and bleeding," *Journal of the American College of Cardiology*, vol. 62, no. 24, pp. 2261–2273, 2013.

[32] T. J. Kunicki and D. J. Nugent, "The genetics of normal platelet reactivity," *Blood*, vol. 116, no. 15, pp. 2627–2634, 2010.

[33] H. Z. Zhang, M. H. Kim, J. Y. Han, and Y. H. Jeong, "Defining predictive values using three different platelet function tests for CYP2C19 phenotype status on maintenance dual antiplatelet therapy after PCI," *Platelets*, 2013.

[34] J. L. Choi, B. R. Kim, J. E. Kim et al., "Association between the microarray-based CYP2C19 genotyping assay and the platelet function test in cardiovascular patients receiving clopidogrel," *International Journal of Laboratory Hematology*, 2014.

[35] M. Prokopi, G. Pula, U. Mayr et al., "Proteomic analysis reveals presence of platelet microparticles in endothelial progenitor cell cultures," *Blood*, vol. 114, no. 3, pp. 723–732, 2009.

[36] S. F. Mause and C. Weber, "Microparticles: protagonists of a novel communication network for intercellular information exchange," *Circulation Research*, vol. 107, no. 9, pp. 1047–1057, 2010.

[37] M. Aatonen, M. Grönholm, and P.-M. Siljander, "Platelet-derived microvesicles: multitalented participants in intercellular communication," *Seminars in Thrombosis and Hemostasis*, vol. 38, no. 1, pp. 102–113, 2012.

[38] J. E. Italiano Jr., A. T. Mairuhu, and R. Flaumenhaft, "Clinical relevance of microparticles from platelets and megakaryocytes," *Current Opinion in Hematology*, vol. 17, no. 6, pp. 578–584, 2010.

[39] E. Shantsila, P. W. Kamphuisen, and G. Y. H. Lip, "Circulating microparticles in cardiovascular disease: implications for atherogenesis and atherothrombosis," *Journal of Thrombosis and Haemostasis*, vol. 8, no. 11, pp. 2358–2368, 2010.

[40] C. N. França, L. F. M. Pinheiro, M. C. O. Izar et al., "Endothelial progenitor cell mobilization and platelet microparticle release are influenced by clopidogrel plasma levels in stable coronary artery disease," *Circulation Journal*, vol. 76, no. 3, pp. 729–736, 2012.

[41] L. M. Biasucci, I. Porto, L. D. Vito et al., "Differences in microparticle release in patients with acute coronary syndrome and stable angina," *Circulation Journal*, vol. 76, no. 9, pp. 2174–2182, 2012.

[42] P. Lackner, A. Dietmann, R. Beer et al., "Cellular microparticles as a marker for cerebral vasospasm in spontaneous subarachnoid hemorrhage," *Stroke*, vol. 41, no. 10, pp. 2353–2357, 2010.

[43] J. Thaler, C. Ay, H. Weinstabl et al., "Circulating procoagulant microparticles in cancer patients," *Annals of Hematology*, vol. 90, no. 4, pp. 447–453, 2011.

[44] S. Robert, P. Poncelet, R. Lacroix et al., "Standardization of platelet-derived microparticle counting using calibrated beads and a Cytomics FC500 routine flow cytometer: a first step towards multicenter studies?" *Journal of Thrombosis and Haemostasis*, vol. 7, no. 1, pp. 190–197, 2009.

[45] F. Mobarrez, J. Antovic, N. Egberg et al., "A multicolor flow cytometric assay for measurement of platelet-derived microparticles," *Thrombosis Research*, vol. 125, no. 3, pp. e110–e116, 2010.

[46] R. Lacroix, S. Robert, P. Poncelet, R. S. Kasthuri, N. S. Key, and F. Dignat-George, "Standardization of platelet-derived microparticle enumeration by flow cytometry with calibrated beads: results of the International Society on Thrombosis and Haemostasis SSC Collaborative workshop," *Journal of Thrombosis and Haemostasis*, vol. 8, no. 11, pp. 2571–2574, 2010.

[47] S. Dangwal and T. Thum, "MicroRNAs in platelet biogenesis and function," *Thrombosis and Haemostasis*, vol. 108, no. 4, pp. 599–604, 2012.

[48] L. C. Edelstein, S. E. McKenzie, C. Shaw, M. A. Holinstat, S. P. Kunapuli, and P. F. Bray, "MicroRNAs in platelet production and activation," *Journal of Thrombosis and Haemostasis*, vol. 11, supplement 1, pp. 340–350, 2013.

[49] P. Willeit, A. Zampetaki, K. Dudek et al., "Circulating microRNAs as novel biomarkers for platelet activation," *Circulation Research*, vol. 112, no. 4, pp. 595–600, 2013.

[50] A. Zampetaki, P. Willeit, L. Tilling et al., "Prospective study on circulating microRNAs and risk of myocardial infarction," *Journal of the American College of Cardiology*, vol. 60, no. 4, pp. 290–299, 2012.

[51] S. Grasedieck, A. Sorrentino, C. Langer et al., "Circulating microRNAs in hematological diseases: principles, challenges, and perspectives," *Blood*, vol. 121, no. 25, pp. 4977–4984, 2013.

Research Article

Association between the Delta Estimated Glomerular Filtration Rate and the Prevalence of Monoclonal Gammopathy of Undetermined Significance in Korean Males

Tae-Dong Jeong, Woochang Lee, Sail Chun, and Won-Ki Min

Department of Laboratory Medicine, Asan Medical Center, University of Ulsan College of Medicine, 88 Olympic-ro 43-gil, Songpa-gu, Seoul 138-736, Republic of Korea

Correspondence should be addressed to Won-Ki Min; wkmin@amc.seoul.kr

Background. We investigated the association between the reduction in the estimated glomerular filtration rate (eGFR) and the prevalence of monoclonal gammopathy of undetermined significance (MGUS) in Korean males. *Methods.* We enrolled 723 healthy Korean males. Serum creatinine concentration, serum electrophoresis, serum immunofixation, and the serum free light chain assay were performed. We calculated delta eGFR per year (ΔeGFR/yr). The prevalence of MGUS was compared based on the ΔeGFR/yr and age group. *Results.* Thirteen (1.8%) of 723 participants exhibited the monoclonal band on serum immunofixation. Prevalence of MGUS by age group was 0.00% (0/172 for 40 years), 1.63% (6/367 for 60 years), and 3.80% (7/184 for >60 years). The median decrease in ΔeGFR/yr was 5.3%. The prevalence of MGUS in participants in their 50s with >5.3% decline in ΔeGFR/yr was significantly higher than those with <5.3% decrease in ΔeGFR/yr (3.16% versus 0.00%; $P = 0.049$). The prevalence of MGUS in participants in their 50s with >5.3% decrease in ΔeGFR/yr was similar to that of healthy males in their 60s. *Conclusion.* Using the rate of reduction in ΔeGFR/yr in healthy Korean males who had their serum creatinine level checked regularly may increase the MGUS detection rate in clinical practice.

1. Introduction

Monoclonal gammopathy of undetermined significance (MGUS) is the most common plasma cell disorder, and its prevalence increases with age [1–4]. The prevalence of MGUS is also affected by race and sex, but MGUS generally develops in older people, African-Americans, and males with a slight predominance [1–5]. In previous studies, the prevalence of MGUS was 4.9% in Caucasian males > 60 years old [2] and 3.8% in Korean males > 65 years old [3].

Several studies of the prevalence of MGUS stratified by age category in each race have been conducted. However, to the best of our knowledge, none has reported the correlation between the degree of estimated glomerular filtration rate (eGFR) reduction and the prevalence of MGUS. And the association between measurement of free kappa and lambda light chains by the serum FLC assay and the prevalence of MGUS has not been well documented either. Thus, in this

study we investigated the correlation between the degree of egfr reduction and MGUS prevalence among Korean healthy males.

2. Materials and Methods

2.1. Subjects. The study included Korean males over 40 years old who visited the hospital for regular health checkups between June 2011 and March 2012. A total of 723 males had regular checkups during the period. According to the review of the electronic medical records, all of the study subjects have not been diagnosed with MGUS previously. This study was approved by the Institutional Review Board of ASAN Medical Center (approval no. 2012-0065).

2.2. Specimen and Data Collection. After general blood chemistry, the remaining 1 mL of serum was collected in two microtubes and stored at −70°C. One of the two microtubes

TABLE 1: Baseline demographic chracteristics of the study population stratified by age.

Variable	40–49 yrs	50–59 yrs	≥60 yrs	All
N	172	367	184	723
Age (yrs)	47.0 ± 1.7	54.3 ± 2.9	65.4 ± 5.2	55.4 ± 7.4
Interval of health checkup (days)	395.6 ± 97.3	394.5 ± 91.7	420.2 ± 113.4	401.3 ± 99.4
Current sCr (mg/dL)	0.989 ± 0.123	0.996 ± 0.155	1.015 ± 0.155	0.999 ± 0.148
Previous sCr (mg/dL)	0.943 ± 0.113	0.941 ± 0.117	0.968 ± 0.129	0.949 ± 0.120
Current eGFR (mL/min/1.73 m^2)	82.6 ± 11.5	80.2 ± 12.6	75.6 ± 12.8	79.6 ± 12.7
Previous GFR (mL/min/1.73 m^2)	87.7 ± 12.6	85.3 ± 11.9	79.8 ± 12.7	84.5 ± 12.6
ΔeGFR/yr (%)	−5.1 ± 9.0	−5.6 ± 8.5	−4.7 ± 8.0	−5.3 ± 8.5
κ FLC (mg/L)	9.77 (2.38–25.91)	10.76 (2.17–292.53)	11.54 (2.17–1,265.95)	11.10 (2.17–1,265.95)
λ FLC (mg/L)	11.13 (6.38–30.31)	11.71 (2.51–34.71)	12.06 (2.51–34.71)	11.84 (2.51–34.71)
κ/λ ratio	0.84 (0.19–1.99)	0.91 (0.33–44.26)	0.94 (0.33–156.68)	0.92 (0.19–156.68)

Data expressed as means ± standard deviation or medians (range).
Abbreviations: CKD-EPI: Chronic Kidney Disease Epidemiology Collaboration; eGFR: estimated glomerular filtration rate; FLC: free light chain; MDRD: Modification of Diet in Renal Disease; sCr: serum creatinine.

was used for serum protein electrophoresis (sPEP) and serum immunofixation electrophoresis (sIFE), while the other was used for the serum free light chain (sFLC) assay. Electronic medical records were used to collect participant data, such as age, date of current health checkup, date of previous health checkup, and current and previous serum creatinine levels.

2.3. Laboratory Tests. Serum creatinine levels of the participants during the study period were measured using a Toshiba 200-FR Neo (Toshiba Medical Systems Co., Tokyo, Japan) instrument with the IDMS-traceable calibrator (c.f.a.s calibrator, Roche Diagnostics, Indianapolis, IN, USA). Previous serum creatinine levels were measured using the Toshiba 200-FR Neo with the same IDMS-traceable calibrator. The Hydrasys 2 (Sebia, Evry, France) instrument was used to perform both sPEP and sIFE based on the manufacturer's instructions. The sIFE was performed to detect kappa and lambda free light chains in sera. The sFLC assay was analyzed using SPAplus (Binding Site, Birmingham, UK) instrument with Freelite (Binding Site) reagents. Both kappa and lambda free light chain concentrations were measured quantitatively to calculate the kappa/lambda FLC ratio. The reference range for the sFLC ratio was 0.26–1.65 [6].

2.4. Calculating eGFR and ΔeGFR. All participants were Korean males. Their current and previous eGFR values were calculated using the four-variable MDRD study equation (eGFR = 175 × standardized serum creatinine$^{-1.154}$ × age$^{-0.203}$). The delta eGFR (ΔeGFR, %) was calculated as the difference between current eGFR and previous eGFR [100 × (current eGFR-previous eGFR)/previous eGFR], whereas the annual rate of decline in eGFR [ΔeGFR/yr (%)] was determined as the difference between the follow-up and baseline eGFR values, with this value divided by the time interval [100 × (current eGFR-previous eGFR)/previous eGFR] × (365/Δdays).

2.5. Definition of MGUS. MGUS is defined as serum monoclonal protein <3 g/dL, clonal bone marrow clonal plasma cells <10%, and absence of end organ damage such as hypercalcemia, renal insufficiency, anemia, and bone lesions (CRAB) that can be attributed to the plasma cell proliferation disorder [7]. In this study, MGUS was defined as an absence of CRAB symptoms and presence of monoclonal protein confirmed by sIFE. The CRAB symptoms were identified through review of the electronic medical records including laboratory findings.

2.6. Statistical Analyses. The participants were grouped by age (40, 50, and >60 years) and ΔeGFR/yr (classified into two groups by median ΔeGFR/yr). The prevalence of MGUS was calculated for each group and the differences were analyzed by the chi-square test or Fisher's exact test. SPSS version 19.0 (SPSS, Inc., Chicago, IL, USA) was used for statistical analyses. A P value <0.05 was considered to indicate significance.

3. Results

3.1. Baseline Characteristics. The mean age of the participants was 55.4 ± 7.4 years (range, 41–90 years) and the average health checkup interval was 401.3 ± 99.4 days (range, 202–768 days). The current serum creatinine level increased by an average of 0.051 ± 0.089 mg/dL from the previous serum creatinine level. eGFR decreased by an annual average of 5.3 ± 8.5%, and 363 participants had ≥5.3% reduction. Median values of serum kappa FLC concentration, serum lambda FLC concentration, and the serum kappa/lambda FLC ratio were 11.10 mg/L, 11.84 mg/L, and 0.92, respectively. The baseline demographic chracteristics of the study population stratified by age are summarized in Table 1.

3.2. sPEP, sIFE, and sFLC Assays. The monoclonal protein was detected in 9 participants by sPEP, 13 by sIFE, and 21 by the sFLC ratio, respectively. Four participants had the monoclonal protein in all three tests. The monoclonal protein was detected in 4 participants by only sIFE and in 17 by only the sFLC assay.
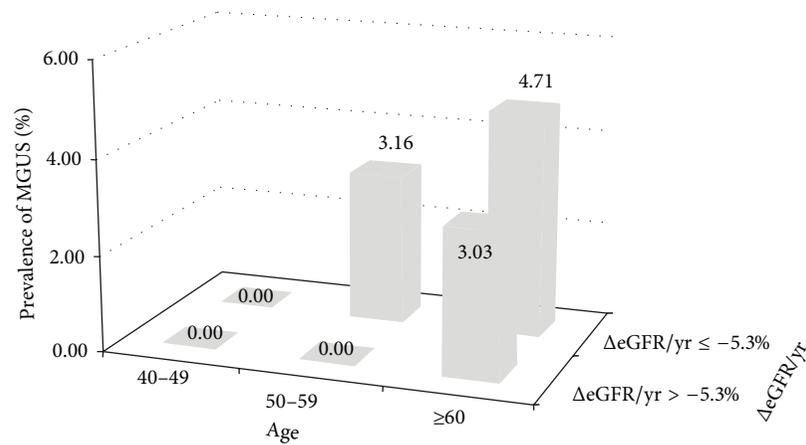
FIGURE 1: Prevalence of monoclonal gammopathy of undetermined significance in Korean males based on delta estimated glomerular filtration rate and age.

3.3. Prevalence of MGUS. Thirteen (1.80%) of the seven hundred and twenty-three participants had the monoclonal band on sIFE. The prevalence of MGUS by age group was 0.00% (0/172, 40 years of age), 1.63% (6/367, 50 years of age), and 3.80% (7/184, ≥60 years of age) (Table 2).

The MGUS prevalence in the group with ≥5.3% decline in ΔeGFR/yr was 2.75% (10/363), almost threefold that in the other groups (0.83%, 3/360); however, the difference was not significant ($P = 0.089$). In an age-stratified analyses, the prevalence of MGUS in 50s with ≥5.3% decline in ΔeGFR/yr group was significantly higher than those with <5.3% decline in ΔeGFR/yr group (3.16% versus 0.00%; $P = 0.049$) (Figure 1). In the 60 years of age or older group, however, the prevalence of MGUS showed no significant difference based on ΔeGFR/yr (4.71% versus 3.03%; $P = 0.438$) (Figure 1).

The MGUS prevalence in participants with kappa or lambda FLC concentrations higher than the reference value on sFLC was 10.91% (6/55), significantly higher than the 1.05% (7/668) in those with a normal serum kappa and lambda FLC concentration.

4. Discussion

We investigated the association between ΔeGFR/yr and prevalence of MGUS in healthy Korean males aged over 40 years. Our results showed that MGUS prevalence values in Korean men in their 40 (0.00%), 50 (1.63%), and >60 years of age (3.80%) were similar to MGUS values for Japanese males in their 40 (1.2%), 50 (2.7%), and >60 years of age (4.3%) and Chinese men 50–65 years (1.2%) [8, 9]. To date, the MGUS prevalence in Koreans has been determined only in elderly people >65 years [3]. In the present study, the prevalence of MGUS in participants >60 years was 3.80% which was similar to those obtained from elderly Korean male aged over 65 years (3.8%) [3].

By definition of MGUS, there is no renal insufficiency. However, excess serum free light chains and intact immunoglobulins that exceed the metabolic ability of kidney function in patients with MGUS can accumulate in the kidney, resulting in subclinical renal insufficiency such as a decline in GFR [10, 11]. On the basis of above consideration, we had assumed that the prevalence of MGUS may be higher in patients with markedly reduction of GFR. And the GFR decline may occur within reference range of serum creatinine. In our study, although the prevalence of MGUS in all participants was not significantly different based on the ΔeGFR, a statistically significant difference was found in the group in their 50s. The difference between the 50s group and those >60 can be partially explained that MGUS is not always a premalignant lesion. Our study indicated that there was apparent association between the MGUS and ΔeGFR; however, a large-scale cohort study is needed to reach the statistical significance.

According to the current MGUS management guideline, MGUS does not require aggressive treatment [12]. However, MGUS is an obvious premalignant lesion that requires careful observation because it progresses to multiple myeloma or other plasma cell-related disorders in some patients [12–15]. In this study, the MGUS prevalence in the group with ≥5.3% decline in ΔeGFR/yr was almost threefold that in the other groups. The prevalence of MGUS in participants in their 50s with a high rate of decrease in ΔeGFR/yr was 3.16%, which was similar to that in the group in their 60s. As 10–20% of those with MGUS in this group are likely to develop multiple myeloma or diverse malignant plasma cell disorders when they reach 60–70 years of age, early detection of MGUS in 50s should be considered.

Measurement of serum creatinine level is included in the National Health Screening Program organized by the National Health Insurance Service for Koreans who are required to undergo a regular health checkup every year or 2 years. And the ΔeGFR can be calculated from those data. We thought that addition of screening for monoclonal protein in those whose ΔeGFR/yr shows a marked reduction may increase the MGUS diagnostic rate.

In this study, we observed 9 samples of false-negative results for sFLC assay based on the sIFE findings. We thought that possible sources of false-negative results of sFLC

TABLE 2: Prevalence of monoclonal gammopathy of undetermined significance (MGUS) in Korean males.

Age (yrs)	Total number of patients	Number of patients with MGUS	Prevalence of MGUS
40–49	172	0	0.00%
50–59	367	6	1.63%
≥60	184	7	3.80%
All	723	13	1.80%

assay were antigen excess [16], FLC polymerization [17], and polyclonal FLC elevation [18]. On the other hand, sFLC assay demonstrated false-positive results for 17 samples based on the sIFE findings. Seventeen participants were normal on the sIFE and sPEP tests but had an abnormal sFLC ratio. Among them, 15 participants showed kappa clonality which means that their sFLC ratio showed more than 1.65 and the remaining 2 participants demonstrated lambda clonality which means that their sFLC ratio is less than 0.26 (data not shown). It has been well documented that sFLC assay could detect monoclonal protein more sensitive than sPEP and sIFE assay [6, 19]. So it is not clear whether 17 samples are true false-positive results. These 17 participants may have monoclonal protein in their sera. So we thought that they need to be monitored to identify monoclonal protein.

In conclusion, the prevalence of MGUS in healthy Korean males in their 50s with a decrease in ΔeGFR/yr of $\geq$5.3% was significantly higher than those with a decrease in ΔeGFR/yr of <5.3%. Additionally, the prevalence of MGUS was similar to that of healthy Korean males in their 60s. Using ΔeGFR/yr in healthy Korean males whose serum creatinine level is checked regularly may facilitate early detection of MGUS.

Conflict of Interests

The authors have no conflict of interests to declare.

Acknowledgments

References

[1] A. Dispenzieri, J. A. Katzmann, R. A. Kyle et al., "Prevalence and risk of progression of light-chain monoclonal gammopathy of undetermined significance: a retrospective population-based cohort study," *The Lancet*, vol. 375, no. 9727, pp. 1721–1728, 2010.

[2] R. A. Kyle, T. M. Therneau, S. V. Rajkumar et al., "Prevalence of monoclonal gammopathy of undetermined significance," *The New England Journal of Medicine*, vol. 354, no. 13, pp. 1362–1369, 2006.

[3] H.-K. Park, K.-R. Lee, Y.-J. Kim et al., "Prevalence of monoclonal gammopathy of undetermined significance in an elderly urban Korean population," *American Journal of Hematology*, vol. 86, no. 9, pp. 752–755, 2011.

[4] R. K. Wadhera and S. V. Rajkumar, "Prevalence of monoclonal gammopathy of undetermined significance: a systematic review," *Mayo Clinic Proceedings*, vol. 85, no. 10, pp. 933–942, 2010.

[5] P. Stratta, L. Gravellone, T. Cena et al., "Renal outcome and monoclonal immunoglobulin deposition disease in 289 old patients with blood cell dyscrasias: a single center experience," *Critical Reviews in Oncology/Hematology*, vol. 79, no. 1, pp. 31–42, 2011.

[6] J. A. Katzmann, R. J. Clark, R. S. Abraham et al., "Serum reference intervals and diagnostic ranges for free κ and free λ immunoglobulin light chains: relative sensitivity for detection of monoclonal light chains," *Clinical Chemistry*, vol. 48, no. 9, pp. 1437–1444, 2002.

[7] N. Korde, S. Y. Kristinsson, and O. Landgren, "Monoclonal gammopathy of undetermined significance (MGUS) and smoldering multiple myeloma (SMM): novel biological insights and development of early treatment strategies," *Blood*, vol. 117, no. 21, pp. 5573–5581, 2011.

[8] M. Iwanaga, M. Tagawa, K. Tsukasaki, S. Kamihira, and M. Tomonaga, "Prevalence of monoclonal gammopathy of undetermined significance: study of 52,802 persons in Nagasaki City, Japan," *Mayo Clinic Proceedings*, vol. 82, no. 12, pp. 1474–1479, 2007.

[9] S. P. Wu, A. Minter, R. Costello et al., "MGUS prevalence in an ethnically Chinese population in Hong Kong," *Blood*, vol. 121, no. 12, pp. 2363–2364, 2013.

[10] G. Cohen and W. H. Hörl, "Free immunoglobulin light chains as a risk factor in renal and extrarenal complications," *Seminars in Dialysis*, vol. 22, no. 4, pp. 369–372, 2009.

[11] A. S. Bargnoux, N. Simon, V. Garrigue et al., "Glomerular filtration rate as a determinant of free light chains in renal transplantation," *Clinical Biochemistry*, vol. 46, no. 16-17, pp. 1764–1766, 2013.

[12] J. Bladé, "Monoclonal gammopathy of undetermined significance," *The New England Journal of Medicine*, vol. 355, no. 26, pp. 2765–2770, 2006.

[13] J. P. Bida, R. A. Kyle, T. M. Therneau et al., "Disease associations with monoclonal gammopathy of undetermined significance: a population-based study of 17,398 patients," *Mayo Clinic Proceedings*, vol. 84, no. 8, pp. 685–693, 2009.

[14] R. A. Kyle and S. Kumar, "The significance of monoclonal gammopathy of undetermined significance," *Haematologica*, vol. 94, no. 12, pp. 1641–1644, 2009.

[15] O. Landgren, G. Gridley, I. Turesson et al., "Risk of monoclonal gammopathy of undetermined significance (MGUS) and subsequent multiple myeloma among African American and white veterans in the United States," *Blood*, vol. 107, no. 3, pp. 904–906, 2006.

[16] S. S. Levinson, "Hook effect with lambda free light chain in serum free light chain assay," *Clinica Chimica Acta*, vol. 411, no. 21-22, pp. 1834–1836, 2010.

[17] C. Li, H. Geng, Z. Yang, and R. Zhong, "Influence of immunoglobulin light chain dimers on the results of the quantitative nephelometric assay," *Clinical Laboratory*, vol. 57, no. 1-2, pp. 53–57, 2011.

[18] S. S. Levinson, "Polyclonal free light chain of Ig may interfere with interpretation of monoclonal free light chain κ/λ ratio," *Annals of Clinical and Laboratory Science*, vol. 40, no. 4, pp. 348–353, 2010.

[19] A. R. Bradwell, H. D. Carr-Smith, G. P. Mead et al., "Highly sensitive, automated immunoassay for immunoglobulin free light chains in serum and urine," *Clinical Chemistry*, vol. 47, no. 4, pp. 673–680, 2001.

Research Article

Erythropoietic Potential of CD34+ Hematopoietic Stem Cells from Human Cord Blood and G-CSF-Mobilized Peripheral Blood

Honglian Jin,[1] Han-Soo Kim,[2] Sinyoung Kim,[1] and Hyun Ok Kim[1]

[1] *Division of Transfusion Medicine and Cell Therapy, Department of Laboratory Medicine, Yonsei University College of Medicine,*
 50 Yonsei-ro, Seodaemun-gu, Seoul 120-752, Republic of Korea
[2] *Innovative Cell and Gene Therapy Center, International St. Mary's Hospital, 25 Simgok-ro, 100 beon-gil, Seo-gu,*
 Incheon 404-834, Republic of Korea

Correspondence should be addressed to Hyun Ok Kim; hyunok1019@yuhs.ac

Red blood cell (RBC) supply for transfusion has been severely constrained by the limited availability of donor blood and the emergence of infection and contamination issues. Alternatively, hematopoietic stem cells (HSCs) from human organs have been increasingly considered as safe and effective blood source. Several methods have been studied to obtain mature RBCs from CD34+ hematopoietic stem cells via *in vitro* culture. Among them, human cord blood (CB) and granulocyte colony-stimulating factor-mobilized adult peripheral blood (mPB) are common adult stem cells used for allogeneic transplantation. Our present study focuses on comparing CB- and mPB-derived stem cells in differentiation from CD34+ cells into mature RBCs. By using CD34+ cells from cord blood and G-CSF mobilized peripheral blood, we showed *in vitro* RBC generation of artificial red blood cells. Our results demonstrate that CB- and mPB-derived CD34+ hematopoietic stem cells have similar characteristics when cultured under the same conditions, but differ considerably with respect to expression levels of various genes and hemoglobin development. This study is the first to compare the characteristics of CB- and mPB-derived erythrocytes. The results support the idea that CB and mPB, despite some similarities, possess different erythropoietic potentials in *in vitro* culture systems.

1. Introduction

Red blood cell transfusion is a well-established and essential therapy for patients with severe anemia. However, the worldwide supply of allogeneic blood faces a serious shortage, and there are many patients around the world whose survival depends on blood transfusion. Around 92 million blood donations are collected annually from all types of blood donors (voluntary unpaid, family/replacement, and paid), but in the report of 39 counties of 159 countries on their collections, donated blood is still not routinely tested for transfusion-transmissible infections (TTIs) including HIV, hepatitis B, hepatitis C, and syphilis [1]. Nevertheless, blood transfusion saves lives, but the transfusion of unsafe blood puts lives at risk because HIV or hepatitis infections can be transmitted to patients through transfusion. However, the financial consequence of discarding unsafe blood creates yet another burden in developing countries.

Research performed on stem cells, specifically hematopoietic stem cells (HSCs), holds promise for the production of mature red blood cells in large quantities through differentiation induction. The classic source of HSCs has been the bone marrow, but bone marrow procurement of cells is an invasive process with risks. The artificial RBCs from stem cells *in vitro* culture can be generated from sources such as embryonic stem cells (ESCs) [2], induced pluripotent stem cells (iPSs) [3], cord blood (CB) [4–6], and peripheral blood (PB) [7]. Of these, ESCs and iPSCs are the least promising due to the low generation efficiency and long-term *in vitro* culture cost hindrances. Currently, granulocyte colony-stimulating factor- (G-CSF-) mobilized peripheral blood (mPB) and CB are therefore

widely researched as a potential alternate source for stem cell procurement. However, this has not been a widespread standard of therapy, and the characteristics of mature red blood cells derived from HSCs after mass production are not yet well known. Our study focuses on comparing CB- and mPB-derived stem cells with respect to their characteristics and function after differentiation.

2. Materials and Methods

2.1. CD34+ HSC Isolation, Culture, and Erythropoietic Differentiation. CB samples from normal full-term deliveries ($n = 7$) were collected in a bag (Green Cross Corp., Yong-in, Korea) containing 24.5 mL of citrate phosphate dextrose A (CPDA-1). Five milliliters of G-CSF-mPB was obtained ($n = 7$) with the written informed consent of normal voluntary allogeneic HSC donors. This study was approved by Severance Hospital IRB (IRB number 4-2011-0081). The CD34+ cells from both sources were isolated using a MACS isolation kit (density, 1.077; Pharmacia Biotech, Uppsala, Sweden) using an antibody against CD34 according to the manufacturer's instructions. And the sorted CD34+ cells were cultured at a density of 1×10^5 cells/mL in a stroma-free condition for 17–21 days as described previously [8, 9]. Briefly, from day 0 to 7, sorted CD34+ cells were continually cultured in serum-free conditioned erythrocyte culture medium with 100 ng/mL SCF (Peprotech, Rehovot, Israel), 10 ng/mL IL-3 (Peprotech), and 6 IU/mL recombinant EPO (Recormon Epoetin beta, Roche) with a half-volume medium change twice a week. Serum-free culture medium consisted of StemPro-34 SFM Complete Medium (Gibco, Grad Island, NY) supplemented with 1% bovine serum albumin (Sigma), 150 μg/mL iron-saturated human transferrin (Sigma), 50 μg/mL insulin (Sigma), 90 ng/mL ferrous nitrate (Sigma), 2 mMol/L L-glutamine (Sigma), 1.6×10^{-4} mol/L monothioglycerol (Sigma), 30.8 μM/L vitamin C (Sigma), 2 μg/mL cholesterol (Sigma), and 1% penicillin-streptomycin solution (Gibco). In the second 7-day period of culture, the medium was replaced with serum-free conditioned medium with 3 IU/mL of recombinant EPO, 50 ng/mL of SCF, and 10 ng/mL of IL-3 for expansion and differentiation. During days 15–18 of culture, only one cytokine (EPO, at 2 IU/mL) was used for erythrocyte differentiation, and poloxamer 188 (Pluronic F68 (F68), Sigma; MW 8400) was added at a concentration of 0.05%. No cytokines were added during days 19–21 of culture, and only poloxamer 188 was added during this period. At the end of each phase, cultured cells were counted using a hemocytometer. The trypan blue stain was used in all cell counts, and only viable cells are included in the fold expansion results. All cultures were maintained at 37°C in a humidified atmosphere of 5% CO_2.

2.2. Assessment of Cell Morphology. Cell morphology was assessed using slides prepared by Cytospin using a cytocentrifuge (Cytospin 3, Shandon Scientific, Tokyo, Japan) at 800 rpm for 4 min followed by Wright-Giemsa staining. Pictures of the stained cells were taken with a digital camera (DP70, Olympus, Tokyo, Japan) at 400x magnification.

2.3. Differential Counting of Cultured Erythroblasts. Five differential countings were enumerated as proerythroblasts, early and late basophilic erythroblasts, polychromatic erythroblasts, and orthochromatic erythroblasts at 1000x magnification.

2.4. Flow Cytometric Analyses of Erythroid Markers. For flow cytometric analyses of cell surface antigens, a total of 1×10^5 cells were stained with phycoerythrin- (PE-) or fluorescein isothiocyanate- (FITC-) conjugated mouse anti-human antibodies against CD45, CD34, CD71, and glycophorin A (GpA) for 15 min, washed, resuspended in FACS buffer, and analyzed using a Cell Lab Quanta SC (Beckman Coulter, Fullerton, CA, USA) using a 488 nm wavelength laser. Cells were analyzed using two-color flow cytometry through WinMDI 2.9. The antibody combinations used were CD45-FITC/CD34-PE and CD71-FITC/GpA-PE, using G1-FITC/G1-PE as a control. All fluorescent conjugated monoclonal antibodies used were purchased from BD Biosciences (San Jose, CA).

2.5. Quantitative Real-Time Polymerase Chain Reaction. To evaluate gene expression levels during erythrocyte differentiation from different sources, we harvested over 1×10^6 cells from cultured erythrocytes at 7, 10, 14, and 17 days and isolated total RNA for quantitative polymerase chain reaction (PCR). Gene expression levels were quantified using the Light Cycler 480 Real-time PCR System (Roche Applied Science). Quantitative real-time polymerase chain reaction (qPCR) was performed using Light Cycler 480 SYBR Green I Master mix (Roche Applied Science) according to the manufacturer's instructions. Primers were designed [10, 11] and generated by Bioneer (Korea) (Table 1). Total RNA (800 ng) was used to generate first-strand cDNA using the Maxime RT Premix Kit (Intron Biotech). Differences between the Cp (crossing point) values of actin and target mRNAs for each sample were used to calculate ΔCp values. The ΔCp values derived from the isolated, undifferentiated CD34+ cells were used as control ΔCp values. Relative expression levels between samples and controls were determined using the formula: relative expression level = $2^{-(S\Delta Cp - C\Delta Cp)}$. Comparative real-time PCR with primers specific for GATA1, GATA2, EKLF, eALAS, and SCL/Tall (Table 1) was performed in triplicate. Reactions were performed at 95°C for 10 min, followed by 45 cycles of 95°C for 30 s, 60°C for 30 s, and 72°C for 30 s.

2.6. Functional Analysis of Hemoglobin. We used a Hemox-Analyzer (TCS, Medical Products Division, Southampton, PA) to measure the oxygen binding and dissociation abilities of the hemoglobin produced in mature erythrocytes derived from the mPB and cord blood. Hemox-Analyzer is an automatic system for recording blood oxygen equilibrium curves and related phenomena [12]. The operating principle of the Hemox-Analyzer is based on dual-wavelength spectrophotometry for the measurement of the optical properties of hemoglobin and a Clark electrode for measuring the oxygen partial pressure in millimeters of mercury. The resulting signals from both measuring systems are fed to the *X-Y* recorder. Both the P_{50} value and observation of the fine

(a)

(b)
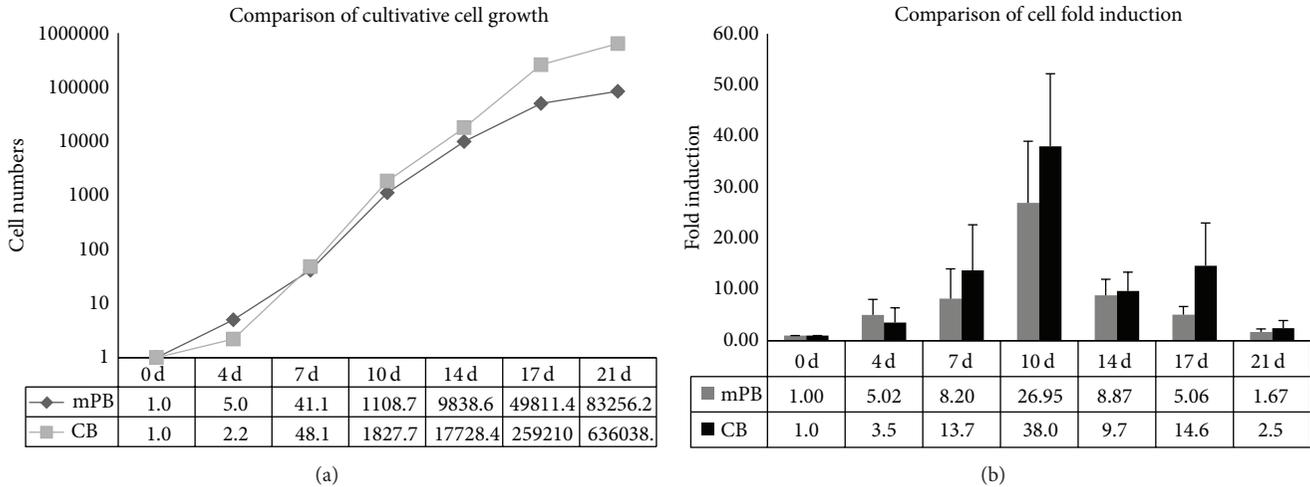
FIGURE 1: Comparison of cell growth in PB- and CB-derived CD34+ cell cultures. Stem cells were cultured for 21 days and counted at the end of each phase. (a) Erythroid cell amplification (mean ± standard deviation) of mPB- and CB-derived CD34+ cells. (b) Numbers of total cells expanded from cultures of mPB- and CB-derived CD34+ cells. CB-CD34+ cells exhibit higher amplification efficiency than mPB cells. $^{*}P < 0.001$.

TABLE 1: Real-time polymerase chain reaction primers.

Gene	Primer sequence
β-actin	
Forward primer	5′-ATTGGCAATGAGCGGTTC-3′
Reverse primer	5′-GGATGCCACAGGACTCCAT-3′
GATA-1	
Forward primer	5′-CACTGAGCTTGCCACATCC-3′
Reverse primer	5′-ATGGAGCCTCTGGGGATTA-3′
GATA-2	
Forward primer	5′-GGCAGAACCGACCACTCATC-3′
Reverse primer	5′-TCTGACAATTTGCACAACAGGTG-3′
eALAS	
Forward primer	5′-GATGTGAAGGCTTTCAAGACAGA-3′
Reverse primer	5′-GGAAAATGGCTTCCTTAGGC-3′
EKLF	
Forward primer	5′-ATCGAGTGAAGAGGAGACCTTCC-3′
Reverse primer	5′-TGAAGATACGCCGCACAACTT-3′
SCL/Tal1	
Forward primer	5′-ACACACAGGATGACTTCCTC-3′
Reverse primer	5′-CCCATGTCCTGCGC-3′

structure of the curve can furnish information about the delivery of oxygen to tissues. CD34+ cells derived from CB and mPB that were cultured for 17 days in three separate phases were analyzed using this system. Normal red blood cells were used as a control.

2.7. Capillary Zone Electrophoresis.

After 17 days of culture, 1 × 10⁸ cells were collected and assessed by capillary zone electrophoresis. Capillary zone electrophoresis was performed as described previously using the Sebia Capillary system (Sebia, Norcross, GA) [13]. Differentiated erythrocytes (5×10^7 cells) were centrifuged at 5,000 rpm for 5 minutes. Thereafter, the culture medium was removed, and the erythrocyte pellet was vortexed for 5 s. Electrophoresis was performed in alkaline buffer (pH 9.4) provided by the manufacturer (Sebia), with separation primarily due to the pH of the solution and endosmosis. The hemoglobin was measured at a wavelength of 415 nm. Electrophoretograms were recorded with the location of specific hemoglobin in specific zones.

2.8. Statistical Analysis.

Student's t-test was performed using Excel (Microsoft). P values less than 0.05 were considered statistically significant.

3. Results

3.1. In Vitro Culture Supports the Differentiation of Erythrocytes.

The number of cell divisions observed significantly increased during the second phase of the culture period. Compared to mPB-CD34+ cells, CB-CD34+ cells have greater proliferative capacity during days 10–21of culture (Figure 1(a)). This difference led to CB cultures achieving a greater total number of cells than that of mPB cultures (636,038 ± 182,817 versus 83,256 ± 8,858). Cell growth in CB cell cultures exceeded that of mPB cell cultures in the second phase and early third phase of culture (Figure 1(b)). Following erythropoietic differentiation, decreased cell size, nuclear condensation, and nuclear extrusion were confirmed by Wright-Giemsa staining. Although there were no significant differences found, our results show that, in the blood type composition count, the CB HSCs have more multipotency while mPB-CD34+ cells show earlier differentiation into mature erythrocytes (Figure 2(a)). These results demonstrate that mPB- and CB-derived CD34+ HSCs have similar growth patterns and morphological characteristics, but mPB-derived CD34+ cells show faster maturation than CB-derived CD34+ cells (Figure 2(b)).

(a)

- ■ Orthochromatic erythroblast
- ■ Polychromatic erythroblast
- ■ Late basophilic erythroblast
- ▨ Early basophilic erythroblast
- ▨ Proerythroblast

(b)
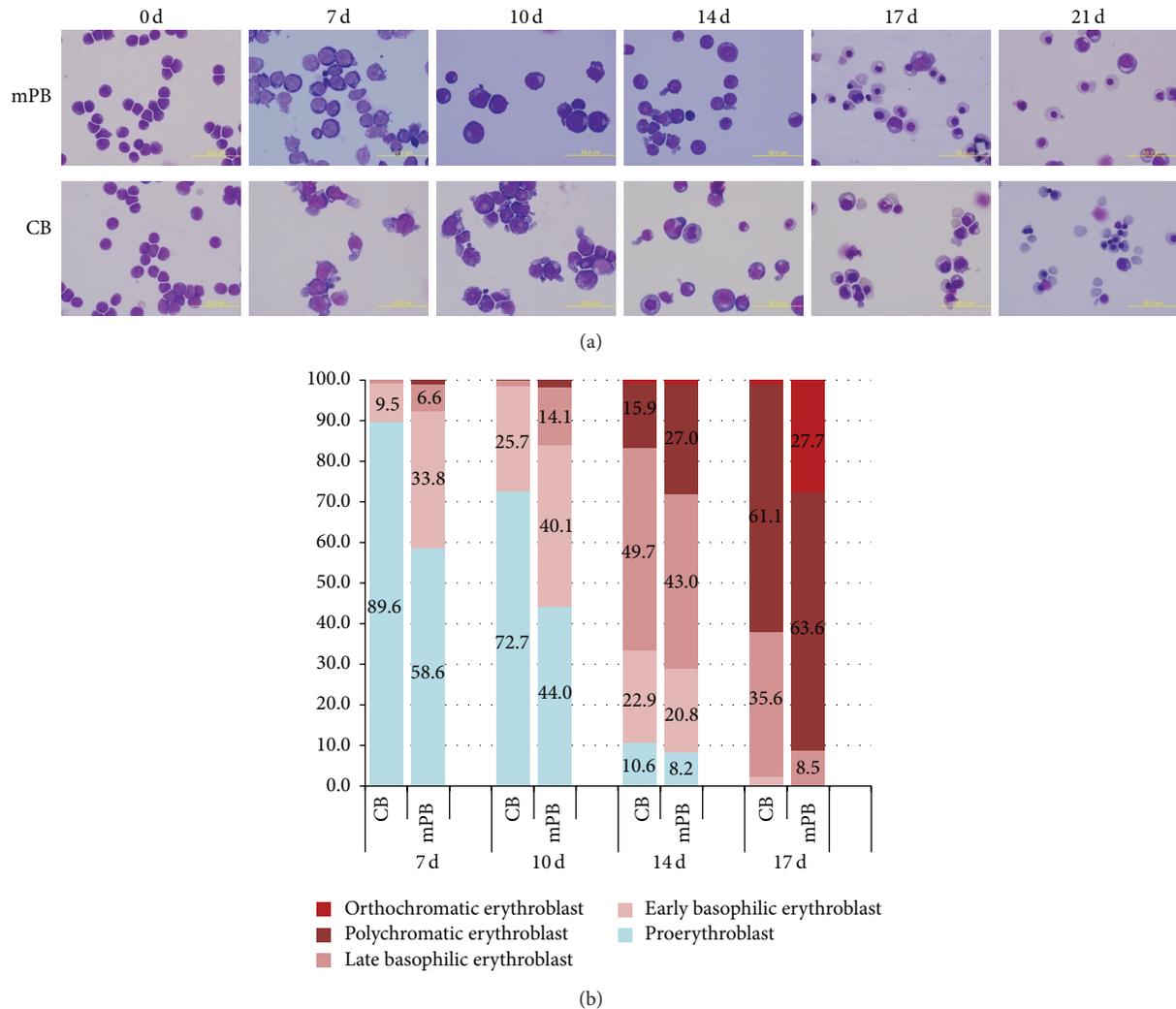
FIGURE 2: Comparison of cell morphological changes in mPB- and CB-derived CD34+ cell cultures. CD34+ cells selected from mPB and CB were cultured for 21 days *in vitro*. Morphological changes in differentiated cells from both sources were similar. No remarkably different patterns were found in the Giemsa staining photos (a). Based on the erythrocyte cell type counting at the end of each phase, the mPB-derived cells matured more rapidly than the cells derived from CB, even though cells from both sources have similar maturation patterns (b).

3.2. Similar Immunophenotypic Patterns.

CD34 and CD45 marker dramatically decreased and finally disappeared from the cells during differentiation, while GPA expression increased during the 21 days of culture. Although CD71 expression increased until early in the third phase of culture, it gradually decreased following final maturation (**Figure 3**). From the immunophenotypic data, we found no significant differences between mPB- and CB-derived CD34+ cells during erythroid cell maturation.

3.3. Different mRNA Expression Levels.

From our data, we can see different patterns in the differentiation of mPB- and CB-derived CD34+ cells. Our data clearly show that GATA-1 expression gradually increases during erythrocyte differentiation, especially in CB cells, while GATA-2 expression gradually decreases following cell maturation. The erythrocyte-specific isoforms ALAS and SCL/Tall are upregulated during erythrocyte differentiation and, in particular, show higher levels in mPB-derived cells than in CB-derived cells. Only one factor, EKLF, which is a β-globin gene transcription factor, increased during erythrocyte differentiation in mPB cells but, in contrast, decreased during differentiation of CB-derived cells (**Figure 4**). These results clearly demonstrate that mPB-derived CD34+ cells differentiate faster into erythrocytes with Hb-β production than CB cells. At the same time, under these *in vitro* culture conditions, CB-derived CD34+ hematopoietic cells exhibit higher multipotency than mPB cells.

3.4. Different Hemoglobin Type Development in mPB- and CB-Derived CD34+ Cells.

Over 80% of the hemoglobin produced by CB-derived CD34+ cells was hemoglobin subtype HbF, while only 17.5% was subtype HbA. Over 95% of the hemoglobin generated by mPB-derived cells was subtype HbA (**Figure 5**).
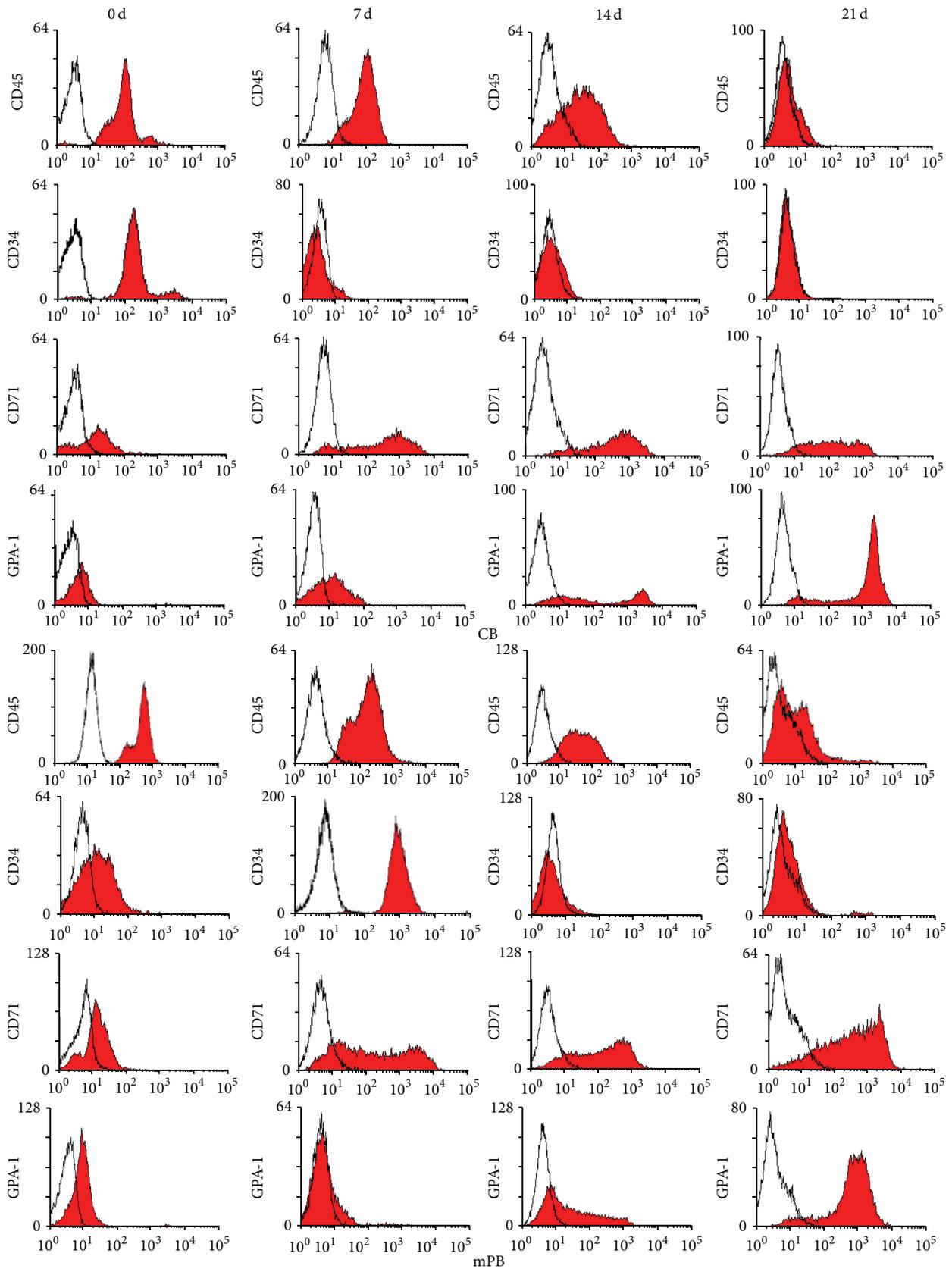
FIGURE 3: Phenotypic markers in erythrocytes differentiated from mPB- and CB-derived CD34+ cells. Cells (3×10^5) from the end of each phase of culture were stained, and hematopoietic and erythropoietic markers were measured. Flow cytometry results show similar patterns in the cultured cells from both sources and no significant differences.
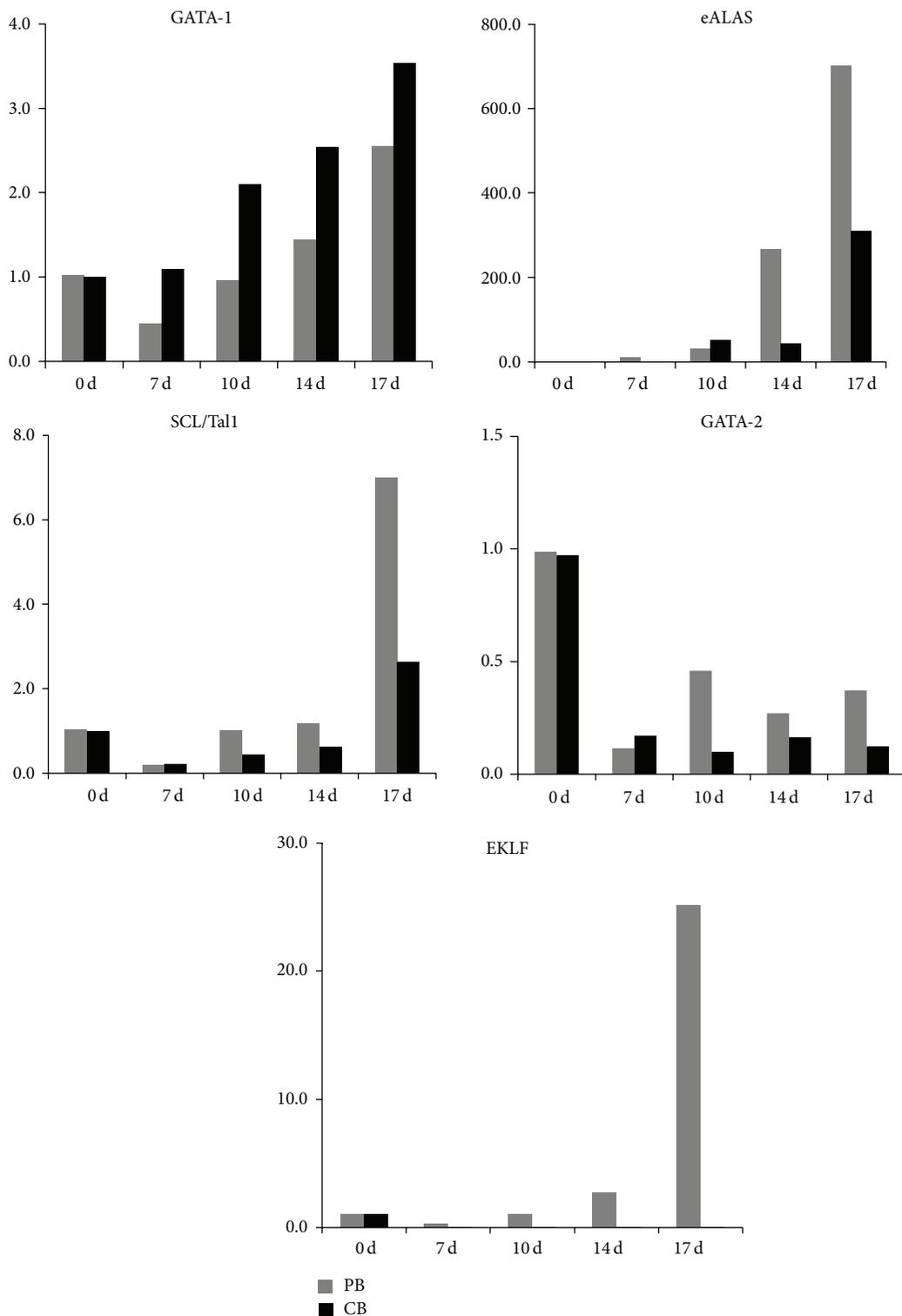
Figure 4: Erythrocyte-specific gene expression in mPB and CB cells. At the end of each phase of culture, cells were harvested, and total RNA was extracted for quantitative PCR. The expression of GATA-1, GATA-2, eALAS, EKLF, and SCL/Tal1 was measured by real-time PCR. The results show an increasing pattern for the GATA-1 transcript and a decreasing pattern for GATA-2, which did not significantly differ between mPB and CB cells. EKLF, eALAs, and SCL/Tall expression levels increased during differentiation but were significantly greater in mPB-derived erythrocytes than in those from CB.
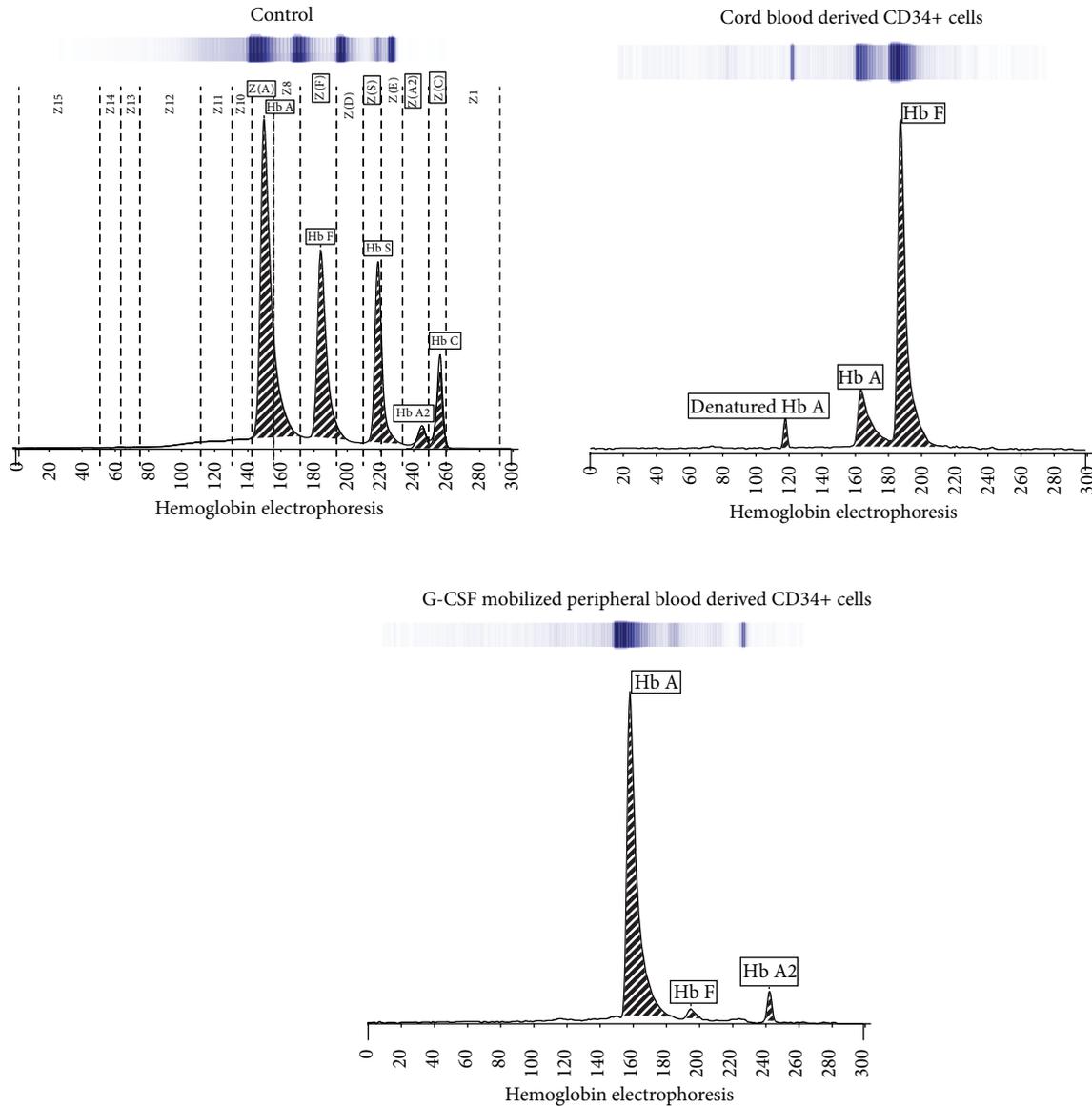
FIGURE 5: Electrophoretic determination of main hemoglobin subtypes in differentiated mPB and CB cells. Capillary zone electrophoresis shows distinct patterns of hemoglobin subtype expression between differentiated mPB and CB cells. About 80% of the hemoglobin produced by CB-CD34-derived erythrocytes is HbF, while only 17.5% is HbA. However, 95.5% of the hemoglobin produced by mPB-CD34-derived erythrocytes is HbA.

3.5. Similar Hemoglobin Dissociation Curve with Mature RBCs from mPB and CB Cells. While erythrocytes derived from each source have different combinations of HbA and HbF, similar hemoglobin dissociation curve was observed (Figure 6). Apart from this hemoglobin subtype variation, this result clearly shows that *in vitro* cultured RBCs can produce hemoglobin with oxygen binding and dissociation abilities equivalent to red blood cells produced *in vivo*.

4. Discussion

The shortage of blood supply and the ever-growing demand for blood transfusion represent a significant emerging issue in transfusion medicine. Shortage of donated blood and the risk of infection have created limitations in the availability of red blood cells available for transfusion. More recently, isolated CD34+ cells from human umbilical CB obtained from discarded maternity products and G-CSF-mPB obtained from healthy volunteers through leukapheresis have emerged as potential alternative sources of HSCs. The HSCs collected from both sources have high rates of proliferation and capacities for differentiation and create mature RBCs under the proper culture conditions through three phases of *in vitro* culture. We note that, though both types of stem cells show similar characteristics in general growth patterns with morphological and immunophenotypic changes, they
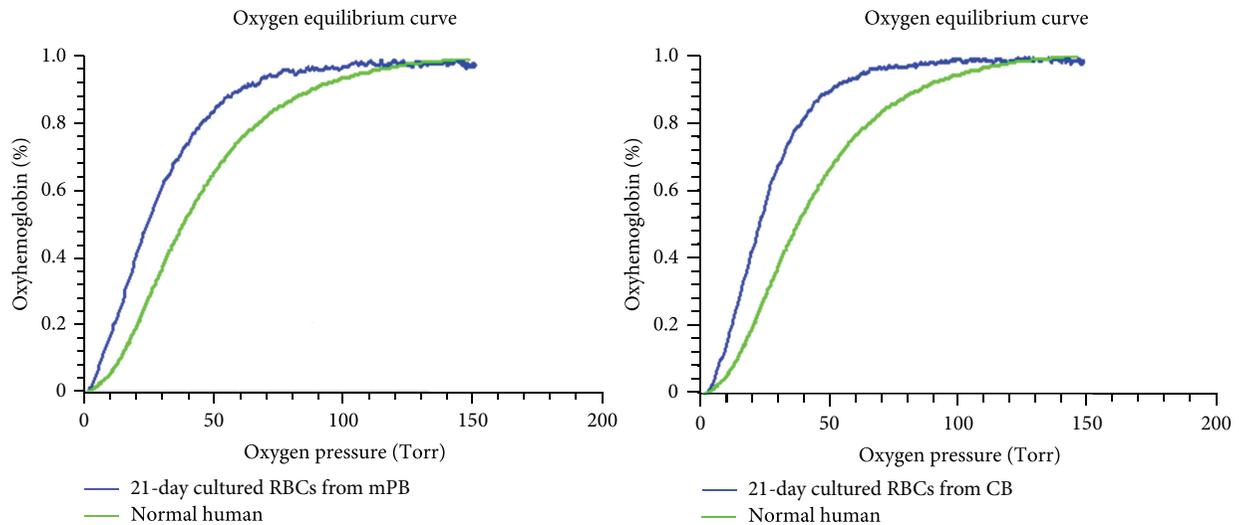
FIGURE 6: Hemox analysis in mPB and CB cells cultured for 21 days. Differentiated erythrocytes were harvested at the end of the 21 days of culture, and oxygen equilibria were measured by Hemox-Analyzer. Erythrocytes derived from mPB and from CB both show greater oxygenation abilities compared with normal human blood. There are no significant differences between differentiated mPB and CB cells.

show different characteristics in gene expression levels and hemoglobin subtype production.

Our results show that both mPB- and CB-derived CD34+ cells began to proliferate extremely quickly during 7–14 days of culture. However, both cell sources produce similar total cell numbers after 21 days of culture. And morphological changes in differentiated cells from both sources were similar, and no remarkable differences were found during the culture except when comparing cell differentiation rates. The mPB cells seemed to mature earlier than CB cells. These results show that mPB cells, from circulating blood, possess more progenitor cells than CB and have the ability of rapid differentiation into the mature RBCs. Following cell growth at the end of each cell culture phase, mPB- and CB-derived CD34+, GPA, and CD70 (transferrin receptor) expression showed similar patterns in flow cytometry analyses. These data are consistent with previous results regarding erythrocyte induction mechanisms [8, 14]. To confirm whether the initial exposition of cells is due to different sources derived differentiation, gene expression profiles were analyzed by quantitative RT-PCR. GATA-1 is a transcription factor that determines erythroid differentiation, survival, and β-globin gene expression [15]. GATA-2 inhibits GATA-1 function. GATA-2 expression exhibited a downregulation following erythropoietin stimulation, and its levels were higher in cultured mPB cells. This can be explained in earlier differentiation into mature RBCs in mPB source cells than in CB. This finding is also consistent with the result of differential counts that mPB showed faster shift from pronormoblasts to orthochromatic normoblasts in comparison to CB. Ikonomi et al. have previously shown that GATA-2 preferentially increases γ-globin gene expression, indicating that the prolonged expression of GATA-2 contributes to the early increase in γ-globin in CB [16]. EKLF binds specifically to the β-globin promoter and is critical in establishing chromatin structure for high-level β-globin transcription via

its acetylation by CREB binding protein [17]. SCL/Tall is required for the progression of erythroid differentiation, and enforced expression of SCL/Tall increases β-globin expression and BFU-E and CFU-E production [18]. Because these transcription factors are closely related to increased β-globin gene expression, changes in their expression may account for the delay and reduction of β-globin expression in CB-derived differentiated cells. The HbA- and HbF-related gene expression tests exhibit different expression levels depending on the cell source. We cultured mPB- and CB-derived CD34+ cells through three phases, harvested them after 17 days of culture, and analyzed them by hemoglobin type testing. These results clearly demonstrated different subtypes of hemoglobin expressed by mPB- and CB-derived mature cells. CB-derived cells mostly express HbF and mPB-derived cells mainly express HbA, but, based on these data, the original sources of these cells appear to possess different propensities for hemoglobin production patterns. These results demonstrate that hemoglobin subtypes are not related to culture conditions and culture time but are strongly affected by the source material. To evaluate the function of the differentiated mPB and CB cells, CD34+ cells derived from each source were expanded and differentiated to large cell numbers of up to a total of 5×10^7 cells, and oxygen equilibria were measured by Hemox-Analyzer. From the result, the oxygen dissociation curves indicate that the cells from both sources do not significantly differ from one another with respect to hemoglobin function. Although the types of hemoglobin expression differed between CB- and mPB-derived mature cells, the oxygen binding and dissociation curves may be similar due to variation among adult type hemoglobin, fetal type hemoglobin, or mixture of both types *in vitro* culture processing after 17 days of culture. The cultured cells, indeed, have slightly greater deoxygenation functionalities compared with normal cells, which showed the immaturity in shift to left.

In summary, mPB and CB are undoubtedly excellent sources for mature RBC production and may be key in contributing to a solution for the RBC supply shortage problem. Our study shows that, despite similar phenotypes and functionalities following erythrocyte maturation, the two are discrete in that they show different Hb types and gene expression levels. This study demonstrates distinctions that should be taken into account when choosing the source of HSCs for artificial mature RBC production form stem cells.

Conflict of Interests

The authors declare that there is no conflict of interests regarding the publication of this paper.

Acknowledgment

References

[1] World Health Organization, "Global Database on Blood Safety (GDBS)," Summary Report 2011, 2011.

[2] Y. Ebihara, F. Ma, and K. Tsuji, "Generation of red blood cells from human embryonic/induced pluripotent stem cells for blood transfusion," *International Journal of Hematology*, vol. 95, pp. 610–616, 2012.

[3] C. Mazurier, L. Douay, and H. Lapillonne, "Red blood cells from induced pluripotent stem cells: hurdles and developments," *Current Opinion in Hematology*, vol. 18, no. 4, pp. 249–253, 2011.

[4] M.-C. Giarratana, L. Kobari, H. Lapillonne et al., "Ex vivo generation of fully mature human red blood cells from hematopoietic stem cells," *Nature Biotechnology*, vol. 23, no. 1, pp. 69–74, 2005.

[5] K. Miharada, T. Hiroyama, K. Sudo, T. Nagasawa, and Y. Nakamura, "Efficient enucleation of erythroblasts differentiated in vitro from hematopoietic stem and progenitor cells," *Nature Biotechnology*, vol. 24, no. 10, pp. 1255–1256, 2006.

[6] E. J. Baek, H.-S. Kim, S. Kim, H. Jin, T.-Y. Choi, and H. O. Kim, "In vitro clinical-grade generation of red blood cells from human umbilical cord blood CD34+ cells," *Transfusion*, vol. 48, no. 10, pp. 2235–2245, 2008.

[7] D. Boehm, W. G. Murphy, and M. Al-Rubeai, "The potential of human peripheral blood derived CD34+ cells for ex vivo red blood cell production," *Journal of Biotechnology*, vol. 144, no. 2, pp. 127–134, 2009.

[8] E. J. Baek, H.-S. Kim, J.-H. Kim, N. J. Kim, and H. O. Kim, "Stroma-free mass production of clinical-grade red blood cells (RBCs) by using poloxamer 188 as an RBC survival enhancer," *Transfusion*, vol. 49, no. 11, pp. 2285–2295, 2009.

[9] H. O. Kim, "*In-vitro* stem cell derived red blood cells for transfusion: are we there yet?" *Yonsei Medical Journal*, vol. 55, pp. 304–309, 2014.

[10] M. Vlaski, X. Lafarge, J. Chevaleyre, P. Duchez, J.-M. Boiron, and Z. Ivanovic, "Low oxygen concentration as a general physiologic regulator of erythropoiesis beyond the EPO-related downstream tuning and a tool for the optimization of red blood cell production ex vivo," *Experimental Hematology*, vol. 37, no. 5, pp. 573–584, 2009.

[11] H. M. Rogers, X. Yu, J. Wen, R. Smith, E. Fibach, and C. T. Noguchi, "Hypoxia alters progression of the erythroid program," *Experimental Hematology*, vol. 36, no. 1, pp. 17–27, 2008.

[12] D. L. Vanhille, R. H. Nussenzveig, C. Glezos, S. Perkins, and A. M. Agarwal, "Best practices for use of the HEMOX analyzer in the clinical laboratory: quality control determination and choice of anticoagulant," *Laboratory Hematology*, vol. 18, pp. 17–19, 2012.

[13] D. F. Keren, D. Hedstrom, R. Gulbranson, C.-N. Ou, and R. Bak, "Comparison of Sebia Capillarys capillary electrophoresis with the Primus high-pressure liquid chromatography in the evaluation of hemoglobinopathies," *American Journal of Clinical Pathology*, vol. 130, no. 5, pp. 824–831, 2008.

[14] H. O. Kim and E. J. Baek, "Red blood cell engineering in stroma and serum/plasma-free conditions and long term storage," *Tissue Engineering A*, vol. 18, no. 1-2, pp. 117–126, 2012.

[15] R. Ferreira, K. Ohneda, M. Yamamoto, and S. Philipsen, "GATA1 function, a paradigm for transcription factors in hematopoiesis," *Molecular and Cellular Biology*, vol. 25, no. 4, pp. 1215–1227, 2005.

[16] P. Ikonomi, C. T. Noguchi, W. Miller, H. Kassahun, R. Hardison, and A. N. Schechter, "Levels of GATA-1/GATA-2 transcription factors modulate expression of embryonic and fetal hemoglobins," *Gene*, vol. 261, no. 2, pp. 277–287, 2000.

[17] W. Zhang, S. Kadam, B. M. Emerson, and J. J. Bieker, "Site-specific acetylation by p300 or CREB binding protein regulates erythroid Krüppel-like factor transcriptional activity via its interaction with the SWI-SNF complex," *Molecular and Cellular Biology*, vol. 21, no. 7, pp. 2413–2422, 2001.

[18] E. Ravet, D. Reynaud, M. Titeux et al., "Characterization of DNA-binding-dependent and -independent functions of SCL/TAL1 during human erythropoiesis," *Blood*, vol. 103, no. 9, pp. 3326–3335, 2004.

Research Article

Evaluation of Three Automated Nucleic Acid Extraction Systems for Identification of Respiratory Viruses in Clinical Specimens by Multiplex Real-Time PCR

Yoonjung Kim,[1] Mi-Soon Han,[1] Juwon Kim,[2] Aerin Kwon,[3] and Kyung-A Lee[1]

[1] Department of Laboratory Medicine, Yonsei University College of Medicine, 211 Eonju-ro, Gangnam-gu,
    Seoul 135-720, Republic of Korea
[2] Department of Laboratory Medicine, Yonsei University Wonju College of Medicine, Wonju, Republic of Korea
[3] Green Cross Laboratories, Yongin, Republic of Korea

Correspondence should be addressed to Kyung-A Lee; kal1119@yuhs.ac

A total of 84 nasopharyngeal swab specimens were collected from 84 patients. Viral nucleic acid was extracted by three automated extraction systems: QIAcube (Qiagen, Germany), EZ1 Advanced XL (Qiagen), and MICROLAB Nimbus IVD (Hamilton, USA). Fourteen RNA viruses and two DNA viruses were detected using the Anyplex II RV16 Detection kit (Seegene, Republic of Korea). The EZ1 Advanced XL system demonstrated the best analytical sensitivity for all the three viral strains. The nucleic acids extracted by EZ1 Advanced XL showed higher positive rates for virus detection than the others. Meanwhile, the MICROLAB Nimbus IVD system was comprised of fully automated steps from nucleic extraction to PCR setup function that could reduce human errors. For the nucleic acids recovered from nasopharyngeal swab specimens, the QIAcube system showed the fewest false negative results and the best concordance rate, and it may be more suitable for detecting various viruses including RNA and DNA virus strains. Each system showed different sensitivity and specificity for detection of certain viral pathogens and demonstrated different characteristics such as turnaround time and sample capacity. Therefore, these factors should be considered when new nucleic acid extraction systems are introduced to the laboratory.

1. Introduction

Respiratory viruses can cause mild to severe illnesses as well as frequent complications. They frequently cause pneumonia in children, especially those younger than 2 years (up to approximately 80%) [1, 2]. For adult patients in the ICU, these pathogens account for 28% of pneumonia cases, with mortality rates comparable to those of bacterial pneumonia [3]. The mean annual incidence of respiratory tract infections in the United States was reported to be 4.2 and 1.2 for the first and the second years of a child's life, respectively. Furthermore, 27% of respiratory tract infections resulted from coinfection with two or more viruses, including rhinovirus, human coronavirus, and adenovirus [4]. Since the year 2000, many new respiratory viruses have been identified including H5N1 avian influenza, SARS-coronavirus, human coronavirus NL63, human coronavirus HKU1, human metapneumovirus, human bocavirus, and human rhinovirus type C [5, 6]. Therefore, simultaneous identification of multiple viruses is needed for timely patient management.

Detection or characterization of the respiratory viruses by conventional diagnostic techniques such as cell culture, direct fluorescent antibody detection (DFA), and serological testing can be difficult and time-consuming [7–9]. Thus, rapid and highly accurate PCR methods have been numerously evaluated and multiplex real-time (RT)-PCR method is currently considered as the best technique for the detection and typing of comprehensive panel for many common respiratory viruses [7, 10, 11].

High-quality nucleic acid extraction is necessary for the multiplex RT-PCR assays as the results are greatly influenced by the nucleic acid quality [12, 13]. As the conventional manual nucleic acid extraction methods are prone to contamination and inter- and intraoperator variability [14, 15], various automated nucleic acid extraction methods have been introduced.

Some automated nucleic acid extraction systems including the easyMGA system (Biomérieux), the Qiasymphony (Qiagen), Biorobot EZ1, and MgaNA pure Compact (Roche) were evaluated for stool, nasal, and nasopharyngeal aspirate samples in previous study [16–18]. However, these automated nucleic acid extraction systems were evaluated using multiplex PCR or multiples real-time PCR assays which are capable of detecting only up to 5 viruses simultaneously in a single patient sample. Only recently, multiple real-time PCR assay which is capable detecting more than 14 viruses simultaneously was developed and widely used [19, 20]. But a comprehensive comparison of the automated extraction systems for these multiplex RT-PCR using nasopharyngeal aspirate samples has never been carried out. The EZ1 Advanced XL and the QIAcube systems have been popularly used in medical laboratories for DNA/RNA extraction, whereas the MICROLAB Nimbus IVD system is newly introduced. Therefore, we evaluated the three different automated nucleic acid extraction systems for multiplex RT-PCR using clinical nasopharyngeal swab specimens.

2. Materials and Methods

2.1. Clinical Specimen Collection. A total of 84 nasopharyngeal swabs (Universal Transport Medium, Copan Diagnostics, Murrieta, CA, USA) were collected from 20 adult and 64 pediatric patients with signs and/or symptoms of the respiratory infection between February and July, 2012. All specimens were stored at 2–8°C for up to 72 hours prior to processing. The study was approved by the Institutional Review Boards of Gangnam Severance Hospital.

2.2. Nucleic Acid Extraction. Three different automated systems were used for the nucleic acid extraction. QIAcube system (Qiagen, Hilden, Germany) with QIAamp MinElute Virus Spin Kit (Qiagen), EZ1 Advanced XL system (Qiagen) with EZ1 Advanced XL Virus Mini kit v2.0 (Qiagen), and MICROLAB Nimbus IVD system (Hamilton, Reno, NV, USA) with STARMag96 Virus kit (Seegene, Seoul, Korea) were evaluated. Three aliquot samples were separated from each of the specimens, and nucleic acid of each aliquot samples was extracted on the same day by three different automated systems in a single laboratory. The sample and elution volumes used in this study were 150 μL and 60 μL for the QIAcube system, 400 μL and 60 μL for the EZ1 Advanced XL system, and 600 μL and 100 μL for the MICROLAB Nimbus IVD system, respectively. For the quality control of the entire nucleic acid extraction process and RT-PCR, 10 μL of bacteriophage MS2 (AnyplexTMII RV16 detection, Seegene) was added to each sample as the internal control in order to check the entire process from nucleic acid extraction

to PCR. cDNA was synthesized using the cDNA Synthesis Premix (Seegene) which included reverse transcriptase and a random hexamer, according to the manufacturer's protocol.

2.3. Real-Time PCR and Melting Curve Analysis. Anyplex II RV16 Detection kit (Seegene) was used to detect 14 RNA viruses and 2 DNA viruses including human adenovirus (ADV), influenza A and B viruses (FluA, FluB), human parainfluenza viruses 1/2/3/4 (PIV1/2/3/4), human rhinovirus A/B/C (RV A/B/C), human respiratory syncytial viruses A and B (RSV-A, RSV-B), human bocaviruses 1/2/3/4 (BoV1/2/3/4), human coronaviruses 229E, NL63 and OC43 (CoV-229E, CoV-NL63, CoV-OC43), human metapneumovirus (MPV), and human enterovirus (EV). A real-time PCR reaction mixture was prepared with as follows: 8 μL cDNA, 4 μL 5x RV primer, 4 μL 8-methoxypsoralen solution, and 4 μL 5x Master Mix. Seegene's unique real-time PCR and melting curve analysis technique called "Tagging Oligonucleotide Cleavage and Extension" assay (http://www.seegene.co.kr/neo/en/introduction/core_toce.php) was performed using CFX96 real-time PCR detection system (Bio-Rad, Hercules, CA, USA) as follows: (1) 1 cycle of initial denaturation at 95°C for 15 min, (2) 50 cycles of denaturation at 94°C for 30 sec, annealing at 60°C for 1 min, and extension at 72°C for 30 sec, (3) 1 cycle of cooling the reaction mixture at 55°C for 30 sec, and (4) melting double-stranded DNA into single strands by raising the temperature to 85°C. The fluorescence was measured continuously during the temperature rise from 55°C. And, the melting peaks were derived from the initial fluorescence (F) versus temperature (T) curves by plotting the negative derivative of fluorescence over temperature versus temperature ($-dF/dT$ versus T) by Seegene software [19]. If internal control was not detected in real-time PCR reaction, the results were sorted as "invalid results" by Seegene software. Plasmids containing the target sequence were included as positive controls.

2.4. Analytical Sensitivity of the Automated Nucleic Acid Extraction Systems. One DNA (ADV) and 2 RNA (RSV-A and FluA) viral reference strains (ATCC VR-3, ADV; ATCC VR-26, RSV-A; ATCC VR-544, FluA) were obtained from the Korean Bank for Pathogenic Viruses (Korea University College of Medicine, Seoul, Republic of Korea). The reference strains were serially diluted with 10-fold saline buffer and they were made as five-level samples: ADV (10^{-6} to 10^{-10}), FluA (10^{-5} to 10^{-9}), and RSV (10^{-4} to 10^{-8}). And each diluted sample was extracted 5 times using the 3 different automated nucleic acid extraction systems.

2.5. Interpretation of the Results. When all 2 or 3 of the automated nucleic acid extraction systems yielded the same results, they were considered as a true positive and we considered it as a true negative when all 3 of the automated nucleic acid extraction systems yielded "not detected." In case of positive results from only 1 of the three automated nucleic acid extraction systems, the confirmatory test performed with the Seeplex RV15 ACE Detection kit (Seegene). When the confirmatory test also yielded negative result, it was

TABLE 1: Distribution of respiratory viruses in 44 positive nasopharyngeal swab specimens.

Virus type	Single infection ($n = 33$)	Dual infection ($n = 8$)	Triple infection[a] ($n = 3$)	Total (%) ($n = 44$)
RV	10	7	2	19 (32.8)
MPV	3	2	3	8 (13.8)
PIV3	5	2	1	8 (13.8)
RSV-A	6	1	0	7 (12.1)
ADV	1	2	2	5 (8.6)
FluB	2	0	1	3 (5.2)
FluA	2	0	0	2 (3.4)
BoV	1	1	0	2 (3.4)
EV	1	1	0	2 (3.4)
CoV-OC43	1	0	0	1 (1.7)
PIV1	1	0	0	1 (1.7)
Total (%)	33 (56.9)	16 (27.6)	9 (15.5)	58 (100.0)

[a]RV + MPV + ADV ($n = 1$), RV + MPV + FluB ($n = 1$) and MPV + ADV + PIV3 ($n = 1$).
RV: human rhinovirus; MPV: human metapneumovirus; PIV3: human parainfluenza virus 3; RSV-A: human respiratory syncytial virus A; ADV: human adenovirus; FluB: influenza B; FluA: influenza A; BoV: human bocavirus; EV: human enterovirus; CoV-OC43: human coronavirus OC43; PIV1: human metapneumovirus.

considered as a false positive [16]. Among these positive results from only 1 of the three automated nucleic acid extraction systems, three pathogens (FluB, HRV, and HBoV) were detected when repeated with the Seeplex RV15 ACE Detection kit (Seegene). These discordant results were also confirmed by PCR and sequencing. The following primers were used for the sequencing analysis: FluB-NF (GTC CAT CAA GCT CCA GTT TT), FluB-NR (TCT TCT TAC AGC TTG CTT GC) (145 bp), HRV-5′NCRF (GCA CTT CTG TTT CCC C), HRV-5′NCRR (CGG ACA CCC AAA GTA G) (380 bp), HBoV-NP1F (GAC CTC TGT AAG TAC TAT TAC), HBoV-NP1R (CTC TGT GTT GAC TGA ATA CAG) (354 bp) [21].

2.6. Statistical Analysis. Statistical analysis was performed using SPSS Statistics 20.0 (SPSS Inc., Chicago, IL, USA) and Analyse-it 2.22 (Analyse-it Software Ltd., Leeds, UK). Kappa coefficients were calculated to estimate the agreement between the results by different utilized methods.

3. Results

3.1. Detection of Respiratory Viruses in Clinical Specimens. Among the 84 nasopharyngeal swab specimens, viral pathogens were detected in 44 specimens (detection rate: 52.4%). A total of 58 pathogens including multiple infections were detected in 44 specimens and the proportions of single and dual and triple infections were 75.0%, 18.2% and 6.8%, respectively. Based on frequency of detection, RV (32.8%) was more than one-third of detected pathogens, followed by MPV (13.8%), PIV3 (13.8%), RSV-A (12.1%), and ADV (8.6%). And RV was the predominant pathogen in case of both single (30.3%, $n = 10/19$) and dual (87.5%, $n = 7/8$) respiratory infections (Table 1).

3.2. Comparison of the PCR Results from 3 Automated Nucleic Acid Extraction Systems. The numbers of positives for respiratory viruses ranged from 54 to 59. The nucleic acids extracted by EZ1 Advanced XL showed higher positive rates for virus detection than the others. Among the discrepant results, three positive nucleic acid extracts, which were obtained by only one of the three automated nucleic acid extraction systems, were confirmed by sequencing. Two positive nucleic acid extracts including RV ($n = 1$) and BoV ($n = 1$) were obtained by the QIAcube system, while one FluB positive nucleic acid extract was obtained with EZ1 Advanced XL (Table 2). On the basis of Section 2.5, sensitivity, specificity, concordance rate, and kappa coefficient for the 3 automated nucleic acid extraction systems are shown in Table 3. The percent sensitivity and specificity of the 3 systems ranged from 87.2% to 93.3% and from 82.9% to 94.6%, respectively. The concordance rates between the true results and the 3 systems ranged from 88.3% to 94.2%. The kappa coefficients ranged from 0.76 to 0.88 ($P < 0.001$ for all values). The QIAcube system yielded the best percent sensitivity and concordance rate, while the MICROLAB Nimbus IVD system demonstrated the lowest sensitivity and the highest specificity. Sensitivity and specificity of the 3 systems were also evaluated for the most commonly detected 5 viral pathogens. The QIAcube system showed the highest sensitivity for the RNA viruses (RV, MPV, PIV3, and RSV-A), while the EZ1 Advanced XL system demonstrated the best percent sensitivity for the ADV.

One of two BoVs was not detected by the EZ1 Advanced XL system, while all three were detected by the QIAcube system (Table 2). For DNA viruses, including ADV and BoV, the QIAcube system and the EZ1 Advanced XL system demonstrated equal sensitivity of 85.7%.

TABLE 2: Comparison of detection of respiratory virus by three automatic extraction methods from nasopharyngeal swab specimens.

Virus	QIAcube	EZ1 advanced XL	MICROLAB Nimbus IVD	Total number of specimens
RV	+	+	+	14
	+	−	+	3
	+	−	−	1[a]
	−	+	+	1
	−	+	−	2[b]
MPV	+	+	+	7
	+	+	−	1
PIV3	+	+	+	8
PIV1	+	+	+	1
	−	+	−	1[b]
PIV4	+	−	−	1[b]
RSV-A	+	+	+	7
	−	+	−	1[b]
ADV	+	+	+	2
	−	+	+	1
	+	+	−	2
	−	+	−	3[b]
FluB	+	+	+	2
	−	+	−	1[a]
FluA	+	+	+	2
BoV	+	+	+	1
	+	−	−	1[a]
EV	+	+	+	2
	+	−	−	1[b]
CoV-OC43	1	1	1	1
CoV-NL63	−	−	+	1[b]
CoV-229E	−	−	+	1[b]
Total	**57**	**59**	**54**	**68**

[a]Virus detected by only 1 of the three automated nucleic acid extraction systems, and we confirmed this result by sequencing analysis and confirmed it as "true positive."
[b]Virus detected by only 1 of the three automated nucleic acid extraction systems, but they were not detected by repeated test with the Seeplex RV15 ACE Detection kit (Seegene).

3.3. Characteristics of the Three Automated Nucleic Acid Extraction Systems.

Basic characteristics of the 3 automated nucleic acid extraction systems are summarized in Table 3. The QIAcube system employs the spin column principle, while the EZ1 Advanced XL and the MICROLAB Nimbus IVD systems use magnetic particles for the nucleic acid extraction. While sample and elution volumes can be adjusted in the QIAcube and the EZ1 Advanced XL systems, they are fixed in the MICROLAB Nimbus IVD system. The EZ1 Advanced XL system demonstrated the shortest turnaround time (TAT) per sample, followed by the QIAcube system and the MICROLAB Nimbus IVD system. The MICROLAB Nimbus IVD system was suitable for the downstream applications as it had the highest sample capacity and the automated PCR setup function.

3.4. Analytical Sensitivity of the Three Automated Nucleic Acid Extraction Systems.

The analytical sensitivity of the 3 automated nucleic acid extraction systems is showed in Table 4. The EZ1 Advanced XL system demonstrated the best analytical sensitivity for all 3 of the viral strains. There was little difference between the QIAcube and the MICROLAB Nimbus IVD systems with regards to analytical sensitivity.

4. Discussion

If a specimen with positive results for the same virus by more than 2 of 3 systems was used as the "gold standard," the performance of the QIAcube system was superior to the EZ1 Advanced XL system and the MICROLAB Nimbus IVD system in sensitivity and concordance rate (Table 3). The EZ1 Advanced XL system showed relatively high number of the discrepant results ($n = 12$) and false positives ($n = 7$), especially for ADV (3 false positives). However, it showed the best analytical sensitivity for ADV-3, FluA, and RSV-A (Table 4) and as well as the highest sensitivity for ADV in clinical specimens (Table 3). As the analytical sensitivity of

TABLE 3: Comparison of the PCR results from 3 automated nucleic acid extraction systems using a total of 84 nasopharyngeal specimens.

	QIAcube	EZ1 advanced XL	MICROLAB Nimbus IVD
Positive results	45 (53.6%)	45 (53.6%)	43 (51.2%)
True positive[a]	42	38	41
False positive[a] (virus type)	3 (PIV4, EV, RSV-B)	7 (PIV1, ADV ($n = 3$), RSV-A, RV ($n = 2$))	2 (CoV-NL63, CoV-229E)
Negative results	39 (46.4%)	39 (46.4%)	41 (48.8%)
True negative[a]	36	34	35
False negative[a] (virus type)	3 (FluB, RV, ADV)	5 (BoV, RV ($n = 4$))	6 (FluB, RV, MPV, BoV, ADV ($n = 2$))
Sensitivity (%)	93.3	88.4	87.2
Specificity (%)	92.3	82.9	94.6
Concordance rate (%)	94.2	88.3	92.2
Kappa coefficient[b] (95% CI)	0.88 (0.79 to 0.97)	0.76 (0.64 to 0.89)	0.84 (0.74 to 0.95)
RV sensitivity/specificity	94.7/100.0	78.9/96.9	94.7/100.0
MPV sensitivity/specificity	100.0/100.0	100.0/100.0	85.0/100.0
PIV3 sensitivity/specificity	100.0/100.0	100.0/100.0	100.0/100.0
RSV-A sensitivity/specificity	100.0/100.0	100.0/98.7	100.0/100.0
ADV sensitivity/specificity	80.0/100.0	100.0/96.2	60.0/100.0
Characteristics of three systems			
Principle	Spin column	Magnetic particle	Magnetic particle
Sample volume (μL)	≤200	100–400	600
Elution volume (μL)	20–150	60–150	100
Turnaround time[c] (min)	90	45	150
Sample capacity	12	14	48
Automated PCR set-up	Impossible	Impossible	Possible

[a]When all three automated nucleic acid extraction systems yielded the same results, they were considered "true positive" or "true negative." If only 1 system yielded negative result, it was considered "false negative." When the pathogen was detected from only 1 system, multiplex PCR and sequencing analysis were performed to confirm the result. [b]$P < 0.0001$ for all values. [c]includes lysis step but not the hands-on time.

TABLE 4: Analytical sensitivity of the three automated nucleic acid extraction systems.

Virus strain dilution factor	ADV-3 (detected/replicates)					FluA (detected/replicates)					RSV-A (detected/replicates)				
	10^{-6}	10^{-7}	10^{-8}	10^{-9}	10^{-10}	10^{-5}	10^{-6}	10^{-7}	10^{-8}	10^{-9}	10^{-4}	10^{-5}	10^{-6}	10^{-7}	10^{-8}
QIAcube (QIAGEN)	5/5	3/5	0/5	0/5	0/5	5/5	2/5	1/5	0/5	0/5	5/5	4/5	0/5	0/5	0/5
EZ1 (QIAGEN)	5/5	5/5	0/5	0/5	0/5	5/5	5/5	2/5	1/5	0/5	5/5	5/5	3/5	1/5	0/5
NIMBUS (Seegene)	5/5	4/5	0/5	0/5	0/5	5/5	4/5	0/5	0/5	0/5	5/5	2/5	1/5	0/5	0/5

the confirming test including the Seeplex RV15 ACE Detection kit (Seegene) and sequencing analysis could be lower than Anyplex II RV16 Detection kit (Seegene) [22], some of these false positive results could include true positive results. Therefore, we discerned that the EZ1 Advanced XL system is more suitable for ADV virus detection. The MICROLAB Nimbus IVD system showed the highest specificity (94.6%, only two false positives), but it demonstrated the lowest sensitivity (87.2%) with 6 false negatives (Table 3).

The sample and elution volumes used in this study were 150 μL and 60 μL for the QIAcube system, 400 μL and 60 μL for the EZ1 Advanced XL system, and 600 μL and 100 μL for the MICROLAB Nimbus IVD system, respectively. The relative concentration ratios of sample volume to elution volume were 2.5 for the QIAcube system, 6.7 for the EZ1 Advanced XL system, and 6.0 for the MICROLAB Nimbus IVD system, respectively. We used QIAcube system with sample volume 150 μL and elution volume 60 μL routinely in our laboratory. Therefore, we adjusted the sample volume and elution volume in the MICROLAB Nimbus IVD system and the EZ1 Advanced XL system similarly, but we could not do this in QIAcube system. Although the QIAcube system was performed with the lowest sample/elution volume ratio, it showed the best performance.

Previously, Chan et al. evaluated the performance of the NucliSens easyMAG (bioMerieux, Marcy l'Etoile, France) and BioRot 9604 automated nucleic acid extraction systems (Qiagen) in comparison with the manual QIAamp extraction method (Qiagen). In their study, these three different methods were evaluated with different sample volumes and elution volumes. The relative concentration ratios of the sample volume to elution volume were 4.5 for the NucliSens easyMAG, 2.5 for the BioRot 9604, and 1.0–2.3 for the manual QIAamp, respectively. However, the nucleic acids obtained by all three methods gave comparable sensitivities in PCR tests, and the three methods gave comparable viral loads [16] Therefore, we thought that the relative concentrative effect of the eluted nucleic acid may have little effect on the results of RT-PCR based methods. In a previous study, the MagNA Pure Compact machine with the MagNAPure Compact Nucleic Acid Isolation Kit I (Roche, Indianapolis, IN, USA) demonstrated more than 4-fold higher DNA recovery from the *S. pyogenes* than the other automated extraction systems including KingFisher-ML (ThermoFisher Scientific Inc., Worcester, MA, USA), Biorobot EZ1 (Qiagen), easyMAG (bioMerieux), and Biorobot MDX (Qiagen); however, it was less efficient in RNA purification from RSV and influenza A virus viruses. This may be due to RNA degradation or inefficient RNA binding to the magnetic beads [17]. Actually, the MagNAPure Compact Nucleic Acid Isolation Kit I was preferred for DNA extraction, although it did not include carried RNA. Inclusion of carried RNA could enhance the yield of a very few target molecules and reduce the chances of viral RNA degradation. In our study, all three extraction kits included carried RNA, and all three systems showed comparable efficiencies of RNA and DNA extraction (Table 4).

Turnaround time (TAT) per sample of the QIAcube system, EZ1 Advanced XL, and the MICROLAB Nimbus IVD systems were 7.5 minutes, 3.2 minutes, and 3.1 minutes,

respectively. Nucleic acid extraction systems using the magnetic particle principle had the shorter TAT per sample than the system which employs the spin column principle, probably due to its simplicity to perform [23].

Therefore, the systems using the magnetic particle may be more preferred for more rapid identification of the viral pathogens. The longer hands-on time of the MICROLAB Nimbus IVD systems was drawback, but it has the capability to run 3-4 fold more samples than other comparison systems at the same time and this system integrates fully automated steps from nucleic extraction to PCR setup function, allowing human errors to be minimized and providing more reliable results. This system is more suitable for laboratory which was carried on large samples for PCR.

5. Conclusion

In the present study, the QIAcube system showed the fewest false negative results and the best concordance rate, and it may be more suitable for detecting various viruses, including RNA and DNA virus strains. However, each system demonstrated different sensitivity and specificity for the detection of certain viral pathogens and different characteristics such as the carrier RNA, TAT, sample capacity, and automated PCR setup function. Therefore, according to the characteristics of the target patient group and the laboratory, these factors should be considered when the new nucleic acid extraction system is introduced into the laboratory.

Conflict of Interests

The authors declare that there is no conflict of interests regarding the publication of this paper.

Authors' Contribution

Yoonjung Kim and Mi-Soon Han contributed equally to this work.

Acknowledgment

References

[1] C. A. Sinaniotis, "Viral pneumonia in children: incidence and aetiology," *Paediatric Respiratory Reviews*, vol. 5, supplement 1, pp. S197–S200, 2004.

[2] C. M. B. Perez, "Prevalence of viral pathogens among pediatric patients admitted for pneumonia in a local tertiary hospital," *PIDSP Journal*, vol. 13, no. 1, 2012.

[3] S. H. Choi, S. B. Hong, G. B. Ko et al., "Viral infection in patients with severe pneumonia requiring intensive care unit admission," *The American Journal of Respiratory and Critical Care Medicine*, vol. 186, no. 4, pp. 325–332, 2012.

[4] M. P. Fairchok, E. T. Martin, S. Chambers et al., "Epidemiology of viral respiratory tract infections in a prospective cohort

of infants and toddlers attending daycare," *Journal of Clinical Virology*, vol. 49, no. 1, pp. 16–20, 2010.

[5] J. Dong, J. P. Olano, J. W. McBride, and D. H. Walker, "Emerging pathogens: challenges and successes of molecular diagnostics," *Journal of Molecular Diagnostics*, vol. 10, no. 3, pp. 185–197, 2008.

[6] E. B. Carstens, "Ratification vote on taxonomic proposals to the International Committee on Taxonomy of Viruses (2009)," *Archives of Virology*, vol. 155, no. 1, pp. 133–146, 2010.

[7] J. D. Fox, "Nucleic acid amplification tests for detection of respiratory viruses," *Journal of Clinical Virology*, vol. 40, supplement 1, pp. S15–S23, 2007.

[8] F. Gharabaghi, A. Hawan, S. J. Drews, and S. E. Richardson, "Evaluation of multiple commercial molecular and conventional diagnostic assays for the detection of respiratory viruses in children," *Clinical Microbiology and Infection*, vol. 17, no. 12, pp. 1900–1906, 2011.

[9] F. Gharabaghi, R. Tellier, R. Cheung et al., "Comparison of a commercial qualitative real-time RT-PCR kit with direct immunofluorescence assay (DFA) and cell culture for detection of influenza A and B in children," *Journal of Clinical Virology*, vol. 42, no. 2, pp. 190–193, 2008.

[10] F. de-Paris, C. Beck, A. B. Machado et al., "Optimization of one-step duplex real-time RT-PCR for detection of influenza and respiratory syncytial virus in nasopharyngeal aspirates," *Journal of Virological Methods*, vol. 186, no. 1-2, pp. 189–192, 2012.

[11] S. Bellau-Pujol, A. Vabret, L. Legrand et al., "Development of three multiplex RT-PCR assays for the detection of 12 respiratory RNA viruses," *Journal of Virological Methods*, vol. 126, no. 1-2, pp. 53–63, 2005.

[12] C. Mengelle, J.-M. Mansuy, K. Sandres-Sauné, C. Barthe, J. Boineau, and J. Izopet, "Prospective evaluation of a new automated nucleic acid extraction system using routine clinical respiratory specimens," *Journal of Medical Virology*, vol. 84, no. 6, pp. 906–911, 2012.

[13] F. Osman, T. Olineka, E. Hodzic, D. Golino, and A. Rowhani, "Comparative procedures for sample processing and quantitative PCR detection of grapevine viruses," *Journal of Virological Methods*, vol. 179, no. 2, pp. 303–310, 2012.

[14] K. Loens, K. Bergs, D. Ursi, H. Goossens, and M. Ieven, "Evaluation of NucliSens easyMAG for automated nucleic acid extraction from various clinical specimens," *Journal of Clinical Microbiology*, vol. 45, no. 2, pp. 421–425, 2007.

[15] S. C. Tan and B. C. Yiap, "DNA, RNA, and protein extraction: the past and the present," *Journal of Biomedicine and Biotechnology*, vol. 2009, Article ID 574398, 10 pages, 2009.

[16] K. H. Chan, W. C. Yam, C. M. Pang et al., "Comparison of the NucliSens easyMAG and Qiagen BioRobot 9604 nucleic acid extraction systems for detection of RNA and DNA respiratory viruses in nasopharyngeal aspirate samples," *Journal of Clinical Microbiology*, vol. 46, no. 7, pp. 2195–2199, 2008.

[17] G. Yang, D. E. Erdman, M. Kodani, J. Kools, M. D. Bowen, and B. S. Fields, "Comparison of commercial systems for extraction of nucleic acids from DNA/RNA respiratory pathogens," *Journal of Virological Methods*, vol. 171, no. 1, pp. 195–199, 2011.

[18] J. Verheyen, R. Kaiser, M. Bozic, M. Timmen-Wego, B. K. Maier, and H. H. Kessler, "Extraction of viral nucleic acids: comparison of five automated nucleic acid extraction platforms," *Journal of Clinical Virology*, vol. 54, no. 3, pp. 255–259, 2012.

[19] H. K. Kim, S. H. Oh, K. A. Yun, H. Sung, and M. N. Kim, "Comparison of Anyplex II RV16 with the xTAG respiratory viral panel and Seeplex RV15 for detection of respiratory viruses," *Journal of Clinical Microbiology*, vol. 51, no. 4, pp. 1137–1141, 2013.

[20] C. H. Cho, C. K. Lee, M. H. Nam et al., "Evaluation of the AdvanSure real-time RT-PCR compared with culture and Seeplex RV15 for simultaneous detection of respiratory viruses," *Diagnostic Microbiology and Infectious Disease*, vol. 79, no. 1, pp. 14–18, 2014.

[21] G. Zhang, Y. Hu, H. Wang, L. Zhang, Y. Bao, and X. Zhou, "High incidence of multiple viral infections identified in upper respiratory tract infected children under three years of age in Shanghai, China," *PLoS ONE*, vol. 7, no. 9, Article ID e44568, 2012.

[22] C. H. Cho, B. Chulten, C. K. Lee et al., "Evaluation of a novel real-time RT-PCR using TOCE technology compared with culture and Seeplex RV15 for simultaneous detection of respiratory viruses," *Journal of Clinical Virology*, vol. 57, no. 4, pp. 338–342, 2013.

[23] M. Kleines, K. Schellenberg, and K. Ritter, "Efficient extraction of viral DNA and viral RNA by the chemagic viral DNA/RNA kit allows sensitive detection of cytomegalovirus, hepatitis B virus, and hepatitis G virus by PCR," *Journal of Clinical Microbiology*, vol. 41, no. 11, pp. 5273–5276, 2003.

Research Article

Detection of Herpes Simplex and Varicella-Zoster Virus in Clinical Specimens by Multiplex Real-Time PCR and Melting Curve Analysis

Yun Ji Hong,[1,2] Mi Suk Lim,[2] Sang Mee Hwang,[1,2] Taek Soo Kim,[1,2] Kyoung Un Park,[1,2] Junghan Song,[1,2] and Eui Chong Kim[1]

[1] *Department of Laboratory Medicine, Seoul National University College of Medicine, Seoul 110-744, Republic of Korea*
[2] *Department of Laboratory Medicine, Seoul National University Bundang Hospital, 173-82 Gumiro, Bundanggu, Seongnam, Gyeonggido 463-707, Republic of Korea*

Correspondence should be addressed to Kyoung Un Park; m91w95pf@snu.ac.kr

Herpes simplex viruses types 1 and 2 (HSV-1 and HSV-2), and varicella-zoster virus (VZV) are common agents resulting in various forms of clinical manifestation from skin vesicle to disseminated viral infection. The aim of the present study was to develop a real-time PCR and melting curve analysis which detect and differentiate HSV-1, HSV-2, and VZV, to compare with PCR-RFLP using clinical specimens, and to introduce the 4-year experience in the clinical laboratory. Three pairs of primers for HSV-1, HSV-2, and VZV were designed. Primers for human endogenous retrovirus-3 (HERV-3), an internal control, were adopted. A hundred selected specimens and many clinical specimens were tested for methods comparison and assay validation. Increased sensitivity and specificity were obtained from real-time PCR. In review of results of clinical specimens submitted to clinical laboratory, a total of 46 of 3,513 specimens were positive in cerebrospinal fluids, blood, skin vesicles, genital swabs, aqueous humor, and ear discharge. Thus, this method could be a rapid and accurate alternative to virus culture and other molecular tests for detection and typing of HSV-1, HSV-2, and VZV.

1. Introduction

Alphaherpesvirinae, a subfamily of Herpesviridae, is a common causative agent of human virus infection and includes herpes simplex viruses types 1 and 2 (HSV-1 and HSV-2) and varicella-zoster virus (VZV). Although they are famous for resulting vesicles in skin, the clinical manifestations which involve other areas than cutaneous area are more concerned. Especially in visceral organs and central nervous system (CNS) involvement, the suspicion of the infection is difficult, let alone the diagnosis, because symptoms and signs are ambiguous [1].

In clinical laboratory, conventional methods for detecting HSV and VSV such as cell culture or direct immunofluorescent assay (DFA) have limitations such as slowness, insensitivity, and nonstandardization in interpretation [2]. Moreover, the illness differences in severity and antiviral regimens according to viral species have been ascertained which requires more time, labor, and cost in traditional methods [3, 4].

Polymerase chain reaction- (PCR-) based techniques, particularly in CNS infection, have replaced the gold standard for the diagnosis of HSV-1, HSV-2, and VZV because cerebrospinal fluid stays positive for up to 1 week in the infection [3]. Various PCR-based methods have been introduced to the clinical laboratory, for example, conventional PCR, nested PCR, and PCR-restriction fragment length polymorphism (RFLP). Also, real-time PCR has been established as an easily available assay of microbiology laboratory recently, with the advantage of rapidity and low contamination rate. The aim of the present study was to develop a real-time PCR and melting curve analysis which detect and differentiate HSV-1, HSV-2, and VZV with LightCycler SYBR Green PCR, to compare with PCR-RFLP using clinical specimens, and to introduce the 4-year experience in the clinical laboratory.

2. Materials and Methods

2.1. Patients and Specimens. Specimens used in this study were classified into two groups: 100 specimens including already known as positives for clinical validation and clinical specimens obtained from patients with signs and symptoms suggestive of HSV or VZV infection for diagnosis. The 100 specimens consisted of 79 cerebrospinal fluids (CSF), 20 vesicle swabs, and 1 plasma sample.

2.2. Shell Vial Culture and Typing. Human lung fibroblast (MRC-5 cells) cultured in modified Eagle's medium (MEM) containing 10% fetal bovine serum, gentamicin, vancomycin, and nystatin was used for the preparation of cell monolayer. Cells were inoculated with 100 μL of filtered clinical specimens and centrifuged at 700 ×g for 40 min. Thereafter, 1 mL of culture medium was added to the shell vials and the cultures were incubated at 37°C. Virus typing was performed on days 2, 4, and 6 after inoculation using monoclonal antibodies specific for HSV-1, HSV-2, or VZV (Light Diagnostics HSV 1/2 DFA and Light Diagnostics Varicella-Zoster DFA; Chemicon International, Temecula, CA, USA).

2.3. Nucleic Acid Extraction. 60 μL of extracted material was obtained from 140 μL of clinical specimen by QIAamp Viral RNA Mini Kit (Qiagen, Valencia, CA, USA) according to the manufacturer's instructions. PCR-RFLP and real-time PCR and melting curve analysis were performed with the identical nucleic acid.

2.4. Polymerase Chain Reaction-Restriction Fragment Length Polymorphism (PCR-RFLP). Genes encoding DNA polymerase of HSV and thymidine kinase of VZV were amplified for PCR-RFLP [5, 6]. After treating the amplified nucleic acid with *Sma* I and *Bam*H I for HSV-1 and HSV-2 and *Sma* I only for VZV, the PCR products were visualized using 2% agarose gel electrophoresis to detect the fragmentation.

2.5. Real-Time PCR and Melting Curve Analysis. The primers used in amplification and the gene targets are shown in Table 1. All primers except a pair for internal control were designed using LightCycler probe design software 2.0 (Roche, Penzberg, Germany). Human endogenous retrovirus-3 (HERV-3) *env* gene was also used to monitor false-positive results due to extraction failure or presence of inhibitors [7, 8]. The reaction mixture (20 μL), containing 3.0 μL of extracted nucleic acid, 1 × LightCycler FastStart DNA Master SYBR Green I (Roche), 3 mM MgCl$_2$, 0.3 μM of primers for HERV-3, and each of the primers for the detection (1.0 μM of primers for VZV or 0.3 μM of each primer for HSV), was denatured initially for 10 min at 95°C and was then treated for 5 sec at 95°C, 3 sec at 65°C, and 10 sec at 72°C for 45 cycles with LightCycler 2.0 (Roche). The program for analytic melting was followed by an increase in temperature to 99°C from 65°C with a 0.1°C/s ramp rate.

2.6. Standard Materials for Evaluation of Analytic Sensitivity of Real-Time PCR. Nucleic acid was amplified by the same
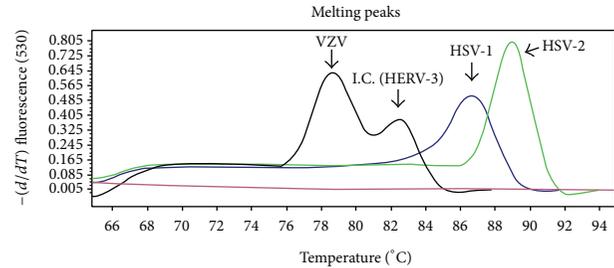
FIGURE 1: Differentiation of HSV-1, HSV-2, and VZV by multiplex real-time PCR-melting curve analysis. Melting peaks of HSV-1, HSV-2, and VZV positive samples by melting curve analysis. The HSV-1 amplicon has a melting temperature around 86.89°C, HSV-2 around 89.08°C, and VZV around 78.58°C, and internal control has a melting temperature around 82.41°C. HSV: herpes simplex virus; VZV: varicella-zoster virus; HERV-3: human endogenous retrovirus; I.C.: internal control.

primers used in multiplex real-time PCR and inserted into pTA2 vector using Target Cloning Kit (Toyoko, Osaka, Japan). Of the transformed, 3 colonies were selected for culture in Luria-Bertani media overnight, and then the plasmid DNA was extracted by GeneAll Exprep Plasmid SV Mini Kit (GeneAll Biotechnology, Seoul, Korea). With the restriction enzymes, *Hin*d III and *Bam*H I, transformation was confirmed and plasmid copy number was calculated. Creating standard curves of 10^2 copies to 10^6 copies per reaction by 10-fold distilled water dilution, the sensitivity of real-time PCR and melting curve analysis was determined.

3. Results

3.1. Validation of Multiplex Real-Time PCR and Melting Curve Analysis. In melting curve analysis, HSV-1, HSV-2, and VZV were distinguishable from each other, as well as HERV-3, the internal control (Figure 1). The melting curve of HSV-1, HSV-2, VZV, and HERV-3 showed the average melting temperature (Tm) to be 87.04°C, 89.32°C, 78.60°C, and 82.00°C, respectively (range: 86.84–87.16°C, 89.04–89.66°C, 77.36–79.20°C, and 81.09–82.89°C). In addition, the limits of detection were 1 copy, 10 copies, and 1 copy for HSV-1, HSV-2, and VZV, respectively (data not shown).

3.2. Comparison of Virus Culture, PCR-RFLP, and Real-Time PCR and Melting Curve Analysis in the Clinical Specimens. Of the total 100 clinical specimens, 9 (9%) were positive in multiplex real-time PCR, 8 (8%) in PCR-RFLP, and 4 (4%) in culture for HSV-1. Furthermore, 4 specimens were found positive only by molecular test and 1 specimen (CSF) was positive by real-time PCR solely. In HSV-2, 6 (6%) were positive in the respective molecular assays, and 4 (4%) were positive in culture. The assay of VZV was positive by real-time PCR and melting curve analysis in 19 (19%) specimens and by PCR-RFLP in 13 (13%) specimens. Of them, 6 specimens (5 CSF and 1 vesicle swab) were positive only by real-time PCR and melting curve analysis. None of the VZV cultures was positive in this study (Table 2).

TABLE 1: Primer sequences used and product sizes of each target genes for HSV-1, HSV-2, VZV, and HERV-3.

Virus	Gene target	Primer sequences (5′ → 3′)	Amplicon (bp)	Reference
HSV-1	gpD	Forward primer: GGTCTCTTTTGTGTGGTGC	84	This study
		Reverse primer: GCCCACTATGACGACAAAC		This study
HSV-2	gpG	Forward primer: TACGCTCTCGTAAATGCTTC	120	This study
		Reverse primer: GCCCACCTCTACCCACAA		This study
VZV	ORF4	Forward primer: GCCCATGAATCACCCTC	79	This study
		Reverse primer: ACTCGGTACGCCATTTAG		This study
HERV-3	envelope	Forward primer: CATGGGAAGCAAGGGAACTAATG	135	Yuan et al., 2001 [7]
		Reverse primer: CCCAGCGAGCAATACAGAATTT		Yuan et al., 2001 [7]

HSV: herpes simplex virus; VZV: varicella-zoster virus; HERV-3: human endogenous retrovirus; gpD: glycoprotein D; gpG: glycoprotein G; ORF4: open reading frame 4.

TABLE 2: Comparison of real-time PCR, PCR-RFLP, and virus culture for the detection of HSV-1, HSV-2, and VZV during the validation phase.

Virus	Real-time PCR		PCR-RFLP		Virus culture	
	Positive	Negative	Positive	Negative	Positive	Negative
HSV-1	9	91	8	92	4	96
HSV-2	6	94	6	94	4	96
VZV	19	81	13	87	0	100

HSV: herpes simplex virus; VZV: varicella-zoster virus.

3.3. Application of the Real-Time PCR and Melting Curve Analysis on Clinical Specimens.

Between January 2008 and May 2012, more than 2,600 specimens were requested for detection of HSV-1, HSV-2, or VZV to Seoul National University Bundang Hospital, the tertiary referral center. The specimens types and number of tested specimens are shown in Table 3. Of 2,642 specimens for HSV-1 or HSV-2, 3 CSF, 1 blood sample, and 1 skin vesicle were positive for HSV-1 and so were 4 CSF, 3 skin vesicles, and 3 genital swabs for HSV-2. Of 871 specimens submitted for VZV, 30 (23 CSF, 2 blood samples, 2 skin vesicles, 2 aqueous humor, and 1 ear discharge) were positive.

Of the 30 virus-positive cases from 28 patients, 17 (60.7%) occurred in male patients and 11 (39.3%) occurred in female patients. The mean age was 54.2 years (range: 16–82 years; median: 59 years). Age, clinical diagnosis, and immunologic status of patients with virus-positive CSF are shown in Table 4. All 3 cases of HSV-1 positive patients resented with mental status changes. HSV-2 infections were diagnosed with meningitis presenting headache and fever in all immunocompetent patients. In cases of VZV, meningitis, myelitis, encephalitis, Ramsay Hunt syndrome, and disseminated viral infection were manifested as an infection.

4. Conclusion

HSV-1, HSV-2, and VZV, highly contagious viruses which belong to Alphaherpesvirinae, cause various forms of clinical manifestation from skin vesicles to disseminated viral infection [9]. Laboratory detection of these virus infections as well as clinical symptoms or signs is also important for

TABLE 3: Summary of specimen types and numbers positive for HSV-1, HSV-2, and VZV.

Specimen type	Number tested		Number positive		
	HSV-1 and HSV-2	VZV	HSV-1	HSV-2	VZV
CSF	2,495	755	3	4	23
Blood					
Serum	62	68	0	0	1
Plasma	15	16	1	0	1
Skin vesicle	16	13	1	3	2
Genital swab	21	0	0	3	0
Oral swab	4	2	0	0	0
Eye					
Corneal scraping	11	0	0	0	0
Vitreous fluid	8	8	0	0	0
Aqueous humor	3	5	0	0	2
Amniotic fluid	5	1	0	0	0
Urine	1	0	0	0	0
BAL	0	2	0	0	0
Ear discharge	0	1	0	0	1
Tissue (skin)	1	0	0	0	0
Total	2,642	871	5	10	30

HSV: herpes simplex virus; VZV: varicella-zoster virus; CSF: cerebrospinal fluid; BAL: bronchoalveolar lavage.

diagnosis, as prompt antiviral therapy improves morbidity and mortality [10]. Many types of diagnostic methods for virus detection have been used in clinical laboratory so far; however, virus isolation in cell culture, known as classical "gold standard," has several limitations in turnaround time, manual labor, and lack of sensitivity. Our results on real-time PCR and melting curve analysis in HSV-1, HSV-2, and VZV clearly indicated increased diagnostic sensitivity compared to shell vial culture. Especially, the detection rates of VZV were markedly improved in the newly developed assay, which correlates with previous report by others [11].

In comparison with PCR-RFLP, real-time PCR and melting curve analysis demonstrated a modest increased sensitivity. General limitation has to be taken into consideration

TABLE 4: Clinical and laboratory findings of the patients positive for the presence of HSV or VZV DNA in CSF by PCR.

Virus detected	Number of positive samples	Age at diagnosis (number of patients)	Clinical diagnosis (number of patients)	Number of immunocompromised patients*/number of immunocompetent patients
HSV-1	3	31–50 (1)	Encephalitis (1)	0/1
		>50 (2)	Encephalitis (2)	1/1
HSV-2	4	31–50 (2)	Meningitis (2)	0/2
		>50 (1)	Meningitis (1)	0/1
VZV	23	10–30 (3)	Meningitis (3)	0/3
		31–50 (7)	Meningitis (6)	1/5
			Myelitis (1)	0/1
		>50 (12)	Encephalitis (6)	4/2
			Meningitis (4)	1/3
			Disseminated viral infection (1)	1/0
			Ramsay Hunt syndrome (1)	0/1

*Immunocompromised patients include patients who were diagnosed with hematologic malignancy (acute myeloid leukemia, diffuse large B-cell lymphoma, and essential thrombocythemia), solid tumor (breast cancer and cervical cancer), rheumatoid arthritis treated with methotrexate, and diabetes mellitus.
HSV: herpes simplex virus; VZV: varicella-zoster virus.

nevertheless: long turnaround time as ever due to cumbersome post-PCR processing and nonnegligible contamination chances transferring amplicons onto agarose gel [12]. In this study, real-time PCR using SYBR green dye was chosen since it does not require setting new probes. SYBR green chemistry intercalates double-stranded DNA, amplifies fluorescent signals a thousandfold as PCR progresses, and finally detects the presence of target DNA. It is suitable for clinical molecular laboratories because it is employable for other PCR items in addition to its inexpensiveness compared with hydrolysis probe. The SYBR green chemistry has limits of nonspecific reaction to double-stranded DNA and possibility of false-positive results; thus it needs optimization in the quantification in assay [13]. However, real-time PCR used in this study, by implementation of melting curve analysis, increased reliability of results and solved the problem of SYBR Green I, which binds to nonspecific double-stranded DNA [14].

HERV-3, relatively well characterized among endogenous retroviruses, is reported to be present in the human genome at a single genomic locus. Because of its properties, HERV-3 is often used to measure both DNA quality and quantity and to monitor PCR inhibitors [7]. There are several reports that undiluted and untreated specimens have a much greater incidence of inhibition [8, 15]. More than 11 types of specimens were submitted to the clinical laboratory and little is known about presence of inhibitors in different kinds of specimens, especially in the rarely requested items. As multiplex real-time PCR assays for HSV-1, HSV-2, and HERV-2 (VZV and HERV for another tube) are devised in this study, it is expected to detect PCR inhibitors.

Laboratory diagnosis and typing of herpesviruses are important for some complications such as meningitis and encephalitis. While HSV-2 is related to recurrent meningitis and meningoencephalitis in immunocompromised patients, HSV-1 is generally known to be the most common cause of sporadic encephalitis [16]. Although positive cases are rare and unfeasible to generalize in the present study, the findings of CSF positive patients were concordant with others. With long-term extensive study, it is expected to define patients' demographics and epidemiology of HSV-1, HSV-2, and VZV.

In summary, the newly developed real-time PCR and melting curve analysis have increased sensitivity and shortened turnaround time in clinical samples. The Accurate and less labor intensive molecular assay in clinical laboratory may help the rapid diagnosis and prompt treatment for patients.

Conflict of Interests

The authors declare that there is no conflict of interests regarding the publication of this paper.

References

[1] D. Olmez, A. Boz, and N. Erkan, "Varicella zoster infection: a rare cause of abdominal pain mimicking acute abdomen," *Journal of Clinical Medicine Research*, vol. 1, no. 4, pp. 247–248, 2009.

[2] C. A. Gleaves, D. H. Rice, R. Bindra et al., "Evaluation of a HSV specific monoclonal antibody reagent for laboratory diagnosis of herpes simplex virus infection," *Diagnostic Microbiology and Infectious Disease*, vol. 12, no. 4, pp. 315–318, 1989.

[3] R. J. Whitley and B. Roizman, "Herpes simplex virus infections," *The Lancet*, vol. 357, no. 9267, pp. 1513–1518, 2001.

[4] A. Sauerbrei and P. Wutzler, "Herpes simplex and varicella-zoster virus infections during pregnancy: current concepts of prevention, diagnosis and therapy. Part 2: Varicella-zoster virus infections," *Medical Microbiology and Immunology*, vol. 196, no. 2, pp. 95–102, 2007.

[5] S. Kido, T. Ozaki, H. Asada et al., "Detection of varicella-zoster virus (VZV) DNA in clinical samples from patients with VZV by the polymerase chain reaction," *Journal of Clinical Microbiology*, vol. 29, no. 1, pp. 76–79, 1991.

[6] F. Rozenberg and P. Lebon, "Amplification and characterization of herpesvirus DNA in cerebrospinal fluid from patients with acute encephalitis," *Journal of Clinical Microbiology*, vol. 29, no. 11, pp. 2412–2417, 1991.

[7] C. C. Yuan, W. Miley, and D. Waters, "A quantification of human cells using an ERV-3 real time PCR assay," *Journal of Virological Methods*, vol. 91, no. 2, pp. 109–117, 2001.

[8] D. M. Whiley, I. M. Mackay, M. W. Syrmis, M. J. Witt, and T. P. Sloots, "Detection and differentiation of herpes simplex virus types 1 and 2 by a duplex LightCycler PCR that incorporates an internal control PCR reaction," *Journal of Clinical Virology*, vol. 30, no. 1, pp. 32–38, 2004.

[9] D. E. Dwyer and A. L. Cunningham, "10: herpes simplex and varicella-zoster virus infections," *Medical Journal of Australia*, vol. 177, no. 5, pp. 267–273, 2002.

[10] S. S. Long, "Delayed acyclovir therapy in neonates with herpes simplex virus infection is associated with an increased odds of death compared with early therapy," *Evidence-Based Medicine*, vol. 18, no. 2, p. e20, 2013.

[11] M. J. Espy, R. Teo, T. K. Ross et al., "Diagnosis of varicella-zoster virus infections in the clinical laboratory by LightCycler PCR," *Journal of Clinical Microbiology*, vol. 38, no. 9, pp. 3187–3189, 2000.

[12] C. A. Heid, J. Stevens, K. J. Livak, and P. M. Williams, "Real time quantitative PCR," *Genome Research*, vol. 6, no. 10, pp. 986–994, 1996.

[13] M. Arya, I. S. Shergill, M. Williamson, L. Gommersall, N. Arya, and H. R. H. Patel, "Basic principles of real-time quantitative PCR," *Expert Review of Molecular Diagnostics*, vol. 5, no. 2, pp. 209–219, 2005.

[14] C. D. Sibley, G. Peirano, and D. L. Church, "Molecular methods for pathogen and microbial community detection and characterization: current and potential application in diagnostic microbiology," *Infection, Genetics and Evolution*, vol. 12, no. 3, pp. 505–521, 2012.

[15] J. Druce, M. Catton, D. Chibo et al., "Utility of a multiplex PCR assay for detecting herpesvirus DNA in clinical samples," *Journal of Clinical Microbiology*, vol. 40, no. 5, pp. 1728–1732, 2002.

[16] R. Kneen, B. D. Michael, E. Menson et al., "Management of suspected viral encephalitis in children-association of British Neurologists and British Paediatric Allergy, Immunology and Infection Group National Guidelines," *Journal of Infection*, vol. 64, no. 5, pp. 449–477, 2012.

Research Article

Significance of Lewis Phenotyping Using Saliva and Gastric Tissue: Comparison with the Lewis Phenotype Inferred from *Lewis* and *Secretor* Genotypes

Yun Ji Hong,[1,2] Sang Mee Hwang,[1,2] Taek Soo Kim,[1,2] Eun Young Song,[1] Kyoung Un Park,[1,2] Junghan Song,[1,2] and Kyou-Sup Han[1]

[1] *Department of Laboratory Medicine, Seoul National University College of Medicine, Seoul 110-744, Republic of Korea*
[2] *Department of Laboratory Medicine, Seoul National University Bundang Hospital, 173-82 Gumiro, Bundanggu, Seongnam, Gyeonggido 463-707, Republic of Korea*

Correspondence should be addressed to Kyoung Un Park; m91w95pf@snu.ac.kr

Lewis phenotypes using various types of specimen were compared with the Lewis phenotype predicted from *Lewis* and *Secretor* genotypes. This is the first logical step in explaining the association between the Lewis expression and *Helicobacter pylori*. We performed a study of the followings on 209 patients who underwent routine gastroscopy: erythrocyte and saliva Lewis phenotyping, gastric Lewis phenotyping by the tissue array, and the *Lewis* and *Secretor* genes genotyping. The results of phenotyping were as follows [Le(a−b−), Le(a+b−), Le(a−b+), and Le(a+b+), respectively, in order]: erythrocyte (12.4%, 25.8%, 61.2%, and 0.5%); saliva (2.4%, 27.3%, 70.3%, and 0.0%); gastric mucosa (8.1%, 6.7%, 45.5%, and 39.7%). The frequency of *Le*, $le^{59/508}$, $le^{59/1067}$, and le^{59} alleles was 74.6%, 21.3%, 3.1%, and 1.0%, respectively, among 418 alleles. The saliva Lewis phenotype was completely consistent with the Lewis phenotype inferred from *Lewis* and *Secretor* genotypes, but that of gastric mucosa could not be predicted from genotypes. Lewis phenotyping using erythrocytes is only adequate for transfusion needs. Saliva testing for the Lewis phenotype is a more reliable method for determining the peripheral Lewis phenotype of an individual and the gastric Lewis phenotype must be used for the study on the association between *Helicobacter pylori* and the Lewis phenotype.

1. Introduction

The Lewis histoblood group system consists of two major antigens, Le^a and Le^b, and three common phenotypes, Le(a−b−), Le(a+b−), and Le(a−b+). The Lewis determinants are oligosaccharides which are synthesized by the sequential addition of sugar units to oligosaccharide chains by fucosyltransferases encoded by *H*, *Secretor*, and *Lewis* genes. The type 2 oligosaccharide chains are expressed mainly on erythrocytes and on vascular endothelial cells, while the type 1 oligosaccharide chains are expressed on the digestive and respiratory tracts and in secretions. The classical Lewis determinants (Le^a and Le^b) are composed of type 1 chains [1]. The Le^a antigen is synthesized from a type 1 precursor substrate

by *Lewis*-encoded $\alpha(1,3/1,4)$fucosyltransferase, while the Le^b antigen is synthesized from a type 1 H substrate by the enzyme.

The eleven *fucosyltransferase* (*FUT*) genes encoding human fucosyltransferases have been isolated [2]. The *FUT1* (*H*) and *FUT2* (*Secretor*) encode $\alpha(1,2)$fucosyltransferases, and the *FUT3*-*FUT9* encode $\alpha(1,3/1,4$ or $1,3)$fucosyltransferases. *FUT1*, *FUT2*, *FUT3*, and *FUT6* are polymorphic [1]. Alpha(1,2)fucosyltransferase adds a fucose molecule to the terminal galactose of a precursor to form the H antigen. There are two distinct $\alpha(1,2)$fucosyltransferases in sera and tissues. One is the *H*-encoded fucosyltransferase (H enzyme) and the other is the *Secretor*-encoded fucosyltransferase (secretor enzyme). The H enzyme regulates the expression of

the H antigen mainly on erythrocyte membranes and in vascular endothelial cells, while the secretor enzyme regulates the expression of the H antigen mainly on the gastrointestinal epithelial cells and in body fluids such as saliva.

The Lewis antigens are not intrinsic to the erythrocytes but adsorbed onto erythrocyte membranes from plasma. Accordingly, the Lewis phenotyping from erythrocytes is difficult and is sometimes misjudged because of weak hemagglutination due to low titers and low specificities of the reagents. There are two alleles at the *Lewis* locus, the *Le* which encodes a functional fucosyltransferase and the *le* which encodes a nonfunctional enzyme. An individual homozygous for *le* expresses neither Le^a nor Le^b antigen and has the Le(a−b−) erythrocyte phenotype. Several polymorphisms have been described in the *Lewis* and *Secretor* genes [3–10]. It is conceivable that Lewis antigen expression in digestive organs is biologically much more important than the expression in erythrocytes. The studies on *Helicobacter pylori* suggested that the adherence of *H. pylori* to the human gastric epithelial lining can be mediated by the blood-group antigen-binding adhesion (BabA) that targets human fucosylated blood group antigens type 1 H and Le^b [11–13]. The presence of the *babA2* gene, encoding for BabA, in the *H. pylori* genome is crucial for *H. pylori*-related pathogenesis [13].

In this study, various Lewis phenotypes using saliva, erythrocytes, and gastric mucosa were compared with the Lewis phenotype predicted from *Lewis* and *Secretor* genotypes to establish the significance of Lewis phenotyping using saliva and gastric tissue. This is the first logical step in explaining the association between the Lewis expression and *Helicobacter pylori*.

2. Materials and Methods

2.1. Blood Sample Processing. The subjects were 209 adult patients who underwent routine gastroscopy at a health promotion center because of upper gastrointestinal symptoms. Specimens were collected after the patients had given informed consent. The procedures in this study were in accordance with the National Institutes of Health Bioethics Resources for research on human specimens and the World Medical Association Declaration of Helsinki (Ethical Principles for Medical Research Involving Human Subjects). Peripheral blood was collected in one EDTA tube and one plain tube. The blood of EDTA tube was separated into buffy coat and plasma on the day of blood sampling. The buffy coat was stored at −70°C. DNA for the determination of the *Lewis* and *Secretor* genotypes was extracted from the buffy coat using the Puregene DNA Kit (Gentra, Minneapolis, MN, USA) according to the manufacturer's instructions.

2.2. Saliva Sample Processing. Saliva samples were donated for detection of Lewis antigens before undergoing endoscopy. Saliva (5 to 10 mL) was collected in a wide-mouthed test tube. The saliva was centrifuged at 1000 ×g for 10 minutes. The supernatant was transferred to a clean test tube and placed in boiling water bath for 10 minutes to inactivate salivary enzymes. After recentrifuging at 1000 ×g for 10 minutes, the

supernatant fluid was diluted with an equal volume of saline and stored at −70°C.

2.3. Erythrocyte Phenotyping for the Lewis Antigens. Ortho BioClone 2.0 anti-Le^a and anti-Le^b monoclonal antibodies (Ortho-Clinical Diagnostics, Inc., Raritan, NJ, USA) were used for hemagglutination tests according to the manufacturer's instructions.

2.4. Saliva Testing for the Lewis Phenotypes. The Lewis antigens in saliva were tested by hemagglutination inhibition methods with Lewis antisera. Doubling dilutions of the appropriate blood grouping reagent were prepared beforehand, for the selection of blood grouping reagent dilution. One drop of 3% saline suspension of red cells was added to one drop of each reagent dilution. Le(a+b−) and Le(a−b+) red cells were used to determine Lewis phenotypes. Each tube was centrifuged and examined macroscopically for agglutination. The highest reagent dilution that gives 2+ agglutination was selected. For the hemagglutination inhibition test, one drop of appropriately diluted blood grouping reagent was mixed with one drop of the appropriate saliva and the mixture was incubated for 10 minutes at room temperature. One drop of 3% saline suspension of washed indicator cells was added to each tube. The tube contents were incubated for 60 minutes at room temperature. Each tube was centrifuged and inspected macroscopically for agglutination. Saline control tube was included in each test.

2.5. Tissue Array Method. Core tissue biopsies (2 mm in diameter) were taken from individual paraffin-embedded gastric tissues (donor blocks) and arranged in a new recipient paraffin block (tissue array block) using a trephine apparatus (Superbiochips Laboratories, Seoul, Korea). Each tissue array block contained up to sixty cases. Sections of 4 μm were cut from each tissue array block, deparaffinized, and dehydrated.

2.6. Gastric Immunostaining for the Lew Phenotypes. Immunohistochemical phenotyping of the gastric tissue specimens for Lewis antigens was performed using a streptavidin peroxidase procedure after an antigen retrieval process using microwaves or autoclaves. The monoclonal antibodies used for detection of gastric Lewis antigens were the antibody to Le^a and the antibody to Le^b (Signet Laboratories, Inc., Dedham, MA, USA). The same pathologist evaluated all slides blindly. The results of immunostaining were considered to be positive if more than 20% of the cells showed staining.

2.7. Genotyping for the Lewis Genes. The *Lewis* genotype was determined for the T59G, G508A, and T1067A polymorphic sites. The $le^{59/508}$ and $le^{59/1067}$ alleles confer very low enzymatic activity relative to the *Le* and Le^{59} alleles [4]. The Le^{59} allele confers about the same enzymatic activity as the *Le* allele [3].

(1) PCR-CTPP for the Detection of the T59G Mutation. The T59G mutation was determined by the polymerase chain

reaction with confronting two-pair primers (PCR-CTPP) [14]. The oligonucleotide primers (Bioneer Corporation, Daejeon, Korea) used in the PCR-CTPP were [15] Le59-F1, 5′-CCA TGG ATC CCC TGG GTG-3′; Le59-R1, 5′-CCA CCA GCA GCT GAA ATA GCC-3′; Le59-F2, 5′-CGC TGT CTG GCC GCA CT-3′; Le59-R2, 5′-GAA GGT GGG AGG CGT GAC TTA-3′. PCR was performed in 25 μL reaction mixture containing 10 pmol each of the four primers, 2 μL of DNA, 0.6 units of *Taq* polymerase (Takara, Shiga, Japan), 0.2 mM dNTPs, 2.5 μL 10x PCR buffer, 1.5 mM MgCl$_2$, and 2.5 μL of glycerol. PCR conditions were 3 minutes of initial denaturation at 94°C, followed by 35 cycles of denaturing at 94°C for 30 seconds, annealing at 66°C for 30 seconds and extension at 72°C for 30 seconds, and final extension at 72°C for 5 minutes. PCR products underwent electrophoresis in a 3% agarose gel and were stained by ethidium bromide. In the T59G detection by the PCR-CTPP, the 329 bp and 81 bp bands represented the T allele and G allele, respectively. A common band of 373 bp appeared for both alleles.

(2) PCR-RFLP for the Detection of the G508A and T1067A Mutations. The G508A and T1067A mutations were determined by the polymerase chain reaction-restriction fragment length polymorphism (PCR-RFLP). For detecting the G508A mutation, genomic DNA was combined with the 508-F (5′-ACT TGG AGC CAC CCC CTA ACT GCC A-3′) and 508-R (5′-TGA GTC CGG CTT CCA GTT GGA CAC C-3′) primers (10 pmol) [6] in 25 μL reaction mixture containing 0.6 units of *Taq* polymerase (Takara, Shiga, Japan), 0.2 mM dNTPs, 2.5 μL 10x PCR buffer, and 1.5 mM MgCl$_2$. Thirty cycles (30 seconds at 94°C, 30 seconds at 70°C, and 30 seconds at 72°C) were run, and then the 206 bp products were digested by *Pvu*II enzyme and subjected to separation through 3% agarose gel electrophoresis.

For the T1067A mutation, the first PCR with the primers [4] Le-F (5′-CTC CCG ACA GGA CAC CAC TCC CA-3′) and Le-R (5′-CTC AAG CTT CGT GCC GTG ATG ATC TCT CTG CAC-3′) was carried out in the same PCR buffer as in the PCR for detection of the G508A mutation. Thirty cycles (30 seconds at 94°C, 30 seconds at 70°C, and 45 seconds at 72°C) were run. For the second PCR amplification, the first PCR products were used as the template by 1067-F (5′-CGC TCC TTC AGC TGG GCA CTG GA-3′) and 1067-R (5′-CGG CCT CTC AGG TGA ACC AAG AAG CT-3′) primers [4]. Thirty cycles (30 seconds at 94°C, 30 seconds at 62°C, and 30 seconds at 72°C) were run in the same PCR buffer. The products were digested by *Hin*dIII enzyme and analyzed by 3% agarose gel electrophoresis. The 109 bp product was cleaved into two fragments, 24 and 85 bp, by the digestion.

2.8. Genotyping for the Secretor Genes. The *Secretor* genotype was determined for the C357T, A385T, and G428A polymorphic sites and the fusion gene. Both *Se* and *Se*^{357} alleles have full enzyme activity. The *se*^{428}, *se*^{385}, *se*$^{357/385}$, and *se*^{fus} alleles confer little or no enzymatic activity relative to the *Se* and *Se*^{357} alleles [5, 8]. The *se*^{fus} allele is due to fusion of the *Secretor* gene and a pseudogene.

(1) PCR-CTPP for the Detection of the A385T Mutation and the Fusion Gene. To detect the A385T mutation and the fusion gene, the genotyping was conducted by means of PCR-CTPP [14]. The primers were as follows [16]: Se5-F0, 5′-TTT CAC TGC CAC CAG CAC CTG-3′; Se385-F1, 5′-ATC AAA GGC ACT GGG ACC CAG-3′; Se385-R1, 5′-GGA CGT ACT CCC CCG GGA T-3′; Se385-F2, 5′-TGG AGG AGG AAT ACC GCC ACT-3′; Se385-R2, 5′-GTC CCC TCG GCG AAC ATG G-3′. Genomic DNA (30–100 ng) was used for each 25 μL reaction mixture containing 0.2 mM dNTPs, 10 pmol each of the five primers, 2.5 μL glycerol, 0.6 units of *Taq* polymerase (Takara, Shiga, Japan), 2.5 μL 10x PCR buffer, and 1.5 mM MgCl$_2$. PCR conditions were 3 minutes of initial denaturation at 94°C, followed by 35 cycles of 30 seconds at 94°C, 30 seconds at 61°C, and 30 seconds at 72°C, and final extension at 72°C for 5 minutes. Amplified DNA was visualized on a 2% agarose gel containing ethidium bromide. In the *Secretor* A385T and the fusion genotyping by the PCR-CTPP, the amplified bands with 284 bp, 216 bp, and 353 bp represented the A allele, T allele, and *se*^{fus} allele, respectively. A common band of 460 bp appeared for the A and T alleles.

(2) PCR-RFLP for the Detection of the C357T and G428A Mutations. The C357T and G428A mutations were determined by PCR-RFLP. For the detection of the C357T mutation, the first PCR amplification with the primers Se-F (5′-CTC GAA TTC GGG CCT CCA TCT CCC AGC TAA C-3′) and Se-R (5′-CTC AAG CTT GCT TCT CAT GCC CGG GCA CTC-3′) was performed [6]. The Se-F and Se-R primers (10 pmol) were added to 5 μL of genomic DNA in total volume of 50 μL containing 0.2 mM of each dNTP, 0.1 unit of *Taq* polymerase (Takara, Shiga, Japan), 5 μL 10x PCR buffer, and 1 mM MgCl$_2$. Thirty cycles (30 seconds at 94°C, 30 seconds at 65°C, and 30 seconds at 72°C) were run. For the second PCR, one μL of the first PCR product was used as the template by the primer sets 357-F (5′-CAG GAT CCC CTG GCA GAA CTA CCA CAT TAA-3′) and 357-R (5′-AGC AGG GGT AGC CGG TGA AGC GGA CGT ACT-3′) [6]. PCR was performed in 25 μL reaction mixture containing 10 pmol each primer, 0.2 units of *Taq* polymerase (Takara, Shiga, Japan), 0.1 mM dNTPs, 2.5 μL 10x PCR buffer, and 4 mM MgCl$_2$. The second PCR was carried out under the same conditions as in the first PCR. The 357-F primer created an *Ase*I site in the second PCR product from the mutant allele having C357T, and the 98 bp product was cleaved into two fragments, 28 and 70 bp, by the digestion.

For detection of the G428A nonsense mutation, the first PCR was performed under the same primers and conditions as in the first PCR for detection of the C357T mutation. The second PCR was performed by the primers, 428-F (5′-CGC TTC ACC GGC TAC CCC TGC TTC T-3′) and 428-R (5′-AAC TTC TGG GCC TCC TCC CGC A-3′) [6]. PCR was performed in 25 μL reaction mixture containing 10 pmol each primer, 0.2 units of *Taq* polymerase (Takara, Shiga, Japan), 0.1 mM dNTPs, 2.5 μL 10x PCR buffer, and 4 mM MgCl$_2$. Thirty cycles (30 seconds at 94°C, 30 seconds at 60°C, and 30 seconds at 72°C) were run. In case of the product having the G428A mutation, the 107 bp product might be separated into two fragments, 23 and 84 bp, by *Xba*I digestion.

TABLE 1: *Lewis* genotype and allele frequencies by erythrocyte Lewis phenotype[*].

	Le(a−b−) (n = 26)	Le(a+b−) (n = 54)	Le(a−b+) (n = 128)	Le(a+b+) (n = 1)	
Le/Le	6[**]	33	69	0	108
Le/le$^{59/508}$	14[**]	20	45	0	79
Le/le$^{59/1067}$	2[**]	1	9	1	13
Le/Le^{59}	0	0	4	0	4
le$^{59/508}$/*le*$^{59/508}$	4	0	1[**]	0	5
Le allele	28	87	196	1	312 (74.6)
le$^{59/508}$ allele	22	20	47	0	89 (21.3)
le$^{59/1067}$ allele	2	1	9	1	13 (3.1)
Le^{59} allele	0	0	4	0	4 (1.0)

[*] Values are number or number (percentage).
[**] Inconsistency between the erythrocyte Lewis phenotypes and the Lewis phenotypes by the inference from *Lewis* genotypes.

TABLE 2: *Secretor* genotype and allele frequencies by erythrocyte Lewis phenotype.

	Le(a−b−) (n = 26)	Le(a+b−) (n = 54)	Le(a−b+) (n = 128)	Le(a+b+) (n = 1)	
Se/Se^{357}	1	0	1	0	2
Se/se^{385}	1	1[*]	0	0	2
Se/se$^{357/385}$	9	4[*]	56	0	69
Se/se^{fus}	0	0	1	0	1
Se^{357}/*Se*^{357}	0	1[*]	1	0	2
Se^{357}/*se*$^{357/385}$	4	2	34	0	40
Se^{357}/*se*^{fus}	2	0	33	0	35
se^{385}/*se*$^{357/385}$	7	18	0	1	26
se$^{357/385}$/*se*$^{357/385}$	2	25	1[*]	0	28
se$^{357/385}$/*se*^{fus}	0	3	1[*]	0	4
Se allele	11	5	58	0	74
Se^{357} allele	7	4	70	0	81
se^{385} allele	8	19	0	1	28
se$^{357/385}$ allele	24	77	93	1	195
se^{fus} allele	2	3	35	0	40

[*] Inconsistency between the erythrocyte Lewis phenotypes and the Lewis phenotypes by the inference from *Secretor* genotypes.

3. Results

Lewis phenotypes (from erythrocyte, saliva, and gastric mucosa), *Secretor* genotypes, and *Lewis* genotypes were determined in 209 patients. The number of individuals with erythrocyte phenotype Le(a−b−), Le(a+b−), Le(a−b+), and Le(a+b+) was 26 (12.4%), 54 (25.8%), 128 (61.2%), and 1 (0.5%), respectively, among the 209 individuals. The number of patients with saliva phenotype Le(a−b−), Le(a+b−), Le(a−b+), and Le(a+b+) was 5 (2.4%), 57 (27.3%), 147 (70.3%), and 0 (0.0%), respectively. Lewis antigen expression on gastric mucosa was as follows: Le(a−b−), 17 (8.1%); Le(a+b−), 14 (6.7%); Le(a−b+), 95 (45.5%); Le(a+b+), 83 (39.7%).

The frequency of occurrence of the *Le*, *le*$^{59/508}$, *le*$^{59/1067}$, and *Le*^{59} alleles was 74.6%, 21.3%, 3.1%, and 1.0%, respectively, among 418 alleles examined in total (Table 1). The *le*$^{59/508}$ allele accounted for 87.3% of the *le* alleles, whereas the *le*$^{59/1067}$ allele was 12.7%. The frequency of the *Se*, *Se*^{357}, *se*^{385}, *se*$^{357/385}$,

and *se*^{fus} alleles was 17.7%, 19.4%, 6.7%, 46.7%, and 9.6%, respectively, among 418 alleles examined in total (Table 2).

Tables 1 and 2 summarized whether Lewis phenotype on erythrocytes and known mutations of *Lewis* gene or *Secretor* gene corresponded. In Table 3, various Lewis phenotypes (saliva, erythrocytes, and gastric mucosa) were compared with the Lewis phenotype predicted from *Lewis* and *Secretor* genotypes. The saliva Lewis phenotype was completely consistent with the Lewis phenotype inferred from *Lewis* and *Secretor* genotypes, but the Lewis phenotype in gastric mucosa could not be predicted from *Lewis* and *Secretor* genotypes.

4. Conclusion

One out of purposes of the present study was to examine the correspondence between Lewis phenotype on RBCs and

TABLE 3: Comparison between various Lewis phenotypes and the Lewis phenotype predicted from *Lewis* and *Secretor* genotypes.

	le/le and −/−			*Le/−* and *se/se*		*Le/−* and *Se/−*				
	le/le Se/Se	*le/le* Se/se	*le/le* se/se	Le/Le se/se	Le/le se/se	Le/Le Se/Se	Le/Le Se/se	Le/le Se/Se	Le/le Se/se	
	Le(a−b−)			Le(a+b−)		Le(a−b+)				
Lewis phenotype in saliva*										
Le(a−b−)	0	4	1	0	0	0	0	0	0	5
Le(a+b−)	0	0	0	31	26	0	0	0	0	57
Le(a−b+)	0	0	0	0	0	3	78	1	65	147
Le(a+b+)	0	0	0	0	0	0	0	0	0	0
Lewis phenotype on erythrocytes										
Le(a−b−)	0	3	1	3	5	0	3	1	10	26
Le(a+b−)	0	0	0	27	19	1	5	0	2	54
Le(a−b+)	0	1	0	1	1	2	70	0	53	128
Le(a+b+)	0	0	0	0	1	0	0	0	0	1
Lewis phenotype in gastric mucosa**										
Le(a−b−)	0	1	1	0	1	0	3	1	10	17
Le(a+b−)	0	0	0	6	4	0	3	0	1	14
Le(a−b+)	0	3	0	1	1	1	44	0	45	95
Le(a+b+)	0	0	0	24	20	2	28	0	9	83

*The saliva Lewis phenotype through the hemagglutination inhibition test was consistent with the Lewis phenotype inferred from *Lewis* and *Secretor* genotypes.
**The Lewis phenotype in gastric mucosa by immunohistochemistry was not predicted from *Lewis* and *Secretor* genotypes.

known mutations of *Lewis* gene. Moreover various Lewis phenotypes (saliva, erythrocytes, and gastric mucosa) were compared with the Lewis phenotype predicted from *Lewis* and/or *Secretor* genotypes.

Erythrocyte phenotyping through the conventional hemagglutination test has been regarded as a simple way of determining the Lewis antigens. However, in view of our study, erythrocyte phenotyping seems to be incapable of determining accurate Lewis phenotypes. The erythrocyte phenotype is influenced by many factors and may not necessarily reflect someone's *Lewis* and *Secretor* genotypes. The adsorption of glycolipid carrying Lewis activities from plasma onto erythrocytes is sometimes prevented. Some diseases are known to decrease the concentration of circulating Lewis-active glycolipids and cause the incompatible expression of Lewis antigens on erythrocytes. The expression of Lewis antigens has also demonstrated to be affected by the presence of tumors in cancer patients [4].

Lewis phenotyping using erythrocytes is only adequate for transfusion needs. Up to the present, many studies, which have been performed to establish if a disease associates with the Lewis blood group, were not correctly determined the Lewis phenotypes. Therefore, for accurate Lewis phenotyping, alternative methods must be used. In this study, the methods of genotyping and gastric immunohistochemical phenotyping resolved the above problems. However, molecular genotyping only provided an adjunct to phenotyping because the genotyping methods were unable to detect as yet undetermined mutations.

We have calculated Hardy-Weinberg equilibrium (HWE) for our data using Arlequin 3.5.1.3 [17]. The distribution of alleles in the population of our study was deviated from

the Hardy-Weinberg equilibrium ($P < 0.05$). Not only our study but also several other studies about *Secretor* and *Lewis* genes shows deviation from HWE [18, 19]. The C357T single nucleotide polymorphism (SNP) is normally present in conjunction with other SNPs of *Secretor* gene. By contrast, the isolated form of the Se^{357} allele was present at a relatively high frequency, which indicates the possibility that other combinations of C357T may exist, involving mutations that were not investigated in this population. It is also attributed to the ethnic composition of the sample and the change in population structures. In addition, HWE generally tends to be due to a deficit of heterozygotes for SNP, since the allelic dropout may be the most prevalent genotyping error [20]. Interestingly, our result of HWE calculation revealed deviation due to a deficit of homozygotes. Another possibility of the HWE disequilibrium may be the use of different amplification methods for genotyping, including different DNA polymerase, among studies [14, 16], and it might lead to misjudging the *FUT2* genotype.

When the Lewis phenotype predicted from *Lewis* and *Secretor* genotypes was compared with various Lewis phenotypes (saliva, erythrocytes, and gastric mucosa), the Lewis phenotype obtained from saliva was completely consistent with the Lewis phenotype predicted from *Lewis* and *Secretor* genotypes, but the Lewis phenotype in gastric mucosa was unpredictable. Saliva testing for the Lewis phenotype appears to be a more reliable method for determining the peripheral Lewis phenotype of an individual because the Lewis antigens are not intrinsic to the erythrocytes but adsorbed onto erythrocyte membranes from plasma. Moreover saliva Lewis phenotyping through the hemagglutination inhibition test seems to be able to be used as a simple substituting method

for determining the Lewis phenotype by the inference from *Lewis* and *Secretor* genotypes. Because the Lewis expression in gastric mucosa is a different one from the Lewis phenotype by the inference from *Lewis* and *Secretor* genotypes, the gastric Lewis phenotype must be used for the study on the association between the Lewis phenotype and *Helicobacter pylori*.

Conflict of Interests

The authors declare that there is no conflict of interests regarding the publication of this paper.

References

[1] Y. Koda, M. Soejima, and H. Kimura, "The polymorphisms of fucosyltransferases," *Legal Medicine*, vol. 3, no. 1, pp. 2–14, 2001.

[2] R. Mollicone, S. E. H. Moore, N. Bovin et al., "Activity, splice variants, conserved peptide motifs, and phylogeny of two New α1,3-fucosyltransferase families (FUT10 and FUT11)," *Journal of Biological Chemistry*, vol. 284, no. 7, pp. 4723–4738, 2009.

[3] R. Mollicone, I. Reguigne, R. J. Kelly et al., "Molecular basis for Lewis α(1,3/1,4)-fucosyltransferase gene deficiency (FUT3) found in Lewis-negative Indonesian pedigrees," *Journal of Biological Chemistry*, vol. 269, no. 33, pp. 20987–20994, 1994.

[4] S. Nishihara, H. Narimatsu, H. Iwasaki et al., "Molecular genetic analysis of the human Lewis histo-blood group system," *Journal of Biological Chemistry*, vol. 269, no. 46, pp. 29271–29278, 1994.

[5] Y. Koda, M. Soejima, Y. Liu, and H. Kimura, "Molecular basis for secretor type α(1,2)-fucosyltransferase gene deficiency in a Japanese population: a fusion gene generated by unequal crossover responsible for the enzyme deficiency," *American Journal of Human Genetics*, vol. 59, no. 2, pp. 343–350, 1996.

[6] T. Kudo, H. Iwasaki, S. Nishihara et al., "Molecular genetic analysis of the human lewis histo-blood group system: II. Secretor gene inactivation by a novel single missense mutation A385T in Japanese nonsecretor individuals," *Journal of Biological Chemistry*, vol. 271, no. 16, pp. 9830–9837, 1996.

[7] Y. Liu, Y. Koda, M. Soejima, N. Uchida, and H. Kimura, "PCR analysis of Lewis-negative gene mutations and the distribution of Lewis alleles in a Japanese population," *Journal of Forensic Sciences*, vol. 41, no. 6, pp. 1018–1021, 1996.

[8] H. Narimatsu, H. Iwasaki, F. Nakayama et al., "*Lewis* and *Secretor* gene dosages affect CA19-9 and DU-PAN-2 serum levels in normal individuals and colorectal cancer patients," *Cancer Research*, vol. 58, no. 3, pp. 512–518, 1998.

[9] E. M. Matzhold, W. Helmberg, T. Wagner et al., "Identification of 14 new alleles at the fucosyltransferase 1, 2, and 3 loci in Styrian blood donors, Austria," *Transfusion*, vol. 49, no. 10, pp. 2097–2108, 2009.

[10] M. Soejima, R. Fujimoto, T. Agusa et al., "Genetic variation of FUT2 in a Vietnamese population: identification of two novel Se enzyme-inactivating mutations," *Transfusion*, vol. 52, no. 6, pp. 1268–1275, 2012.

[11] T. Borén, P. Falk, K. A. Roth, G. Larson, and S. Normark, "Attachment of *Helicobacter pylori* to human gastric epithelium mediated by blood group antigens," *Science*, vol. 262, no. 5141, pp. 1892–1895, 1993.

[12] D. Ilver, A. Arnqvist, J. Ögren et al., "*Helicobacter pylori* adhesin binding fucosylated histo-blood group antigens revealed by retagging," *Science*, vol. 279, no. 5349, pp. 373–377, 1998.

[13] M. Gerhard, N. Lehn, N. Neumayer et al., "Clinical relevance of the *Helicobacter pylori* gene for blood-group antigen-binding adhesin," *Proceedings of the National Academy of Sciences of the United States of America*, vol. 96, no. 22, pp. 12778–12783, 1999.

[14] N. Hamajima, T. Saito, K. Matsuo, and K. Tajima, "Competitive amplification and unspecific amplification in polymerase chain reaction with confronting two-pair primers," *Journal of Molecular Diagnostics*, vol. 4, no. 2, pp. 103–107, 2002.

[15] A. Shibata, N. Hamajima, Y. Ikehara et al., "ABO blood type, *Lewis* and *Secretor* genotypes, and chronic atrophic gastritis: a cross-sectional study in Japan," *Gastric Cancer*, vol. 6, no. 1, pp. 8–16, 2003.

[16] N. Hamajima, A. Shibata, Y. Ikehara et al., "Lack of consistency in the associations of *Helicobacter pylori* seropositivity with Se and *Le* polymorphisms among Japanese," *Gastric Cancer*, vol. 5, no. 4, pp. 194–200, 2002.

[17] L. Excoffier, G. Laval, and S. Schneider, "Arlequin (version 3.0): an integrated software package for population genetics data analysis," *Evolutionary Bioinformatics Online*, vol. 1, pp. 47–50, 2005.

[18] Y. Koda, T. Ishida, H. Tachida et al., "DNA sequence variation of the human ABO-secretor locus (FUT2) in New Guinean populations: possible early human migration from Africa," *Human Genetics*, vol. 113, no. 6, pp. 534–541, 2003.

[19] T. C. Corvelo, S. de Loiola Rdo, D. C. Aguiar et al., "The Lewis histo-blood group system: molecular analysis of the 59T > G, 508G > A, and 1067T > A polymorphisms in an Amazonian population," *PLoS ONE*, vol. 8, no. 7, Article ID e69908, 2013.

[20] S. Sen and M. Burmeister, "Hardy-Weinberg analysis of a large set of published association studies reveals genotyping error and a deficit of heterozygotes across multiple loci," *Human genomics*, vol. 3, no. 1, pp. 36–52, 2008.

Review Article

Role of G Protein-Coupled Receptors in Control of Dendritic Cell Migration

Yuan Liu and Guixiu Shi

Department of Rheumatology and Clinical Immunology, The First Affiliated Hospital, Xiamen University,
No. 55, Zhenhai Road, Xiamen 361003, China

Correspondence should be addressed to Guixiu Shi; guixiu.shi@gmail.com

Dendritic cells (DCs) are highly efficient antigen-presenting cells. The migratory properties of DCs give them the capacity to be a sentinel of the body and the vital role in the induction and regulation of adaptive immune responses. Therefore, it is important to understand the mechanisms in control of migration of DCs to lymphoid and nonlymphoid tissues. This may provide us novel insight into the clinical treatment of diseases such as autoimmune disease, infectious disease, and tumor. The chemotactic G protein-coupled receptors (GPCR) play a vital role in control of DCs migration. Here, we reviewed the recent advances regarding the role of GPCR in control of migration of subsets of DCs, with a focus on the chemokine receptors. Understanding subsets of DCs migration could provide a rational basis for the design of novel therapies in various clinical conditions.

1. Introduction

Migration of immune cells is a fundamental biological process involved in normal physiology. This process increases the chance that lymphocytes will encounter the antigen and is also critical to the development of an inflammatory response. Abnormal immune cells migration is always associated with the development and progression of autoimmune diseases [1–3]. Many studies have provided strong support for this idea, and clinical studies have indicated that pharmacological inhibitors on immune cells migration can be highly effective in certain disease conditions [4, 5].

Dendritic cells (DCs) are highly efficient antigen-presenting cells (APC). Several subsets of DCs exist in mice and humans with distinct immunological activities, tissue distribution, and migratory properties. Following uptake of Antigen and in response to inflammatory signals, DCs reside within peripheral tissue become mature and migrate to lymph nodes where they initiate the acquired immunity [6]. In addition to activating the immune response, DCs are also decisive in creating tolerance [7]. The migratory properties of DCs give them capacity to be a sentinel of the body in recognizing the alloantigens, xenoantigens, autoantigens, and neoantigens, and give them the vital role in the induction and regulation of adaptive immune responses. Therefore, it is important to understand the mechanisms in control of migration of DCs, which may provide us novel insight into the clinical treatment of diseases such as autoimmune disease, infectious disease, and tumor.

G protein-coupled receptors (GPCR), the 7 transmembrane receptors, encoded by more than 800 genes, are activated by a large variety of factors ranging from small amines to hormones and chemokines [8]. Chemokines are the most well-known factors in the induction of immune cell migration, and all chemokine receptors identified so far are membrane-bound GPCRs. Besides chemokines, several bioactive lipids or hormones such as Sphingosine 1-phosphate (S1P), Lysophosphatidic acid (LPA), and angiotensin II can also regulate the migration of DCs by binding to receptors coupled to G proteins [9–11]. GPCRs play a central role in control of DCs migration. In this review, we focused on the role of chemokine receptors in control of migration of DCs.

Thymus
DC progenitor
Sirpα^- CD11b$^-$ CD8α^{hi} DCs
Sirpα^+ CD11b$^+$ CD8α^- DCs
pDCs

Bone marrow

Spleen
CD4$^-$ CD8α^+ DC
CD4$^-$ CD8α^- DC
CD4$^+$ CD8α^- DC

Blood circulation

DC precursor
cDC
pDC

Newly generated and experienced DCs

Secondary lymphoid organ

Other lymphoid tissues

Lymph node
CD8α^+ DC
CD8α^+ DC
CD8^{int} LFA-1^{int} DC

Peripheral tissues

Skin
Langerhans cells
Dermal DCs

Intestine
PP CD103$^+$ DC
LP CD103$^+$ DC
LP CD103$^-$ DC

Lung
CD103$^+$ CD11b^{lo} CD11c$^+$ DC
CD103$^-$ CD11b^{hi} CD11c$^+$DC,

Other periphery tissues

Figure 1: Schematic illustration of routes of migration of mouse DCs. DC precursors are released from the BM into the blood; DC progenitors can also be found in multiple locations including the thymus, blood, lymph, and most visceral organs. DC precursors seeded peripheral lymphoid tissues and nonlymphoid tissues and differentiated them into committed DCs. cDCs in peripheral tissues can access afferent lymph upon receiving a mobilization signal and travel to the draining LNs during both inflammation and steady-stated. pDCs travel to the LNs and spleen via hematogenous route. Some DCs might exit lymph nodes (LN) and start a still undefined pathway to recirculate. The circulating DCs in the blood contain both DC precursors and differentiated DC subsets, which are a mixture of newly generated cells from the BM and experienced DCs which have reentered the circulation from peripheral tissues.

2. Subsets of Dendritic Cells and Routes of Dendritic Cells Trafficking

Definition of subsets of DCs is still evolving with new technology. Dendritic cell was first discovered in peripheral lymphoid organs in the late 1970s [12]. Soon after that, DCs populate in nonlymphoid tissue such as Langerhans cell (LC) were identified. Classical mouse DCs in lymphoid tissue were further subdivided into two subsets by the presence or absence of CD8 expression (CD8$^+$ and CD11b$^+$ cDCs), and DCs in nonlymphoid tissue were subdivided by the expression of integrin CD103 (CD103$^+$ CD11b$^-$ and CD11b$^+$ cDCs) [13, 14]. However, human DCs did not express CD8, they can be split into CD1c$^+$ and CD141$^+$ subsets which share homology with mouse classical DCs expressing either CD11b (CD1c$^+$ DCs) or CD8/CD103 (CD141$^+$ DCs) [15].

In recent years, a population of DCs which morphologically resemble plasma cells but, upon exposure to viral stimuli, produce enormous amounts of interferon (IFN)-α, was identified and named as plasmacytoid dendritic cells (pDCs). The definition of classical DCs (cDCs) then came out which referred to DCs other than pDCs. DCs can also be classified into myeloid DCs and lymphoid DCs based on their origin. Phenotype characteristics and immune function of subsets of DCs were summarized by Merad et al. [16]. Subsets of DCs are different in migratory routes.

Most of the conclusions about the migration of DCs came from researches on mouse DCs. All DCs are thought to be ultimately derived from bone marrow (BM) [17]. Many DCs begin their journey with their release from the BM into the blood. Circulating DCs in the blood contain both DC precursors and differentiated DC subsets, which are a mixture of newly generated cells from the BM and experienced DCs. DCs in the blood subsequently traffic to lymphoid and nonlymphoid tissues. DCs in peripheral tissues such as skin, lung, and intestine migrate to draining lymph nodes to initiate acquired immunity during inflammation state, and this migration also happens in steady-state. A small fraction of these experienced DCs can reenter into the blood circulation and begin another cycle of journey. Unlike cDCs, pDCs are rarely found in peripheral tissues except for the intestine and enter the LN via the high endothelial venules (HEV) instead of afferent lymphatics. pDCs have been reported to migrate to sites of inflammation and to infiltrate tumors as well as solid organ transplants [18]. The routes of migration of mouse DCs are schematic illustrated in Figure 1.

3. Chemokine Receptors and DCs Migration

Chemokines are small molecular weight chemoattractant peptides first identified and characterized as being induced at sites of inflammation and thought to orchestrate the influx of leucocytes to the inflamed tissue. To date, more than 40 chemokines have been identified and classified into four families, C, CC, CXC, and CX3C, according to the motif displayed by the first two of four cysteine residues at the N terminus of the molecule [19]. The specific effect of chemokines is mediated by their G protein-coupled receptors. DCs migration is largely mediated by the interaction of chemokines with their G protein-coupled receptors. Selective expression of chemokine receptors on DCs tightly regulates the normal and inflammatory trafficking within lymphoid and nonlymphoid tissues [20].

There are 18 chemokine receptors that have been identified so far, receptors for fractalkine (CX3CR1) and lymphotactin (XCR1), 5 receptors that selectively bind certain CXC chemokines named as CXCR1 to CXCR5, 9 receptors which bind to CC chemokine named as CCR1 to CCR9, D6 which has been termed as CCR10 by some research group, and receptor which can bind to both CXC and CC chemokines known as the Duffy antigen receptor for chemokines (DARC) [21].

Studies on the in vitro derived DCs (CD34$^+$ stem cell or bone marrow-derived DCs) found that immature DCs can express CCR1, CCR2, CCR5, CCR6, CXCR1, CXCR2, and CXCR4, with these expression patterns differing somewhat among DC subsets. However, chemokine receptors expression profile from the in vitro study may not accurately mirror the changes that occur on DCs in vivo. It has been indicated that several chemokine receptors including CCR1, CCR2, CCR3, CCR5, CCR6, CCR7, CCR9, CCR10, CXCR3, CXCR4, CXCR5, and ChemR23 are involved in control of different subsets of DCs recruitment to periphery tissues and migration to secondary lymphoid tissues or migration within lymphoid tissues.

3.1. Chemokine Receptors and Mouse DCs Migration

3.1.1. CCR1. Expression of CCR1 can be detected on immature DCs. Its ligand CCL9, also known as MIP-γ, is constitutively secreted by the follicle-associated epithelium (FAE) within the dome regions of the Peyer's patches in mouse, and it may play a role in the recruitment of CD11b$^+$ DCs in the dome regions of the Peyer's patches in addition to the CCR6-dependent manner [22]. Study also indicated the possible role of CCR1 as well as CCR5 in regulation of recruitment of immature DC precursors into resting airway tissues and during acute bacterial-induced inflammation by using Met-RANTES, which retained high binding affinity to CCR1 and CCR5. However, the effect of CCR1 in control of DCs migration appeared to depend on the nature of the eliciting stimulus, because the recruitment of DCs was not affected by Met-RANTES in inflammation induced by Sendai virus infection and after aerosol challenge of sensitized animals with the soluble recall Ag OVA [23]. These data suggest that CCR1 might play a role in recruitment of immature DCs to

periphery tissues during both steady-state and inflammatory-state. However, all of these conclusions came from some indirect data, the direct effect of CCR1 in the DCs migration still needs to be proved.

3.1.2. CCR2. CCR2 is expressed on immature DCs, and its expression can be also detected in mature DCs [54]. Its main ligand is CCL2 [55]. Several studies demonstrated the central role of CCR2 in the recruitment of DCs to the lung during inflammation by using CCR2 knockout mice. Robays and his colleague showed that CCR2 was involved in the recruitment of DCs in the lung during allergic inflammation and may mediate the release of DC precursors into the bloodstream, and CCR2 was critical in inducing Th2 responses [24, 25]. However, controversy existed about the role of CCR2 in the Th1 or Th2 induction. In the situation of fungal pathogen and mycobacterium tuberculosis infection, CCR2 was shown to be involved in recruitment of myeloid DCs and CD11c$^{\text{dim/intermediate}}$ DCs to the lung, respectively, and it was supposed to mount Th1 immune responses [26, 27]. Besides the role of CCR2 in the immature DCs trafficking, it can also regulate the migration of some activated DCs to the draining LNs. Study using CCR2-null mice showed that migration of Langerhans cell from skin to draining lymph nodes was impaired with reduced Th1-inducing DCs (CD8α^+ DC) in the spleen and impaired infection-induced relocalization of CD11c$^+$ DC from the marginal zone (MZ) to the T cell areas in spleen [28].

3.1.3. CCR5. CCR5 is the major HIV-1 coreceptors for R5 strains. CCR5 is shown to be expressed by immature blood DCs in human, and in vitro maturation of blood DCs resulted in median 3-fold increases in CCR5 expression [56]. Its ligands CCL3, CCL4, and CCL5 are produced in the inflamed LNs of humans and/or mice [57, 58]. In mice, the role of CCR5 in the migration of pDCs to LNs has been demonstrated by several studies. By using CCR5 deficient pDCs (derived from BM of CCR5 −/− mice), Diacovo proved that migration of pDCs from blood to inflamed peripheral lymph nodes relied in part on CCR5 rather than CXCR3 [29].

3.1.4. CCR6. CCR6 is expressed by immature DCs, different in subsets of DCs (absent from CD8α^+ lymphoid DC), and the expression level of CCR6 decreases progressively as DCs mature [59]. Its ligand CCL20 is expressed by inflamed skin, mucosal epithelium, and mucosal-associated lymphoid tissue epithelium, and it plays an important role in recruitment of immature DCs to inflamed skin or mucosa [20]. Study on the CCR6 deficient mice showed that myeloid CD11c$^+$ CD11b$^+$ dendritic cells were absent from the subepithelial dome of Peyer's patches, which indicated the role of CCR6 in recruitment of myeloid DCs to the Peyer's patches [30, 31]. Similarly, studies also demonstrated the role of CCR6 in recruitment of myeloid DCs to the inflamed epithelial tissues such as skin [32]. Study also indicated that in some situation such as consecutive to an initial CCR7-mediated recruitment from blood into lymphoid tissues draining inflamed epithelia, pDCs might be conditioned to acquire CCR6 and CCR10

expression and migrate into inflamed epithelia of mucosae or skin. This study suggests an unexpected pDCs migratory model, after CCR7-mediated extravasation of blood pDCs into lymphoid tissues draining inflamed epithelia, they may be instructed to up-regulate CCR6 and/or CCR10 allowing their homing into inflamed epithelia (in mucosae or skin) [33].

3.1.5. CCR7. CCR7 has been identified as a key regulator of lymphocytes trafficking to secondary lymphoid organs [60]. It is expressed by mature DCs [61]. CCL19 and CCL21 (also known as secondary lymphoid-tissue chemokine) are the two ligands of CCR7 which are found to express in the afferent lymphatic vessel and LN paracortex and subcapsular sinus (SCS) in mice [62]. The role of CCR7 in DCs migration has been well studied in mice DCs. Several studies demonstrated the role of CCR7 in control of tissue-resident myeloid dendritic cells from periphery tissues such as skin and mucosa migration to draining LNs via the afferent lymphatics under inflammatory and steady-state conditions [34, 63]. The role of CCR7 in migration of pDCs remains controversial. Some studies showed that murine pDCs were CCR7 negative or low, and functionally were considered unresponsive to CCR7 ligands [64, 65]. However, studies using CCR7-deficient mice demonstrated the role of CCR7 in regulation of pDCs migration to secondary lymphoid organs. Sebastian found that ex vivo derived nonstimulated and naive pDC express CCR7, CCR7-deficient pDC showed impaired homing to resting as well as inflamed LN, and identified that CCR7 was an important LN homing receptor for pDC under both steady-state and inflammatory conditions [35]. Umemoto showed that CCR7 as well as CXCR4 were both critical chemokine receptors required for pDCs to migrate into white pulp in the spleen under steady-state conditions [36].

3.1.6. CCR9. CCR9 has first been identified on T cells as a chemokine receptor that directs these cells to migrate to the intestine. The CCR9 receptor is not unique to T cells and has also been reported on both myeloid and pDCs, and the expression level of CCR9 was inversely related to the maturation state of DCs [66]. CCL25, also known as thymus-expressed chemokine (TECK), is the ligand of CCR9, which is found in the thymic cortex and in the small intestinal mucosa [67, 68]. It was reported that CCR9 controlled the migration of pDC to the small intestine under both steady-state and inflammatory conditions [37]. The CCR9$^+$ pDCs in tissue was thought to be immunosuppressive population [69, 70]. However, the role of CCR9 in myeloid DCs migration still needed to be investigated.

3.1.7. CXCR3. Study using the human CXCR3-specific monoclonal antibodies showed that CXCR3 was expressed in certain dendritic cells subsets, specifically myeloid-derived CD11c$^+$ cells both in normal lymphoid organs and inflammatory conditions [71]. Study also showed that CXCR3 was functionally expressed in pDCs and induced migration of

pDCs. By using CXCR3 (−/−) mice, Yoneyama et al. demonstrated that CXCR3 played an important role in recruitment of pDC precursors to inflamed lymph nodes through high endothelial venules (HEV) in propionibacterium acnes-primed or HSV-infected mice [38]. And similarly, Asselin-Paturel showed that murine CMV infection and systemic injection of TLR7 and TLR9 ligands can induce migration and clustering of splenic pDCs in the spleen marginal zone, which was dependent on CXCR3 [39]. However, in the study of Diacovo, it was showed that CCR5 instead of CXCR3 was required for pDC migration in response to heat-killed mycobacterium tuberculosis. This difference might be due to the different inflammatory conditions [29].

3.1.8. CXCR4. CXCR4 is the major HIV-1 coreceptors for X4 HIV-1 strains. The expression of CXCR4 on immature DCs is low and is up-regulated during maturation [56]. Its ligand CXCL12 is one of the three most important chemokines (CCL19, CCL21, and CXCL12) which directs DCs migrate from sites of infection to secondary lymphoid organs. Kabashima found that CXCR4 was highly expressed on migrated cutaneous DCs and its ligand, CXCL12, was detected in the LYVE-1(+) lymphatic vessels in the skin. By using CXCR4 antagonist 4-F-Benzoyl-TN14003, they demonstrated that CXCR4 was required for migration of cutaneous dendritic cells to LNs [40]. Umemoto showed that CXCR4 as well as CCR7, cooperatively regulated pDCs migration to the splenic white pulp under steady-state conditions [36].

3.1.9. CXCR5. It was thought that expression of CXCR5 was restricted to mature, recirculating B cells as well as small subpopulations of CD4$^+$ and CD8$^+$ T lymphocytes [72]. Study also indicated that CXCR5 can be expressed by activated DCs and may be involved in their migration to draining LNs. The CXCR5 ligand CXCL13, also known as B lymphocyte chemoattractant or (BLC), is highly expressed in B cell zones of secondary lymphoid organs. Saeki showed that activated dermal type DCs expressed CXCR5 and these DCs utilize CXCR5 and BLC as a possible mechanism to migrate to B cell zones as well as T cell zones (TCZ) in draining LN in vivo. However, in vitro murine bone marrow derived DCs displayed less CXCR5 expression than the activated skin DCs, and they do not migrate to BLC [41, 73].

3.1.10. ChemR23. ChemR23 is a previously orphan protein G coupled receptor highly expressed in immature pDCs and at lower levels in myeloid DCs. Chemerin is the natural ligand of the ChemR23 and a chemoattractant factor for human immature dendritic cells (DCs), macrophages, and NK cells [74]. It played a central role in human pDCs migration. It was reported that ChemR23 was not present on mouse DCs [75]. However, Souphalone demonstrated that ChemR23 was functionally expressed by mouse DCs and mediated an anti-inflammatory activity in a lung disease model [74]. These controversies on the expression of ChemR23 on mouse DCs are presumably the result of the different sensitivity of the Abs used in these studies.

TABLE 1: Chemokine receptors and chemokines involved in migration of mouse DCs subsets.

Receptor	Ligands	Cellular distribution	Role in migration	Reference
CCR1	MIP-1γ/CCL9	Immature DCs	Recruitment of CD11b$^+$ DCs to the dome regions of Peyer's patch	[22]
			Recruitment of DC precursors into airway epithelium during bacterial inflammation and steady-state	[23]
CCR2	CCL2/MCP-1	Immature DCs	Recruitment of DCs in the lung during allergic inflammation, and supposed to be critical in inducing T(H)2 responses	[24, 25]
			Recruitment of CD11c$^{dim/intermediate}$ DCs in the lung during mycobacterium tuberculosis infection and cDCs during Cryptococcus neoformans infection, may be important in inducing T(H)1 responses	[26, 27]
		Mature DCs	Activated LC migrate from skin to draining LNs and regulate infection-induced relocalization of CD11c$^+$ DC in spleen	[28]
CCR5	MIP-1α/CCL3 MIP-1β/CCL4 Rantes/CCL5	Immature DCs mature DCs	Recruitment of pDC to inflamed peripheral lymph nodes	[29]
CCR6	CCL20/MIP-3α	Immature myeloid DC, subsets of pDCs	Recruitment of myeloid CD11c$^+$ CD11b$^+$ dendritic cells to the dome regions of Peyer's patches	[30, 31]
			Recruitment of myeloid DCs to the inflamed epithelial tissues such as skin	[32]
			mediate pDC recruitment to inflamed epithelia	[33]
CCR7	CCL19/MIP-3β CCL21/SLC	Mature DCs	essential for directing the antigen-loaded mature cDCs to the T cell-rich areas of the draining lymph node during inflammatory and steady-state conditions	[34]
			Migration of pDCs to LNs via HEV under both steady-state and inflammatory conditions	[35]
			Migration of pDC to the splenic white pulp under steady-state conditions	[36]
CCR9	CCL25	Myeloid and pDC	Controls the migration of pDC to the small intestine under both steady-state and inflammatory conditions	[37]
CCR10	CCL27 CCL28	Subset of tonsil pDCs, IL-3-cultured blood pDCs	Mediate pDC homing into inflamed epithelia	[33]
CXCR3	CXCL9 CXCL10/IP-10 CXCL11	pDC precursors pDC CD11c$^+$ myeloid DCs monocyte-derived iDC	Migration of pDC to inflamed LNs via HEV	[38]
			migration and clustering of splenic plasmacytoid DCs in the spleen marginal zone	[39]
CXCR4	CXCL12/SDF-1α	Immature DCs mature DCs pDC	Migration of skin dendritic cells to LNs	[40]
			Migration of pDC to the splenic white pulp under steady-state conditions	[36]
CXCR5	CXCL13/BLC/BCA-1	Activated skin DC	Activated dermal DC migrate to draining LNs	[41]

3.2. Chemokine Receptors in Human DCs Migration and Their Role in Diseases. Studies on the role of CCRs in human DCs migration are relatively few compared to studies in mouse. Most conclusions came from indirect evidence by using specific antibody or by analyzing their expression to speculate their role in human DCs migration.

Sato et al. indicated the role of CCR1 and CCR3 in human peripheral blood monocyte-derived dendritic cells migration by using monoclonal antibody (MoAb) to CCR1 and CCR3

[42]. Human cytomegalovirus may use a mechanism by down-regulating CCR1 and CCR5 expression on human DCs to paralyze the early immune response of the host [76], and filarial infection can also down-regulate the CCR1 expression on monocyte-derived DCs which may alter DCs migration [77].

By analyzing the expression of CCR2 and CCR6 on subsets of DCs as well as the ligands of CCR2 and CCR6 expression in different sites in the body, Vanbervliet

TABLE 2: Chemokine receptors and chemokines involved in migration of human DCs subsets.

Receptor	Ligands	Cellular distribution	Role in migration	Reference
CCR1	MIP-1γ/CCL9	Immature DCs	May be involved in human peripheral blood monocyte-derived dendritic cells migration	[42]
CCR2	CCL2/MCP-1	Immature mature DCs	Recruitment of circulating blood DCs and monocytes to inflamed tissue	[43]
CCR3	Eotaxin eotaxin-2	Immature DCs mature DCs	May be involved in dendritic cells migration	[42, 44]
CCR5	MIP-1α/CCL3 MIP-1β/CCL4 Rantes/CCL5	Immature DCs mature DCs	Attract DCs to migrate cross the human intestinal epithelium and sample luminal virions	[45]
			May contribute to the recruitment of blood myeloid DC to cerebrospinal fluid in multiple sclerosis patients and acute optic neuritis.	[46]
			May be involved in the altered homing of blood DCs during the alloimmune response	[47]
CCR6	CCL20/MIP-3α	pDCs	May be involved in leukemic pDCs and blood pDCs from melanoma patients recruitment to lesions of skin	[48, 49]
			Recruitment of circulating blood DCs and monocytes to inflamed tissue	[43]
CXCR3	CXCL9 CXCL10/IP-10 CXCL11	pDCs immature CD1a$^+$ DC	Might be involved in the recruitment of pDC and immature CD1a$^+$ DCs to tissue lesions	[50, 51]
ChemR23	Chemerin	Immature pDCs	Migration plasmacytoid dendritic cells to lymphoid organs and inflamed skin	[52, 53]

indicated the possible role of CCR2 and CCR6 in control DCs migration by raising a novel model of how DCs in the blood migrate to inflamed epithelial surfaces: CCR2(+) circulating DC or DC precursors are mobilized into the tissue via the expression of MCP by cells lining blood vessels, and these cells traffic from the tissue to the site of pathogen invasion via the production of MIP-3alpha/CL20 by epithelial cells and the up-regulation of CCR6 in response to the tissue environment [43].

CCR3 is the chemokine receptor initially discovered on eosinophils. Study showed that it was also expressed by human DCs that differentiated from blood monocytes, DCs that emigrated from skin (epidermal and dermal DCs), and DCs derived from CD34$^+$ hemopoietic precursors in bone marrow and umbilical cord blood. Unlike other chemokine receptors, such as CCR5 and CCR7, the expression of CCR3 is not dependent on the state of maturation. Indirect study by using CCR3 antibodies indicated the possible role of CCR3 in the DCs migration induced by its ligand eotaxin and eotaxin-2 [42, 44]. Studies on the role of CCR3 in the DCs migration are few, and the specific role of CCR3 in control of subsets of DCs migration is still not clear.

In human, the role of CCR5 has also been indicated in DCs migration in some situations such as in HIV-1 infection and Acute Graft-Versus-Host Disease [45–47]. However, unlike mice pDCs, the recruitment of pDCs appeared to be CCR5 independent. Pashenkov showed that expression of CCR5 was elevated on blood myeloid (CD11c$^+$) DC in multiple sclerosis (MS) and optic neuritis patients compared

to noninflammatory controls, its ligands RANTES and MIP-1beta were expressed in MS lesions, and the expression of CCR5 by myeloid DC in blood correlated with numbers of these cells in cerebrospinal fluid (CSF), which suggest that CCR5 may contribute to recruitment of myeloid DC (CD11c$^+$) to the CSF in these patients, but recruitment of plasmacytoid DC to CSF appeared to be CCR5-independent [46].

Studies also showed that CCR6 was expressed on leukemic pDCs and blood pDCs from melanoma patients and involved in the recruitment of pDC to lesions of skin [48, 49].

Most of the conclusions about the role of CCR7 on the human DCs migration came from the research on mouse DCs. The specific role of CCR7 in subsets of human DCs migration still needed to be confirmed as in mouse DCs.

It was found that in some inflamed situations such as in psoriatic lesions, pDCs found in the lesions were nearly all CXCR3(+), indirectly implicated the possible role for CXCR3 in mediating the recruitment of pDCs into the periphery tissue and developing lesions in human [50]. Besides its ligand CCL9–11, research about uveitis indicated that CXCR3 was involved in the immature DCs migration induced by retinal autoantigens S-antigen (S-Ag) and interphotoreceptor retinoid binding protein (IRBP), suggesting its role in the autoimmune disease [51].

In human DCs, it was found that ChemR23 was expressed both on pDCs and myeloid DCs. Its ligand can induce the transmigration of plasmacytoid and myeloid
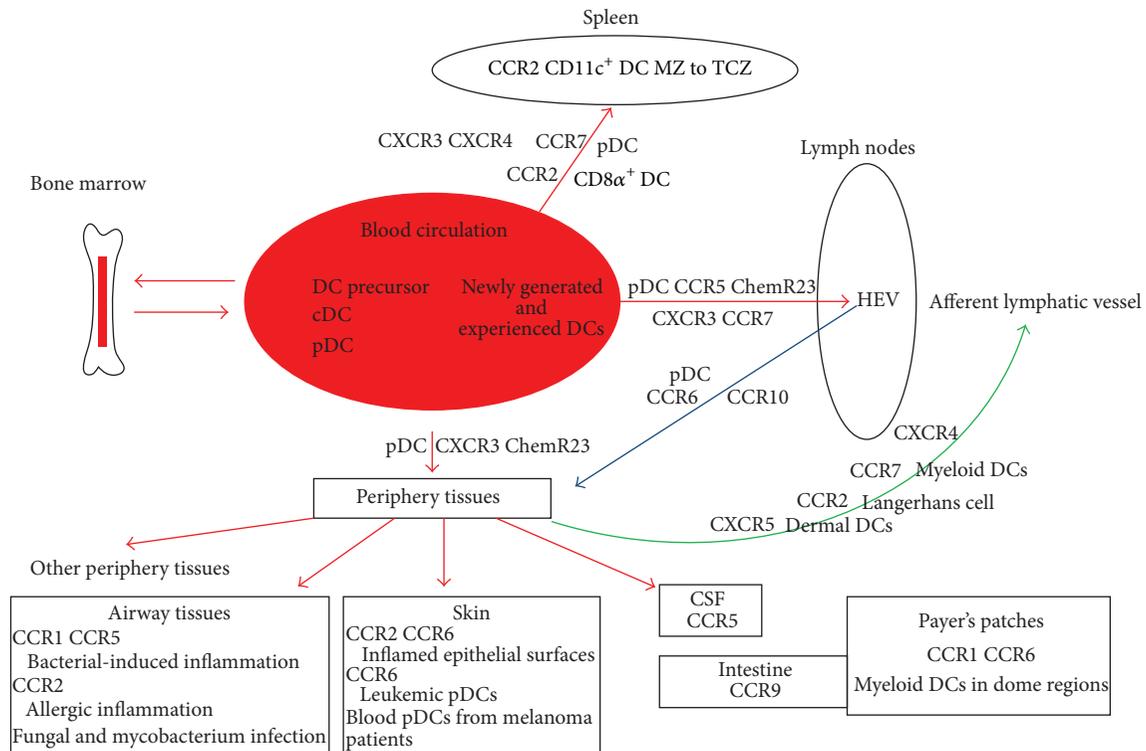
FIGURE 2: Chemokine receptors involved in migration of mouse and human DCs subsets. CCR7, CXCR4, CCR2, and CXCR5 are involved in subsets of cDCs migration from periphery tissues to draining LNs in both inflammation and steady-state. CCR5, ChemR23, CXCR3, and CCR7 are involved in migration of pDCs to LNs via hematogenous route. CCR2 is implicated in control of CD8α$^+$ DC to the spleen and relocalization of CD11c$^+$ DC from the marginal zone to the T cell areas in spleen. CCR7, CXCR3, and CXCR4 are shown to be involved in pDCs migration from blood to spleen. CCR1, CCR2, CCR5, and CCR6 are involved in the recruitment of cDCs to different tissues in specific situations. CCR9 is shown to have a role in controlling the migration of pDC to the small intestine under both steady-state and inflammatory conditions. In other situations of inflammation or tumor, CXCR3, ChemR23, and CCR6 are implicated to be involved in pDCs migration to periphery tissues.

DCs across an endothelial cell monolayer in vitro. The Chemerin (+) endothelial cells were found to be surrounded by ChemR23(+) pDCs, which suggest a key role of the ChemR23/Chemerin axis in directing plasmacytoid DC trafficking [52]. Similarly, De Palma found that Chemerin was associated with tubular epithelial cells and renal lymphatic endothelial cells in patients with lupus nephritis but not in normal kidneys, and ChemR23-positive DCs had infiltrated the kidney tubulointerstitium in patients with severe lupus nephritis. The induced Chemerin can result in an efficient transendothelial migration of pDCs measured in transwell systems. These data suggest the role of ChemR23 in the recruitment of pDCs within the kidney in lupus nephritis patients [53].

The role of chemokines receptor in control of subsets of mouse and human DCs migration was summarized in Tables 1 and 2 and Figure 2.

4. Signaling Pathways Involved in Chemokine Receptor Signaling

All chemokine receptors are thought to couple to G proteins. The heterotrimeric G-proteins consist of a α-subunit that binds and hydrolyses GTP as well as a β- and a γ-subunit that form an undissociable complex. Based on the types of their α subunits, G proteins can be grouped into four subfamilies, they are Gαi, Gαs, Gαq/11, and G12/13, each subfamily contains several members of G proteins [78].

The mechanism involved in the CCR7 signaling has been well studied; it is a multimodule model with the involvement of Gαi, Gαq, and Gα12 [79]. It was thought that chemotaxis induced by chemokine receptors was mainly through the Gαi subfamily. The ligation of CCR7 and its ligands mediated the activation of G proteins induced by the binding of GTP to Gαi and the release of free $\beta\gamma$ subunits. The $\beta\gamma$ subunits subsequently activated downstream effectors such as PI3K which regulate the Akt pathway [80]. However, it seemed that these enzymes did not regulate either chemotaxis or the speed of DCs but regulated CCR7-dependent DC survival [81, 82]. MAPK members ERK1/2, JNK, and p38 were also found to be activated and depended on Gαi in the CCR7 signaling cascades and played an important role in regulating DCs chemotaxis. Besides the role of Gαi in the chemokine receptors signaling pathway, in recent years, chemokine receptors coupled to other G protein subfamilies has also been demonstrated. Study found that Gnaq −/− DCs

were unable to migrate to inflammatory sites and LNs in vivo, which indicated the role of Gαq in the chemokine receptor signaling. Gαq, like CD38, regulated the extracellular calcium entry in chemokine-stimulated cells [83]. In addition to Gαq, CCR7 also used another pathway involving Rho/Pyk2/cofilin and presumably depended on G12/G13 to control the migratory speed of DCs [81].

5. Perspectives

Several families of chemokines receptors and their chemokine ligands orchestrate subsets of DCs trafficking. For cDCs, CCR7 plays a central role in the migration of mature DCs to the draining LNs via lymphatic vessels during both inflammation and steady-state conditions, with a multimodule signaling model that involved Gαi, Gαq, and Gα12. CXCR4, CCR2, and CXCR5 have also been implicated to be involved in some subsets of cDCs migration from periphery tissues to draining LNs. CCR2 is also implicated in control of CD8α⁺ DC to the spleen and relocalization of CD11c⁺ DC from the marginal zone to the T cell areas in spleen. CCR1, CCR2, CCR5, and CCR6 are involved in the recruitment of cDCs to different tissues in specific situations. pDCs use a very different migratory patterns compared with cDCs. For pDCs, CCR5, ChemR23, CXCR3, and CCR7 are involved in migration of pDCs to LNs via hematogenous route, though the role of CCR5 versus CXCR3 and role of CCR7 in pDCs migration remains controversial. CCR7, CXCR3, and CXCR4 are shown to be involved in pDCs migration from blood to spleen. CCR9 is shown to have a role in controlling the migration of pDC to the small intestine under both steady-state and inflammatory conditions. In other situations of inflammation or tumor, CXCR3, ChemR23, and CCR6 are implicated to be involved in pDCs migration to periphery tissues.

However, there are still some limitations in the present studies on the role of chemokines receptors in the control of DCs migration. Some conclusions on the role of chemokines receptors in subsets of DCs migration came from indirect evidence by studying the expression change of chemokine receptors on DCs or by using an antagonist of a chemokine receptor to draw a possible conclusion. Experiments using chemokines receptors knockout mice also have their limitations, because it can affects a wide variety of cells potentially implicated in the inflammation. Studies using in vitro derived DCs may not accurately mirror the situations occurring in vivo. The role of chemokines receptors in the control of migration of a specific subset of DCs remains to be defined which causes the different roles of subsets of DCs in immune regulation. Understanding this complex orchestration of chemokines receptors in the subsets of DCs migration will be essential to manipulate efficiently the function of a specific subset of DCs and facilitate our clinical treatment in multiple diseases in which DCs are involved.

Conflict of Interests

The authors declare that there is no conflict of interests.

Acknowledgments

References

[1] R. M. Thurlings, C. A. Wijbrandts, R. J. Bennink et al., "Monocyte scintigraphy in rheumatoid arthritis: the dynamics of monocyte migration in immune-mediated inflammatory disease," *PLoS ONE*, vol. 4, no. 11, Article ID e7865, 2009.

[2] M. U. Norman and M. J. Hickey, "Mechanisms of lymphocyte migration in autoimmune disease," *Tissue Antigens*, vol. 66, no. 3, pp. 163–172, 2005.

[3] J. Marsal and W. W. Agace, "Targeting T-cell migration in inflammatory bowel disease," *Journal of Internal Medicine*, vol. 272, no. 5, pp. 411–429, 2012.

[4] C. R. Mackay, "Moving targets: cell migration inhibitors as new anti-inflammatory therapies," *Nature Immunology*, vol. 9, no. 9, pp. 988–998, 2008.

[5] A. D. Luster, R. Alon, and U. H. von Andrian, "Immune cell migration in inflammation: present and future therapeutic targets," *Nature Immunology*, vol. 6, no. 12, pp. 1182–1190, 2005.

[6] J. Banchereau and R. M. Steinman, "Dendritic cells and the control of immunity," *Nature*, vol. 392, no. 6673, pp. 245–252, 1998.

[7] R. M. Steinman, "Some interfaces of dendritic cell biology," *APMIS*, vol. 111, no. 7-8, pp. 675–697, 2003.

[8] V. Katritch, V. Cherezov, and R. C. Stevens, "Structure-function of the G protein-coupled receptor superfamily," *Annual Review of Pharmacology and Toxicology*, vol. 53, pp. 531–556, 2013.

[9] Y. Maeda, H. Matsuyuki, K. Shimano, H. Kataoka, K. Sugahara, and K. Chiba, "Migration of CD4 T cells and dendritic cells toward sphingosine 1-phosphate (S1P) is mediated by different receptor subtypes: S1P regulates the functions of murine mature dendritic cells via S1P receptor type 3," *Journal of Immunology*, vol. 178, no. 6, pp. 3437–3446, 2007.

[10] L. C. Chan, W. Peters, Y. Xu, J. Chun, R. V. Farese Jr., and S. Cases, "LPA3 receptor mediates chemotaxis of immature murine dendritic cells to unsaturated lysophosphatidic acid (LPA)," *Journal of Leukocyte Biology*, vol. 82, no. 5, pp. 1193–1200, 2007.

[11] M. Jurewicz, D. H. McDermott, J. M. Sechler et al., "Human T and natural killer cells possess a functional renin-angiotensin system: further mechanisms of angiotensin II-induced inflammation," *Journal of the American Society of Nephrology*, vol. 18, no. 4, pp. 1093–1102, 2007.

[12] R. M. Steinman and Z. A. Cohn, "Identification of a novel cell type in peripheral lymphoid organs of mice. I. Morphology, quantitation, tissue distribution," *Journal of Experimental Medicine*, vol. 137, no. 5, pp. 1142–1162, 1973.

[13] K. Shortman and W. R. Heath, "The CD8+ dendritic cell subset," *Immunological Reviews*, vol. 234, no. 1, pp. 18–31, 2010.

[14] J. Helft, F. Ginhoux, M. Bogunovic, and M. Merad, "Origin and functional heterogeneity of non-lymphoid tissue dendritic cells in mice," *Immunological Reviews*, vol. 234, no. 1, pp. 55–75, 2010.

[15] M. Collin, N. McGovern, and M. Haniffa, "Human dendritic cell subsets," *Immunology*, vol. 140, no. 1, pp. 22–30, 2013.

[16] M. Merad, P. Sathe, J. Helft, J. Miller, and A. Mortha, "The dendritic cell lineage: ontogeny and function of dendritic cells

and their subsets in the steady state and the inflamed setting," *Annual Review of Immunology*, vol. 31, pp. 563–604, 2013.

[17] S. H. Naik, P. Sathe, H.-Y. Park et al., "Development of plasmacytoid and conventional dendritic cell subtypes from single precursor cells derived in vitro and in vivo," *Nature Immunology*, vol. 8, no. 11, pp. 1217–1226, 2007.

[18] K. McKenna, A.-S. Beignon, and N. Bhardwaj, "Plasmacytoid dendritic cells: linking innate and adaptive immunity," *Journal of Virology*, vol. 79, no. 1, pp. 17–27, 2005.

[19] D. Rossi and A. Zlotnik, "The biology of chemokines and their receptors," *Annual Review of Immunology*, vol. 18, pp. 217–243, 2000.

[20] M.-C. Dieu, B. Vanbervliet, A. Vicari et al., "Selective recruitment of immature and mature dendritic cells by distinct chemokines expressed in different anatomic sites," *Journal of Experimental Medicine*, vol. 188, no. 2, pp. 373–386, 1998.

[21] C. Murdoch and A. Finn, "Chemokine receptors and their role in inflammation and infectious diseases," *Blood*, vol. 95, no. 10, pp. 3032–3043, 2000.

[22] X. Zhao, A. Sato, C. S. Dela Cruz et al., "CCL9 is secreted by the follicle-associated epithelium and recruits dome region Peyer's patch CD11b+ dendritic cells," *Journal of Immunology*, vol. 171, no. 6, pp. 2797–2803, 2003.

[23] P. A. Stumbles, D. H. Strickland, C. L. Pimm et al., "Regulation of dendritic cell recruitment into resting and inflamed airway epithelium: use of alternative chemokine receptors as a function of inducing stimulus," *Journal of Immunology*, vol. 167, no. 1, pp. 228–234, 2001.

[24] L. J. Robays, T. Maes, S. Lebecque et al., "Chemokine receptor CCR2 but not CCR5 or CCR6 mediates the increase in pulmonary dendritic cells during allergic airway inflammation," *Journal of Immunology*, vol. 178, no. 8, pp. 5305–5311, 2007.

[25] S. Provoost, T. Maes, G. F. Joos, and K. G. Tournoy, "Monocyte-derived dendritic cell recruitment and allergic TH2 responses after exposure to diesel particles are CCR2 dependent," *Journal of Allergy and Clinical Immunology*, vol. 129, no. 2, pp. 483–491, 2012.

[26] J. J. Osterholzer, J. L. Curtis, T. Polak et al., "CCR2 mediates conventional dendritic cell recruitment and the formation of bronchovascular mononuclear cell infiltrates in the lungs of mice infected with cryptococcus neoformans," *Journal of Immunology*, vol. 181, no. 1, pp. 610–620, 2008.

[27] W. Peters, J. G. Cyster, M. Mack et al., "CCR2-dependent trafficking of F4/80dim macrophages and CD11cdim/intermediate dendritic cells is crucial for T cell recruitment to lungs infected with *Mycobacterium tuberculosis*," *Journal of Immunology*, vol. 172, no. 12, pp. 7647–7653, 2004.

[28] N. Sato, S. K. Ahuja, M. Quinones et al., "CC chemokine receptor (CCR)2 is required for langerhans cell migration and localization of T helper cell type 1 (Th1)-inducing dendritic cells: absence of CCR2 shifts the Leishmania major—resistant phenotype to a susceptible state dominated by Th2 cytokines, B cell outgrowth, and sustained neutrophilic inflammation," *Journal of Experimental Medicine*, vol. 192, no. 2, pp. 205–218, 2000.

[29] T. G. Diacovo, A. L. Blasius, T. W. Mak, M. Cella, and M. Colonna, "Adhesive mechanisms governing interferon-producing cell recruitment into lymph nodes," *Journal of Experimental Medicine*, vol. 202, no. 5, pp. 687–696, 2005.

[30] D. N. Cook, D. M. Prosser, R. Forster et al., "CCR6 mediates dendritic cell localization, lymphocyte homeostasis, and immune responses in mucosal tissue," *Immunity*, vol. 12, no. 5, pp. 495–503, 2000.

[31] R. Varona, R. Villares, L. Carramolino et al., "CCR6-deficient mice have impaired leukocyte homeostasis and altered contact hypersensitivity and delayed-type hypersensitivity responses," *Journal of Clinical Investigation*, vol. 107, no. 6, pp. R37–R45, 2001.

[32] M. Le Borgne, N. Etchart, A. Goubier et al., "Dendritic cells rapidly recruited into epithelial tissues via CCR6/CCL20 are responsible for CD8+ T cell crosspriming in vivo," *Immunity*, vol. 24, no. 2, pp. 191–201, 2006.

[33] V. Sisirak, N. Vey, B. Vanbervliet et al., "CCR6/CCR10-mediated plasmacytoid dendritic cell recruitment to inflamed epithelia after instruction in lymphoid tissues," *Blood*, vol. 118, no. 19, pp. 5130–5140, 2011.

[34] L. Ohl, M. Mohaupt, N. Czeloth et al., "CCR7 governs skin dendritic cell migration under inflammatory and steady-state conditions," *Immunity*, vol. 21, no. 2, pp. 279–288, 2004.

[35] S. Seth, L. Oberdörfer, R. Hyde et al., "CCR7 essentially contributes to the homing of plasmacytoid dendritic cells to lymph nodes under steady-state as well as inflammatory conditions," *Journal of Immunology*, vol. 186, no. 6, pp. 3364–3372, 2011.

[36] E. Umemoto, K. Otani, T. Ikeno et al., "Constitutive plasmacytoid dendritic cell migration to the splenic white pulp is cooperatively regulated by CCR7- and CXCR4-mediated signaling," *Journal of Immunology*, vol. 189, no. 1, pp. 191–199, 2012.

[37] M. Wendland, N. Czeloth, N. Mach et al., "CCR9 is a homing receptor for plasmacytoid dendritic cells to the small intestine," *Proceedings of the National Academy of Sciences of the United States of America*, vol. 104, no. 15, pp. 6347–6352, 2007.

[38] H. Yoneyama, K. Matsuno, Y. Zhang et al., "Evidence for recruitment of plasmacytoid dendritic cell precursors to inflamed lymph nodes through high endothelial venules," *International Immunology*, vol. 16, no. 7, pp. 915–928, 2004.

[39] C. Asselin-Paturel, G. Brizard, K. Chemin et al., "Type I interferon dependence of plasmacytoid dendritic cell activation and migration," *Journal of Experimental Medicine*, vol. 201, no. 7, pp. 1157–1167, 2005.

[40] K. Kabashima, N. Shiraishi, K. Sugita et al., "CXCL12-CXCR4 engagement is required for migration of cutaneous dendritic cells," *American Journal of Pathology*, vol. 171, no. 4, pp. 1249–1257, 2007.

[41] M.-T. Wu and S. T. Hwang, "CXCR5-transduced bone marrow-derived dendritic cells traffic to B cell zones of lymph nodes and modify antigen-specific immune responses," *Journal of Immunology*, vol. 168, no. 10, pp. 5096–5102, 2002.

[42] K. Sato, H. Kawasaki, H. Nagayama et al., "CC chemokine receptors, CCR-1 and CCR-3, are potentially involved in antigen-presenting cell function of human peripheral blood monocyte-derived dendritic cells," *Blood*, vol. 93, no. 1, pp. 34–42, 1999.

[43] B. Vanbervliet, B. Homey, I. Durand et al., "Sequential involvement of CCR2 and CCR6 ligands for immature dendritic cell recruitment: possible role at inflamed epithelial surfaces," *European Journal of Immunology*, vol. 32, no. 1, pp. 231–242, 2002.

[44] S. Beaulieu, D. F. Robbiani, X. Du et al., "Expression of a functional eotaxin (CC chemokine ligand 11) receptor CCR3 by human dendritic cells," *Journal of Immunology*, vol. 169, no. 6, pp. 2925–2936, 2002.

[45] M. Cavarelli, C. Foglieni, M. Rescigno, and G. Scarlatti, "R5 HIV-1 envelope attracts dendritic cells to cross the human intestinal epithelium and sample luminal virions via engagement of the CCR5," *EMBO Molecular Medicine*, vol. 5, no. 5, pp. 776–794, 2013.

[46] M. Pashenkov, N. Teleshova, M. Kouwenhoven et al., "Elevated expression of CCR5 by myeloid (CD11c+) blood dendritic cells in multiple sclerosis and acute optic neuritis," *Clinical and Experimental Immunology*, vol. 127, no. 3, pp. 519–526, 2002.

[47] K. Shahin, M. Sartor, D. N. Hart, and K. F. Bradstock, "Alterations in chemokine receptor CCR5 expression on blood dendritic cells correlate with acute graft-versus-host disease," *Transplantation*, vol. 96, no. 8, pp. 753–762, 2013.

[48] J. Charles, J. Di Domizio, D. Salameire et al., "Characterization of circulating dendritic cells in melanoma: role of CCR6 in plasmacytoid dendritic cell recruitment to the tumor," *Journal of Investigative Dermatology*, vol. 130, no. 6, pp. 1646–1656, 2010.

[49] N. B. Vermare, L. Chaperot, M. Peoc'h et al., "In situ leukemic plasmacytoid dendritic cells pattern of chemokine receptors expression and in vitro migratory response," *Leukemia*, vol. 18, no. 9, pp. 1491–1498, 2004.

[50] S.-C. Chen, M. De Groot, D. Kinsley et al., "Expression of chemokine receptor CXCR3 by lymphocytes and plasmacytoid dendritic cells in human psoriatic lesions," *Archives of Dermatological Research*, vol. 302, no. 2, pp. 113–123, 2010.

[51] O. M. Z. Howard, F. D. Hui, B. S. Shao et al., "Autoantigens signal through chemokine receptors: uveitis antigens induce CXCR3- and CXCR5-expressing lymphocytes and immature dendritic cells to migrate," *Blood*, vol. 105, no. 11, pp. 4207–4214, 2005.

[52] W. Vermi, E. Riboldi, V. Wittamer et al., "Role of ChemR23 in directing the migration of myeloid and plasmacytoid dendritic cells to lymphoid organs and inflamed skin," *Journal of Experimental Medicine*, vol. 201, no. 4, pp. 509–515, 2005.

[53] G. De Palma, G. Castellano, A. Del Prete et al., "The possible role of ChemR23/Chemerin axis in the recruitment of dendritic cells in lupus nephritis," *Kidney International*, vol. 79, no. 11, pp. 1228–1235, 2011.

[54] A. Vecchi, L. Massimiliano, S. Ramponi et al., "Differential responsiveness to constitutive vs. inducible chemokines of immature and mature mouse dendritic cells," *Journal of Leukocyte Biology*, vol. 66, no. 3, pp. 489–494, 1999.

[55] F. Jimenez, M. P. Quinones, H. G. Martinez et al., "CCR2 plays a critical role in dendritic cell maturation: possible role of CCL2 and NF-κB," *Journal of Immunology*, vol. 184, no. 10, pp. 5571–5581, 2010.

[56] B. Lee, M. Sharron, L. J. Montaner, D. Weissman, and R. W. Doms, "Quantification of CD4, CCR5, and CXCR4 levels on lymphocyte subsets, dendritic cells, and differentially conditioned monocyte-derived macrophages," *Proceedings of the National Academy of Sciences of the United States of America*, vol. 96, no. 9, pp. 5215–5220, 1999.

[57] N. Tedla, H.-W. Wang, H. P. McNeil et al., "Regulation of T lymphocyte trafficking into lymph nodes during an immune response by the chemokines macrophage inflammatory protein (MIP)-1α and MIP-1β," *Journal of Immunology*, vol. 161, no. 10, pp. 5663–5672, 1998.

[58] N. Tedla, P. Palladinetti, D. Wakefield, and A. Lloyd, "Abundant expression of chemokines in malignant and infective human lymphadenopathies," *Cytokine*, vol. 11, no. 7, pp. 531–540, 1999.

[59] T. Kucharzik, J. T. Hudson, R. L. Waikel, W. D. Martin, and I. R. Williams, "CCR6 expression distinguishes mouse myeloid and

lymphoid dendritic cell subsets: demonstration using a CCR6 EGFP knock-in mouse," *European Journal of Immunology*, vol. 32, no. 1, pp. 104–112, 2002.

[60] R. Förster, A. Schubel, D. Breitfeld et al., "CCR7 coordinates the primary immune response by establishing functional microenvironments in secondary lymphoid organs," *Cell*, vol. 99, no. 1, pp. 23–33, 1999.

[61] G. J. Randolph, J. Ochando, and S. Partida-Sánchez, "Migration of dendritic cell subsets and their precursors," *Annual Review of Immunology*, vol. 26, pp. 293–316, 2008.

[62] G. Vassileva, H. Soto, A. Zlotnik et al., "The reduced expression of 6Ckine in the plt mouse results from the deletion of one of two 6Ckine genes," *Journal of Experimental Medicine*, vol. 190, no. 8, pp. 1183–1188, 1999.

[63] M. H. Jang and M. Miyasaka, "CCR7 is critically important for migration of dendritic cells in intestinal lamina propria to mesenteric lymph nodes," *Journal of Immunology*, vol. 176, no. 2, pp. 803–810, 2006.

[64] P. Brawand, D. R. Fitzpatrick, B. W. Greenfield, K. Brasel, C. R. Maliszewski, and T. De Smedt, "Murine plasmacytoid pre-dendritic cells generated from Flt3 ligand-supplemented bone marrow cultures are immature APCs," *Journal of Immunology*, vol. 169, no. 12, pp. 6711–6719, 2002.

[65] M. D. Gunn, "Chemokine mediated control of dendritic cell migration and function," *Seminars in Immunology*, vol. 15, no. 5, pp. 271–276, 2003.

[66] M. L. Drakes, P. J. Stiff, and T. G. Blanchard, "Inverse relationship between dendritic cell CCR9 expression and maturation state," *Immunology*, vol. 127, no. 4, pp. 466–476, 2009.

[67] A. M. Norment, L. Y. Bogatzki, B. N. Gantner, and M. J. Bevan, "Murine CCR9, a chemokine receptor for thymus-expressed chemokine that is up-regulated following pre-TCR signaling," *Journal of Immunology*, vol. 164, no. 2, pp. 639–648, 2000.

[68] K. A. Papadakis, C. Landers, J. Prehn et al., "CC chemokine receptor 9 expression defines a subset of peripheral blood lymphocytes with mucosal T cell phenotype and Th1 or T-regulatory 1 cytokine profile," *Journal of Immunology*, vol. 171, no. 1, pp. 159–165, 2003.

[69] H. Hadeiba, T. Sato, A. Habtezion, C. Oderup, J. Pan, and E. C. Butcher, "CCR9 expression defines tolerogenic plasmacytoid dendritic cells able to suppress acute graft-versus-host disease," *Nature Immunology*, vol. 9, no. 11, pp. 1253–1260, 2008.

[70] S. Mizuno, T. Kanai, Y. Mikami et al., "CCR9+ plasmacytoid dendritic cells in the small intestine suppress development of intestinal inflammation in mice," *Immunology Letters*, vol. 146, no. 1-2, pp. 64–69, 2012.

[71] M. Á. García-López, F. Sánchez-Madrid, J. M. Rodríguez-Frade et al., "CXCR3 chemokine receptor distribution in normal and inflamed tissues: expression on activated lymphocytes, endothelial cells, and dendritic cells," *Laboratory Investigation*, vol. 81, no. 3, pp. 409–418, 2001.

[72] R. Förster, T. Emrich, E. Kremmer, and M. Lipp, "Expression of the G-protein-coupled receptor BLR1 defines mature, recirculating B cells and a subset of T-helper memory cells," *Blood*, vol. 84, no. 3, pp. 830–840, 1994.

[73] H. Saeki, M. T. Wu, E. Olasz, and S. T. Hwang, "A migratory population of skin-derived dendritic cells expresses CXCR5, responds to B lymphocyte chemoattractant in vitro, and co-localizes to B cell zones in lymph nodes in vivo," *European Journal of Immunology*, vol. 30, no. 10, pp. 2808–2814, 2000.

[74] S. Luangsay, V. Wittamer, B. Bondue et al., "Mouse ChemR23 is expressed in dendritic cell subsets and macrophages, and

mediates an anti-inflammatory activity of chemerin in a lung disease model," *Journal of Immunology*, vol. 183, no. 10, pp. 6489–6499, 2009.

[75] B. A. Zabel, A. M. Silverio, and E. C. Butcher, "Chemokine-like receptor 1 expression and chemerin-directed chemotaxis distinguish plasmacytoid from myeloid dendritic cells in human blood," *Journal of Immunology*, vol. 174, no. 1, pp. 244–251, 2005.

[76] S. Varani, G. Frascaroli, M. Homman-Loudiyi, S. Feld, M. P. Landini, and C. Söderberg-Nauclér, "Human cytomegalovirus inhibits the migration of immature dendritic cells by down-regulating cell-surface CCR1 and CCR5," *Journal of Leukocyte Biology*, vol. 77, no. 2, pp. 219–228, 2005.

[77] R. T. Semnani, L. Mahapatra, B. Dembele et al., "Expanded numbers of circulating myeloid dendritic cells in patent human filarial infection reflect lower CCR1 expression," *Journal of Immunology*, vol. 185, no. 10, pp. 6364–6372, 2010.

[78] Y. Wang, Y. Li, and G. Shi, "The regulating function of heterotrimeric G proteins in the immune system," *Archivum Immunologiae et Therapiae Experimentalis*, vol. 61, no. 4, pp. 309–319, 2013.

[79] N. Sánchez-Sánchez, L. Riol-Blanco, and J. L. Rodríguez-Fernández, "The multiple personalities of the chemokine receptor CCR7 in dendritic cells," *Journal of Immunology*, vol. 176, no. 9, pp. 5153–5159, 2006.

[80] A. Del Prete, W. Vermi, E. Dander et al., "Defective dendritic cell migration and activation of adaptive immunity in PI3Kγ-deficient mice," *EMBO Journal*, vol. 23, no. 17, pp. 3505–3515, 2004.

[81] L. Riol-Blanco, N. Sánchez-Sánchez, A. Torres et al., "The chemokine receptor CCR7 activates in dendritic cells two signaling modules that independently regulate chemotaxis and migratory speed," *Journal of Immunology*, vol. 174, no. 7, pp. 4070–4080, 2005.

[82] N. Sánchez-Sánchez, L. Riol-Blanco, G. De La Rosa et al., "Chemokine receptor CCR7 induces intracellular signaling that inhibits apoptosis of mature dendritic cells," *Blood*, vol. 104, no. 3, pp. 619–625, 2004.

[83] G. Shi, S. Partida-Sánchez, R. S. Misra et al., "Identification of an alternative Gαq-dependent chemokine receptor signal transduction pathway in dendritic cells and granulocytes," *Journal of Experimental Medicine*, vol. 204, no. 11, pp. 2705–2718, 2007.